PURIFICATION AND CHARACTERISATION OF GLIADIN FRACTIONS FROM WHEAT FLOUR.

by

Nana Asare Yeboah, B.Sc. (Hons) (Kumasi), M.Sc. (London).

A thesis submitted to the University of Kent at Canterbury in part fulfilment of the requirements for the award of the degree of Doctor of Philosophy (Biochemistry) of the Faculty of Natural Sciences.

Biological Laboratory,

August, 1991.

DECLARATION

Unless otherwise stated, the work presented in this thesis is entirely my own. No part has been submitted in support of an application for any degree, or qualification, of the University of Kent at Canterbury, or any other institute of learning.

(signed)

N.A. Yeboah

August, 1991.

To

Elizabeth Amanda

with love and appreciation.

ABSTRACT

Three gliadin fractions designated γ_{III}-gliadin, γ_V-gliadin and ω-gliadin were purified to homogeneity from milled flour (variety Chinese Spring) in good yield. The proteins were characterised in terms of amino acid compositions and N-terminal amino acid sequences; these confirmed that they were typical gliadins. M_r values by SDS-PAGE and by gel filtration in GuHCl, were 41K for the γ_{III}-gliadin by both methods, 47K and 44K respectively for the γ_V-gliadin and 76K and 90K for the ω-gliadin.

The chemical characterisation was extended using the physical techniques of fluorescence and circular dichroism spectroscopy to derive information on the proteins' conformational properties, and using time-resolved fluorescence to probe dynamic properties. Studies in the presence of various concentrations of urea were carried out in order to monitor unfolding of the native conformation, and the proteins' stabilities to unfolding.

The wavelength of maximum fluorescence emission (approximately 350nm) indicated that the tryptophan residues of the proteins were exposed to solvent in the native state; this was confirmed by the high values obtained for the Stern-Volmer quenching constants (12-18 M^{-1}), indicating considerable accessibility to exogenous quencher. Time-resolved fluorescence studies indicated rotational correlation times for the tryptophan side-chains of 3-6ns indicative of free mobility of these side-chains. The far-uv CD spectra of the proteins indicated some regular secondary structure; the spectra were suggestive of some α-helices in the γ-gliadins and some ß-turns in the ω-gliadin.

Exposure of the proteins to high concentrations of urea led to some loss of far-uv CD spectral features indicating secondary structure, implying that the proteins became

unfolded to some extent. However, these conditions produced only small changes in fluorescence intensity and wavelength of maximum emission and led to minimal changes in the near-uv CD spectra. These results indicate that there is little change in the environments of aromatic residues on unfolding, consistent with the interpretation that these residues are exposed in the native state.

Preliminary conformational and denaturation analyses were also carried out using two peptides derived from a related γ-gliadin fraction corresponding to its repetitive proline-rich N-terminal and non-repetitive S-rich C-terminal domains respectively. The properties of these peptides indicated that the properties of the intact γ-gliadins could be regarded as the sums of those of the isolated domains.

CONTENTS

ACKNOWLEDGEMENTS

It gives me great pleasure to acknowledge the support and encouragement I have received prior to, and during, this Ph.D studentship. Foremost, I must thank my supervisors, Prof. Robert Freedman and Prof. Peter Shewry for their personal interest, close supervision and inspiration. I am also indebted to Dr K.B Egyankor (University of Science & Technology, Kumasi) and Prof. Dr and Frau Dr. F. Deinhardt (Max von Pettenkofer Institut, München) for their unwavering support and encouragement throughout the years.

At Rothamsted Experimental Station where the first and final years of the period of research were spent, I would like to thank Drs Arthur Tatham and Nigel Halford (presently at Long Ashton Research Station, Bristol), Mrs Saroj Parmar and Mrs Susan Smith for the help while working in their laboratories. I am also grateful to Arthur and Nigel for reading parts of this thesis, and especially to Nigel for his morale-boosting advice and encouragement. I must also express my gratitude to Dr Judith Palmer for the training/travel/logistics grants and for arranging the use of the CUED PC laboratory facilities, Mr Gordon Higgins, Mrs Linda Castle and the staff of the Photography Department for help with all my photographic requirements and finally, the Rothamsted Overseas Housing Association for accommodation during my stay.

At the University of Kent at Canterbury, I am grateful to the Director and staff of the Biological Laboratory for their assistance in all the time I spent there, and also to all my friends and colleagues for their support. I am especially grateful to Drs Amina Sheikh, Neil Bulleid, Richard Williamson, Gordon Wright and all the RBF clones (RBF1 - RBF∞) and the wild-type, for their companionship and support.

I must also thank my present boss, Dr Nazlin Howell (University of Surrey) for her understanding and encouragement, and also the following for their technical assistance, Mr John Tiley (amino acid sequencing), the staff of The Molecular Recognition Centre, University of Bristol (amino acid composition analysis), Dr Gordon Wright (fluorescence spectroscopy) and Dr Alex Drake (CD spectroscopy).

I would like to take the opportunity to thank my family (my mother, brothers, sisters, and their families) for being there always when I needed them. Finally, to my best friend Elizabeth Amanda, for her love, the typing, the final proof-reading and for doing all the things that few people will find worthwhile to do.

The Ph.D studentship was supported by a grant from the Science and Engineering Research Council and financial contributions from the Lawes Agricultural Trust.

GLOSSARY

ABBREVIATIONS

AR	analytical reagent
>	greater than
<	less than
e	log to the base e
FT-IR	Fourier transformation infra-red
g	gram
μg	microgram
ΔG	Gibbs free energy change
HSA	Human Serum Albumin
K	10^3
l	litre
μl	microlitre
M_r	Relative molecular mass
ml	millilitre
M	molar
mM	millimolar
mg	milligram
mA	milliampere
mdeg	millidegrees
mol %	mole per cent

nm	nanometer
nmole	nanomole
ns	nanosecond
psi	pounds per square inch
Q	Quencher
pmole	picomole
SD	standard deviation
SERC	Science and Engineering Research Council
TM	registered trade mark
v/v	volume to volume
w/v	weight to volume

AMINO ACID SYMBOLS

Residue	One Letter Symbol	Three Letter Symbol
Alanine	A	Ala
Valine	V	Val
Leucine	L	Leu
Isoleucine	I	Ile
Proline	P	Pro
Phenylalanine	F	Phe
Tryptophan	W	Trp
Tyrosine	Y	Tyr

Residue	One Letter Symbol	Three Letter Symbol
Methionine	M	Met
Glycine	G	Gly
Serine	S	Ser
Threonine	T	Thr
Cysteine	C	Cys
Asparagine	N	Asn
Aspartic Acid	D	Asp
Glutamine	Q	Gln
Glutamic Acid	E	Glu
Lysine	K	Lys
Arginine	R	Arg
Histidine	H	His

CHAPTER 1

GENERAL INTRODUCTION

FOREWORD

Wheat is the world's most widely cultivated crop. It is a major world crop in terms of production, consumption and trade. Wheat cultivation can be traced to early Persian and Egyptian civilisations and has persisted and flourished until the present day. Its main end uses are as food for humans and feed for poultry and livestock. As a component of human food, a major use of wheat is in bread-making and it is this aspect that this thesis is concerned with. In addition to all the available statistics, two other observations support the global significance of wheat as a crop and as food. Firstly, the emblem of the United Nations incorporates bearded wheat inflorescences or spikes and secondly, the latin motto of one of its organs, the Food and Agriculture Organisation (FAO), *Fiat Panis*, actually translates as 'let there be bread'.

The science of wheat, including the technological properties which affect its processing into food, has received a great deal of attention spanning several centuries and in order to put this thesis in an appropriate perspective, this chapter attempts a concise review of relevant knowledge published to date. Relevant terms and the scope of the thesis are also defined.

EVOLUTION OF COMMON BREAD WHEAT *Triticum aestivum*.

Cereals are the fruits of cultivated grasses and are members of the *Gramineae*, a

monocotyledonous family. Wheat belongs to the genus *Triticum*, a group of several species only three of which are of any commercial importance. *Triticum aestivum* is believed to have descended from the primitive archetypal wild wheat species *Triticum monococcum* commonly referred to as einkorn. This is a diploid with 14 chromosomes. Sometime in the course of its evolution, *Triticum monococcum* is thought to have been fertilised by a wildgrass, *Aegilops speltoides* or *Triticum speltoides* another diploid with 14 chromosomes. Chromosome doubling of the infertile hybrid gave rise to a tetraploid, 28 chromosome species, *Triticum turgidum* commonly called emmer. Durum wheat which is used for producing pasta is a subspecies of *Triticum turgidum*. Tetraploid emmer either in the wild or in cultivation was then thought to have been crossed with another wild grass *Aegilops squarrosa* (also known as *Triticum tauschii*) giving rise to the hexaploid 42-chromosome hybrid species *Triticum aestivum*. Today, the arable fields of the temperate world are dominated by the thousands of *Triticum aestivum* varieties. An illustration of the possible origin of the hexaploid genomes of common bread wheat, *Triticum aestivum* is shown in Figure 1.1.

THE WHEAT SEED

Figure 1.2 shows a longitudinal section of a typical wheat grain. The pericarp or dry fruit coat surrounds the seed, and is made up of a number of layers of cells. The aleurone layer in contrast to the pericarp, is only one cell thick and part of the starchy endosperm. The vegetative part of the fruit is the germ or embryo. The largest tissue in the grain is the starchy endosperm which constists largely of starch granules embedded in a protein matrix. Most of the protein in the grain is present in the

Figure 1.1
THE ORIGINS OF THE HEXAPLOID GENOMES OF *T. aestivum*

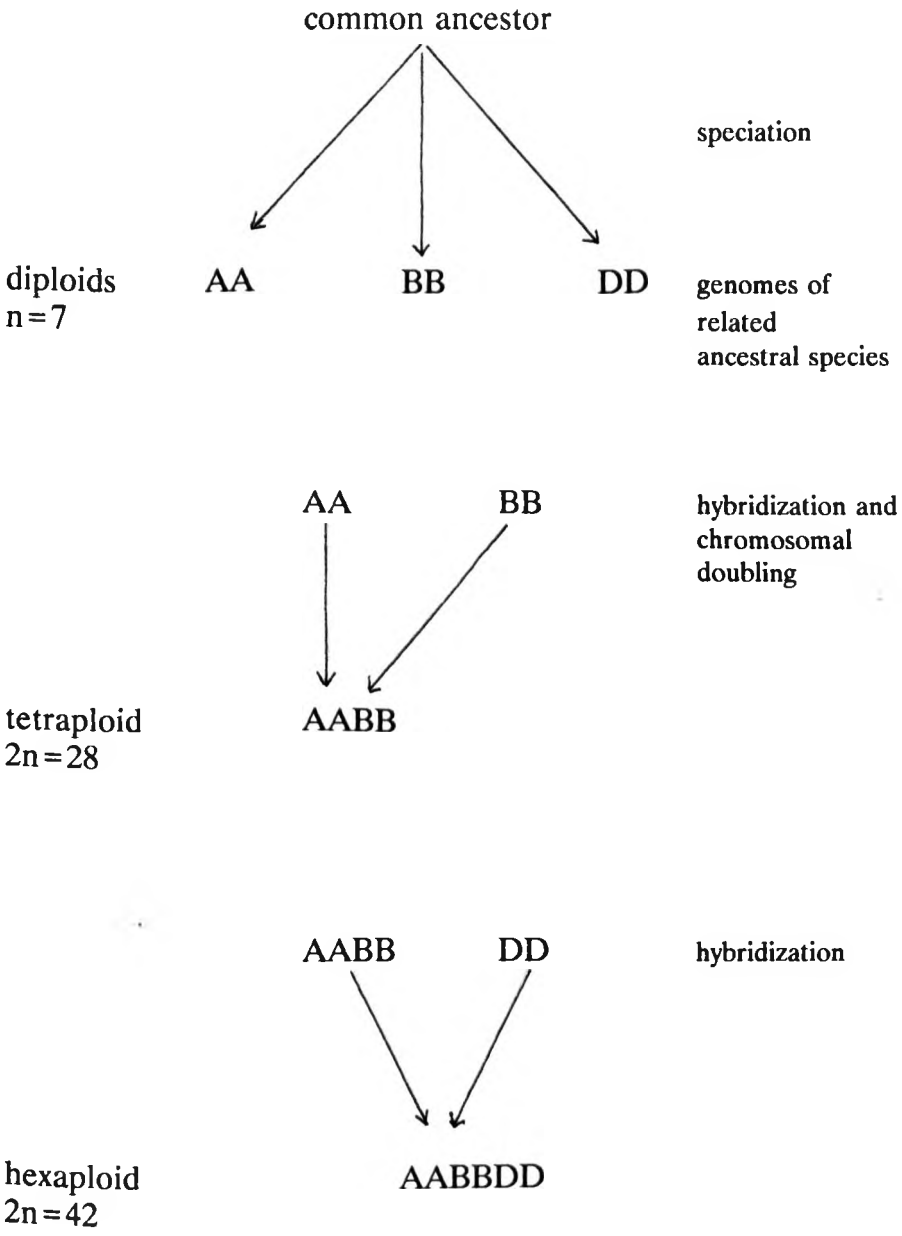

Figure 1.2
LONGITUDINAL SECTION OF A WHEAT SEED

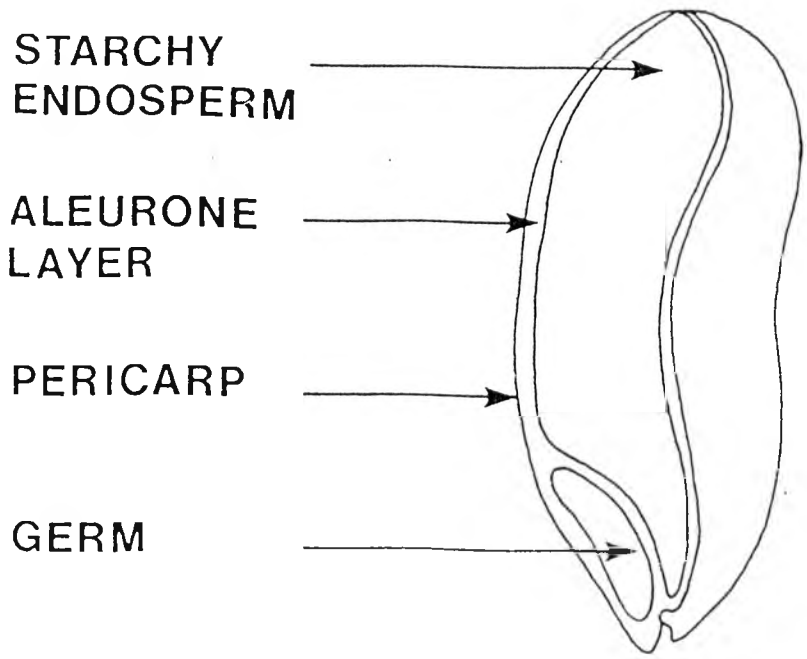

endosperm, mostly in the form of prolamins, proteins soluble in aqueous alcohols and characterised by high contents of proline and glutamine. To date, prolamins have only been described in grasses (Shewry and Miflin, 1985). Although other biochemical factors determine the quality of wheat required for bread-making, hard wheat is traditionally considered more suitable for bread-making than soft wheat.

The average weight of a typical bread wheat grain is about 40mg. 80-85% of the mature grain comprises the contents and cell walls of the endosperm and these constitute the bulk of wheat flour after milling. Up to 15% by weight of commercial wheat flour is made up of proteins with the rest being made up of carbohydrates, lipids, mineral matter and vitamins. Of the protein fraction, 50-60% are synthesized in the developing wheat endosperm and subsequently stored in membrane bound protein bodies. The remainder are mainly metabolic and structural proteins. As the grain matures, the protein bodies become compressed into the rigid protein matrix of the mature seed endosperm. Evidence from scanning electron microscopy (Hoseney, 1986), suggests that in hard wheat there is a tight physical association between protein molecules and starch granules of a nature that is not yet fully understood. However, in dough the protein and starch molecules are easily separated by gentle washing under running water. Bread dough washed in this way until all the starch is removed leaves gluten.

Gluten is important for various reasons. Its notable physical properties are viscosity and elasticity, and the fine balance between these two contrasting properties determines the ability of wheat doughs to be baked into leavened bread. About 80% of the dry weight of gluten is protein, 2% is lipid and the rest is made up of carbohydrates and mineral matter (Hesser, 1987). With such a high content of proteins, gluten prepared by

Beccari in Italy in 1728, is considered by many to be the first protein to be isolated from a plant source. Prior to this the widely held view was that proteins only came from animal sources.

Wheat gluten is unique among cereals in its ability to form a cohesive dough that retains gas and produces a light baked product, hence it is preferred to other cereal flours for bread-making.

GLUTEN PROTEINS

The classification of the major wheat gluten proteins is shown in Figure 1.3. There are two broad groups: the gliadins, which are soluble in aqueous alcohol and the glutenins which are insoluble in aqueous alcohol under non-reducing conditions but soluble if treated with reducing agents such as 2-mercaptoethanol. The gliadins are monomeric proteins which associate by non-covalent hydrophobic interactions and hydrogen bonding whereas the glutenins consist mainly of subunits covalently cross-linked by disulphide bonds into polymers with M_rs in excess of $1x10^6$. Traditionally, the gliadins are classified in increasing order of electrophoretic mobility at acid pH as the ω-, γ-, β- and α-gliadins each of which is known to consist of a complex mixture of closely-related proteins. Reduction of disulphide bonds in the glutenin fraction results in two groups of subunits classified according to their M_rs by polyacrylamide gel electrophoresis in the presence of sodium dodecyl sulphate (SDS-PAGE), as the high molecular weight (HMW) and the low molecular weight (LMW) glutenin subunits.

The gliadins and glutenins are both considered to be prolamins. These and related prolamins from barley and rye differ from one another in their amino acid composition

Figure 1.3
CLASSIFICATION OF GLUTEN PROTEINS

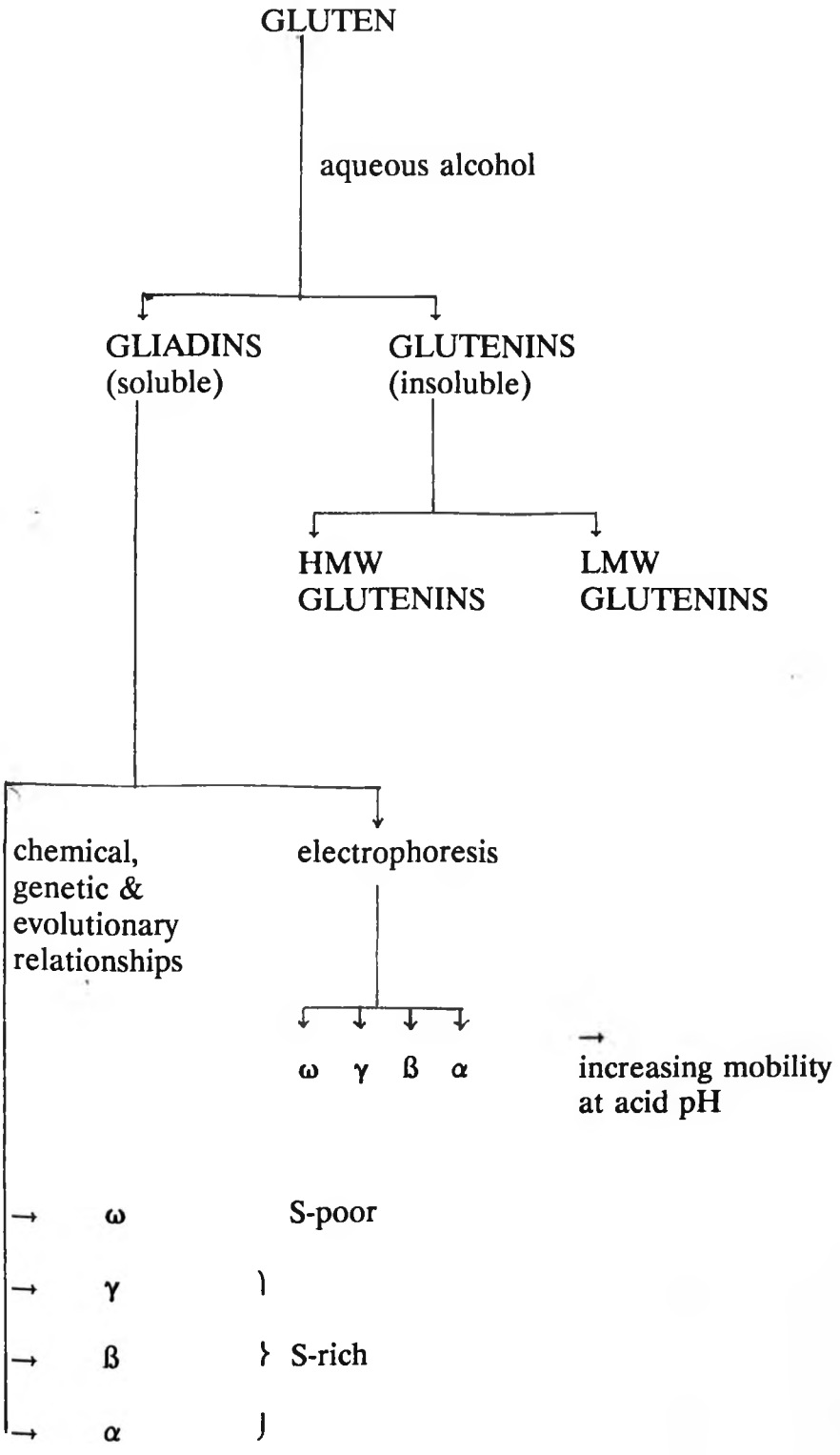

and sequence, genetic control, and evolutionary relationships. Shewry *et al.* (1986) therefore, classified them on the basis of the above molecular relationships into three alternative groups as described below.

1. sulphur (S)-rich
2. S-poor
3. high molecular weight (HMW).

Among the gluten proteins, the ω-gliadins correspond to the S-poor prolamins. They contain little or no cysteine and methionine, small amounts of basic amino acids, and their amino acid composition is characterised by high contents of glutamine, proline and phenylalanine, these three residues accounting for nearly 80% of the total. Although complete amino acid sequences of the ω-gliadins have not been reported, N-terminal sequences are available (Figure 3.3). Their M_rs by SDS-PAGE, are between 44-74K, with most above 50K (Kasarda *et al.*, 1983).

The α-, β-, γ-gliadins and the LMW glutenins correspond to the S-rich prolamins. The monomeric α-, β- and γ-gliadins all contain cysteine residues which form intramolecular disulphide bonds. In addition, they are characterised by higher contents of glutamine/glutamic acid and lower contents of proline when compared with the glutenins. It is also known on the basis of amino acid sequence data (chapter 3) that the α- and β-gliadins are closely-related and it is now usual to refer to both as the α-type gliadins (in contrast to the γ-type gliadins). The most widely studied α-type gliadin is the aggregable α-gliadin, A-gliadin. Its M_r by SDS-PAGE is 32K, which is typical of the group.

The M_rs of the γ-type gliadins on the other hand, are higher than those of the α-type

(although some overlaps may exist). Typically, they are between 38-42K by SDS-PAGE but higher M_rs have also been reported (Popineau and Pineau, 1988). Proteins related to the γ-type gliadins have also been described in other members of the *Triticeae* and in more distantly-related tribes of grasses and as a result, they are considered an ancestral type of S-rich prolamin (Shewry and Miflin, 1985).

Less is known about the structure of the individual LMW glutenin subunits. However, they can be separated by two-dimensional SDS-PAGE/isoelectric focusing (IEF) into a number of components with M_rs between 36-44K by SDS-PAGE. Their overall amino acid compositions are similar to those of the monomeric S-rich gliadins and some of the polymers containing them are also soluble in aqueous alcohol and may be extracted with the gliadins. These have been variously referred to as the high molecular weight gliadins, low molecular weight glutenins or aggregated gliadins (Shewry *et al.*, 1986).

The HMW glutenins, on the other hand, have been studied more extensively mainly because specific subunits are linked with good or poor bread-making quality in wheat doughs (Burnouf and Bouriquet, 1980; Moonen *et al.*, 1983, 1984; Branlard and Dardavet, 1985; Bushuk and Ng, 1987). Their M_r by SDS-PAGE vary with the gel system used (Bunce *et al.*, 1985) from between 95 to 136K. However, a true range of 69-88K, based on amino acid sequencing has been determined (Anderson *et al.*, 1988). Their amino acid compositions differ from those of the S-rich gliadins mainly in having higher contents of glycine.

The interactions of the individual gluten proteins are known to influence the properties of gluten and the ability of wheat doughs to be baked into leavened bread. Like all prolamins, the gluten proteins do not possess any biological activity and their only

known function is storage. In this role, they act as sources of nitrogen, carbon and sulphur to nourish the developing seedlings. They are tissue-specific, only being synthesised in the starchy endosperm of the seed. The amounts and types of protein synthesised are influenced by factors such as nutrient availability, climate and genotype. Thus, grain quality and yield differ according to wheat variety and region of cultivation.

GLIADIN GENETICS (based on Payne, 1987)

The extensive polymorphism of gluten proteins is a direct consequence of their genetic control. *Triticum aestivum* is hexaploid, containing three sets of chromosomes designated A, B and D (Figure 1.1). Each of the A, B and D sets is made up of 7 pairs of chromosomes, each set constituting a genome. Within a genome, chromosomes are numbered 1 to 7, followed by the genome assignment i.e 1A to 7A for the A genome, 1B to 7B for the B genome and 1D to 7D for the D genome. Pairs of chromosomes within a genome are homologous, whereas those of different genomes are homoeologous. Methods of determination of the chromosomal locations of prolamin genes include deletion and addition of specific chromosomes. Thus, the 1A chromosomes may be deleted from a wheat variety such as Chinese Spring and replaced with additional 1D chromosomes and the resulting line compared with a normal Chinese Spring line. The absence of storage proteins in the former, would indicate that the genes responsible for the missing proteins are located on chromosome 1A. By similar selective deletions of the short (S) or long (L) arms of the same pair of chromosomes, the arm location of the genes can also be determined. Although such approaches have been used to determine the chromosomal locations of the genes encoding the major gluten

proteins, they do not distinguish between the location of structural and regulatory genes. As a result, the term 'controlling gene', was used to describe these genes. However, it is now considered more appropriate to refer to them as 'structural genes' (Thompson *et al.*, 1983; Harberd *et al.*, 1985). Further details of the determination of the chromosomal locations of the major wheat storage proteins are presented in the reviews by Payne *et al.* (1984; 1987).

The genes encoding the ω-gliadins and the γ-gliadins have been known for some time to form clusters at a single major loci on the short arms of the 1A, 1B and 1D chromosomes (Mecham *et al.*, 1978; Payne *et al.*, 1982 a; b; Sozinov and Poperelya, 1982). The individual loci are designated *Gli-A1*, *Gli-B1* and *Gli-D1* respectively, in accordance with the Recommended International Rules for Gene Symbols in Wheat (Anonymous, 1968). More recently, a third family of genes which encode the LMW subunits have been reported to be present at each of the *Gli-1* loci (Jackson *et al.*, 1983; Payne *et al.*, 1984). Biochemical and molecular biology studies of the ω-gliadins, γ-gliadins and the LMW subunits, have provided further details about these loci. The three types of proteins are thought to be encoded by a total of 9-15 genes per *Gli-1* locus (Harberd *et al.*, 1985) but the actual number of proteins known to be expressed is lower. Thus, in Chinese Spring eight major proteins, comprising three each of ω-gliadin and γ-gliadin and two LMW subunits, are encoded by *Gli-B1* (Payne *et al.*, 1984). Although some minor proteins are also encoded by this locus, it is not clear whether these are the products of different genes expressed in small amounts, or whether they represent post-translational modification products of the major proteins. What is thought to be likely however, is that each major protein is the product of one or more different genes.

The α-gliadins and β-gliadins are encoded by genes at the *Gli-2* locus on the short arms of chromosome 6A, 6B and 6D. Despite their distinctive electrophoretic mobilities at acid pH, the primary sequences as well as gene sequences of the two gliadins, are closely-related (Anderson *et al.*, 1984; Rafalski *et al.*, 1984). The *Gli-2* locus therefore, is thought to contain one gene family, in contrast to the three thought to be present at the *Gli-1* locus. Varying estimates of the size of the gene family at the *Gli-2* locus have been reported as 9-12 (Harberd *et al.*, 1985) and as 33 genes (Okita *et al.*, 1985). A number of different two-dimensional electrophoretic procedures (Wrigley *et al.*, 1973; Payne *et al.*, 1982 a; b; Lafiandra *et al.*, 1984) have also shown that the number of major proteins encoded by genes on chromosomes 6A, 6B and 6D range between 5 and 10. It is possible therefore that each protein is the product of one or two genes.

ROLE OF GLUTEN PROTEINS IN DETERMINING BREAD-MAKING QUALITY OF DOUGHS

The basic ingredients required for bread-making are flour, yeast, water, fats, sugar and salt. Generally, yeast acts on the fermentable sugars releasing CO_2 gas in the process. The CO_2 thus released is trapped and held in gluten pockets providing a lift which eventually produces the light or leavened loaf of bread. Gluten is able to hold the gas bubbles because of its unique visco-elastic properties which are largely determined by the interactions between the individual gluten proteins.

The observation that tetraploid durum wheat which differs from hexaploid bread wheat only in its lack of the D genome, is of poor bread-making quality, provided early indication of the importance of the D genome in determining bread-making quality. The

evidence for the role of specific gluten proteins, however, came from correlation of quality of different cultivars of wheat with the presence or absence of specific gluten proteins (Payne *et al.*, 1979; 1981 a; b; 1984) and also from evidence of the contribution of physical and chemical factors involved in the processing of doughs as reviewed by Wall (1979) and Miflin *et al.* (1983). Further correlations have been reported and specific protein subunits have been linked with good or poor quality (Burnouf and Bouriquet, 1980; Pogna *et al.*, 1982 a; b; 1983; Moonen *et al.*, 1982; 1983; Peruffo *et al.*, 1985; Branlard and Dardavet, 1985; Bushuk and Ng, 1987). The presence of so called good quality subunits, however, does not always imply that a cultivar is going to yield good quality dough; perhaps another indication that the complex interactions of the proteins with themselves and other components are also important in determining bread-making quality.

THE CHEMICAL BASIS OF GLUTEN STRUCTURE AND FUNCTIONALITY

There are two schools of thought on the relationship between gluten proteins, gluten structure and the bread-making quality of wheat doughs. One stresses the importance of covalent disulphide bonds, the other, the importance of non-covalent hydrophobic interactions and hydrogen bonding. Involvement of disulphide bonds in determining the processing properties of dough derives from three main lines of evidence:

1. substances such as 2-mercaptoethanol which cleave disulphide bonds are known to affect dough behaviour

2. cleavage of disulphide bonds leads to a lowering of the apparent molecular weight of glutenin preparations (Meredith and Wren, 1966)

3. addition of 2-mercaptoethanol increases the solubility of gluten proteins (Danno *et al.*, 1974; Miflin *et al.*, 1980).

Ewart (1968) was the first to hypothesize on the structure and rheology of dough. His original idea, which has now been modified, (Ewart, 1972; 1977 a; b; 1981) envisages linkage of glutenin molecules through disulphide bridges into linear polymeric structures with little chain branching. During processing of the dough, secondary forces induce tension while viscous flow is attributed to molecular slip, mechanical scission and disulphide interchange.

Other hypotheses have evolved after Ewart's, and also stress the importance of disulphide bonds. In particular, Bloksma (1975) mentions the central role of disulphide bonds in creating a branched network of polymers in which viscous flow is determined by disulphide interchange. Wall (1979) and Khan and Bushuk (1978, 1979) also point out the importance of both covalent and non-covalent interactions in defining gluten structure. However, contrary to the linear hypothesis of Ewart, Kasarda and Bernadin (Kasarda *et al.*, 1967; 1976; Bernadin, 1978) put forward an alternative hypothesis based on their study of A-gliadin, which reversibly aggregates under conditions of low ionic strength and pH. Significantly, they do not discount the importance of intermolecular disulphide bonds and Ewart's hypothesis. However, they stress the importance of intramolecular disulphide bonds in maintaining conformations of individual proteins which ultimately facilitates aggregation.

These hypotheses stimulate interest and act as starting points for further investigation. On the question of gluten visco-elasticity, the combination is unique although elasticity is a common characteristic of rubber, plastic and other synthetic polymers which are

capable of undergoing deformation under stress but quickly recover their original form upon removal of the stress. But, gluten is extensible whereas rubber and synthetic polymers are not. Elasticity is enhanced by cross-linking and chain flexibility. The S-rich gluten proteins are capable of disulphide cross-linkages by virtue of their cysteine residues whereas the HMW subunits may be flexible in view of their high content of glycine which allows freer rotation about its peptide bonds than any other amino acid.

RATIONALE FOR FOLDING STUDIES OF GLUTEN PROTEINS

It is clear from the different hypotheses of gluten structure that interactions between amino acid residues are important for determining the quality of wheat doughs. The folded conformation of a polypeptide is the result of all the covalent and non-covalent interactions between the residues in its primary sequence (chapter 4). Hence, folding studies of gluten proteins could provide a means of elucidating these interactions. In addition, information on the basic structural organisation of cereal storage proteins relevant to such studies, is also available (Shewry *et al.*, 1987; Tatham *et al.*, 1990b).

There are other factors relevant to adopting protein chemistry principles to the study of gluten proteins. Cereal protein research has kept abreast with fast developing techniques in molecular biology, protein separation and tissue culture. For instance, lactate-PAGE systems have long replaced starch gel electrophoresis in the analysis of gliadin fractions, and HPLC does not only afford faster, accurate and more reproducible means of fractionating gliadin fractions, it also provides a faster means of identifying or 'fingerprinting' varieties of wheat.

Folding studies could also provide structural details which may be useful for successful

manipulation of the genes that encode gluten proteins in order to improve the quality. Central to this objective is the ability to transform monocotyledonous plants including wheat. For many years this received a lot of attention without any success. Very recently, however, separate reports have appeared detailing successful Agrobacterium-mediated transformation of rice [*Oryza sativa L.*] (Raineri, *et al.*, 1990), regeneration of green plants from embryogenic suspension culture protoplasts of wheat [*Triticum aestivum L.*] (Vasil, *et al.*, 1990) and successful transformation of maize (Gordon-Kamm *et al.*, 1990; Fromm *et al.*, 1990). The implications of these developments for future attempts at manipulating gluten protein structure are enormous and optimistic.

RATIONALE FOR DEVELOPING WHEAT GRAIN OF IMPROVED QUALITY

There is more than just an academic interest in understanding details of wheat gluten protein structure. Gluten is increasingly becoming an important industrial commodity (the various industrial applications of gluten, all of which relate to its unique visco-elastic properties, are shown in Figure 1.4). Moreover, The United Kingdom has traditionally produced soft wheat of poor bread-making quality. The country therefore imports high quality wheats at considerable cost for blending with the home-grown grain. Although plant breeding practices and improvements in baking technology have both contributed towards increasing the proportion of the home-grown grain in the bread-making grist from about 40% to about 80%, it still costs about £100 million per annum to import extra foreign hard grain. Genetic engineering of the home-grown grain in order to improve quality remains an untried approach. It is logical and in line with current scientific know-how, and the prospects of it leading to the development of a U.K wheat

Figure 1.4
INDUSTRIAL USES OF GLUTEN (based on Hesser, 1987)

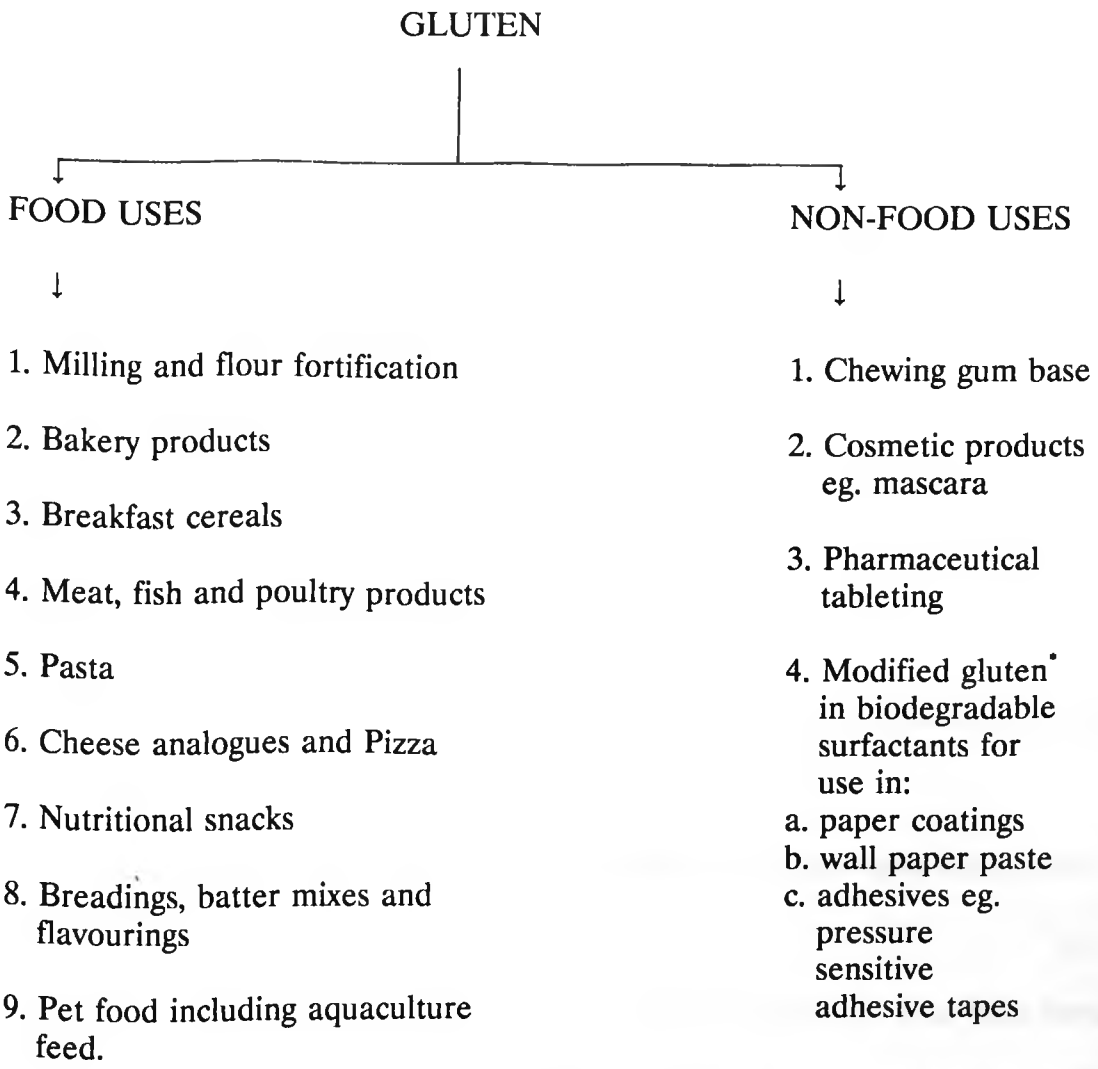

* the potential (but not actual application) has been demonstrated to date.

grain of improved bread-making quality appear brighter each day. Beyond the scope of this thesis, development of wheat grain of improved technological quality also holds vast implications for future attempts to modify the nutritional value of other cereal grains.

SCOPE OF THE PROJECT

The broad objective of the project was to study the pathway and mechanism of folding of wheat gluten proteins. In view of their extensive polymorphism however, the γ-gliadins of the variety Chinese Spring were chosen as a representative model for the reasons below.

1. γ-Gliadins are monomeric proteins with known DNA-derived amino acid sequences (Figures 2.1)

2. Cloned genes encoding γ-gliadins are available, hence mutant gliadins could be generated, whose folding characteristics may provide clues about the role of key residues in the folding of the authentic or wild-type proteins.

3. γ-Gliadins are considered ancestral and so information obtained on them could form a sound basis for analysing the other prolamin groups.

4. The genetics and molecular biology of Chinese Spring are well understood and widely studied.

In order to study the folding of any protein, it has to be obtained in a pure form, and monomers are preferred because unfolding and refolding is known to be less complicated for monomeric proteins than for oligomeric proteins. Gluten proteins are known to possess distinctive amino acid compositions, N-terminal amino acid sequences and M_rs which provide a means of characterising any purified fractions. Unfolding of the

polypeptide chain may be achieved in several ways including heating and addition of denaturants such as urea and guanidinium chloride (GuHCl). Refolding can then be induced by cooling or removal of the denaturant by dilution. Both unfolding and refolding may be monitored by the physical techniques of circular dichroism (CD) and fluorescence spectroscopy, which are sensitive to changes in the conformation of proteins. In the process, information on the relative conformational stabilities as well as clues about the possible mechanisms of folding of different polypeptides may be obtained and compared. Of the two the application of CD to the study of the structures of prolamins is more widely reported (chapters 4 and 5). Fluorescence spectroscopy is not known to have been applied to the prolamins in spite of the fact that they are intrinsically fluorescent (chapter 4).

Thus, in the attempt to achieve the set objective, individual γ-gliadin monomers were purified from milled flour and characterised in terms of their M_rs, amino acid compositions and N-terminal sequences. Following this, the physical techniques of circular dichroism and fluorescence spectroscopy were used to extend their preliminary characterisation to include the characterisation of their behaviour in solution, as well as the stability of their folded conformations to chemical-induced denaturation. It was envisaged that the disulphide structures of the purified fractions would also be determined as a preliminary step to using disulphide bonds as probes for monitoring the folding pathway as in the procedure reported for bovine pancreatic trypsin inhibitor (Creighton, 1978). Alongside this project, two related projects were also in progress with the aims of :

1. developing an expression system for cloned genes encoding γ-gliadins

2. establishing a system for raising monoclonal antibodies specific for γ-gliadins.

In collaboration with these two projects, it was envisaged that comparative studies of the folding characteristics of authentic and mutant γ-gliadins as well as the characterisation of their specific conformations using available monoclonal antibodies, would be undertaken. The scope was amended later to include characterisation of a purified ω-gliadin fraction in similar terms as described above for the γ-gliadins. Although the main reason for doing this was to allow a comparison with the purified γ-gliadins, it was also influenced by other considerations. Firstly, the ω-gliadins have not been studied in detail, and most of the available structural information on the S-poor prolamins are based on studies of the C hordein fraction of barley. Secondly, the purification of individual γ-gliadins resulted in the recovery of pure ω-gliadins in very good yield.

SUMMARY

This thesis represents the findings of this project. It is presented in six chapters as outlined in the table of contents. In this introductory chapter, an attempt has been made to provide a concise background derived from published work in the field. Relevant terms have been defined where appropriate and the reasons behind the approach adopted and their wider implications have also been discussed. Subsequent chapters are based on experimental work carried out by the author and summarised in Figure 1.5. Each chapter comprises an introduction, materials and methods, results, discussion and conclusions. In chapter 6, the overall results are discussed with reference to the stated objectives and their implications for further research. The abbreviations used throughout the thesis are also explained in the glossary.

Figure 1.5
THE PLAN OF RESEARCH

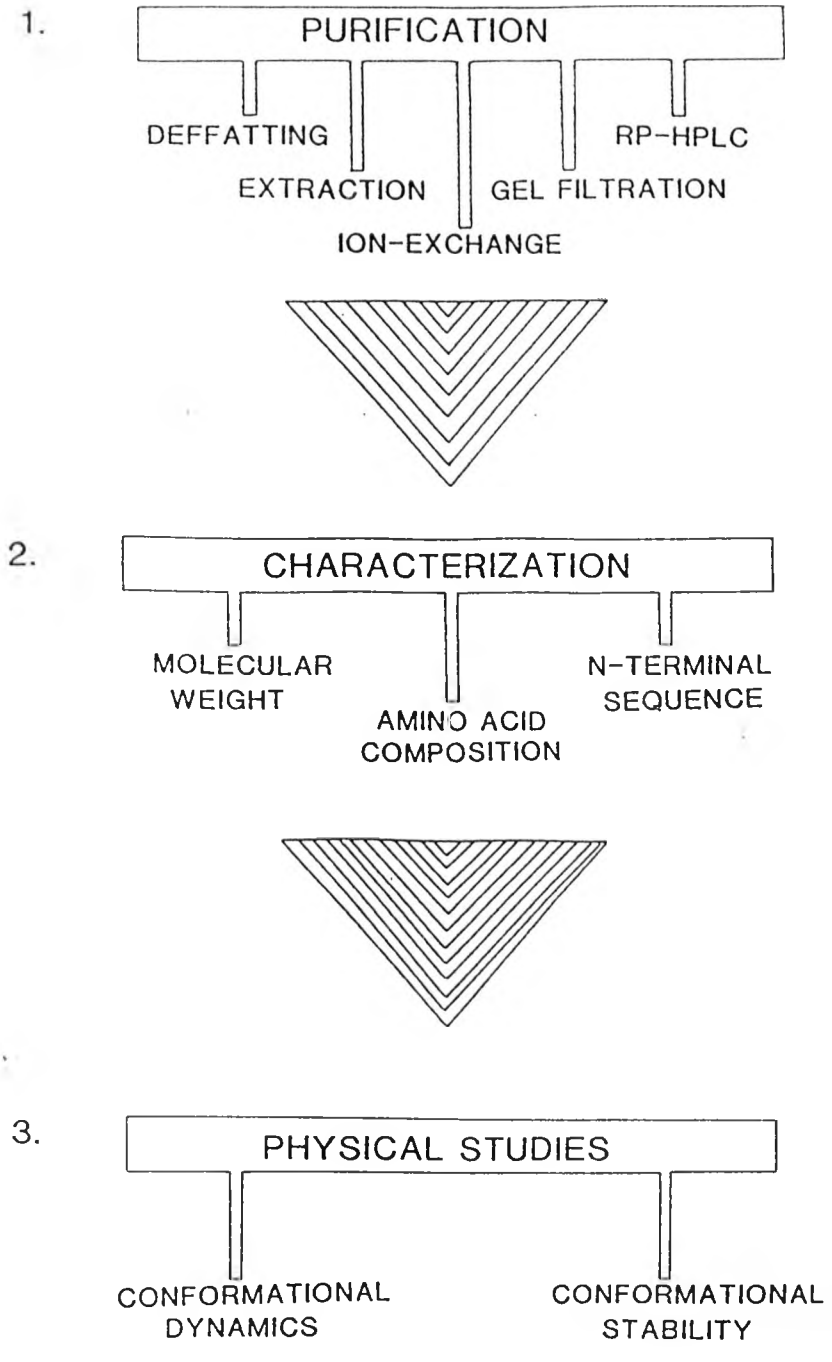

CHAPTER 2

PURIFICATION OF GLIADIN FRACTIONS

INTRODUCTION

An important prerequisite for the study of any protein is that it should be available in a homogeneous form. Protein purification uses highly selective chemical and physical procedures to isolate fractions of interest from the pool of cellular components. Purification strategies are numerous and diverse but they all share a common feature of progressive elimination of unrequired fractions accompanied by a simultaneous retention and enrichment of the target fractions. Essentially, purification begins with an extraction based on the solubility of the fraction of interest in a solubilizing medium. Crude protein extracts obtained this way may vary in their chemical, physical and biological characteristics, reflecting diversity of the components present, or they may show similarities in their characteristics if the components are closely-related. The crude extract may then be further fractionated into individual components on the basis of their:

1. solubility
2. molecular size
3. electric charge or isoelectric point
4. differences in adsorption characteristics
5. biological affinity for other molecules.

The field of biomolecular separation is rich in history and still represents a rapidly

changing area of scientific endeavour. Advances in procedures and instrumentation have led to improved, consistent and accurate recoveries of purified proteins in many cases.

This chapter reviews published work on gluten protein separation including a review of experimental techniques, as a background to the purification of individual gliadin fractions. It also includes sections on the materials and methods used, the results obtained and discussions of these.

BACKGROUND TO EXPERIMENTAL PROCEDURES

The classical work of T.B. Osborne around the turn of the century classified proteins into four groups on the basis of their solubility as follows:

1. albumins - soluble in water
2. globulins - soluble in dilute salt solutions
3. prolamins - soluble in aqueous alcohol solutions
4. glutelins - soluble in dilute acid or alkali

The Osborne classification still provides a useful starting point for most purification protocols although some minor modifications have been introduced to accomodate later developments such as the demonstration of disulphide bonds in proteins by F.G. Hopkins in 1925.

GLIADIN PURIFICATION

Virtually all the characteristics of gliadins which influence their extraction and subsequent fractionation into individual constituents may be associated with their amino

acid compositions.

The complete DNA derived amino acid sequence of a γ-gliadin clone of the variety Chinese Spring is shown in Figure 2.1. As expected of a prolamin, the amino acid composition is high in proline and glutamine. In addition, the sequence is made up of predominantly uncharged hydrophobic residues. Out of a total of 275 residues, only 15 are charged. Of these, the acidic residues comprise 2 aspartic acid and 3 glutamic acid residues, while the basic residues are made up of 3 lysine, 5 histidine and 2 arginine residues. This unusual amino acid composition coupled with other factors such as the structural organisation and folding (chapters 4 and 5), affects the purification of gliadins in a number of ways. For instance, gliadin solubility is enhanced in alcohol solutions and organic solvents, and in aqueous environments they tend to associate through hydrophobic interactions which sometimes leads to the formation of insoluble aggregates.

EXTRACTION OF GLIADINS

Lipids are present in wheat flours at a level of about 2.0% by weight (Hesser, 1987). Gluten proteins are also known to bind lipids (Lásztity *et al.*, 1987) and so these are extracted in organic solvents prior to the extraction of gliadins from flour. It is also known that defatting from flour is more efficient than from dough because defatting of dough results in the extraction of only 0.3% by weight of lipids (Hoseney, 1986). Commonly used solvents for defatting wheat flours include hexane, cyclohexane, butanol and petroleum ether. Although most reported fractionation protocols of gliadins include an initial defatting step, there is little agreement between different workers on the actual effect of this step on the subsequent recovery of gliadins (Wren and Nutt, 1967;

Figure 2.1
DNA-DERIVED PRIMARY SEQUENCE OF γ-GLIADIN FROM CHINESE SPRING
(based on Bartels *et al.* (1986))

```
                                                    20
N M Q V D P S S Q V Q W P Q Q Q P V P Q
                                                    40
P H Q P F S Q Q P Q Q T F P Q P Q Q T F
                                                    60
P H Q P Q Q Q F P Q P Q Q P Q Q Q P L Q
                                                    80
P Q Q P F Q Q P Q Q P Y P Q Q P Q Q P F
                                                   100
P Q T Q Q P Q Q L F P Q S Q Q P Q Q Q F
                                                   120
S Q P Q Q Q F P Q P Q Q P Q Q S F P Q Q
                                                   140
Q P P F I Q P S L Q Q Q V N P C K N F L
                                                   160
L Q Q C K P V S L V S S L W S M I W P Q
                                                   180
S D C Q V M R Q Q C C Q Q L A Q I P Q Q
                                                   200
L Q C A A I H T V I H S I I M Q Q E Q Q
                                                   220
Q G M H I L L P L Y Q Q Q Q V G Q G T L
                                                   240
V Q G Q G I I Q P Q Q P A Q L E A I R S
                                                   260
L V L Q T L P T M C N V Y V P P E C S I
                                                  275
I K A P F S S V V A G I G G Q*
```

* last detected residue.

Charbonnier, 1973; Miflin *et al.*, 1980; Byers *et al.*, 1983).

Gliadins have traditionally been extracted using a solution of 70% (v/v) ethanol at 4°C. Although the superior efficiency of higher temperature and three-carbon alcohols for extracting prolamins is well known, (Shewry and Miflin, 1985), extraction with 70% (v/v) ethanol at 4°C is preferred as this excludes HMW glutenins from the pool of recovered proteins. In addition, 70% (v/v) ethanol at 4°C is close to conditions under which gliadins precipitate out of solution (Dill and Alsberg, 1925) and this is facilitated by the addition of a concentrated solution of sodium chloride. The crude total gliadin is recovered by centrifugation along with some soluble glutenins which co-precipitate under the same conditions. The efficiency of extraction is enhanced by optimising the choice of solvent:flour ratio. The composition of the total gliadin extract can then be analysed by electrophoresis.

CHROMATOGRAPHY OF GLIADINS

Ion exchange and gel filtration chromatography have historically been used to fractionate gliadins. It has also been demonstrated that sufficient differences exist in the surface hydrophobicities of different gliadin polypeptides (Popineau and Godon, 1982) for them to be separated by hydrophobic interaction chromatography (HIC) (Popineau and Pineau, 1985 b). In recent years, the advent of high pressure liquid chromatography has led some workers to analyse and fractionate cereal proteins on ion-exchange, gel filtration and reverse-phase columns with a high degree of resolution. A review of this application is provided by Bietz (1986).

SEPARATION OF GLIADINS BY ION-EXCHANGE CHROMATOGRAPHY

Because of the net positive charge on gliadins at low pH, cation exchangers have long been used to fractionate them. The first isolation of a wheat gliadin, a γ-type gliadin from the variety Ponca, was reported in 1963 (Woychik, 1963). Purification of this fraction was performed on a carboxymethyl cellulose (CMC) cation exchanger using a pH gradient. Following this, several modifications of this procedure were reported (Ewart, 1975; 1977 b; 1981) in which total gliadin was loaded onto a CMC column, equilibrated with sodium acetate buffer maintained at pH 3.5 with acetic acid. The buffer also contained dimethyl formamide (DMF) to enhance the solubility of the gliadins. Elution was performed using a combination of stepwise and gradient increase in the concentration of sodium chloride. Charbonnier and Mossé (1980) used ion-exchange chromatography on the cation exchanger sulphopropyl Sephadex (SPS) and a buffer system comprising urea, ethylenediamine, hydrochloric acid, acetic acid and sodium acetate at pH 3.1 to achieve significant resolution of total gliadin extract. This method formed the initial step in the later protocol of Popineau and Pineau (1985 a and b) which was extended to include a further ion-exchange step on a newly developed cation-exchanger, sulphopropyl Trisacryl M (SP-Trisacryl M). The buffer system comprised acetic acid, urea and hydrochloric acid at pH 2.6. Sample elution was by a linear gradient of sodium chloride. In all these protocols, significant separation of component gliadin monomers was achieved and although some fractions were enriched in particular gliadin monomers, no single isolated fraction was entirely homogeneous.

SEPARATION BY GEL FILTRATION CHROMATOGRAPHY

The ion-exchange protocols described above essentially separated total gliadin into the classical electrophoretic groups: α-, β-, γ- and ω-gliadins. They were, however, each cross-contaminated by other proteins and gliadin groups. Charbonnier and Mossé (1980) therefore used gel filtration chromatography to further separate soluble glutenins and albumins from gliadin fractions obtained from the initial ion-exchange separation on SP-Sephadex. The gel filtration matrix was Sephadex G-100 of superfine grade and the buffer system comprised urea, sodium chloride and acetic acid, although in practice, any solvent system in which gliadins are soluble can be used. For example, Popineau and Pineau (1985 b) were able to remove soluble glutenins and other cross-contaminants from ion-exchange fractions of gliadins by gel filtration on Sephadex G-100 equilibrated with aluminium lactate buffer, pH 3.6.

SEPARATION BY HYDROPHOBIC INTERACTION CHROMATOGRAPHY (HIC)

The protocol of Popineau and Pineau (1985 b) extended the purification procedure to include a final separation step on a phenyl Sepharose HIC column. The column was initially equilibrated with aluminium lactate buffer, pH 3.6. Protein was initially eluted with the same buffer followed by a linear gradient of ethanol in ammonia solution. This combination of different chromatographic separations led to the successful isolation of six γ-gliadin components, each of which had a distinct electrophoretic mobility.

SEPARATION OF GLIADINS BY HIGH PERFORMANCE LIQUID CHROMATOGRAPHY (HPLC)

The advent of HPLC has brought a new dimension to the field of cereal protein isolation and analysis, notably in terms of enhanced rapidity, simplicity, high level of resolution and sensitivity. HPLC is a more precise procedure mainly by virtue of its superior instrumentation. Hence, factors such as flow rates, rigidity and stability of column matrices, operating temperatures and pressures which have for long, limited traditional open column chromatography, are controlled within accurate limits of experimental error in HPLC.

Early development of HPLC columns gave small silica-based columns which could withstand pressures and flow rates higher than previously envisaged or experienced with traditional open columns. These columns provided improved speed, sensitivity, resolution, reproducibility and ease of use, but their relatively small pore size (80-100Å) limited their application, to low-molecular weight organic molecules and peptides. Present day silica-based HPLC columns however, are of wider pore sizes, typically in excess of 300Å which extends their application to larger molecules like proteins. As in traditional open column chromatography, HPLC columns may be ion-exchange (IE-HPLC) gel filtration or size exclusion (SE-HPLC) or hydrophobic interaction (RP-HPLC) type. They differ mainly in the nature of the covalent modification of the silanol groups on the surface of the silica matrix which ultimately defines the functionality of the column. Thus, SE-HPLC columns have bonded phases on the surface of their matrix which do not interact with proteins, offering rather relative degrees of penetration of the matrix to protein molecules according to their molecular sizes. Similarly, IE-HPLC

columns have ionizable groups bonded to their surfaces while RP-HPLC columns are modified to incorporate hydrophobic groups on their surfaces. In RP-HPLC, which is the high performance equivalent of HIC, proteins are adsorbed on the basis of their hydrophobicity and subsequently, selectively desorbed from the column matrix by a gradient of relatively polar or aqueous solvents. Bietz, who pioneered RP-HPLC analysis of wheat and maize proteins (1983) has also presented a comprehensive review of the optimal conditions for isolating specific cereal proteins (Bietz, 1986).

A commonly used solvent for RP-HPLC of cereal proteins is acetonitrile (CH_3CN) but the polar phase is always water. To this solution of solvent and water is always added a low percentage by volume, typically up to 0.1%, of trifluoroacetic acid (TFA) which acts as an ion-pairing reagent and binds to free silanol groups to diminish their reactivity towards proteins. The sensitivity of HPLC requires that all the solvents used are of high purity. In most instances, commercial HPLC grade solvents and reagents are available to counter the solvent purity problem. In addition, HPLC columns are fitted with prefilters and in the purification of prolamins, preliminary open column chromatography is used to obtain relatively pure samples prior to further fractionation by HPLC. Also important is a preliminary analytical run to establish optimal conditions of fractionation such as sample load per run, elution gradient range, operating temperature, flow rates and operating pressure before scale up to preparative columns. At a high detector sensitivity, microgram quantities (or nanograms in some cases) of prolamins may be loaded on analytical HPLC columns, but on a preparative scale, up to 50mg may be loaded per run (Bietz, 1986). In contrast, much larger samples may be loaded on open columns. For example, Charbonnier and Mossé (1980) loaded 20g of crude gliadin on

a 10 x 90cm preparative ion-exchange column. Whereas a typical HPLC run may take up to an hour to complete, the total run time of the protocol of Charbonnier and Mossé (1980) was over 300hr. Hence, the precision and rapidity of HPLC allows runs to be repeated and fractions recovered in a more reproducible manner.

POLYACRYLAMIDE GEL ELECTROPHORESIS OF GLIADINS

Chromatography and electrophoresis are the most widely used separation techniques in the analysis of gluten proteins. As gluten proteins lack any biological activity, a convenient way of assaying peak fractions during purification is by electrophoresis. Elton and Ewart (1962) catalogue the development of gel electrophoresis of gluten proteins from the 1930s when evidence from ultracentrifuge analysis and diffusion measurements suggested that gliadin was composed of more than one individual protein. Jones *et al.* (1959) demonstrated the heterogeneity of gliadin proteins by moving boundary electrophoresis in an aluminium lactate buffer maintained at an acidic pH of 3.2. Woychik (1961) and Elton and Ewart (1962) used starch gel electrophoresis and aluminium lactate buffer, pH 3.2, with and without 2M urea to study gliadin extracts. They identified four distinct major bands which were designated ω, γ, β and α in increasing order of their mobility. Advances in gliadin research showed that each type of gliadin comprised several more components. Wrigley (1976) used 2-dimensional (isoelectric focusing, IEF/acid-PAGE) electrophoresis to resolve gliadin into 46 'separate' proteins. More recently, Tkachuk and Mellish (1987) showed that gliadins from the variety Neepawa could be resolved into over 100 protein spots using 2-D (IEF/SDS-PAGE) electrophoresis.

Gel electrophoresis of gluten proteins in one dimension falls into 2 broad types:

1. polyacrylamide gel electrophoresis at acid pH (Acid-PAGE)

2. polyacrylamide gel electrophoresis in the presence of sodium dodecyl sulphate (SDS-PAGE).

Acid-PAGE resolves gliadin extracts into the classical α- β-, γ-and ω- types and is useful in purification procedures in which peak fractions eluting from chromatography columns need to be analysed for their content. In order to monitor the progress of purification, however, it is important to know the homogeneity of isolated peak fractions. Used in conjunction with reducing agents such as 2-mercaptoethanol or dithiothreitol (DTT), and the chaotropic agent urea, SDS-PAGE affords the analysis of protein complexes which have been dissociated into component subunits. This provides a clearer picture of the extent of purity of isolated peak fractions.

STRATEGY OF PURIFICATION OF INDIVIDUAL GLIADIN FRACTIONS

With many protocols available for the purification of individual gliadin fractions, it was decided as an initial step to evaluate various reported protocols with the intention of adopting the one that gave reasonable yields of ω-gliadin and γ-gliadin fractions in a rapid and reproducible manner. Of the reported ion-exchange protocols, the three discussed below were evaluated.

1. SPS C50 ion-exchange (Charbonnier and Mossé, 1980) involved a simple elution step and up to 5g of total gliadin could be loaded at a time, but the procedure was not very rapid due to the use of lower flow rates. In addition, the γ-gliadin and β-gliadin fractions were not sufficiently resolved although the ω-gliadins and α-gliadins eluted as

distinct components in the initial and final column washes respectively.

2. SP-Trisacryl M presented two problems. Although it has been reported (Popineau and Pineau, 1985 a and b) to have been effective in fractionating 'whole' γ-gliadin into individual components, attempts to apply it to the fractionation of total gliadin was not successful. Its use therefore, required a preliminary fractionation step for total gliadin. It also required the use of low pH buffers which could cause deamidation of glutamine and asparagine residues (Popineau and Pineau, 1985 b). Although attempts were made to modify elution conditions by increasing the pH of buffers to between 3.5 and 4.5, this led to irreversible binding of proteins to the column matrix especially in the presence of high salt concentration. This problem was also encountered by other workers (Pratt, 1990).

3. CM52 (Booth and Ewart, 1969; Ewart, 1975; 1977 b) had the advantage of permitting larger sample loads and higher flow rates, and total gliadin was also separated into components enriched in α-, β-, γ-and ω- gliadins in good yield and in a reproducible manner. An additional gel filtration step was, however, required in order to remove cross-contaminating ω- and β-gliadins as well as soluble glutenins from the γ-gliadin enriched fractions.

Analytical RP-HPLC of fractions resulting from gel filtration chromatography was used to establish optimal conditions prior to semi-preparative fractionation. A summary of the entire purification procedure is shown in Figure 2.2.

Figure 2.2
PLAN OF PURIFICATION

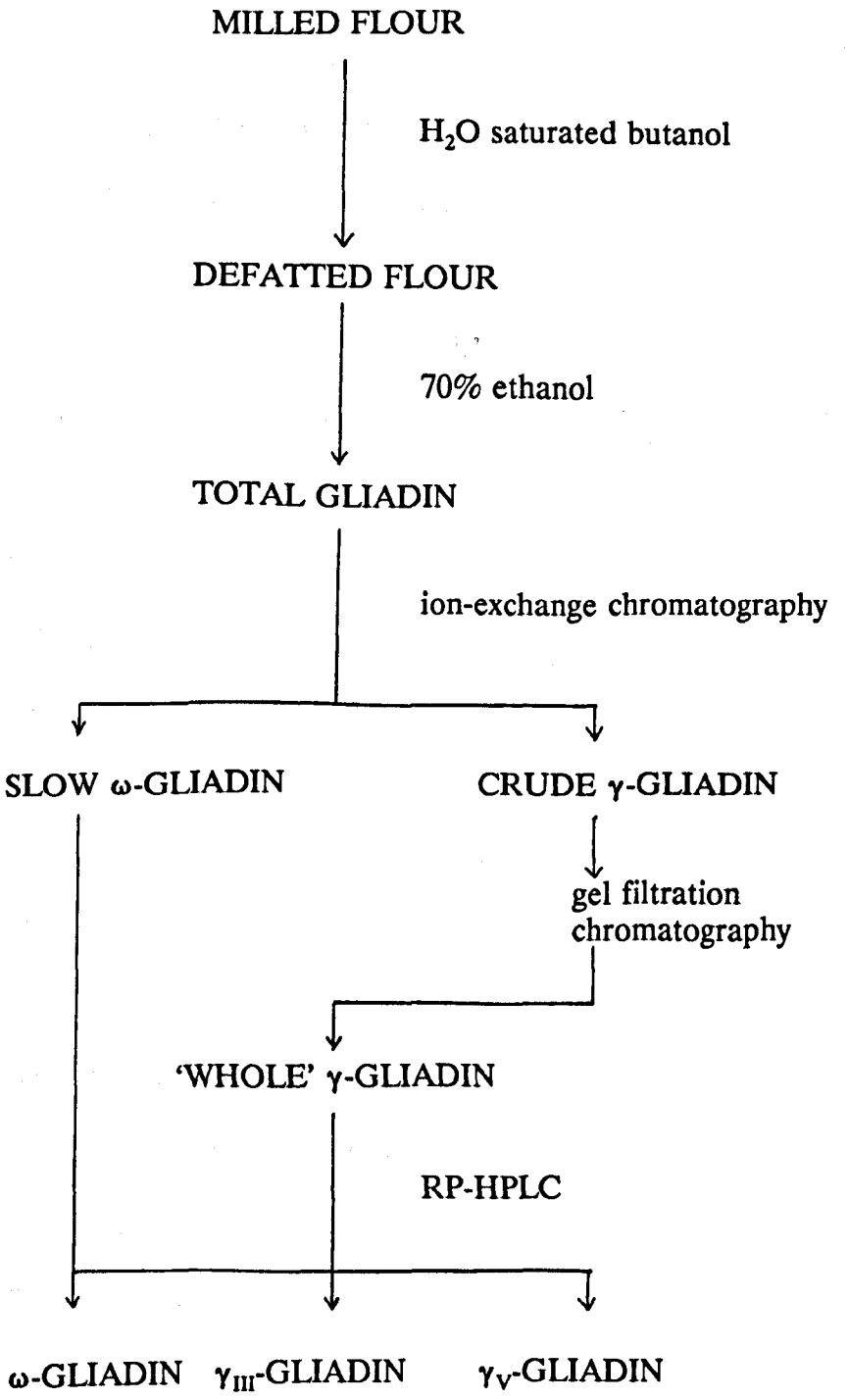

AIMS

In view of the extensive polymorphism of gliadins and the fact that physical analysis of any protein requires that it be obtained in a homogeneous form, the aims of the purification were to isolate individual ω-gliadin and γ-gliadin fractions from milled endosperm flour of the wheat variety Chinese Spring in good yield and to use SDS-PAGE analysis to establish the homogeneity of each isolated fraction.

MATERIALS

Milled wheat endosperm flour was a gift from Dr J. Michael Field of ICI Seeds, U.K Ltd.

CHEMICALS

PRODUCT		SOURCE
Acetic acid (glacial)	AR	Fisons Ltd
Acetonitrile (ACN) (HPLC grade)		Romil Chemicals
Acrylamide (electrophoresis grade)		BDH Ltd
bis-Acrylamide "		"
Aluminium lactate	AR	May & Baker Ltd
Amberlite mixed bed resin	AR	BIO-RAD
Ammonium persulphate (APS)	AR	BDH Ltd
L-Ascorbic acid	AR	"
Bromophenol blue		Sigma
Butan-1-ol	AR	Fisons Ltd
Carboxymethyl cellulose (CM52) resin		Whatman

PRODUCT		SOURCE
Coomassie brilliant blue R250		BDH Ltd
Dimethyl formamide (DMF)	AR	"
Dithiothreitol (DTT)	AR	Sigma
Ethanol (absolute)		Fisons Ltd
Ferrous sulphate ($FeSO_4.7H_2O$)	AR	BDH Ltd
Glycerol	AR	Fisons Ltd
Glycine (chromatographic grade)		BDH Ltd
Guanidine hydrochloride ('grade I')		Sigma
Helium gas		Union Carbide
Hydrogen peroxide H_2O_2 (30%)	AR	Fisons Ltd
D-/L- Lactic acid (85%)	AR	BDH Ltd
2-Mercaptoethanol	AR	Sigma
Methanol	AR	Fisons Ltd
Methanol (HPLC grade)		Romil Chemicals
Rosaniline hydrochloride		BDH Ltd
Sephadex G-100 (superfine grade)		Pharmacia
Sodium acetate	AR	Fisons Ltd
Sodium chloride	AR	BDH Ltd
Sodium dodecyl (lauryl) sulphate (SDS)		"
TEMED (N,N,N^1,N^1-tetramethylenediamine)		Sigma
Trichloroacetic acid (TCA)	AR	May & Baker Ltd
Trifluoroacetic acid (TFA) (HPLC grade)		Romil Chemicals

PRODUCT		SOURCE
Tris ([hydroxymethyl]aminoethane)		Sigma
urea	AR	Fisons Ltd

SOLUTIONS AND BUFFERS

8M Urea

urea		480.48g
H_2O	to	1l

the solution was deionized by passing through amberlite mixed bed resin, stored at room temperature and used within 3 days.

Stock 500mM sodium acetate, pH 3.5 with acetic acid

sodium acetate		41.0g
H_2O	to	300ml

the pH was adjusted to 3.5 using 400-500ml glacial acetic acid and H_2O was added to a final volume of 1l.

5mM sodium acetate, 1M DMF, pH 3.5 with acetic acid

stock 500mM sodium acetate		10ml
DMF		77.3ml
H_2O	to	1l

the pH was adjusted to 3.5 by dropwise addition of glacial

acetic acid when necessary.

HPLC buffer A, 10% (v/v) ACN

acetonitrile		100ml
TFA		1ml
H_2O	to	1l

HPLC buffer B, 90% (v/v) ACN

acetonitrile		900ml
TFA		1ml
H_2O	to	1l

HPLC buffer C, 50% (v/v) ACN

acetonitrile		500ml
H_2O	to	1l

all the solutions used for the HPLC buffers were filtered prior to mixing using 22μm organic and inorganic millipore filters as appropriate. The buffers were prepared fresh, degassed under vacuum and used on the same day.

Stock 32% (w/v) acrylamide solution

acrylamide	32g
bis-acrylamide	1g

H_2O	to	100ml

The solution was deionised by stirring with amberlite mixed bed resin (AR) for 30min, filtered and stored at 4°C in dark reagent bottles for up to 14 days.

Stock 5.6% (w/v) acrylamide solution

acrylamide		5.6g
bis-acrylamide		0.28g
H_2O	to	100ml

The solution was deionised, filtered and stored as described above.

10% (w/v) (0.3% bis) resolving gel solution (2 gels)

stock 32% acrylamide solution	25ml
$FeSO_4.7H_2O$ (3.2mg ml^{-1} solution)	10ml
stock (85%) lactic acid	400μl
L-ascorbic acid	80μg
H_2O	44ml

The solution was degassed under vacuum, precooled at -20°C till ice crystals appeared, then 60μl 0.2% (v/v) H_2O_2 was added to start polymerization

4.5% (w/v) (0.2% bis) stacking gel solution (2 stacks)

stock 5.6% acrylamide solution		10ml
aluminium lactate buffer, pH 3.1	1.25ml	
$FeSO_4.7H_2O$		200μg
L-ascorbic acid		12.5mg
H_2O		1.1ml

The solution was degassed and precooled as above, then 15μl 0.2% (v/v) H_2O_2 was added to start polymerisation.

Upper electrode buffer, aluminium lactate, pH 3.1 with lactic acid

aluminium lactate		1g
D-/L- lactic acid (85%)		1.6ml
H_2O	to	1l

Lower electrode buffer, lactic acid pH 2.6

D-/L- lactic acid (85%)		16ml
H_2O	to	4l

The pH was adjusted to 2.6 when necessary by dropwise addition of lactic acid

Sample buffer

ethanol (absolute)		70ml
rosaniline hydrochloride		2mg
glycerol		10ml
H_2O	to	100ml

SDS-PAGE

60% (w/v) stock acrylamide solution

acrylamide		60g
bis-acrylamide		0.9g
H_2O	to	100ml

The solution was filtered, stored in dark reagent bottles at room temperature and used within 14 days.

25% (w/v) stock acrylamide solution

acrylamide		25g
bis-acrylamide		3.5g
H_2O	to	100ml

The solution was filtered and stored as above.

Urea/SDS solution

SDS		0.2g
stock 8M urea solution	to	100ml

The solution was prepared fresh and used the same day. For reducing SDS-PAGE gels, 2mM DTT was added.

3M Tris buffer, pH 8.8 with HCl

Tris (pH range 9-7)		36.3g
H_2O	to	70ml

The base was dissolved by gentle warming, allowed to cool and the pH adjusted by dropwise addition of concentrated HCl. H_2O was then added to the final volume of 100ml.

0.5M Tris buffer, pH 6.8 with HCl

Tris		6.05g
H_2O	to	80ml

After dissolving the base, the pH was adjusted and H_2O was added as described above.

Resolving gel solution (2 gels)

stock 3M Tris, pH 8.8	10ml
urea/SDS(/DTT) solution	40ml
0.8% (w/v) APS solution (prepared fresh)	6.8ml
TEMED	20μl

In general, 10% (w/v), 12.5% (w/v) and 14% (w/v) acrylamide gels were prepared by adding the appropriate volume of 60%

(w/v) stock acrylamide solution and H_2O to the above solution up to a final volume of 80ml. TEMED was added last to initiate polymerisation. For reducing SDS-PAGE gels, 2mM DTT was included in the urea/SDS solution.

3.4% (0.5% bis) (w/v) stacking gel solution (2 stacks)

stock 0.5M Tris, pH 6.8	4ml
urea/SDS(/DTT) solution	8ml
stock 25% (w/v) acrylamide solution	2.2ml
0.8% (w/v) APS (prepared fresh)	2ml

The solution was mixed as above and 10μl TEMED was added to start polymerisation. 2mM DTT was added to reducing SDS-PAGE gels.

Electrophoresis buffer

0.19M glycine		56.8g
0.1% (w/v) SDS		4g
0.025M Tris		12.12g
H_2O	to	4l

Sample buffer

bromophenol blue		1mg
glycerol		1ml
SDS		2g
0.063M Tris		0.76g
H_2O	to	100ml

The pH was adjusted to 6.8 by dropwise addition of dilute HCl when necessary. 5% (v/v) 2-mercaptoethanol was included in the reducing sample buffer.

Staining solution

coomassie brilliant blue R250		2g
methanol (AR)		800ml
TCA		200g
H_2O	to	2l

The solution was filtered and stored at room temperature.

Destaining solution

TCA		200g
H_2O	to	2l

EQUIPMENT

PRODUCT	SOURCE
Vydac RP-HPLC analytical column Type 218TP104	Technicol
Vydac RP-HPLC semi-preparative column Type 218TP1010	"
SP 8700 solvent delivery system	Spectra Physics
UV detection system	"
Data integrator	"
Data organiser	"
Protean II™ electrophoresis system	BIO-RAD
FPLC™ SYSTEM	Pharmacia
Mono S HR 5/5 column	"

METHODS

DEFATTING OF FLOUR

Milled flour was defatted with water-saturated butan-1-ol using 5ml per gram of flour. The suspension was stirred for 30min and the supernatant was discarded. The extraction was repeated until the resulting supernatant remained colourless between successive extractions and the flour pellet was retained. In general, batches of 200g of flour were processed.

TOTAL GLIADIN EXTRACTION

The defatted flour pellet was dispersed in 70% (v/v) ethanol precooled at 4°C. Gliadin was extracted using 5ml ethanol per gram of starting weight of flour. The suspension was stirred on ice for 1hr and centrifuged. The supernatant was saved and the extraction repeated. The supernatant solutions were then combined and mixed with 2 volumes of 1.5M NaCl and left to stand at 4°C overnight. The precipitate was recovered by centrifugation and redissolved in 100-200ml of 8M urea after which the urea was removed by exhaustive dialysis against 8l of 50mM acetic acid. Dialysis was continued for at least 120hr with a minimum of 3 changes each 24hr period. The dialysed extract was then freeze-dried to yield approximately 6g of crude total gliadin per 200g batch of processed flour.

ION-EXCHANGE CHROMATOGRAPHY

COLUMN PREPARATION

Ion-exchange chromatography was used to fractionate the total gliadin extract.

50g of carboxymethyl cellulose resin CM52, was pretreated according to manufacturer's instructions. The resin was then equilibrated in 0.2M sodium acetate buffer, pH 3.5 with acetic acid, and allowed to settle overnight. The supernatant was discarded and the resin was washed in 3l of water and poured into a 5 x 30cm column to a height of 25.5cm, to give approximately 500cm^3 of total bed volume. The column was then equilibrated in 2l of starting buffer, 5mM sodium acetate, 1M DMF, pH 3.5 with acetic acid.

SAMPLE PREPARATION AND APPLICATION

The preparation of samples for loading was based on Booth and Ewart (1969). Freeze-dried total gliadin was dissolved by stirring overnight in starting buffer. Batches of 12g protein dissolved in 120ml starting buffer were loaded per run, with six runs carried out. The pH of the sample solution was adjusted to 3.5 when necessary by addition of glacial acetic acid before loading onto the column.

SAMPLE ELUTION

From the start of sample loading, 500ml of eluate corresponding to one column volume, was collected and discarded before fraction collection was started. The ion-exchange column was then washed with 500ml starting buffer. Sample elution was by a modification of the method of Booth and Ewart (1969) and Ewart (1975, 1977 and 1981), involving five consecutive steps in which sodium chloride concentration increased from 0 to 0.5M as shown in Table 2.1. The flow rate was maintained at 42ml hr^{-1} and 10ml fractions were collected. The elution of peak fractions was monitored by the absorbance at 280nm. The fractions were then analysed by Acid-PAGE, at pH 3.2 using total gliadin as standard. Fractions of identical mobility were pooled, dialysed exhaustively against 50mM acetic acid as described above and freeze-dried. Those containing bands with mobilities similar to γ-gliadins were retained for further analysis. Other peak fractions whose mobilities corresponded to the slowest moving ω-gliadin band in the total gliadin standard, were designated 'slow ω-gliadin' and retained for further analysis. After washing, the column was equilibrated at the initial conditions and chromatography was repeated in the absence of protein. Flow rates and fraction collection were as described

Table 2.1
CM52 ION-EXCHANGE ELUTION CONDITIONS

Stage	Total volume of buffer (ml)	[NaCl] (M)
1	700	0 - 0.025
2	1400	0.025
3	1400	0.045
4	1400	0.065 - 0.090
5	700	0.100 - 0.500

above and the refractive indices (RIs) of the fractions collected in the absence of protein were measured using a refractometer. The RI of a series of standard solutions containing the column buffer and 0-0.6M NaCl in steps of 0.1M was also measured. A standard curve of RI versus NaCl concentration was then plotted from which the NaCl concentration in the elution buffer was obtained. The chromatographic conditions described above, including the NaCl gradients, were reproducible in three separate experiments.

COLUMN REGENERATION

The chromatography column was regenerated according to manufacturer's instructions and chromatography was repeated for another batch of total gliadin extract.

GEL FILTRATION CHROMATOGRAPHY

COLUMN PREPARATION

Fractions from CM52 ion-exchange which were enriched in γ-gliadins were further fractionated by gel filtration chromatography to remove cross-contaminating gliadins and soluble glutenins. On the basis of their Acid-PAGE patterns, the slow ω-gliadin fractions did not appear to contain cross contaminants and were therefore not fractionated further. 3g of Sephadex G-100 powder was preswollen and resuspended in 2l of 1% (v/v) acetic acid according to manufacturer's instructions. The gel slurry was degassed under vacuum, poured into a 6 x 75cm glass column and equilibrated in a further 2l of 1% (v/v) acetic acid.

SAMPLE PREPARATION AND ELUTION

1g aliquots of the peak fractions from ion-exchange chromatography enriched in γ-gliadins were dissolved by stirring overnight in 5ml of 1% (v/v) acetic acid according to Charbonnier and Mossé (1980). The sample solution was loaded onto the chromatography column by means of a three-way sample applicator valve. The flow rate during loading was 10ml hr^{-1} after which it was increased to 12ml hr^{-1}. Elution of peak fractions was monitored by uv detection at 280nm and the recovered fractions were analysed by Acid-PAGE as described above. Fractions were pooled on the basis of their electrophoretic mobilities and freeze-dried. Those with mobilities corresponding to γ-gliadins were retained for further analysis. Five batches of γ-gliadin enriched fractions were analysed using the above procedure to yield approximately 2.4g of 'whole' γ-gliadins.

COLUMN REGENERATION

The chromatography column was washed with 2l of column buffer after the elution of the last detectable peak fraction and a fresh sample solution was loaded.

REVERSE PHASE-HPLC SEPARATION OF GLIADIN FRACTIONS

The 'whole' γ-gliadin fraction from gel filtration chromatography and the slow ω-gliadins from ion-exchange were further fractionated by RP-HPLC on a semi-preparative scale using the method of Bietz (1986).

Preliminary analytical runs were carried out to determine the optimal fractionation parameters shown in Table 2.2. The protein concentration was 1mg ml^{-1} and 50μl aliquots corresponding to 50μg protein was loaded. The gradient range within which the proteins eluted was determined initially, using a broad gradient of 0-100% buffer B corresponding to 10%-90% (v/v) acetonitrile. The ω-gliadin was eluted by 25-37% buffer B in 16min, while elution of the γ-gliadin was achieved in 40min using 30-60% buffer B (Table 2.3). The temperature was also varied between 25°C and 75°C and the resolution at various temperatures compared. In general, resolution improved with increasing temperature. However, in view of the stabilities of both the column and protein samples, 50°C was used for all analytical separations. Taking into account the quantities of proteins loaded, the absorption of peptide bonds was considered more sensitive for monitoring the elution of fractions. Hence, a wavelength of 230nm was used. By increasing the detector sensitivity at this wavelength, an improved detection was obtained. However, below a sensitivity of 0.32 absorbance units full scale (AUFS), increases in background noise resulted in uneven baselines and spectra. Thus,

sensitivities of 0.32 and 0.64 AUFS were used as appropriate.

The maximum sample load for the semi-preparative separation was based on Bietz (1986) and was 25mg per 500μl. Increases above this resulted in highly viscous solutions which affected the ease of sample injection. In contrast to the analytical procedure, however, the larger sample loading meant that the absorption of aromatic amino acids at 280nm and a sensitivity of 1.28AUFS were used to monitor the elution of peak fractions. A rate of change of gradient identical to that of the analytical procedure was also used for the semi-preparative runs. However, the lack of an appropriate heating block for the bigger column meant that separations were carried out at room temperature. The flow rates used in both procedures were based on the column manufacturer's recommendations.

SAMPLE PREPARATION AND LOADING

For the analytical runs, 1mg freeze-dried protein was dissolved in 1ml 6M GuHCl with vortexing and 50μl was loaded per run. For the semi-preparative runs, 25mg freeze-dried protein was dissolved in 6M GuHCl to a final volume of 500ul and loaded per run. 50μl and 500μl sample loops were used for the analytical and semi-preparative runs respectively, and samples were loaded via a manual injector and valve.

SAMPLE ELUTION

The analytical and semi-preparative columns were both washed at the initial gradient conditions (time 0, Table 2.3) for 5min after sample loading. The elution of the ω-gliadin fraction on the semi-preparative column was achieved using 20-35% buffer B in

Table 2.2
ANALYTICAL AND SEMI-PREPARATIVE RP-HPLC FRACTIONATION PARAMETERS

FRACTIONATION PARAMETER	ANALYTICAL RP-HPLC	SEMI-PREPARATIVE RP-HPLC
rate of change of gradient	0.75% min^{-1}	0.75% min^{-1}
detector wavelength	230nm	280nm
sensitivity	0.32/0.64 AUFS	1.28 AUFS
operating temperature	50°C	room temperature
maximum operating pressure	2500psi	2500psi
flow rate	1ml min^{-1}	5ml min^{-1}
sample size	10-50μg run^{-1}	25mg run^{-1}

20min, while 28-52% buffer B was used to elute the γ-gliadins in 32min. After the elution of the last detectable peak, both columns were washed as described in Table 2.3. The upper end of the elution gradient conditions was held for 5min and then sharply increased to 100% buffer B in a further 5min. The washing was held at 100% buffer B for another 5min and finally returned to the initial conditions, then a fresh sample was loaded. The total run times for the analytical and semi-preparative separations of the slow ω-gliadin were 41 and 45min, and for the 'whole' γ-gliadin, 65 and 57min respectively. Peak fractions were pooled separately, dialysed exhaustively against 50mM acetic acid and analysed by Acid-PAGE at pH 3.1, and by SDS-PAGE under reducing

conditions.

COLUMN CARE

In order to ensure optimal performance of all the RP-HPLC columns, sample solutions were clarified by spinning at 13,000rpm for up to 20min and loaded within seconds. The columns were stored overnight in 100% buffer B and over weekends and longer periods of time in 100% buffer C.

SEPARATION OF γ_{III}-GLIADIN AND γ_{V}-GLIADIN BY ION-EXCHANGE FPLC

Fast protein liquid chromatography (FPLC) on the analytical ion-exchanger Mono S HR 5/5, was used in an attempt to further fractionate individual components from the γ_{III}-gliadin and γ_{V}-gliadin fractions. Two buffers were used. Buffer A consisted of 5mM sodium acetate, 4M urea, pH 3.5 with acetic acid and buffer B contained 1M NaCl dissolved in buffer A.

1mg of freeze-dried γ-gliadin fractions from HPLC peaks III and V, were dissolved in 1ml of buffer A by stirring overnight. The pH was adjusted to 3.5 with acetic acid. The column was then equilibrated in 100% buffer A and 200μl aliquot of the sample solution was loaded. The column was washed in 100% buffer A for 5min after the sample was loaded and sample elution was achieved by increasing the concentration of buffer B from 0 to 50% in 10min. The column was then washed by an increase in the concentration of buffer B from 50% to 100% in 5min. Finally, the column was re-equilibrated to the initial conditions prior to the loading of a fresh sample. The flow rate was 1ml min^{-1} and sample elution was monitored by the absorption at 280nm using a detector sensitivity of

0.5AUFS. Peak fractions were analysed by SDS-PAGE under reducing conditions.

ACID-PAGE

Gliadin fractions from various stages of the purification procedure were analysed by electrophoresis at acid pH according to the method of Clements (1987) using 10% (w/v) acrylamide gels containing 0.3% bis-acrylamide in a total volume of 40ml. Each gel also contained 0.4mg ml^{-1} $FeSO_4$ and 1mg ml^{-1} ascorbic acid as catalysts. The pH was adjusted to 3.1 with lactic acid and the solution was precooled at -20°C until ice crystals appeared. A 60μl aliquot of 0.2% (v/v) H_2O_2 was then added to start polymerization and the solution was poured into precooled glass plates separated by 3mm spacers. Polymerisation was completed in 5min.

A 4.5% (w/v) acrylamide stacking gel containing 0.2% bis-acrylamide, 16μg ml^{-1} $FeSO_4$ and 1mg ml^{-1} ascorbic acid in 12.5ml total volume was also prepared. The pH of this solution was adjusted to 3.1 by the addition of a 1.25ml aliquot of 0.1% (w/v) aluminium lactate buffer, pH 3.1 and the solution was precooled as described above. 15μl of 0.2% (v/v) H_2O_2 was then added to start polymerisation and the stack was poured onto the resolving gel.

Samples were prepared by dissolving 1mg protein in 1ml sample buffer containing rosaniline dye in 1% (v/v) glycerol and 70% (v/v) ethanol. 10-20μl aliquots were loaded in each well and electrophoresis was carried out at 40-45mA per gel, with the lower electrode as cathode for 3-3.5hr. The upper electrode buffer comprised aluminium lactate buffer, pH 3.1 with lactic acid, and the lower electrode buffer was a solution of lactic acid, pH 2.6.

Table 2.3
RP-HPLC SAMPLE ELUTION CONDITIONS

SEPARATION PROCEDURE	FRACTION	TIME (min)	% A	% B	FLOW RATE (ml min^{-1})
analytical	ω-gliadin	0	75	25	1.00
		5	75	25	
		21	63	37	
		26	63	37	
		31	0	100	
		36	0	100	
		41	75	25	
semi-preparative	"	0	80	20	5.00
		5	80	20	
		25	65	35	
		30	65	35	
		35	0	100	
		40	0	100	
		45	80	20	
analytical	γ-gliadin	0	70	30	1.00
		5	70	30	
		45	40	60	
		50	40	60	
		55	0	100	
		60	0	100	
		65	70	30	
semi-preparative	"	0	72	28	5.00
		5	72	28	
		37	48	52	
		42	48	52	
		47	0	100	
		52	0	100	
		57	72	28	

Each gel was fixed in 250ml of 12% (w/v) TCA with gentle shaking for 30min, and 5ml of 0.5% (w/v) aqueous Coomassie brilliant blue R250 solution was then added. Protein bands were normally visible in 30-60min and gels were washed in water without the need for destaining.

SDS-PAGE

The gliadin fractions were analysed for homogeneity by SDS-PAGE under reducing conditions using a modification of the method of Laemmli (1970). The separating gel contained 14% (w/v) acrylamide, 0.2% (w/v) bis-acrylamide, 0.1% (w/v) SDS, 0.3M Tris, pH 8.8 with HCl, 4M urea, 0.07% (w/v) ammonium persulphate and 1mM DTT in 39.5ml total volume. 20μl aliquot of TEMED was added to start polymerisation and the solution was poured into glass plates separated by 3mm spacers. Polymerisation was completed in 15-20min.

The stacking gel contained 3.4% (0.5% bis) (w/v) acrylamide, 0.12M Tris, pH 6.8 with HCl, 4M urea, 0.01% (w/v) SDS, 1mM DTT and 0.1% (w/v) APS in 8.1ml total volume. 10μl aliquot of TEMED was added and the stack solution was poured on top of the resolving gel.

Sample solutions contained 1mg protein dissolved in 1ml sample buffer consisting of 0.001% (w/v) bromophenol blue, 2% (w/v) SDS, 0.063M Tris, pH 6.8 with HCl, 1% (v/v) glycerol and 5% (v/v) 2-mercaptoethanol. The sample solutions were boiled for 1-2min and 10-20μl aliquots were loaded in each well.

The electrophoresis buffer, comprising 25mM Tris, 190mM glycine, 0.1% (w/v) SDS, pH 8.8, was poured into the upper and lower electrode chambers. Electrophoresis normally

proceeded for 5hr with the upper electrode as cathode. Each gel was stained overnight in 250ml 0.2% (w/v) Coomassie brilliant blue R250 solution containing 40% (v/v) methanol and 10% (w/v) TCA, followed by destaining in 10% (w/v) TCA for at least 6hr.

RESULTS

TOTAL GLIADIN EXTRACTION AND ION-EXCHANGE CHROMATOGARPHY

The recoveries of fractions at various stages of the purification procedure are shown in Table 2.4. 1300g of milled flour were processed in six batches of 200g and one of 100g to yield approximately 43.2g of total gliadin.

The standard curve used to determine NaCl concentration in the CM52 fractions (Table 2.5) is shown in Figure 2.3. CM52 ion-exchange chromatography using a mixture of gradient and stepwise increases in NaCl concentration, resolved total gliadin into 5 major peaks (Figure 2.4). Acid-PAGE analysis (Figure 2.5 a) suggested that the first peak was composed of a single group of gliadins with mobilities similar to that of the slow moving ω-gliadin band in the total gliadin standard. They were eluted in the initial wash using only starting buffer, indicating that they were the least charged of the gliadin groups recovered. Two other peak fractions (Figure 2.5 a, lanes 2 and 3) whose mobilities did not correspond to any in the total gliadin, were also eluted. In further CM52 separations, fractions with similar mobilities to these were consistently detected by Acid-PAGE. However, attempts to freeze-dry them for further analysis were not successful, possibly due to the fact that they were not present in sufficient amounts. The top of the gels, representing the bottom of the stacking wells, was also intensely stained suggesting

Table 2.4
RECOVERY OF GLIADIN FRACTIONS AT DIFFERENT STAGES OF THE PURIFICATION

STEP	FRACTION	RECOVERY
START	MILLED FLOUR	1300g
70% ETHANOL EXTRACTION	TOTAL GLIADIN	42.3g
CM52 ION-EXCHANGE	SLOW ω-GLIADINS	1.23g
	CRUDE γ-GLIADINS	6.69g
G-100 GEL FILTRATION	'WHOLE' γ-GLIADINS	2.43g
RP-HPLC	γ_{III}-GLIADIN	664mg
	γ_{V}-GLIADIN	218mg

the presence of polymers which did not enter the matrix of the gel because of their molecular sizes.

The fractions from the second CM52 peak were eluted by an increase in NaCl concentration from 0-25mM. In contrast to the fractions from the first peak, these were composed of at least 2 different gliadin types whose mobilities at acid pH corresponded broadly to those of the fast moving ω-gliadin and the slow moving γ-gliadin bands of the total gliadin standard (Figure 2.5 b). The fraction was designated 'crude γ-gliadin' fraction and retained for further analysis.

The Acid-PAGE patterns of the fractions from the third peak are shown in Figure 2.5

Table 2.5
NaCl CONCENTRATIONS OF CM52 FRACTIONS

FRACTION NUMBER	RI (1.34---)	[NaCl] (M)	FRACTION NUMBER	RI (1.34---)	[NaCl] (M)
20	130	0	40	130	0
60	130	0	80	132	0.010
100	137	0.019	120	138	0.023
140	139	0.025	160	139	0.025
180	139	0.025	200	139	0.025
220	139	0.025	240	139	0.025
260	139	0.025	280	140	0.027
300	141	0.029	320	143	0.033
340	144	0.037	360	145	0.039
380	146	0.043	400	147	0.045
420	149	0.052	440	151	0.055
460	155	0.065	480	159	0.073
500	160	0.078	520	163	0.083
540	165	0.091	560	210	0.205
580	251	0.302	600	298	0.425

c. The bands were intensely stained and the resolution was not clear due to the presence of high concentrations of samples. However, they corresponded broadly to γ-gliadin, β-gliadin and traces of ω-gliadin and no further attempts were made to improve the resolution. The elution of these fractions was achieved by holding the NaCl concentration at 25mM.

A stepwise increase in NaCl concentration to 45mM resulted in the elution of fractions whose Acid-PAGE patterns are shown in Figure 2.5 d. These were from the fourth peak of CM52 ion-exchange and comprised mainly a mixed range of fractions including ω-gliadins, γ-gliadins, β-gliadins and α-gliadins. Finally, the Acid-PAGE patterns of the fractions corresponding to the last peak in the CM52 elution profile (Figure 2.5 e), suggested that they were composed predominantly of α-gliadins. They were eluted by increasing NaCl concentration from 65mM to 90mM.

Although the 'slow mobility' ω-gliadin fraction, in contrast to the other recovered fractions was not cross-contaminated by other gliadin types, it was, like the others, not entirely homogeneous. The order of elution of the fractions was related to their mobility at acid pH with the ω-gliadins eluting first and the α-gliadins, eluting last.

GEL FILTRATION

The gel filtration profile of the separation of the crude γ-gliadin fraction is shown in Figure 2.6. The Acid-PAGE patterns of corresponding peak fractions are also shown in Figures 2.7 a and b. The mobilities of fractions 85-138 were similar to that of the fast moving ω-gliadin band present in both the starting material and in the total gliadin standard. A 5ml fraction size was used. Hence, the elution of this fraction occured

fraction occured between 425-690ml. The high optical density readings of fractions 88-92 were not reflected in the intensities of staining of their protein bands. Turbid solutions were collected in these fractions which may have contributed to the high A_{280} readings. Aggregation is the normal cause of turbidity in protein solutions and it is likely that a significant amount may have occurred in these fractions.

The samples eluted between fractions 140-208 corresponded to elution volumes of 700-1040ml and had mobilities similar to that of the slow moving γ-gliadin band in the starting material and total gliadin standard. These fractions appeared to be free of cross-contaminants and were therefore referred to as 'whole' γ-gliadins. Attempts to isolate γ-gliadins present as traces with β-gliadins in the third CM52 peak, led to very low yields. Further isolation of 'whole' γ-gliadin was therefore confined to the 'crude' γ-gliadin fraction. The gel filtration profiles as well as the elution volumes of the ω-gliadin and γ-gliadin fractions were all reproducible in replicate gel filtration separations.

RP HPLC

The analytical and semi-preparative RP-HPLC separation profiles of 'whole' γ-gliadin are shown in Figures 2.8 a and b respectively. The recovery of the RP-HPLC peak fractions is also shown in Table 2.6.

The analytical separation gave 3 peaks with retention times of 12.7, 19.0 and 26.0 minutes. The semi-preparative run, on the other hand resulted in 5 peaks, 3 major and 2 minor. The retention times of the major peaks were 12.8, 19.0 and 26.8 minutes, and were in good agreement with those of the analytical separation. The minor peaks were shoulders on the first and second major peaks and were consistent with smaller shoulders

Figure 2.3
STANDARD CURVE FOR THE DETERMINATION OF NaCl (M) CONCENTRATION IN CM52 FRACTIONS

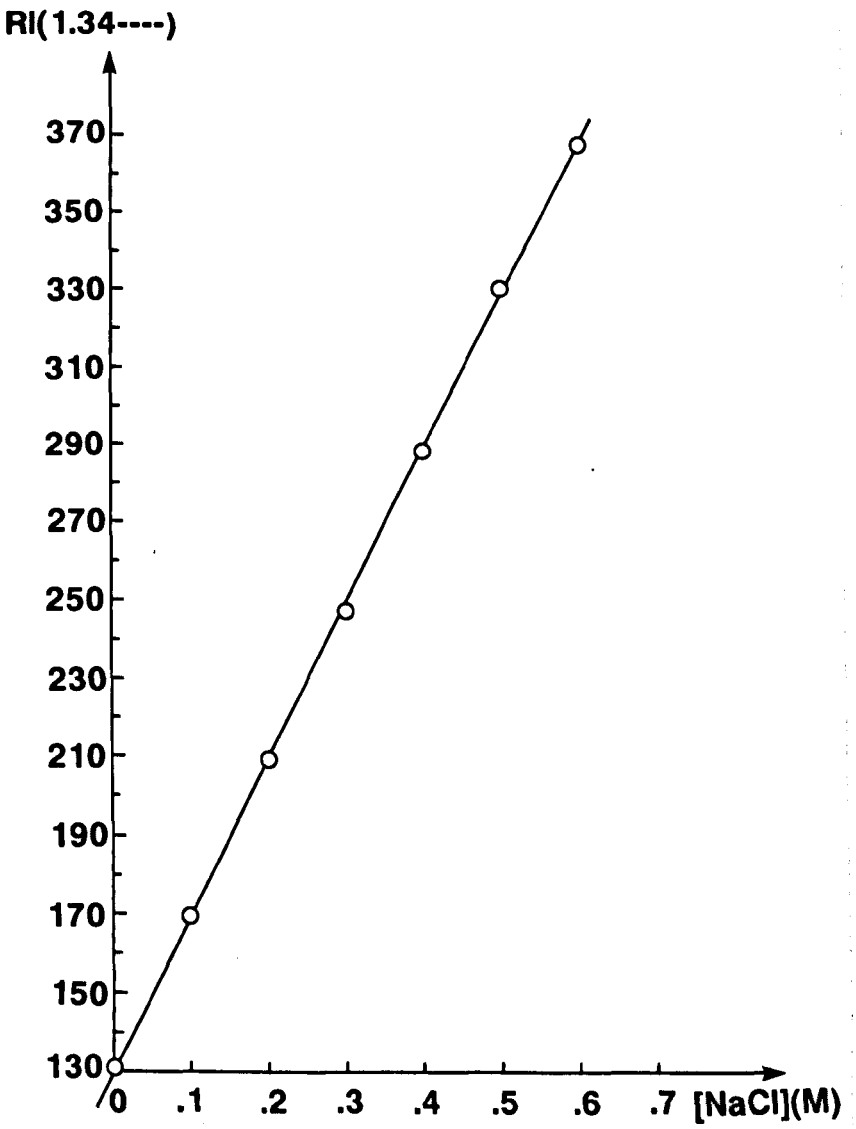

Figure 2.4
FRACTIONATION OF TOTAL GLIADIN BY ION-EXCHANGE CHROMATOGRAPHY ON CM52, 5mM SODIUM ACTETATE BUFFER, 1M DMF, pH 3.5

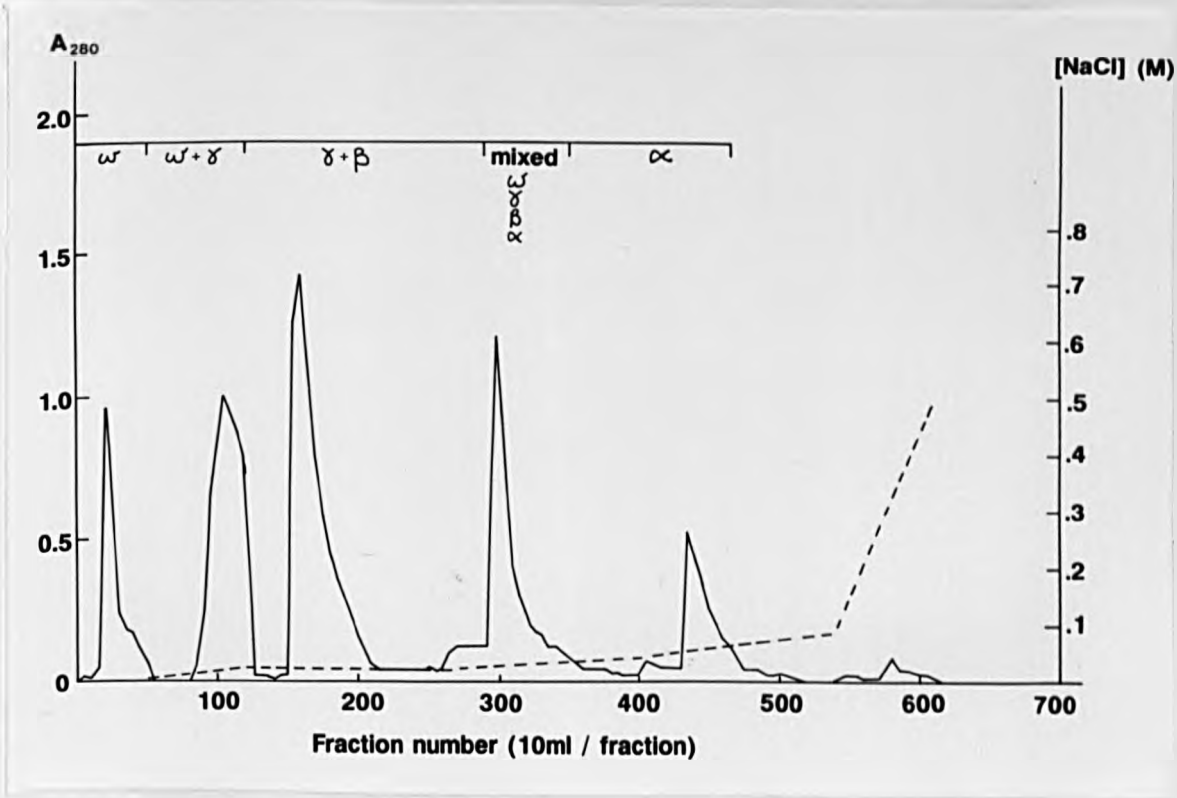

Figures 2.5 a - e
ACID-PAGE PATTERNS OF CM52 PEAK FRACTIONS
a

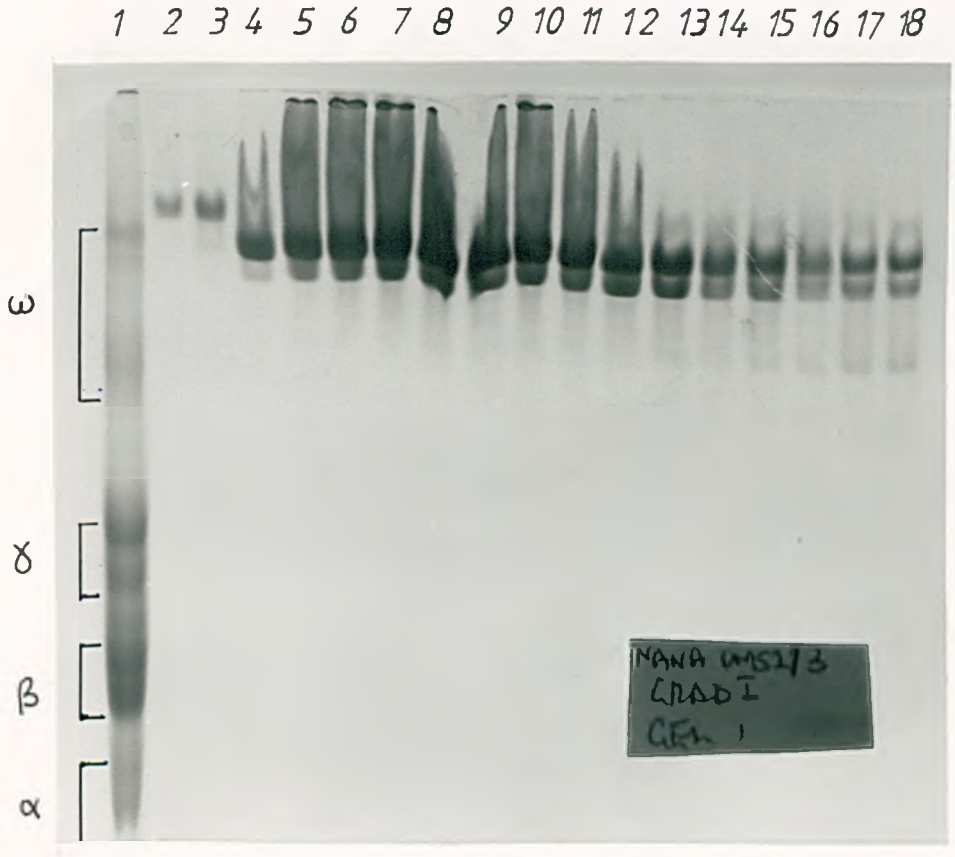

Footnotes for Figure 2.5 a.

Lane	Peak Fraction
1	total gliadin standard
2	12
3	14
4	16
5	18
6	20
7	22
8	24
9	26
10	28
11	30
12	32
13	34
14	36
15	38
16	40
17	42
18	44

b

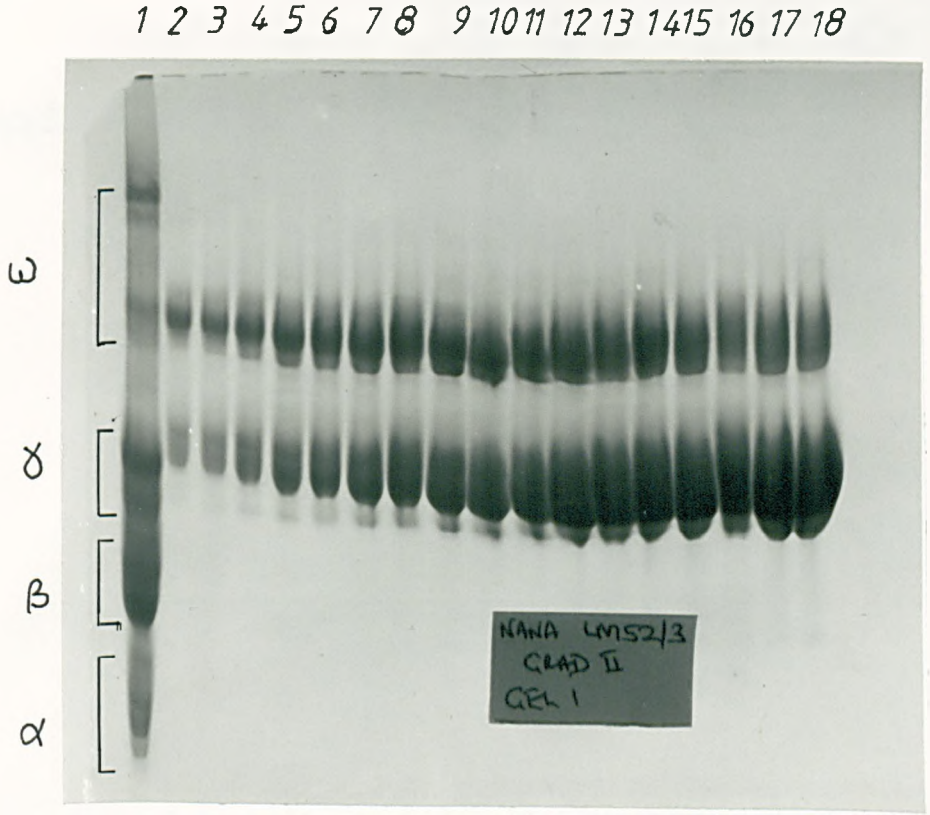
1 2 3 4 5 6 7 8 9 10 11 12 13 14 15 16 17 18
ω
γ
β
α
NANA CMS2/3
GRAD II
GEL 1

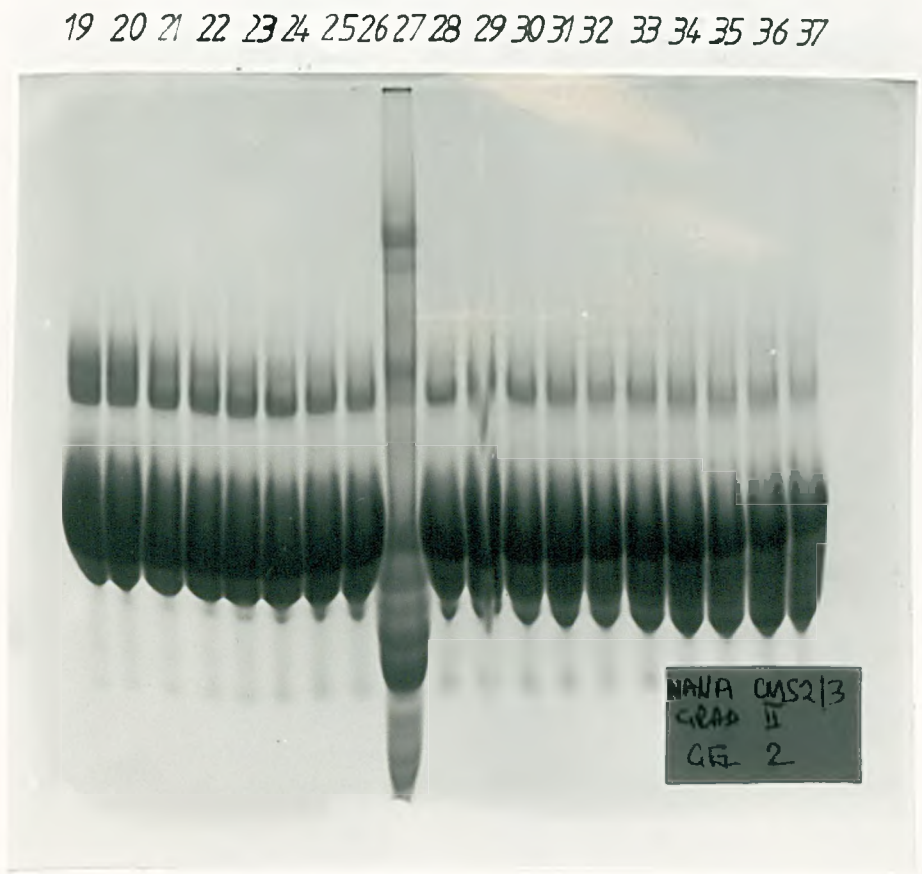
19 20 21 22 23 24 25 26 27 28 29 30 31 32 33 34 35 36 37
NANA CMS2/3
GRAD II
GEL 2

Footnotes for Figure 2.5 b.

Lane	Peak Fraction	Lane	Peak Fraction
1	total gliadin standard	19	116
2	82	20	118
3	84	21	120
4	86	22	122
5	88	23	124
6	90	24	126
7	92	25	128
8	94	26	130
9	96	27	total gliadin standard
10	98	28	156
11	100	29	158
12	102	30	160
13	104	31	162
14	106	32	164
15	108	33	166
16	110	34	168
17	112	35	170
18	114	36	172
		37	174

c

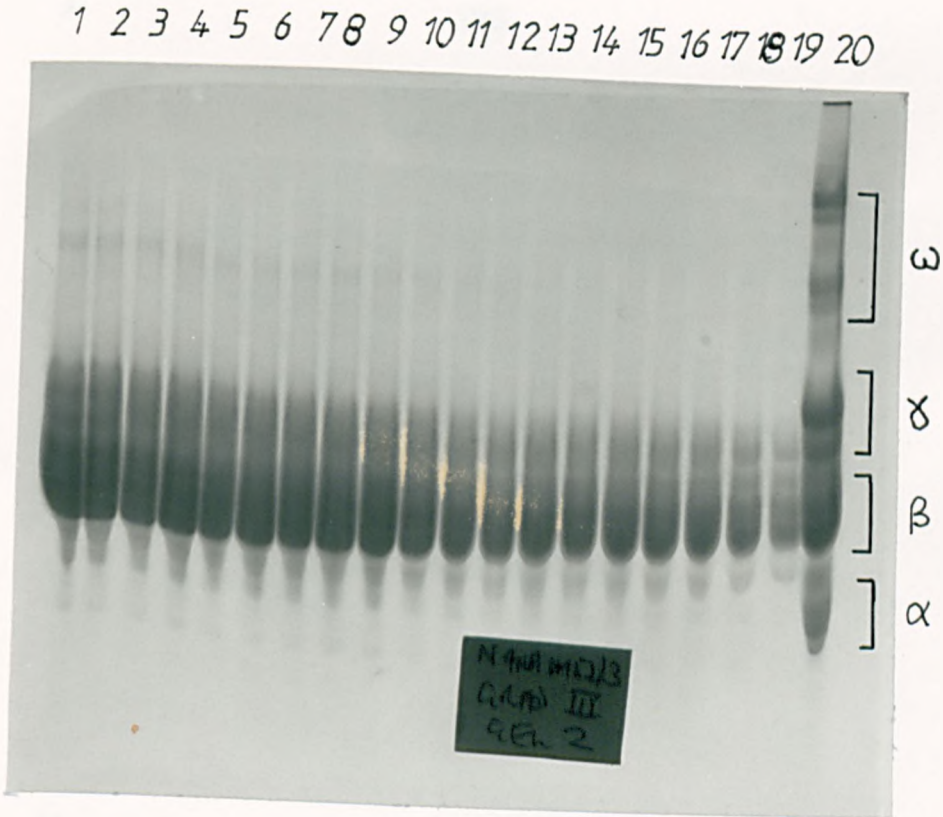

Footnotes for Figure 2.5 c.

Lane	Peak Fraction
1	176
2	178
3	180
4	182
5	184
6	186
7	188
8	190
9	192
10	194
11	196
12	198
13	200
14	202
15	204
16	206
17	208
18	210
19	212
20	total gliadin standard

d

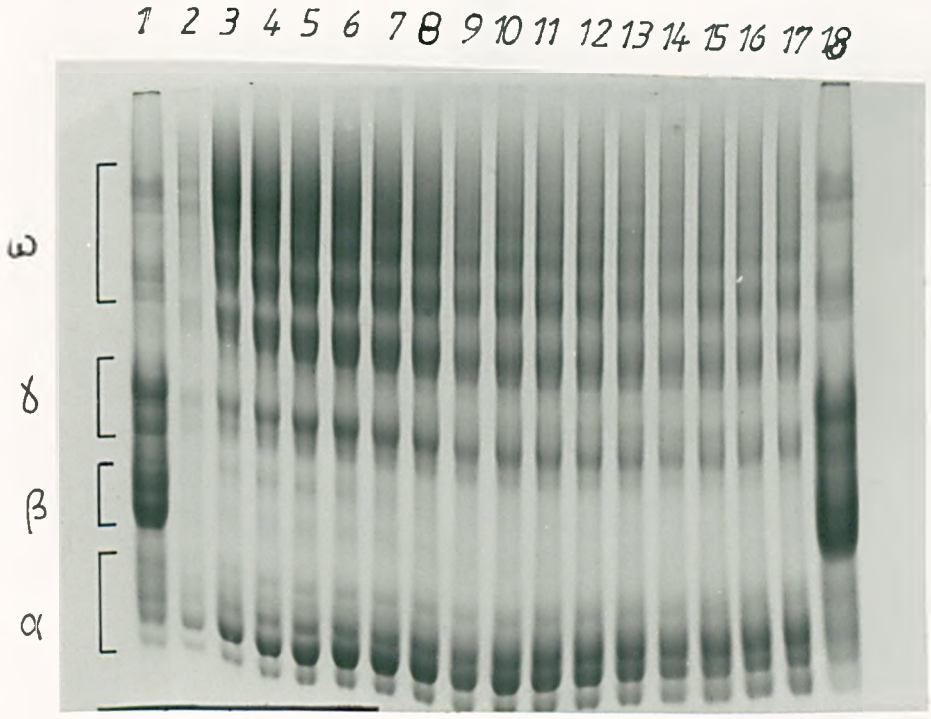

Footnotes for Figure 2.5 d.

Lane	Peak Fraction
1	total gliadin standard
2	290
3	292
4	294
5	296
6	298
7	300
8	302
9	304
10	306
11	308
12	310
13	312
14	314
15	316
16	318
17	320
18	total gliadin standard

e

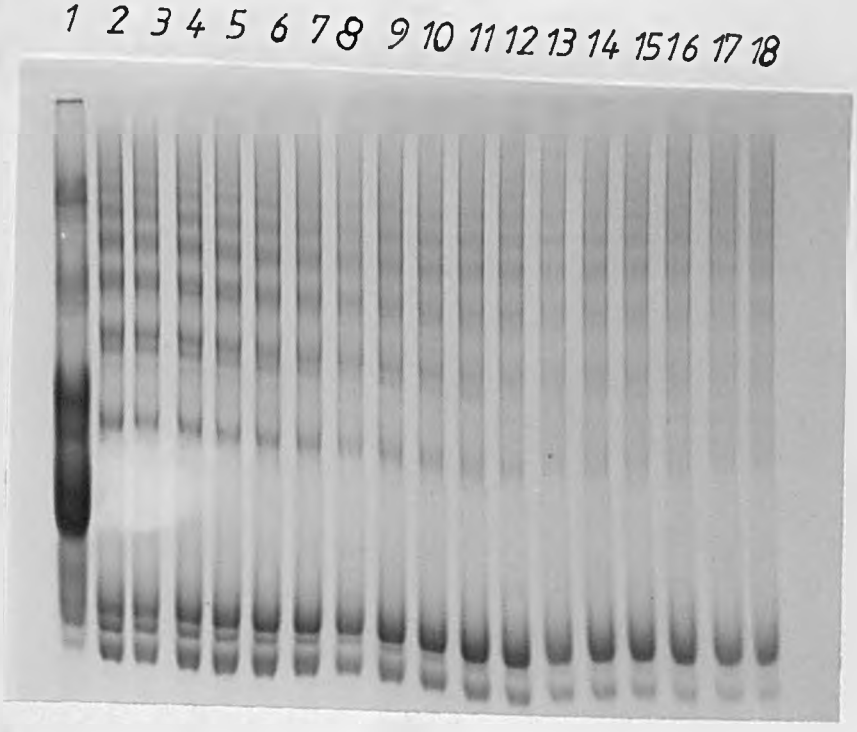

Footnotes for Figure 2.5 e.

Lane	Peak Fraction
1	total gliadin standard
2	430
3	432
4	434
5	436
6	438
7	440
8	442
9	444
10	446
11	448
12	450
13	452
14	454
15	456
16	458
17	460
18	462

Figure 2.6
THE GEL FILTRATION PROFILE OF THE SEPARATION OF 'CRUDE' γ-GLIADIN ON SEPHADEX G-100, 1% (v/v) ACETIC ACID

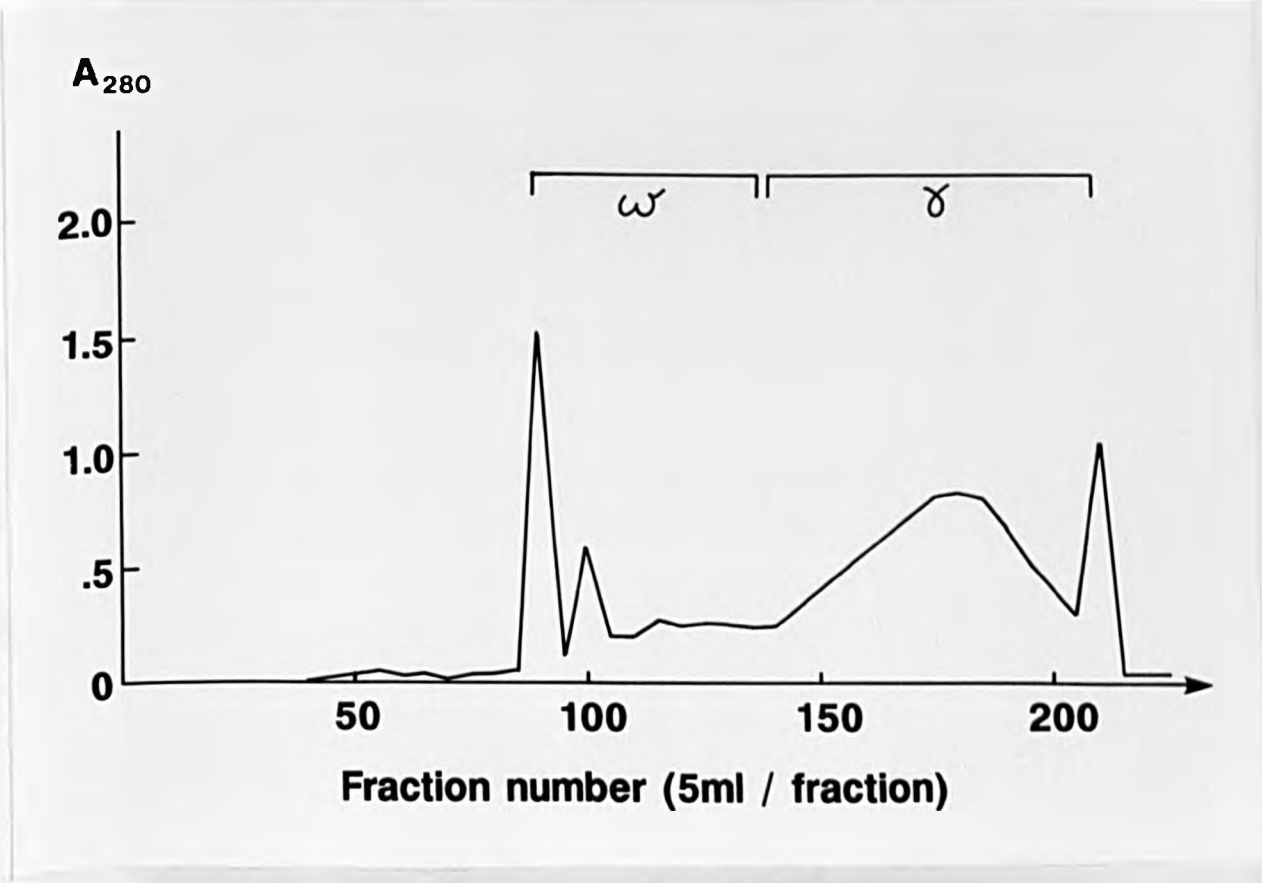

Figures 2.7 a & b
ACID-PAGE PATTERNS OF GEL FILTRATION PEAK FRACTIONS

a

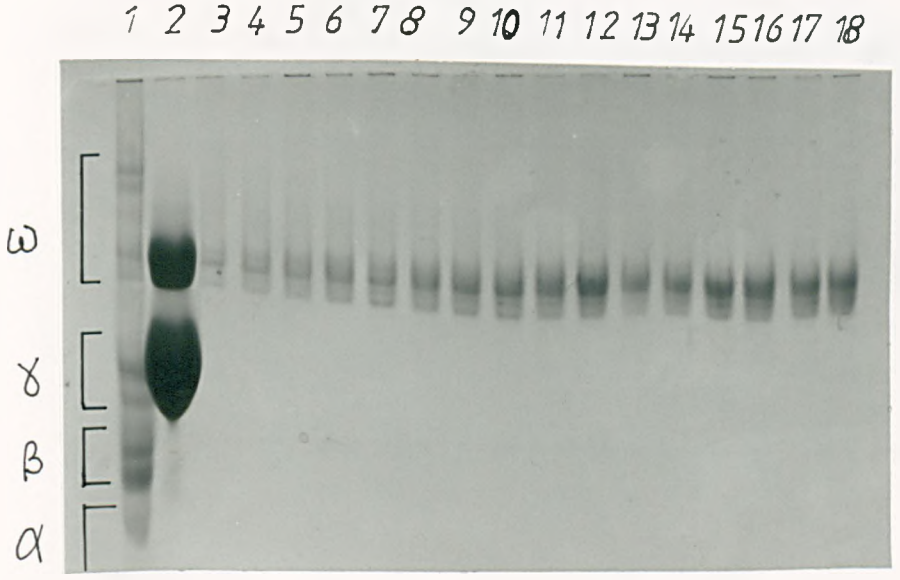

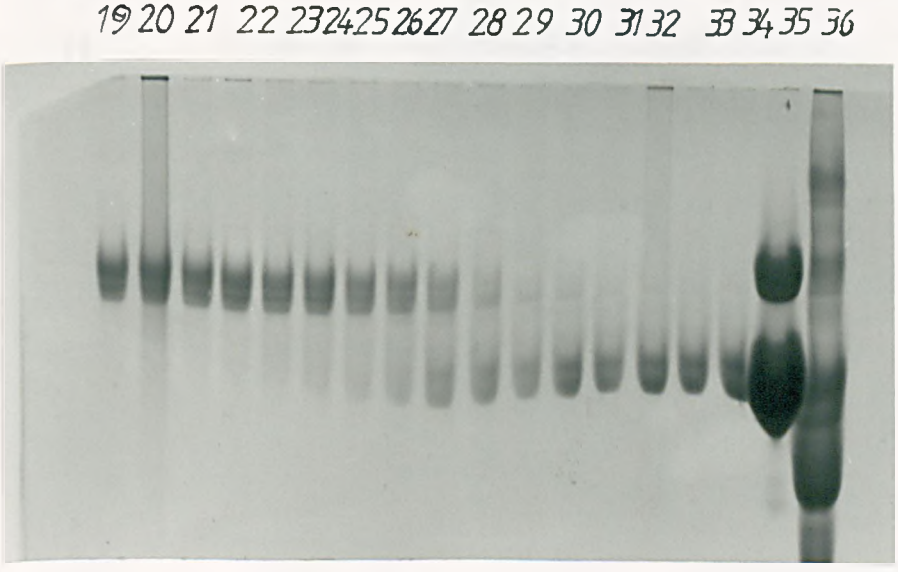

b

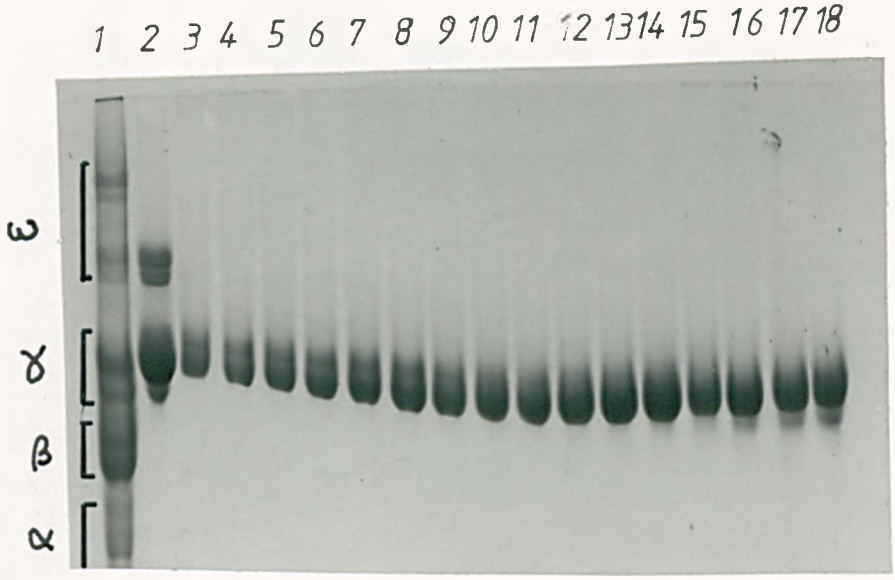
1 2 3 4 5 6 7 8 9 10 11 12 13 14 15 16 17 18
ε
γ
β
α

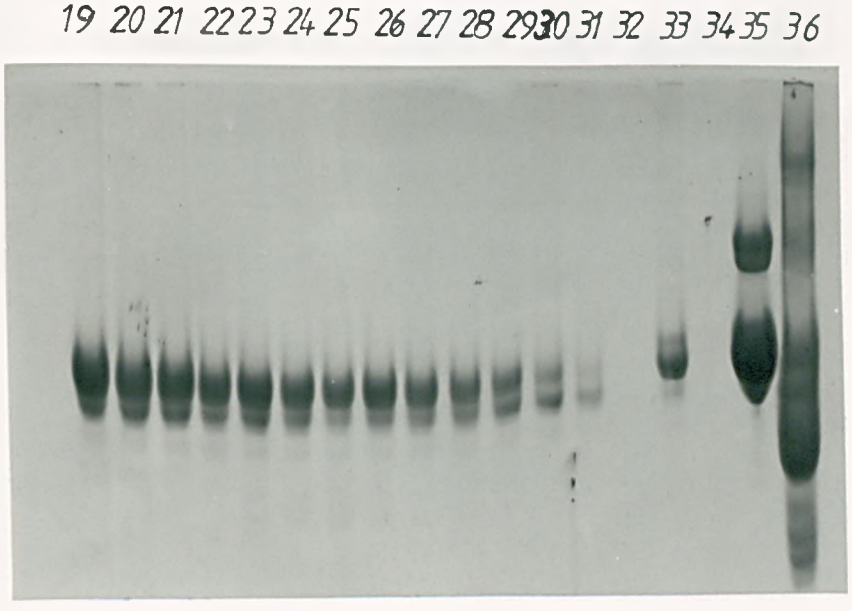
19 20 21 22 23 24 25 26 27 28 29 30 31 32 33 34 35 36

Footnotes for Figure 2.7 b.

Lane	Peak Fraction	Lane	Peak Fraction
1	total gliadin standard	19	185
2	CM52 ω + γ-gliadin*	20	187
3	153	21	189
4	155	22	191
5	157	23	193
6	159	24	195
7	161	25	197
8	163	26	199
9	165	27	201
10	167	28	203
11	169	29	205
12	171	30	207
13	173	31	209
14	175	32	211
15	177	33	213
16	179	34	GF 3(i) γ-gliadin#
17	181	35	CM52 ω + γ-gliadin*
18	183	36	total gliadin standard.

*. as above. #. 'whole' γ-gliadin from previous gel filtration run.

(arrowed) observed in the analytical separation. The peaks of the semi-preparative run were numbered I-V in order of their elution.

SDS-PAGE analysis under reducing conditions (Figures 2.9 a and b), showed that none of the peak fractions was entirely homogeneous. The mobilities of the components of peak II were more similar to that of the ω-gliadin band in the total gliadin standard. Thus, the order of elution was not related to their mobilities at acid pH. Fractions from peaks III and V gave the most reproducible band patterns and contained 2-3 major components compared to at least 4 in the fractions from peaks I and IV. In addition, peaks III and V were recovered in yields of approximately 660mg and 217mg respectively. The two fractions were designated γ_{III}-gliadin and γ_{V}-gliadin respectively

Table 2.6
RECOVERY OF HPLC PEAK FRACTIONS

PEAK FRACTION	RETENTION TIME (min)	RECOVERY (mg)
I	13.0	187.4
II	14.5	50.4
III	20.0	663.9
IV	23.0	65.4
V	26.0	217.7

Figures 2.8 a & b
ANALYTICAL (a) AND SEMI-PREPARATIVE (b) RP-HPLC SEPARATION OF 'WHOLE' γ-GLIADINS

a

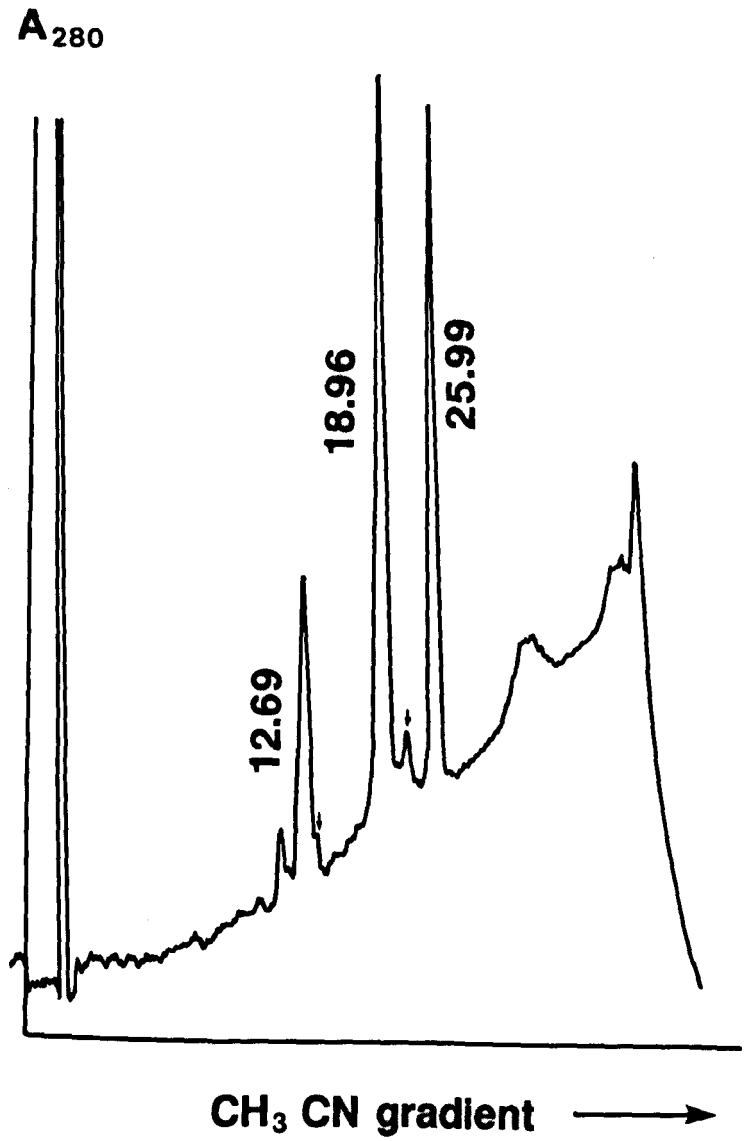

A280
0.00
1.63
2.05
I
12.8
II
14.85
19.03
III
IV
23.81
V
26.82
CH3 CN gradient

Figures 2.9
SDS-PAGE ANALYSIS OF PEAK FRACTIONS FROM THE SEMI-PREPARATIVE RP-HPLC SEPARATION OF 'WHOLE' γ-GLIADIN

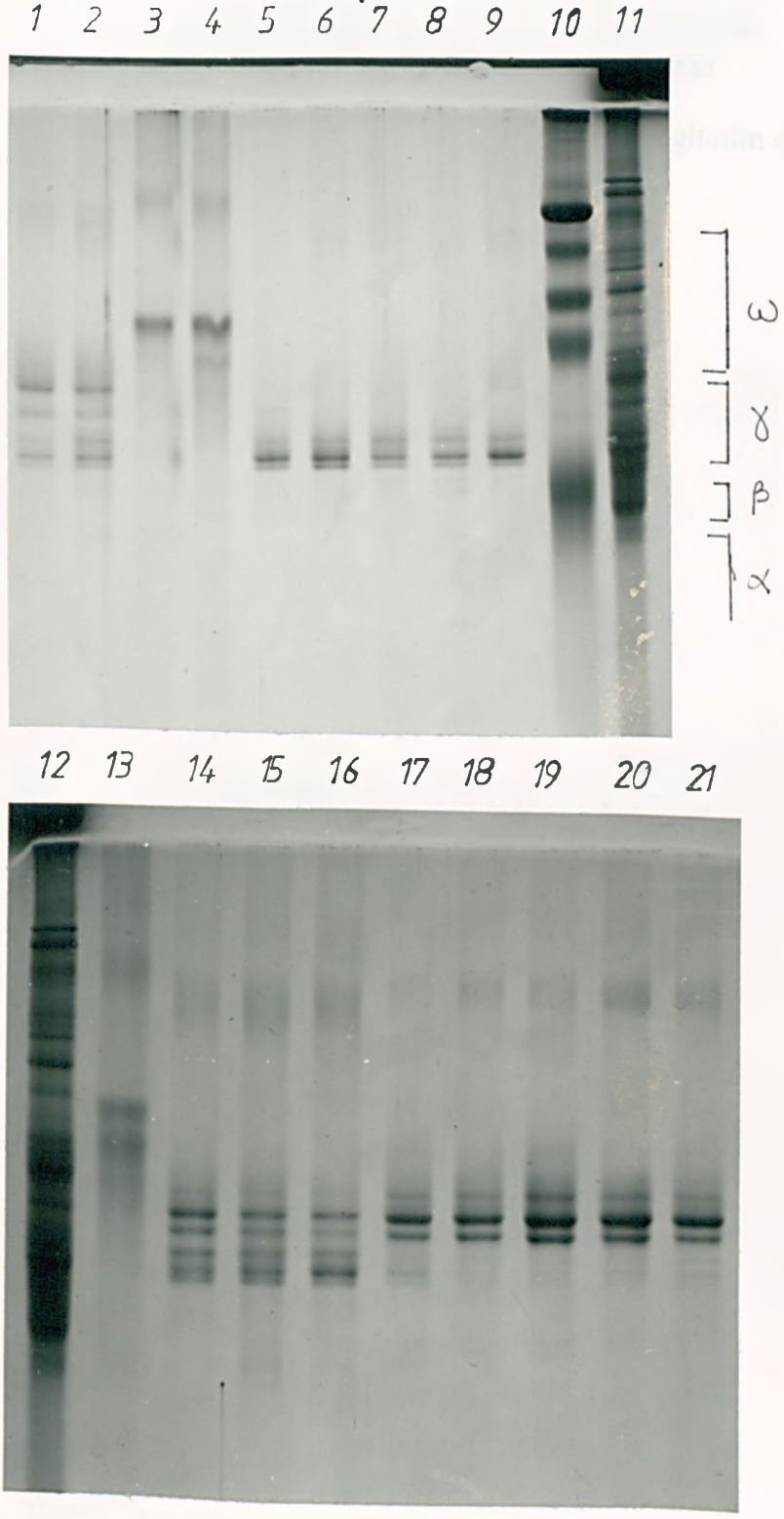

Footnotes for Figure 2.9.

Lane	HPLC Peak Fraction	Lane	HPLC Peak Fraction
1	I	12	total gliadin standard
2	I	13	IV
3	II	14	IV
4	II	15	IV
5	III	16	IV
6	III	17	V
7	III	18	V
8	III	19	V
9	III	20	V
10	standard proteins[1]	21	V
11	total gliadin standard		

1.

α2-Macroglobulin	180K
ß-Galactosidase	116K
Fructose 6-phosphate kinase	84K
Pyruvate kinase	58K
Fumarase	48.5K
Lactic dehydrogenase	36.5K

Figures 2.10 a & b
ANALYTICAL (a) AND SEMI-PREPARATIVE (b) RP-HPLC SEPARATION OF 'SLOW' ω-GLIADINS

a

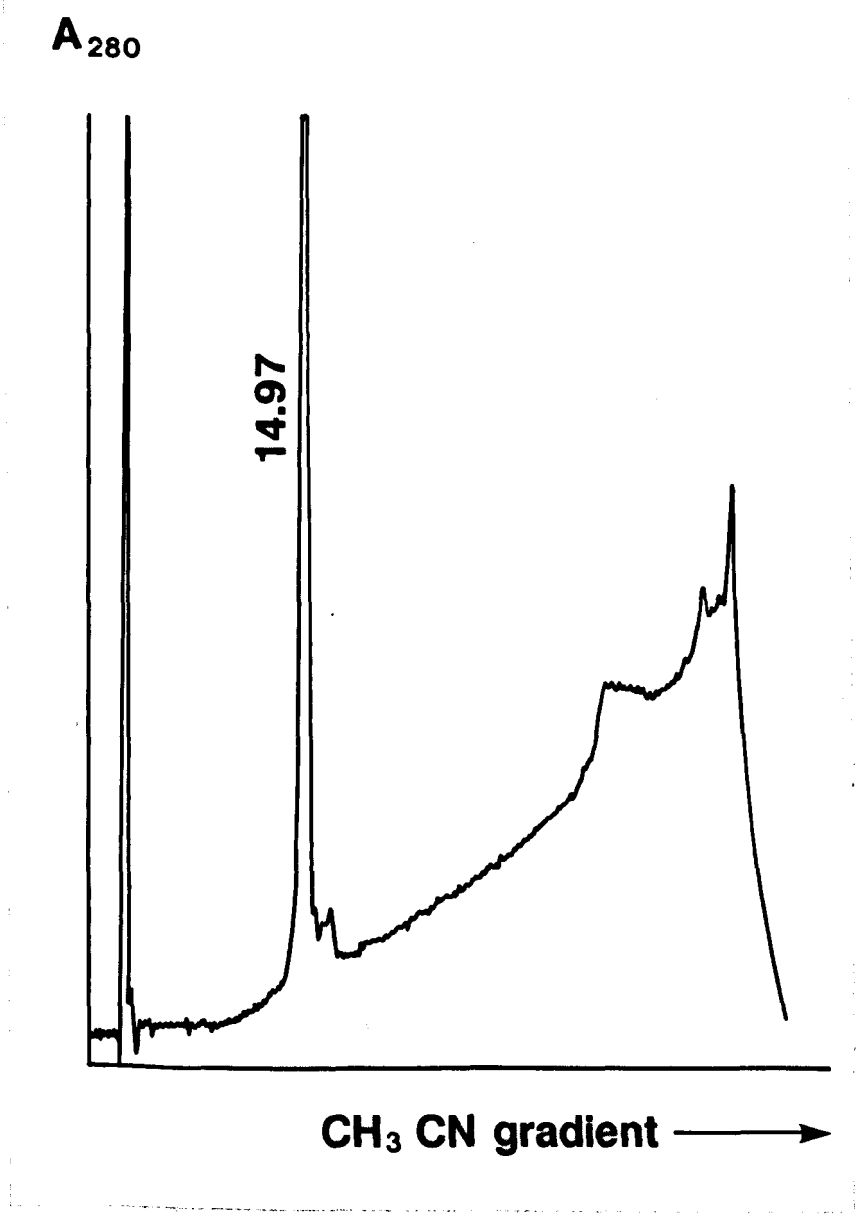

b

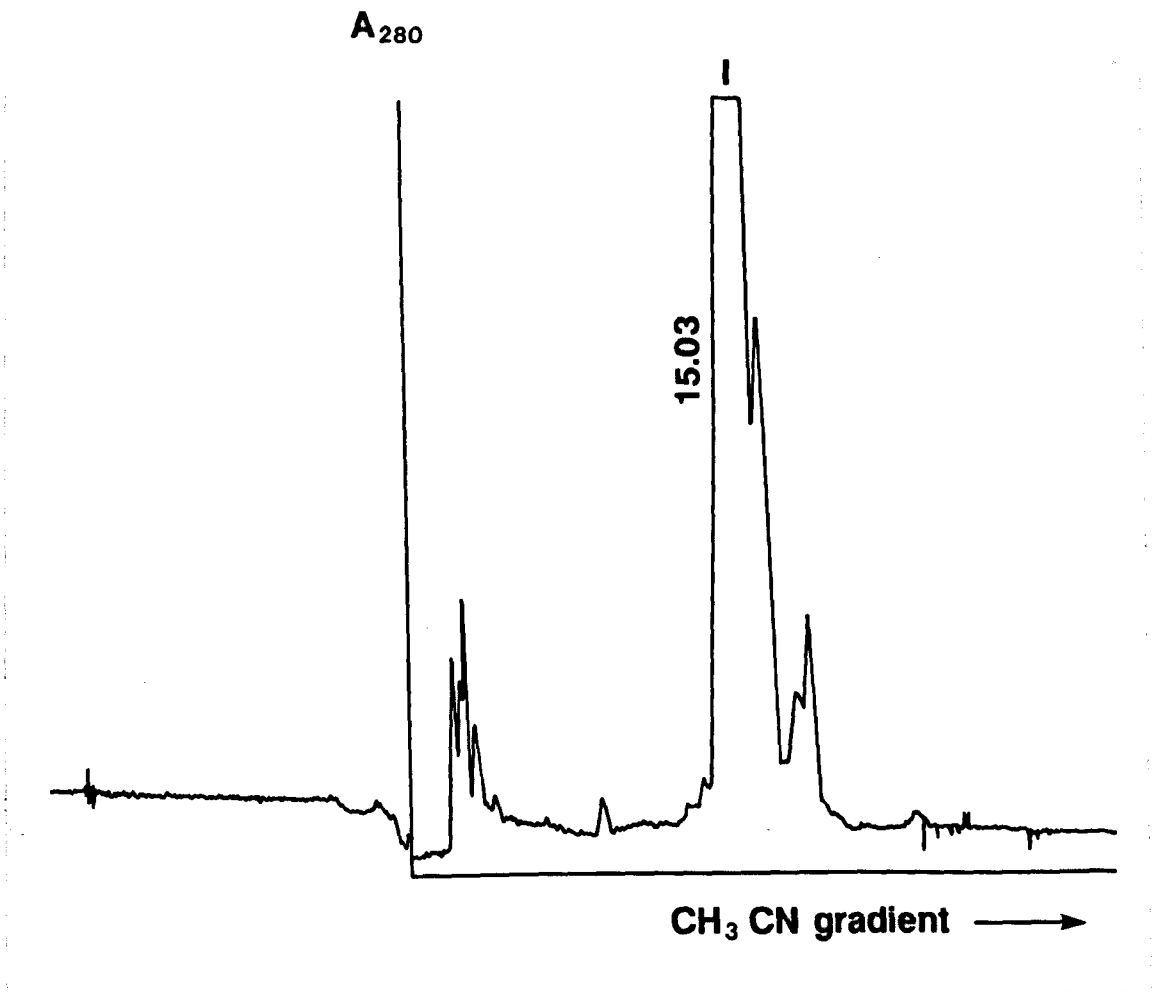

Figure 2.11
SDS-PAGE ANALYSIS OF THE SEMI-PREPARATIVE RP-HPLC SEPARATION OF 'SLOW' γ-GLIADINS

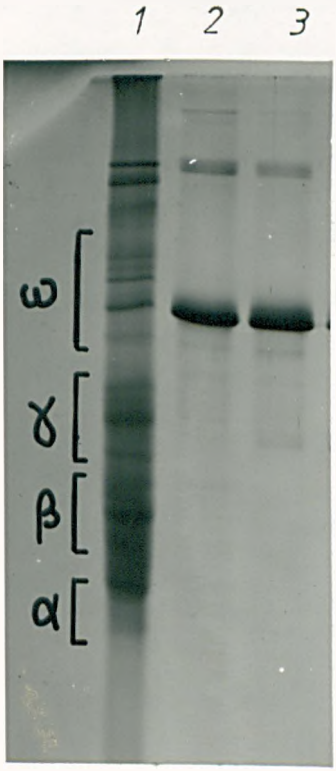

Lane	Fraction
1	total gliadin standard
2	CM52 ω-gliadin
3	RP-HPLC ω-gliadin

and retained for further analysis.

The analytical and semi-preparative RP-HPLC separation profiles of the 'slow' ω-gliadins are shown in Figure 2.10 a and b respectively. A single major peak with a shoulder was obtained in each case. The retention times of the two peaks were in good agreement. The SDS-PAGE patterns of the starting material and the recovered HPLC peak fraction are shown in Figure 2.11. The patterns of the two were similar, each fraction comprising a single component. The presence of a faint contaminating band in each fraction was also observed. Nevertheless, the ω-gliadin fraction was considerably more homogeneous than the corresponding γ-gliadin RP-HPLC fractions. The mobility of the contaminating band was similar to that of a slower moving band in the total gliadin standard suggesting that it was a gliadin of a higher M_r than the ω-gliadins. These patterns suggested that the 'slow' ω-gliadin fraction from CM52 ion exchange was sufficiently homogeneous. It was, therefore, retained for analysis without further RP-HPLC purification.

ANALYTICAL IE-FPLC

Results of the attempted fractionation of the γ_V-gliadin fraction by IE-FPLC are shown in Figure 2.12. Two distinct peaks, numbered 1 and 2, were eluted with NaCl concentrations of 0.12M and 0.26M and retention times of 10.04 and 13.80 minutes respectively. This suggested that the fractions from the two peaks differed significantly from each other in their charge properties. However, SDS-PAGE analysis showed that the band patterns of fractions from the two were similar to each other (Figure 2.13). Thus, despite the separate peaks no significant resolution of the observed bands was achieved. Both the FPLC profile and the SDS-PAGE patterns were reproducible in

several runs and identical patterns were also obtained for the γ_{III}-gliadin fraction. The Acid-PAGE and SDS-PAGE patterns of various fractions at the different stages of the purification are compared in Figure 2.14 a and b respectively.

DISCUSSION

Fractions enriched in 'slow' ω-gliadins were recovered in very high yields, and in a relatively homogeneous state without the need for any further fractionation. Acid-PAGE analysis showed intense staining of bands at the bottom of the stacking wells indicating the presence of soluble glutenins which were extracted along with the gliadins (Figure 2.5a). These were not observed at subsequent fractionation stages and it was assumed that those present were removed at the ion exchange stage. There were other fractions whose mobility did not correspond to any in the total gliadin standard. These could not be recovered possibly because they were present in low amounts, and as a result they were not characterized. However, Charbonnier and Mossé (1980), used gel filtration to remove an albumin fraction from gliadin fractions obtained from ion-exchange on SPS C50. Taking into account the aqueous conditions used in the extraction of the total gliadin, the presence of some albumins can not be totally ruled out. It is likely that their concentrations in total gliadin (in contrast to that in the ion-exchange fractions) may have been too dilute to be detected.

Ion-exchange on CM52 also resulted in the recovery of a γ-gliadin enriched fraction which showed traces of ω-gliadins possessing a faster mobility. The two were successfully separated by gel filtration Sephadex G-100. Some aggregation appeared to have occurred in some of the early fractions of the ω-gliadin component and it is possible that

Figure 2.12
ION-EXCHANGE FPLC SEPARATION OF γ_V-GLIADIN

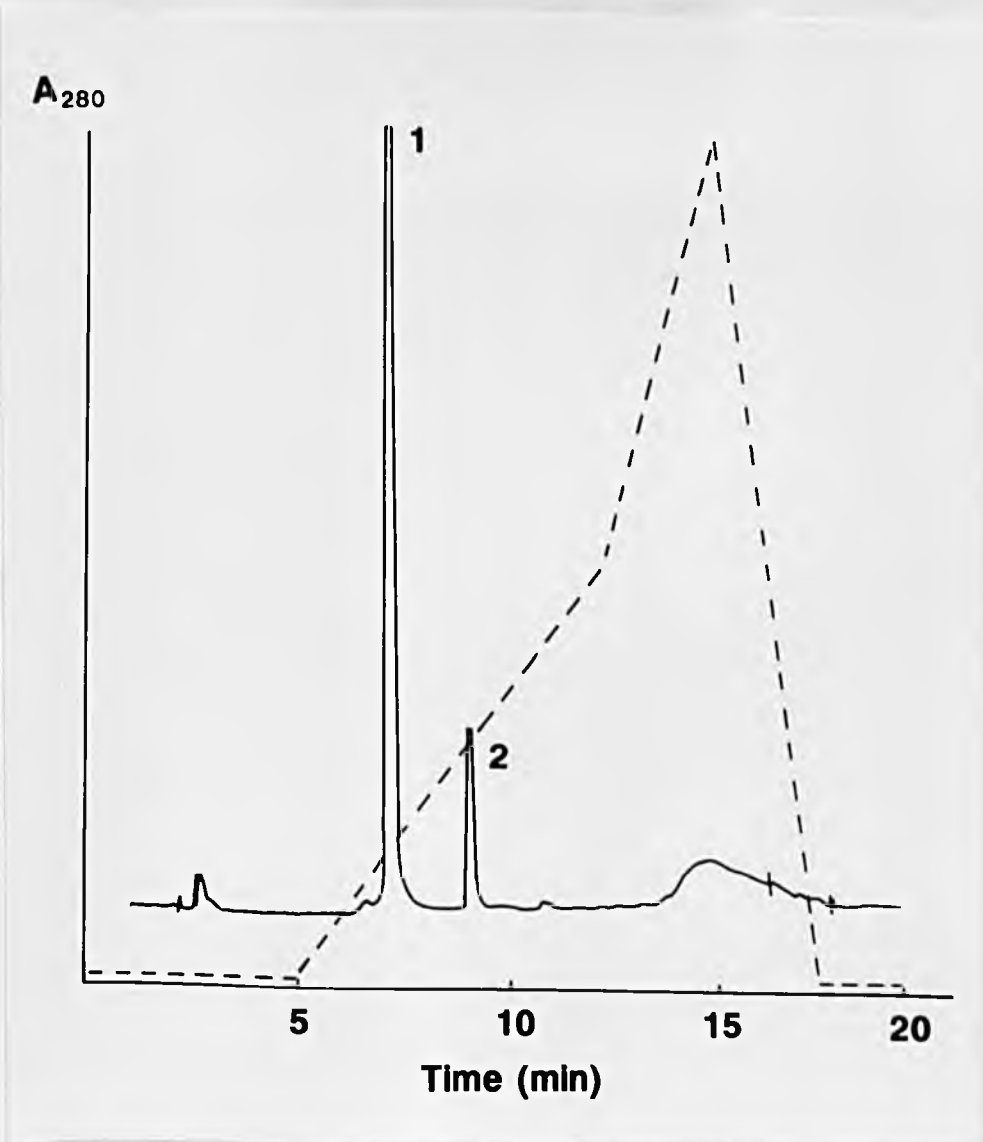

Figure 2.13
SDS-PAGE PATTERNS OF IE-FPLC PEAK FRACTIONS

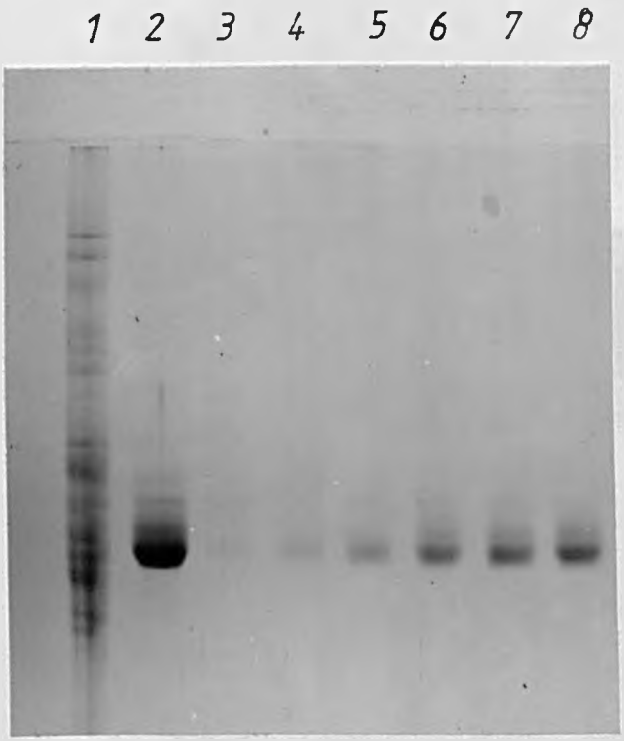

Lane	Fraction
1	total gliadin standard
2	starting material (γ_V-gliadin)
3	peak 2, 5μl
4	peak 2, 20μl
5	peak 2, 40μl
6	peak 1, 5μl
7	peak 1, 5μl
8	peak 1, 5μl

Figure 2.14
PURIFICATION SUMMARY: CORRESPONDING ACID-PAGE (a) AND SDS-PAGE (b) PATTERNS OF FRACTIONS FROM THE DIFFERENT STAGES

a

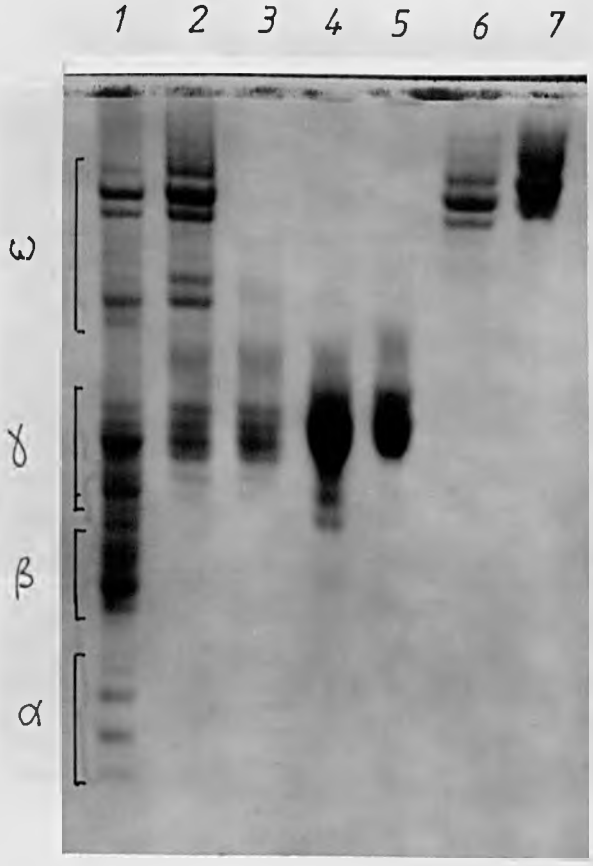

b

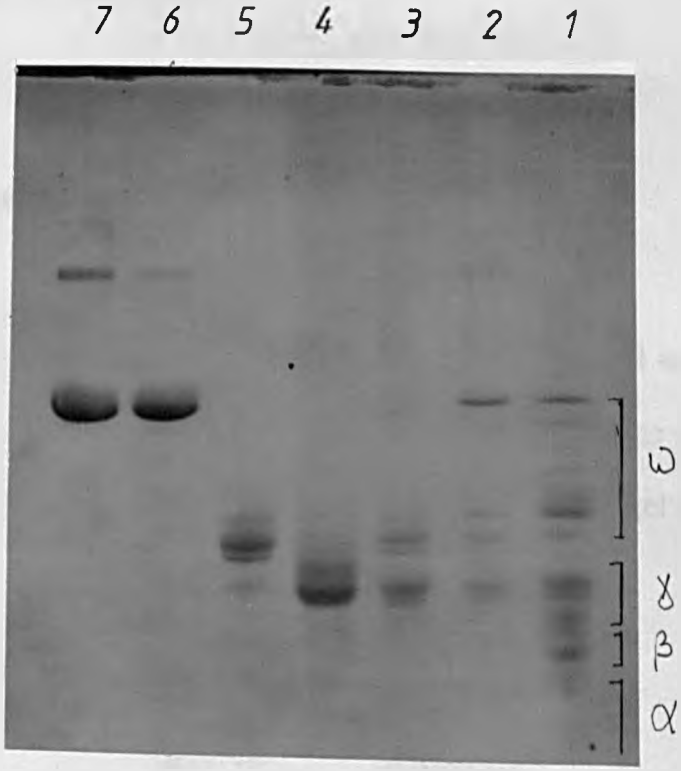

Footnotes for Figures 2.14 a. & b.

Lane	Fraction	Purification Stage
1	total gliadin	70% (v/v) ethanol extraction
2	crude γ-gliadin	CM52 ion-exchange chromatography
3	'whole' γ-gliadin	Sephadex G-100 gel filtration
4	γ_{III}-gliadin	RP-HPLC
5	γ_{V}-gliadin	RP-HPLC
6	'slow' ω-gliadin	RP-HPLC
7	ω-gliadin	RP-HPLC

high concentrations may have caused this. Studies of the aggregable α-gliadin A-gliadin, showed that variation in pH, ionic strength and temperature could induce aggregation (Cole *et al.*, 1983). However, it is unlikely in this case since the gel filtration column was equilibrated in 1% (v/v) acetic acid, in the absence of salt. Hence, variations in the pH and ionic strength would not be expected. In addition, the column was run at room temperature and was shielded from light and sources of heat.

Bietz's (1983; 1986) work on RP-HPLC analysis of cereal storage proteins had led to speculation about the possibility of large scale fractionation of gliadins using this technique. However, at the start of this project, there had been no reported successful use of the procedure to obtain pure gliadin fractions. The doublet of bands observed after SDS-PAGE analysis of the γ_{III}-gliadin and γ_{V}-gliadin fractions could not be resolved any further by RP-HPLC. IE-FPLC of the same fractions produced 2 distinct peaks, a major peak which was eluted with 0.12M NaCl and a minor one which eluted with 0.26M NaCl. Both peak fractions, however, showed SDS-PAGE band patterns closely resembling each other and that of the original material.

Despite the lack of success at further resolution, both the γ_{III}-gliadin and γ_{V}-gliadin fractions showed characteristic electrophoretic mobilities and consistent band patterns, and were relatively pure compared with the γ-gliadin fractions from the other RP-HPLC peaks.

CONCLUSION

Ion-exchange chromatography on cation exchanger CM52 followed by gel filtration on Sephadex G-100 and RP-HPLC using water:acetonitrile mixtures was used to fractionate

total gliadin obtained after ethanol extraction of defatted milled flour. 1.2g of 'slow' ω-gliadins, 660mg of γ_{III}-gliadin and 217mg of γ_{V}-gliadin were prepared in relatively high purity. Their electrophoretic mobilities at acid pH and on SDS-PAGE were consistent with their identification as ω-gliadin and γ-gliadin fractions. SDS-PAGE analysis showed that each of the γ-gliadin fractions contained at least two major bands. In view of several unsuccessful attempts to isolate the components corresponding to these bands, it was decided to characterise the γ_{III}-gliadin and γ_{V}-gliadin fractions as well as the 'slow' ω-gliadins, which were recovered in a relatively more homogeneous form, without further attempts at purification.

CHAPTER 3

CHEMICAL CHARACTERISATION OF THE PURIFIED GLIADIN FRACTIONS

INTRODUCTION

Protein characterization employs conventional techniques to derive the physical, chemical and biological properties of proteins. It provides a means of assigning an identity to a purified protein and also allows it to be compared to other proteins. In the process, comparison of amino acid sequences for instance, may suggest similarities in functionality or reveal a common ancestry between different proteins.

For cereal storage proteins characterisation may involve the determination of molecular weights and chemical content, notably amino acid composition and sequence, all factors which influence their classification. In this chapter, estimations of the molecular weights (M_rs) and the results of automated amino acid analyses and N-terminal amino acid sequencing of the purified gliadin fractions are presented and discussed.

MOLECULAR WEIGHTS OF GLIADINS

M_rs of cereal storage proteins have been determined by SDS-PAGE, gel filtration chromatography or ultracentrifugation. The M_rs of the S-rich gliadins have been reported as 32-44K by SDS-PAGE and as 30-37K by ultracentrifugation (Miflin *et al.*, 1983). Higher M_rs by SDS-PAGE than those above have also been reported for γ_{44}-gliadin and γ_{46}-gliadin (Popineau and Pineau, 1988). In both instances, it was suggested that the presence of longer repetitive domains resulted in extended structures and higher

hydrodynamic volumes which in turn, accounted for the unexpected high M_rs. The M_rs of the S-poor gliadins are 44-74K by SDS-PAGE with most above 50K (Kasarda *et al.*, 1983) and 27-79K by ultracentrifugation (Miflin *et al.*, 1983). M_rs by gel filtration of the gliadins, especially the S-poor, are less widely reported. Hamauzu and Yonezawa (1978) reported M_rs by gel filtration for gliadins they designated gliadin III and gliadin IV which corresponded to α+ß-gliadins and α-gliadins as 37K and 33K respectively. More recently, Popineau and Pineau (1985 b) reported M_rs for γ_{44}-gliadin, γ_{46}-gliadin and γ_{50+51}-gliadin as 35K, 31K and 29.5K respectively.

ESTIMATION OF MOLECULAR WEIGHTS OF GLIADIN FRACTIONS BY SDS-PAGE

Some anionic and cationic detergents whose hydrocarbon chains contain in excess of 10 carbon atoms bind to most globular proteins. Such detergents disrupt the compact conformations of these proteins and denature them. Among this group of detergents, the action of sodium dodecyl (lauryl) sulphate, SDS, is well characterized (Nielsen and Reynolds, 1978). In a fully denatured protein, SDS binds in an approximate ratio of 1.4g per gram of protein. This confers a uniformity of charge on all the polypeptides bound in such a way that although migration in an electric field is driven by charge, observed differences in mobility between different polypeptides are effectively due to their molecular sizes. The relative mobility of a given protein in the gel is defined by its R_f value which is the ratio of the distance moved by the protein to the distance moved by a marker dye. Using standard proteins of known molecular weights, a given gel system is calibrated by measuring the relative mobilities of the standard proteins. From

a semi-logarithmic plot of molecular weight versus R_f, the M_r of an unknown protein is then obtained using its experimentally determined R_f value. However, in order to obtain accurate results certain criteria have to be met (Neilsen and Reynolds, 1978).

1) All polypeptides including standards and unknowns must bind an equal amount of SDS on a per gram basis.

2) All polypeptides must have the same conformation when complexed with SDS.

3) The intrinsic net charge of the polypeptide must have a negligible effect on the net charge of the polypeptide-SDS complex.

4) All polypeptides must be run in the same gel system to ensure that they are all subjected to the same electric field strength, gel pore size and medium viscosity.

Estimates of M_rs of prolamins by SDS-PAGE using different gel systems (Bunce *et al.*, 1985) are shown in Table 3.1. In general, inconsistencies are encountered when SDS-PAGE is used to estimate M_rs of prolamins. According to Bunce *et al* (1985), these may follow three main patterns as described below.

1) over-estimation of M_rs compared with those determined by physical methods or deduced from protein sequences

2) increases in M_r values when urea is included in the gel system

3) differences in M_r values determined in the absence of urea by different gel systems.

The authors (Bunce *et al.*, 1985) attributed the source of the over-estimation to the conformational structure of the proline-rich regions of prolamins. Thus, in the S-poor prolamins where the proline-rich region is more extended compared to the S-rich prolamins (Figure 3.2 a and b), the observed inconsistencies are correspondingly more pronounced.

Table 3.1
ESTIMATES OF M_rS OF GLIADINS BY SDS-PAGE IN DIFFERENT GEL SYSTEMS

Gliadin fraction	M_r by (gel system) Tris/borate	Modified Laemmli	Modified Laemmli+urea
S-poor			
ω-gliadin-1	59.4(0.20)	61.5(1.23)	82.6(0.88)
ω-gliadin-2	50.8(0.20)	50.3(0.83)	68.6(0.45)
S-rich			
gliadin-1	45.0(0.07)	44.0(0.48)	50.9(0.34)
gliadin-2	36.4(0.32)	35.4(0.70)	36.9(0.25)

standard errors of the means are in parentheses

SDS-PAGE estimation of the M_rs of proteins still provides an inexpensive, rapid and simple means of characterizing protein sizes. In view of the inconsistencies associated with the prolamins, however, it is necessary to complement its use by other methods of M_r estimation such as those based on chromatography and physical techniques. In addition, for those prolamins with known complete DNA-derived sequences, M_rs can be calculated from the primary sequence.

ESTIMATION OF MOLECULAR WEIGHTS BY GEL FILTRATION CHROMATOGRAPHY

Gel filtration chromatography is also used extensively to estimate M_rs of proteins. It has several advantages over electrophoretic methods especially in its applicability to both native and denatured proteins. As in SDS-PAGE, the gel filtration column is calibrated

with standard proteins for M_r estimation. A calibrated gel filtration column on the other hand, allows the separation of protein molecules in addition to its use for M_r determinations. Calibration of the column is simply achieved. The total volume, V_t is determined directly from the volume of water required to fill it completely or by calculation from its geometric dimensions. The void volume, V_o is determined by measuring the elution volume of a high molecular weight compound such as Dextran 2000 which is distributed only in the mobile phase and is totally excluded from the internal volume of the stationary gel phase. By measuring the elution volume (V_e) of various molecular weight standards, K_{av} values are calculated for each standard protein according to the equation below.

$$K_{av} = \frac{V_e - V_o}{V_t - V_o} \qquad (1)$$

From a semi-logarithmic plot of M_r versus K_{av}, the M_r of an unknown protein can be obtained once a K_{av} value has been calculated from its experimentally determined V_e. K_{av} is a separation parameter related to the partition of solute species between the stationary gel and mobile liquid phases of the column. The normal precautions required for optimal performance of a gel filtration separation system also apply to the accurate and efficient determination of M_rs by the same system.

THE AMINO ACID CONTENTS OF PROTEINS

The amino acid composition of a protein is the relative proportions of the different amino acids present in it. The amino acid sequence on the other hand, is the basic level

of structural organisation of the protein. It identifies a protein, distinguishing it from all others including those which may have similar amino acid compositions. The primary sequence defines chemical and biological properties as well as higher levels of structural organisation. As a protein can have only one N-terminus, N-terminal sequence analyses in most cases provide a means of establishing the homogeneity of a purified protein. Polypeptide chains can be hydrolyzed completely by boiling with excess 6M HCl or 6M NaOH, at 100-120°C, in a sealed evacuated tube for a period of 10-24hr. Under these conditions, peptide bonds are readily hydrolyzed to give protein hydrolyzates and free amino acids. Acid hydrolysis of proteins destroys tryptophan and causes loss of serine and threonine. In addition, asparagine and glutamine residues undergo complete acid hydrolysis to give free aspartic acid and glutamic acid residues. Alkaline hydrolysis is generally used for the sole determination of tryptophan. The protein hydrolyzates are then separated in an automated amino acid analyzer by ion-exchange chromatography. Amino acids in the hydrolyzates are identified by comparing their elution profiles with those of a standard amino acid mixture run on the same column.

The most widely used procedure for determining the amino acid sequence of proteins is the Edman degradation process (Figure 3.1). This has the attractive feature of removing one residue at a time from the amino terminus of the polypeptide chain. In the process, the α-NH_2 group of the terminal residue reacts quantitatively with phenylisothiocyanate (PITC) in alkaline medium to give the phenylthiocarbamyl or PTC-derivative of the polypeptide. The presence of the PTC group on the terminal residue destabilizes the first peptide bond making it more susceptible to hydrolysis under conditions where the other peptide bonds remain intact. Subsequent treatment with

strong anhydrous acid such as trifluoroacetic acid (TFA) leads to the liberation of the thiazolinine-derivative of the terminal residue which rearranges under aqueous conditions to the phenylthiohydantoin or PTH-derivative. The polypeptide chain is regenerated but one residue shorter and ready for a repeat cycle of the same procedure. In this way, residues are sequentially released from the N-terminus of the polypeptide chain. The released residues are analysed as their PTH-derivatives at each cycle by RP-HPLC. Modern methods of sequencing are largely automated and this has led to a rapid means of analyzing amino acid residues in a number of proteins. Like many automated repetitive processes however, limitations in automated sequencing tend to be cumulative. Background material can therefore build up leading to an inability to detect residues generated during the cycle being processed.

The cause of low yield per cycle encountered in automated sequencing of proteins may be due to a number of reasons as described below.

1) The inability of the PTC-peptide to undergo cyclization and cleavage as a result of conversion of PTC derivatives to isocyanate derivatives.

2) Loss of PTC derivatives from the reaction chamber due to complete solubilization of the derivative.

In order to limit these, modern protein sequencers incorporate steps which alkylate isocyanate derivatives and preclude them from subsequent cycles while PTC-peptides are attached to solid supports to prevent loss through solubilization. Because of the sensitivity and precision of modern automated amino acid analyzers and sequencers, nanomolar concentrations of samples can still give accurate amino acid compositions and sequences respectively.

Figure 3.1
THE ESSENTIAL STEPS OF THE EDMAN DEGRADATION PROCESS

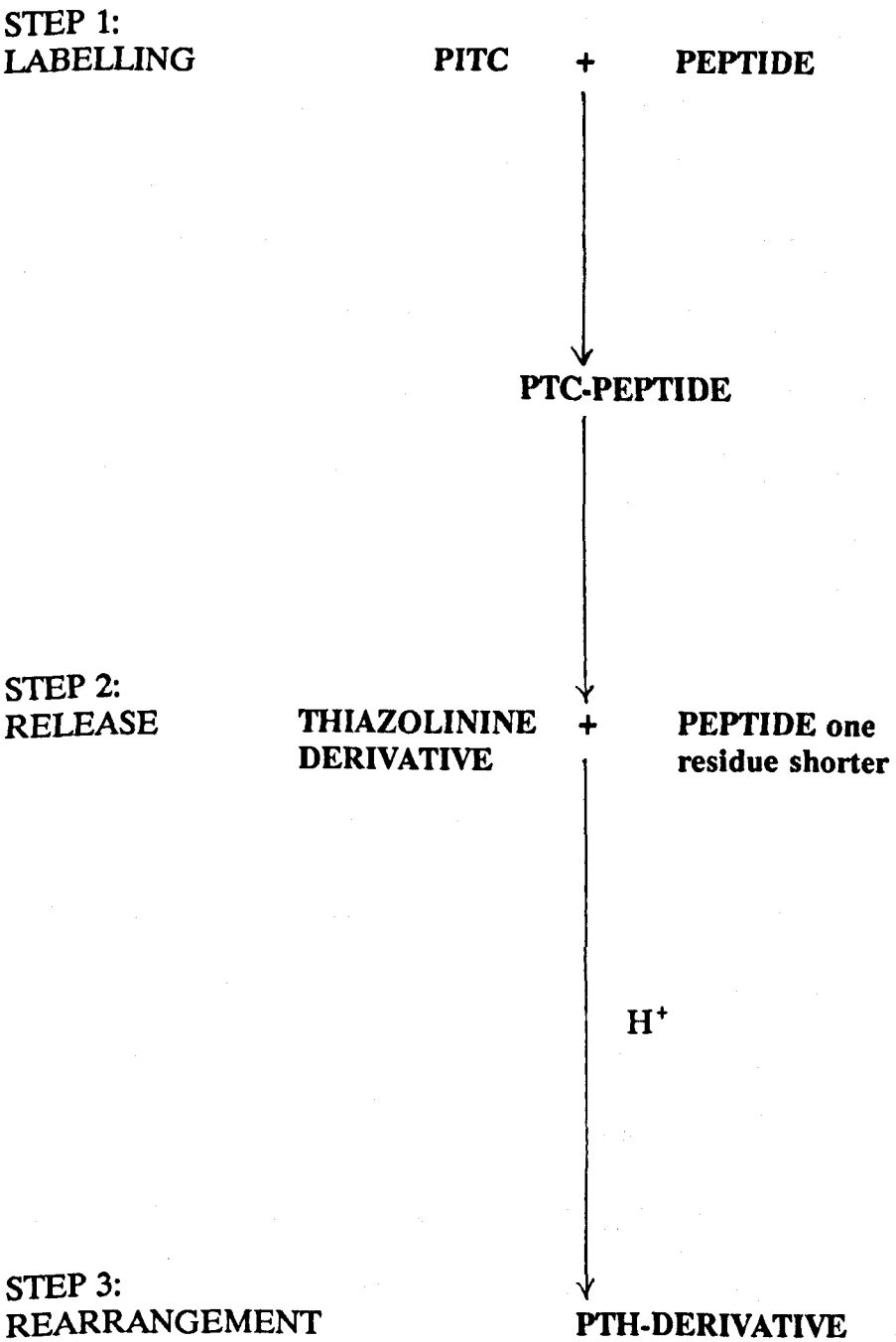

AMINO ACID COMPOSITIONS OF GLIADINS

Although gliadins are characterised by high contents of proline and glutamine, the major groups differ from each other in their contents of specific residues. Table 3.2 shows the amino acid compositions of total gliadin and those of the ω-, γ-, β- and α-gliadins. The S-rich or the α-, β- and γ-gliadins on the whole, have compositions which are similar to each other as well as to that of the total gliadin. These include 37-40 mol % glutamine/glutamic acid, 14-18 mol % proline, 2 mol % cysteine, 1 mol % methionine and 3-6 mol % phenylalanine. The composition of the ω-gliadin fraction on the other hand has none of the sulphur-containing residues. Instead, it is characterized by higher contents of glutamine/glutamic acid (40-50 mol %), proline (20-30 mol %) and phenylalanine (8-9 mol %). Together, these three residues make up nearly 80% of the total.

AMINO ACID SEQUENCES OF GLIADINS

The primary sequences of gliadins, in common with other prolamin groups, comprise at least 2 distinct regions. One region is rich in proline, contains repeated blocks of amino acid residues and corresponds broadly to the N-terminal region. The other region is non-repetitive and corresponds to the C-terminal region. In the S-rich α-type and γ-type gliadins, the non-repetitive sequences contain all the cysteine residues (Figure 3.2 a). The repetitive sequences in the α-type and γ-type gliadins are preceded by short unique N-terminal sequences comprising 5 and 12 residues respectively. Among the S-poor prolamins, the C1 hordein fraction of barley has been studied in detail as a representative model. Significant structural homology and similarities in amino acid

composition exist between it and the other S-poor prolamins, such as ω-gliadins from wheat and ω-secalins from rye. In C hordein, the region of repeated blocks of amino acids constitute the bulk of the primary sequence (Figure 3.2 b). This is flanked by a 12 residue N-terminus and a 6 residue C-terminus. The repetitive region in general, may vary within different fractions as a result of additions and deletions of blocks of amino acids. This in turn, affects the amino acid compositions and M_rs of these fractions. For instance, the ω-gliadins encoded by the B genome are known to have higher M_rs than those encoded by the A and D genomes of bread wheat (Shewry *et al.*, 1987).

Various types of N-terminal sequences have been reported for different gliadin fractions (Bietz *et al.*, 1977; Autran *et al.*, 1979; Kasarda *et al.*, 1983). A comparison of N-terminal amino acid sequences of various S-poor and S-rich prolamin fractions is shown in Figure 3.3. Each type is designated by the single letter symbols for the first three amino acid residues of their sequences. On this basis, the α-type N-terminal sequences correspond to the VRV-type (#18, Figure 3.3) and the two variants representative of the γ-type sequences are the NIQ-type (#19, Figure 3.3) and the NMQ-type (#20, Figure 3.3) (Kasarda *et al.*, 1983). The ω-type sequences reported to date fall into three broad types. The KEL-type (#12-15, Figure 3.3) is associated with the slowest-moving gliadin component on Acid-PAGE. The SRL-type (#16, Figure 3.3) on the other hand, is associated with the fast-moving ω-gliadin bands on Acid-PAGE which contain relatively high proportions of basic residues (lysine, histidine, arginine) and bind dye molecules resulting in more intensely stained bands (Kasarda *et al.*, 1983). The third ω-gliadin type sequence comprises three variants designated RQL- (#1-4, Figure 3.3), ARQ- (#5 and #8-9, Figure 3.3) and ARE- (#10-11, Figure 3.3). The regions of homology in sequences

Figure 3.2
STRUCTURAL ORGANISATION OF THE γ- AND α- TYPE GLIADINS (a), AND OF C HORDEIN (b), THE S-POOR PROLAMIN FROM BARLEY (Shewry *et al.*, 1987).

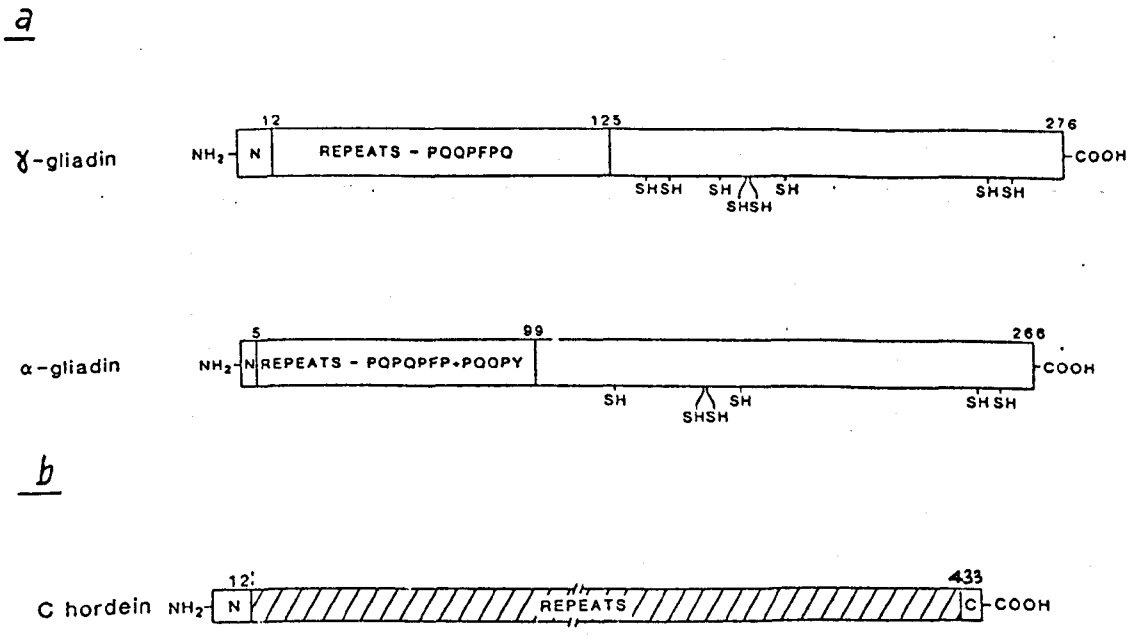

Table 3.2
AMINO ACID COMPOSITIONS (mol %) OF GLIADIN FRACTIONS

	Total gliadin[1]	ω-gliadin[2]	α-gliadin[3]	ß-gliadin[4]	γ-gliadin[4]
Asn/Asp	2.5	0.8	2.9	2.5	2.2
Thr	2.3	1.7	1.5	2.0	2.1
Ser	5.5	5.9	5.3	5.4	5.1
Gln/Glu	36.1	42.8	38.2	37.4	39.6
Pro	17.7	29.1	14.7	17.5	16.3
Gly	2.4	1.1	2.6	3.3	3.3
Ala	3.0	0.6	2.6	3.2	3.4
Cys	3.9	0	2.1	2.4	2.1
Val	4.1	0.4	4.6	4.5	4.4
Met	1.1	0	0.8	0.6	1.6
Ile	3.7	1.6	4.5	4.2	4.2
Leu	7.0	4.1	8.3	7.0	6.7
Tyr	2.0	1.5	3.2	1.5	1.6
Phe	4.5	8.9	3.8	5.4	4.6
His	1.7	0.8	2.1	1.1	1.4
Lys	0.6	0.3	0.5	0.5	0.5
Arg	1.8	0.6	1.8	1.4	1.4
Trp	nd	nd	0.4	nd	nd

1. Belton *et al.* (1985)
2. Kasarda *et al.* (1983)
3. Platt and Kasarda (1971)
4. Charbonnier (1973)
nd not determined

Figure 3.3
N-TERMINAL AMINO ACID SEQUENCES OF GLIADINS (Kasarda *et al.*, 1983)

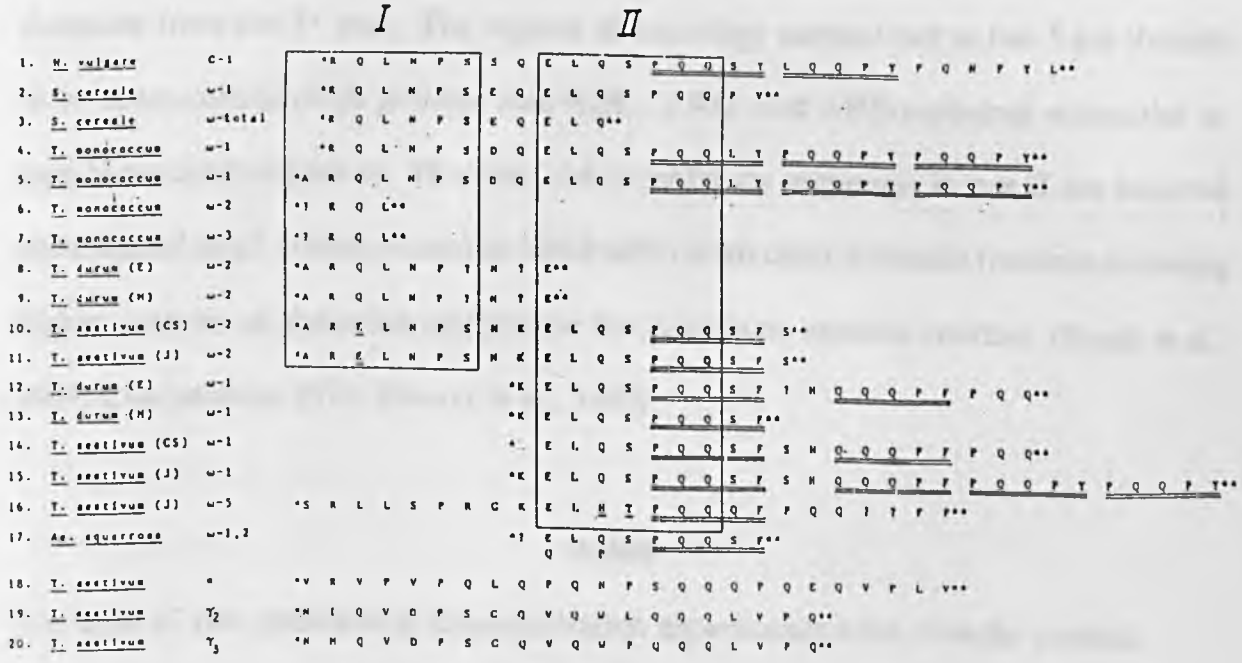

are indicated in boxes (#1-16, Figure 3.3). The RQL-, ARQ- and the ARE-types are essentially homologous. The RQL type, which has been reported in C hordein of barley, the ω-secalins of rye and in *T. monococcum* (Shewry *et al.*, 1980; Kasarda *et al.*, 1983) is thought to be the ancestral type (Kasarda *et al.*, 1983). The KEL-type genes on the other hand, are thought to have arisen from the ARE-type genes as a result of deletions from the 5′ end. The regions of homology marked out in box I are thought to be characteristic of all proteins with RQL-, ARQ- and ARE-variations within the ω-type N-terminal sequences. However, the homologous sequences in box II are believed to be shared by all ω-type prolamins which differ from other prolamin fractions in having higher contents of glutamine and proline but contain no cysteine residues (Booth *et al.*, 1969; Charbonnier, 1974; Shewry *et al.*, 1980).

AIMS

The aims of the preliminary characterisation experiments were broadly twofold.

1) To characterise each purified gliadin fraction in terms of its apparent molecular weight (M_r), amino acid composition and N-terminal amino acid sequence.

2) To draw conclusions on the relative purity of each fraction on the basis of the uniqueness or otherwise of its N-terminal amino acid sequence.

MATERIALS

Amino acid composition analysis was carried out in the Molecular Recognition Centre, University of Bristol, using a PICO-TAG SYSTEM. N-terminal amino acid sequence determination was carried out by Jaytee Biosciences Ltd., at the Research and

Development Centre, University of Kent, Canterbury, using a JAYTEE 8710 SEQUENCER linked to a SHIMADZU HPLC SYSTEM.

CHEMICALS

ESTIMATION OF M_r BY GEL FILTRATION

PRODUCT		SOURCE
Dithiothreitol (DTT)	AR	Sigma
GuHCl (grade I)		"
Iodoacetamide (IAM)	AR	"
Molecular weight calibration kit:		"
Ribonuclease A		"
Chymotrypsinogen A		Sigma
Ovalbumin		"
Bovine serum albumin (BSA)		"
Phosphorylase b		"
β-Galactosidase		"
di-Sodium orthophosphate	AR	Fisons Ltd
Sodium di-hydrogen phosphate	AR	"
Sepharose CL-6B resin		Pharmacia

SOLUTIONS AND BUFFERS

0.1M sodium phosphate, 6M GuHCl, pH 7.0

Solution A

di-Sodium orthophosphate $Na_2HPO_4.7H_2O$		35.81g
GuHCl		573.18g
H_20	to	1l

Solution B

Sodium di-hydrogen phosphate NaH_2PO_4		3.90g
H_2O	to	250ml

Solution A was titrated with solution B till pH 7.0

ESTIMATION OF M_r BY SDS-PAGE

CHEMICALS

PRODUCT	SOURCE
Molecular weight calibration kit:	Sigma
α-Lactalbumin	"
Trypsin inhibitor	"
Trypsinogen	"
Carbonic anhydrase	"
Glyceraldehyde 3-phosphate dehydrogenase	"
Egg albumin	"

PRODUCT	SOURCE
Bovine serum albumin	Sigma
Phosphorylase b	"
β-Galactosidase	"

All other chemicals, buffers and equipment for SDS-PAGE estimation of M_r were as described in chapter 2.

METHODS

ESTIMATION OF M_rS

1. GEL FILTRATION CHROMATOGRAPHY

COLUMN PREPARATION

Sepharose CL-6B was supplied as a pre-swollen gel. 100ml was rinsed thoroughly with water in a Buchner funnel and resuspended in 100ml of column buffer, 100mM sodium phosphate, 6M GuHCl, pH 7.0 with gentle mixing. The gel supension was degassed under vacuum before being packed into a 1.55 (i.d) x 90cm column. The column was then equilibrated with 500ml of column buffer at a constant flow rate of 3ml hr^{-1}.

SAMPLE PREPARATION

The protein samples comprising ω-gliadin, γ_{III}-gliadin, γ_V-gliadin and molecular weight standards were reduced and alkylated according to the method of Waxdall *et al.* (1968). 10mg of protein dissolved in 1ml column buffer, was initially incubated at 37°C for 30min. 40mM DTT was then added and the incubation was allowed to proceed for a further 4hr at the same temperature. The mixture was then transferred onto ice and pre-

cooled for approximately 10min. 100mM iodoacetamide (IAM) was added and the mixture was kept on ice in the dark for a further 1hr to alkylate free sulphydryl groups. Excess IAM was removed initially by the addition of dry Sephadex G-10. Sephadex G-10 was then removed after approximately 2hr by centrifugation and the protein solution was dialysed in 1l column buffer for up to 4hr to remove residual IAM.

COLUMN CALIBRATION

V_t of the column was determined by direct measurement of the volume of water required to fill it completely and also by calculation from its geometric dimensions. V_o of the column was determined by measuring the volume of buffer eluted from the column between the loading of Blue Dextran 2000 and the appearance of the first peak monitored at 620nm. Concentration of Blue Dextran 2000 was 1mg ml^{-1}. In order to obtain V_e values for the reduced and alkylated molecular weight standards, each standard protein (10mg ml^{-1}) was loaded and run separately. The flow rate during sample loading was 2ml hr^{-1}. This was increased to 3ml hr^{-1} after loading and elution of peak fractions was monitored at 280nm. V_e for each protein was obtained by measuring the volume of buffer collected between loading, and the appearance of the first peak. K_{av} values were calculated according to equation (1) above and a calibration curve of log molecular weight versus K_{av} was plotted (Figure 3.9).

10mg ml^{-1} aliquots of reduced and alkylated ω-gliadin, γ_{III}-gliadin and γ_V-gliadin fraction were loaded and run separately on the calibrated gel filtration column as described above for the molecular weight standards. V_e for each fraction was determined as described above and the M_rs of the fractions were obtained from the calibration curve

using their respective K_{av} values. The average time taken to run each protein including the equilibration of the column was over 100hr. As a result, single determinations were carried out.

2. SDS-PAGE UNDER REDUCING CONDITION

SDS-PAGE analysis was used concurrently with gel filtration to estimate the M_rs of the purified fractions. The method used was essentially that of Laemmli (1970) as described in Chapter 2. Molecular weight standards and the purified gliadin fractions were run together on 14% (w/v) acrylamide gels and the power was switched off immediately after the dye marker reached the bottom edge of the gel. The length of the separating gel was then measured as the distance moved by the dye marker. The migration of each protein band was divided by this value in order to obtain the respective R_f values. M_r estimates were carried out in duplicate. For each gel system, a separate standard curve of log molecular weight versus R_f was plotted and from this, the M_rs of the purified fractions were obtained by extrapolation from their experimentally determined R_f values.

N-TERMINAL AMINO ACID SEQUENCE ANALYSIS OF THE PURIFIED GLIADIN FRACTIONS

N-terminal amino acid sequence analysis of ω-gliadin, γ_{III}-gliadin and γ_V-gliadin fractions was carried out using an automated liquid phase Edman degradation process on a JAYTEE 8710 SEQUENCER linked to a SHIMADZU HPLC SYSTEM. 100pmole PTH-amino acid standard was used and the gliadin concentrations were approximately 15-20nmole ml^{-1}.

AMINO ACID COMPOSITION ANALYSIS OF THE PURIFIED GLIADIN FRACTIONS

The amino acid analyzer was a PICO-TAG SYSTEM and analysis was by a modification of the procedure reported by Bidlingmeyer *et al.* (1984). Acid hydrolysis was carried out in the gas phase at 150°C for 90min using 6M HCl. Tryptophan and cysteine were not determined. 200pmole Pierce/Taurine standard was used and the concentrations of the gliadin fractions were approximately 10-20nmole ml^{-1}.

RESULTS

1. CALIBRATION OF SEPHAROSE CL-6B GEL FILTRATION COLUMN

Results of the calibration of the gel filtration column are shown in Figures 3.4-3.9 and Table 3.3. V_t was calculated from the dimensions of the column as 170ml but the amount of water required to fill it completely was 172ml. Although there was good agreement, the measured value was considered the more appropriate as it represented the actual volume available within the column.

The elution profiles of the standards are shown separately for clarity. Blue Dextran 2000 ($M_r > 2x10^6$) eluted in a retention volume of 66ml. In view of its size, it was excluded from the internal area of the stationary phase. Hence, this volume corresponded to V_o of the column.

Like Blue Dextran 2000, the elution volume measured for each standard protein was inversely related to its M_r. Thus, the lowest V_e was obtained for ß-galactosidase (M_r 116K) and the highest, for ribonuclease A (M_r 13.7). Although one protein sample was loaded and analysed at a time, two peaks were obtained in each case by monitoring the

Figure 3.4 ESTIMATION OF M_rS BY GEL FILTRATION CHROMATOGRAPHY: THE ELUTION OF BLUE DEXTRAN 2000 (V_0) AND RIBONUCLEASE A, SEPHAROSE CL-6B, SODIUM PHOSPHATE BUFFER, pH 7.0

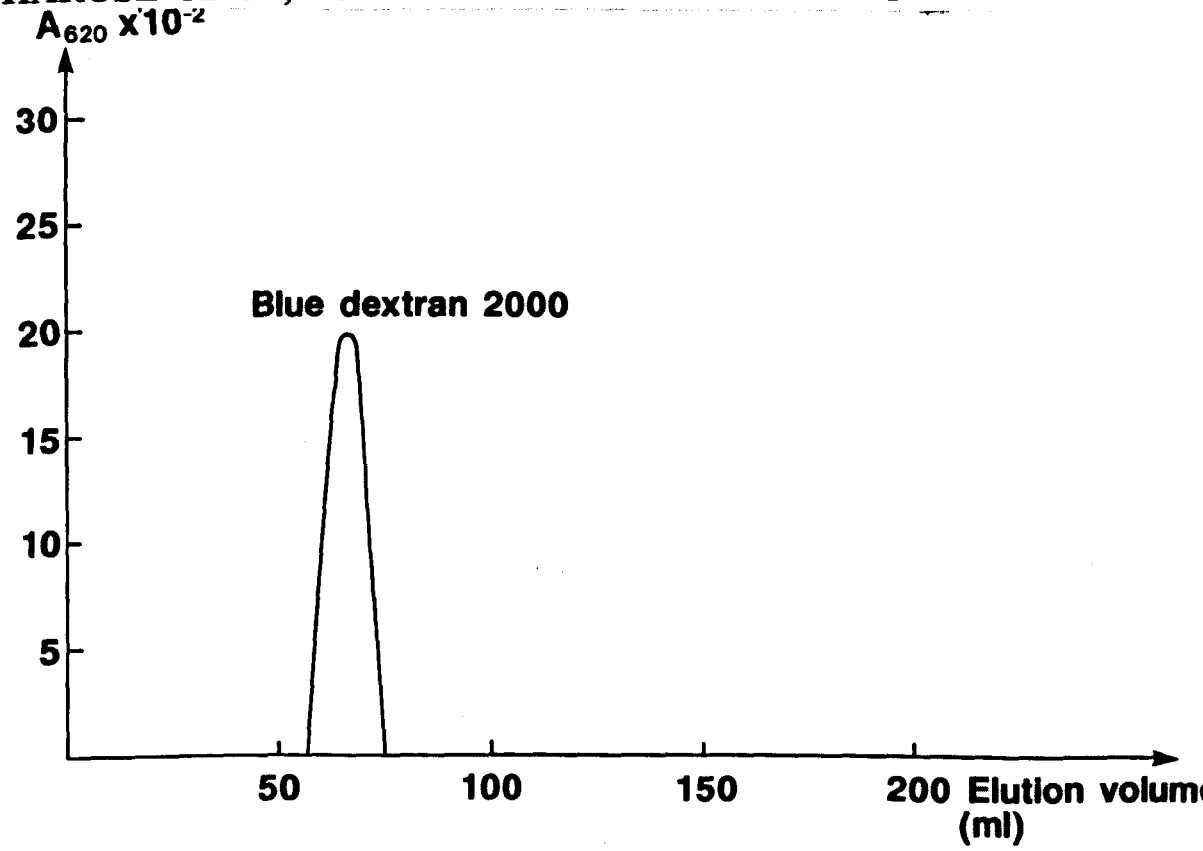

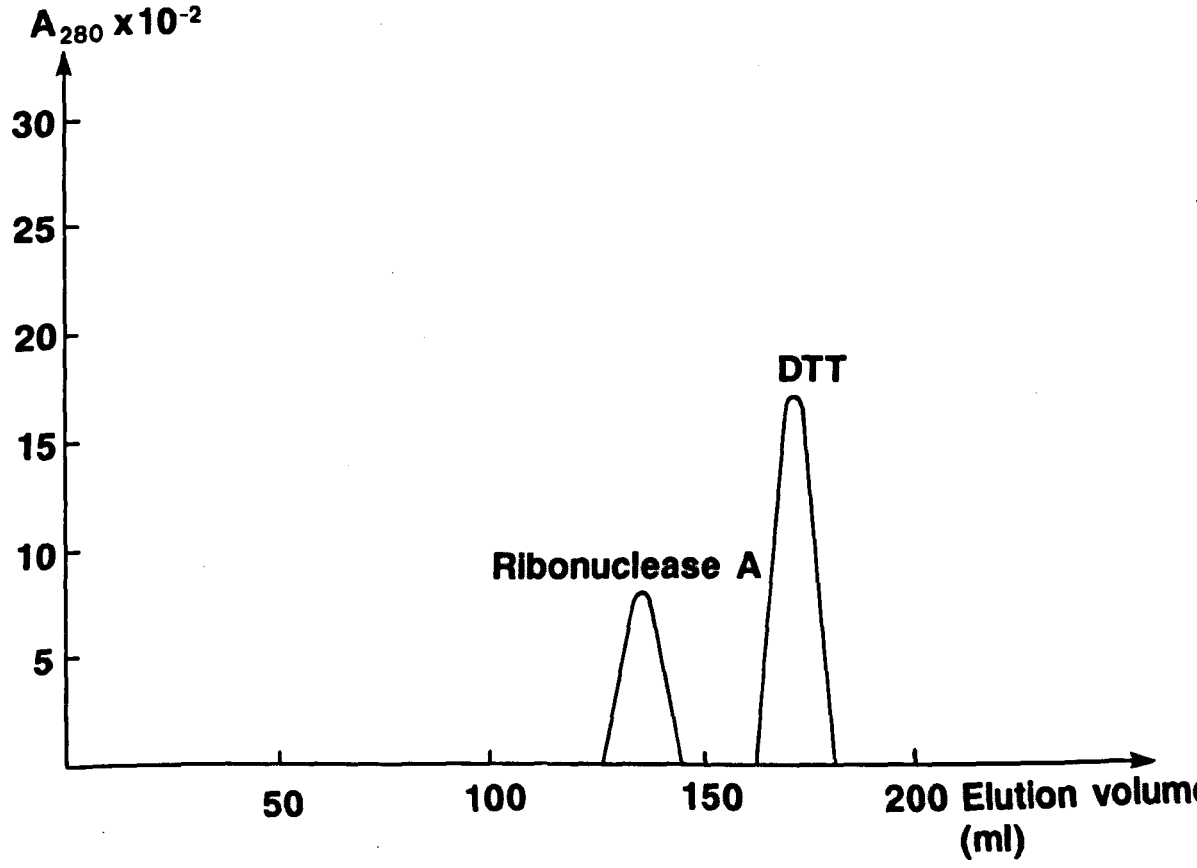

Figure 3.5 ESTIMATION OF M_rS BY GEL FILTRATION CHROMATOGRAPHY: THE ELUTION OF CHYMOTRYPSINOGEN A AND OVALBUMIN, SEPHAROSE CL-6B, SODIUM PHOSPHATE BUFFER, pH 7.0

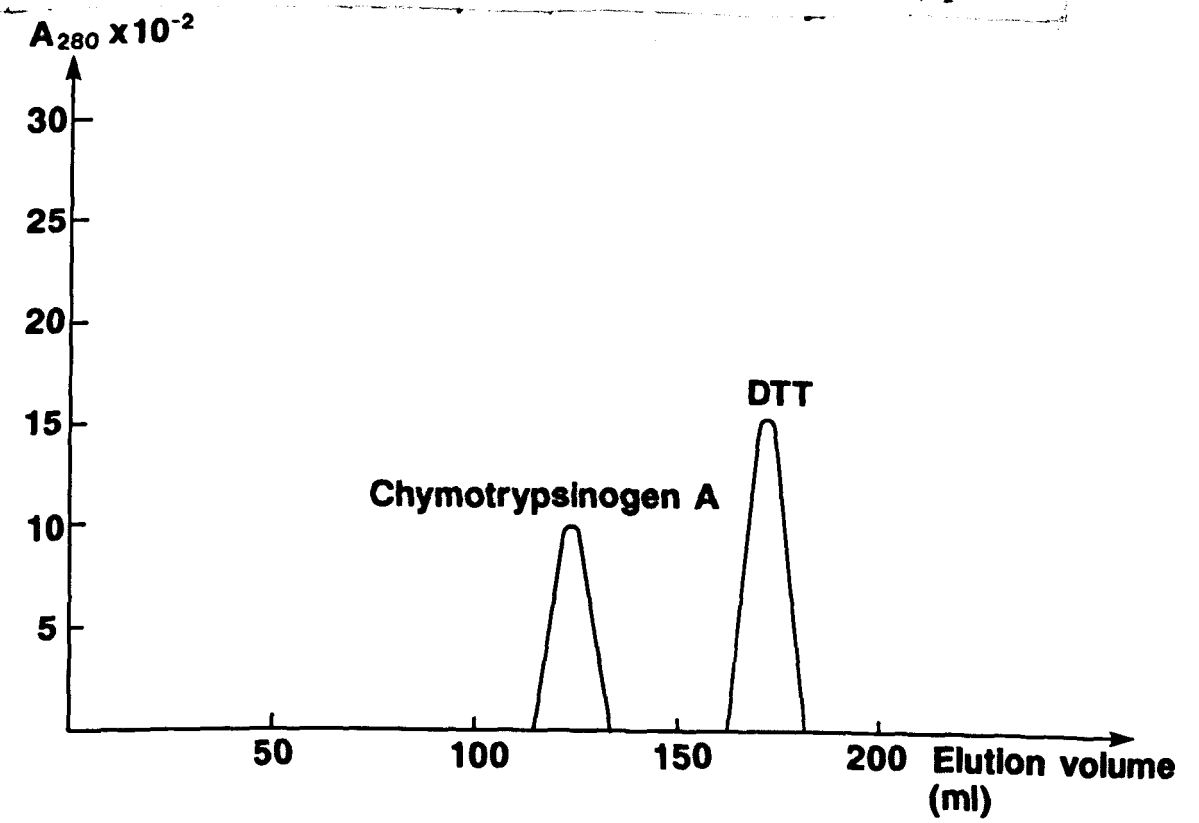

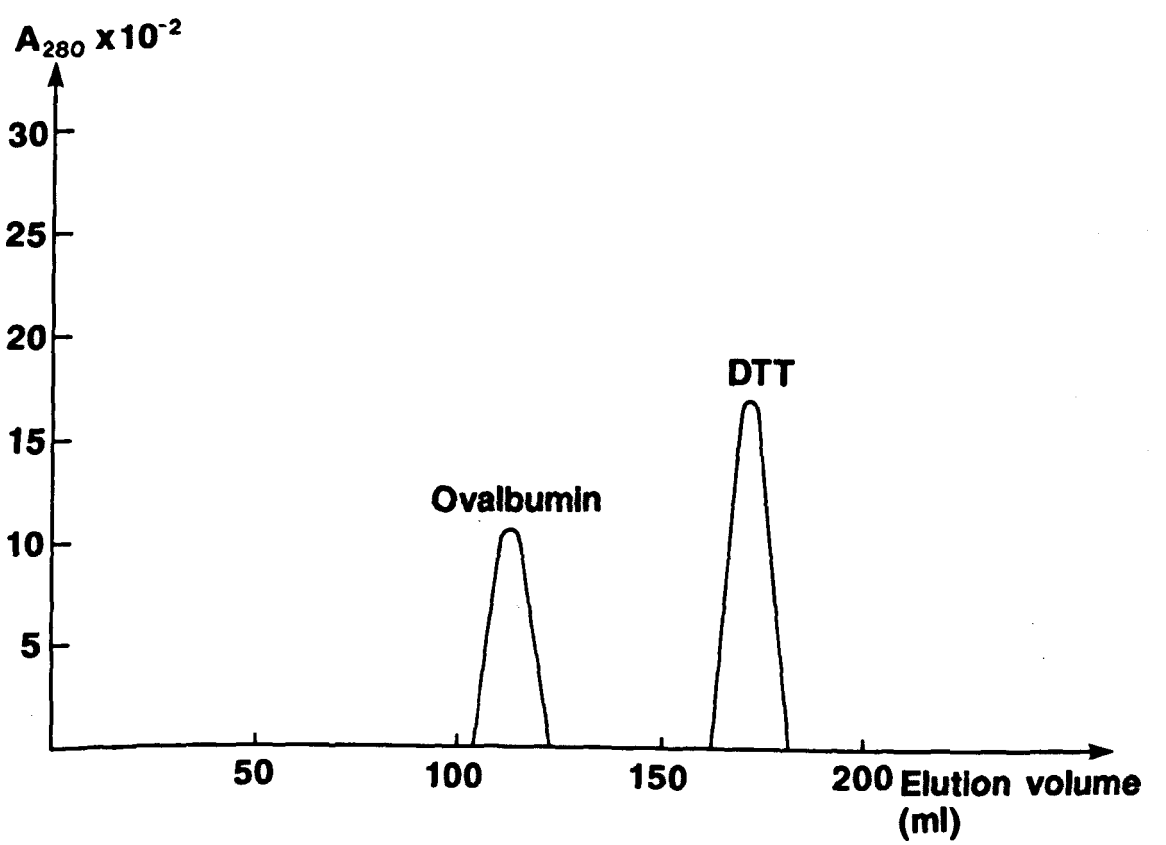

Figure 3.6 ESTIMATION OF M_rS BY GEL FILTRATION CHROMATOGRAPHY: THE ELUTION OF BOVINE SERUM ALBUMIN (BSA) AND PHOSPHORYLASE B, SEPHAROSE CL-6B, SODIUM PHOSPHATE BUFFER, pH 7.0

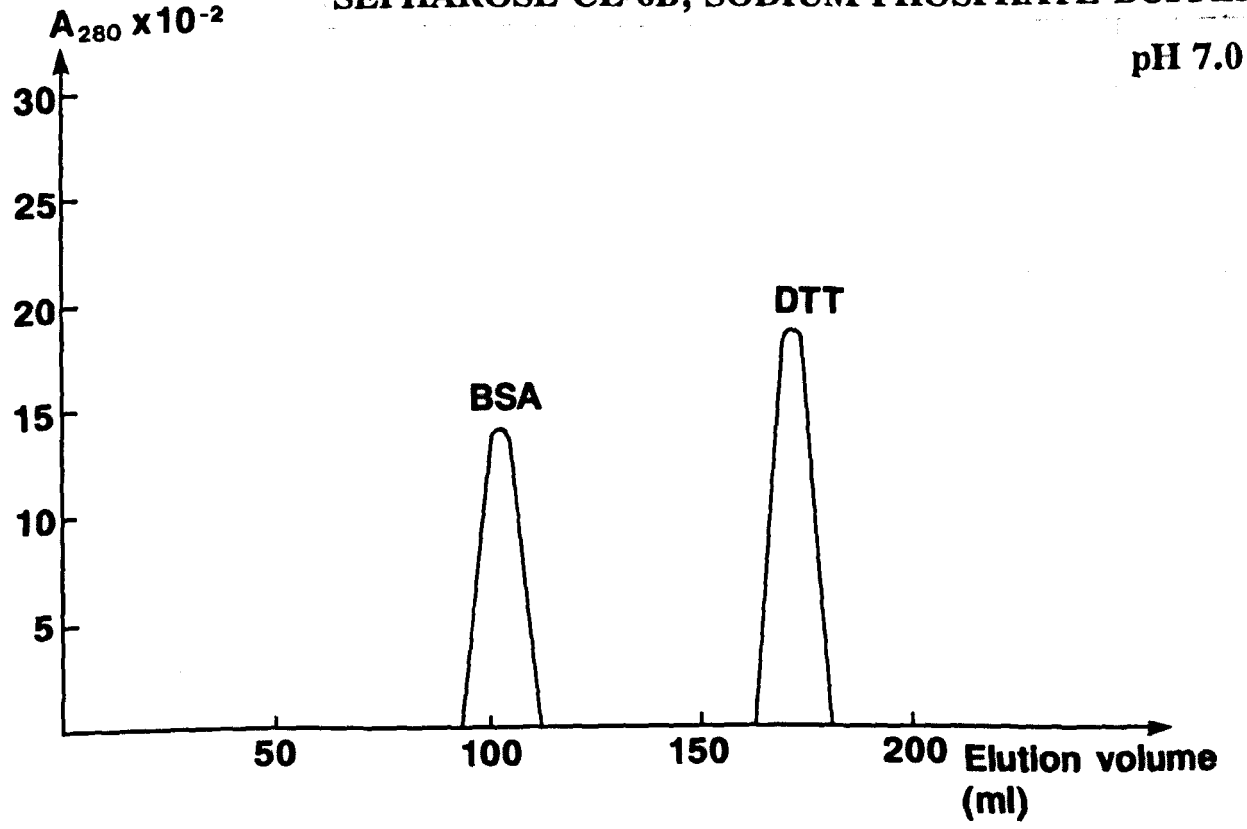

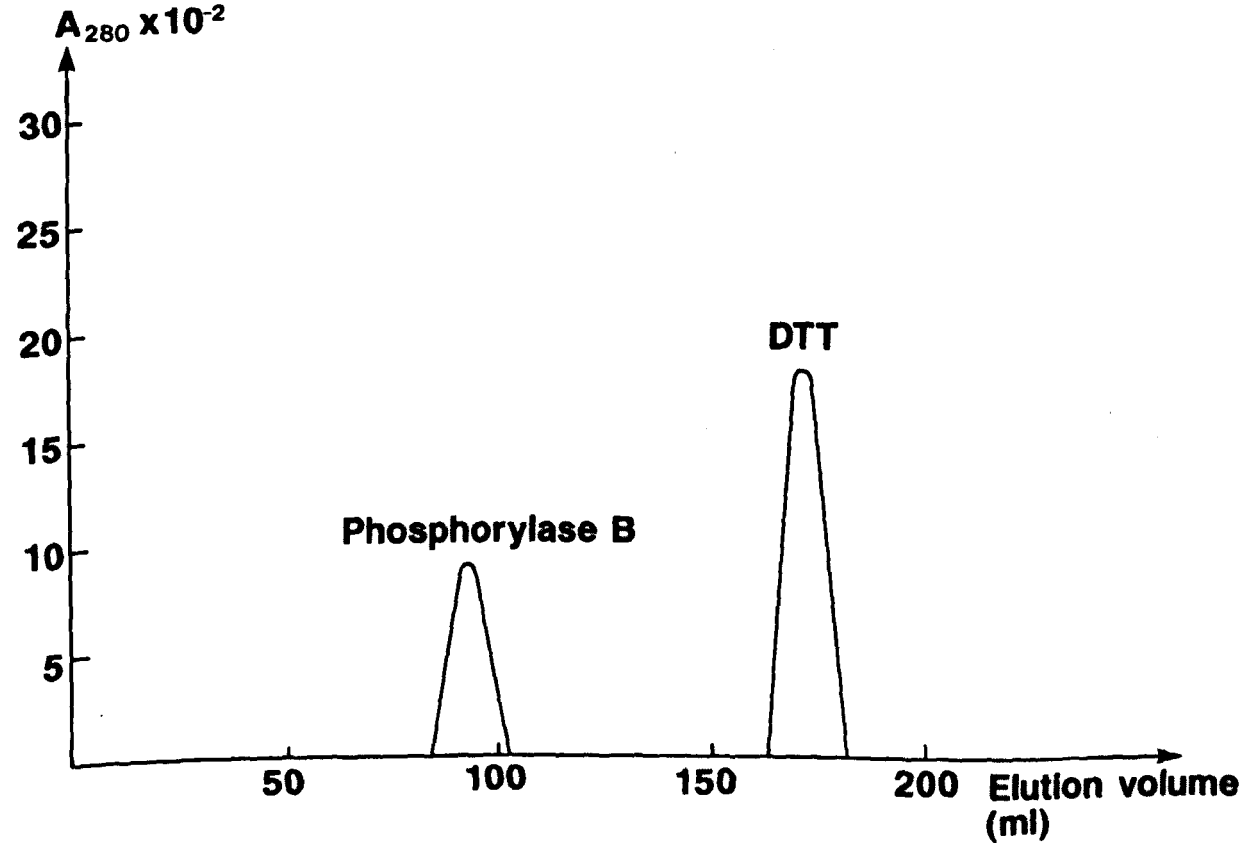

Figure 3.7 ESTIMATION OF M_rS BY GEL FILTRATION CHROMATOGRAPHY: THE ELUTION OF ß-GALACTOSIDASE AND ω-GLIADIN,
SEPHAROSE CL-6B, SODIUM PHOSPHATE BUFFER, pH 7.0

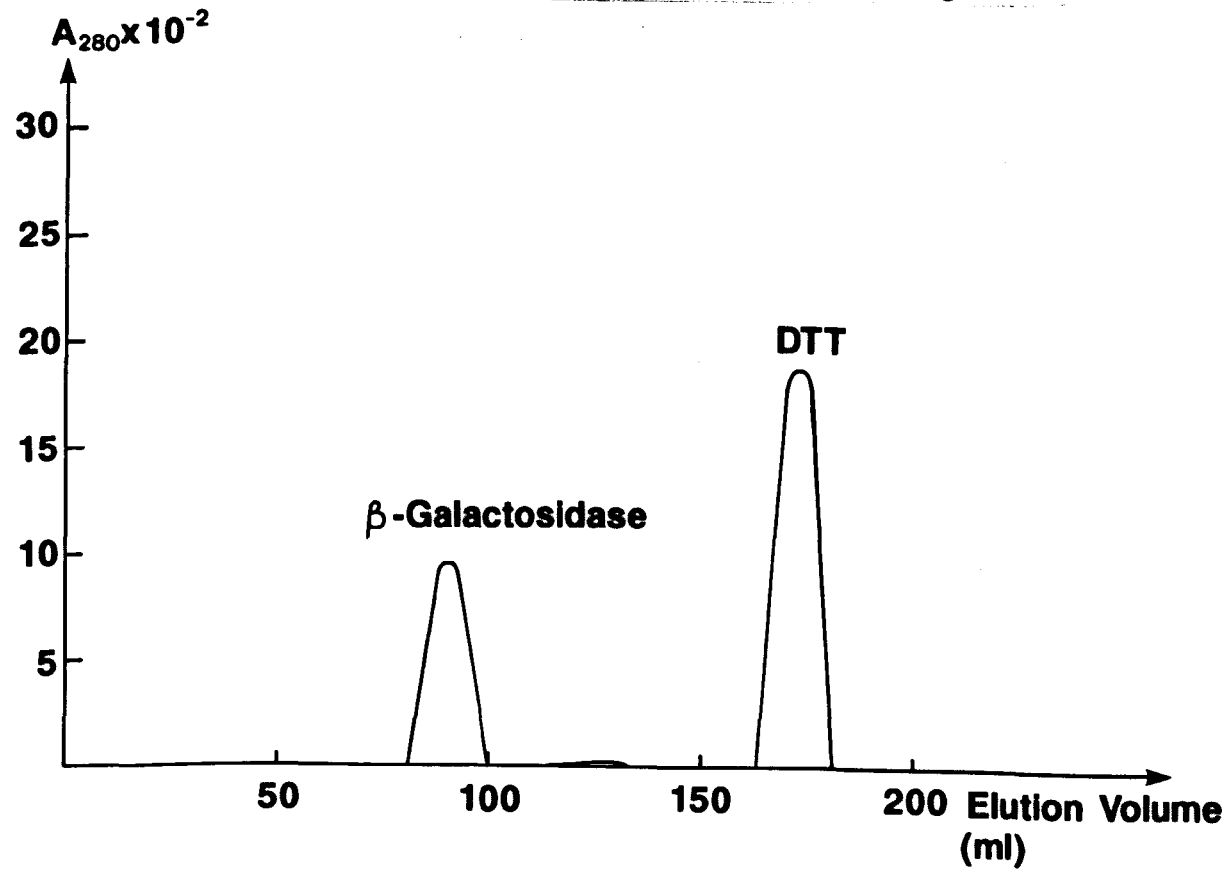

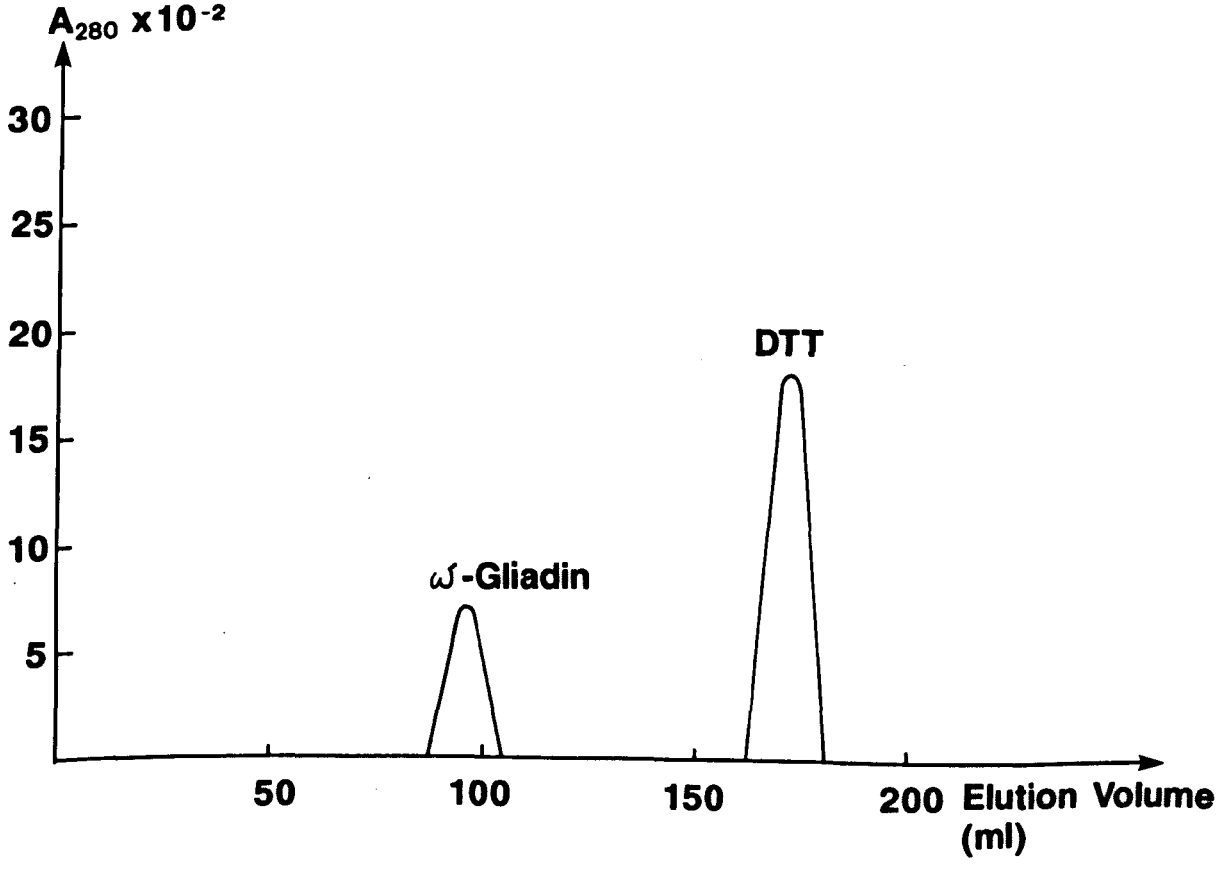

Figure 3.8 ESTIMATION OF M_rS BY GEL FILTRATION CHROMATOGRAPHY: THE ELUTION OF γ_{III} -GLIADIN AND γ_V-GLIADIN,
SEPHAROSE CL-6B, SODIUM PHOSPHATE BUFFER, pH 7.0

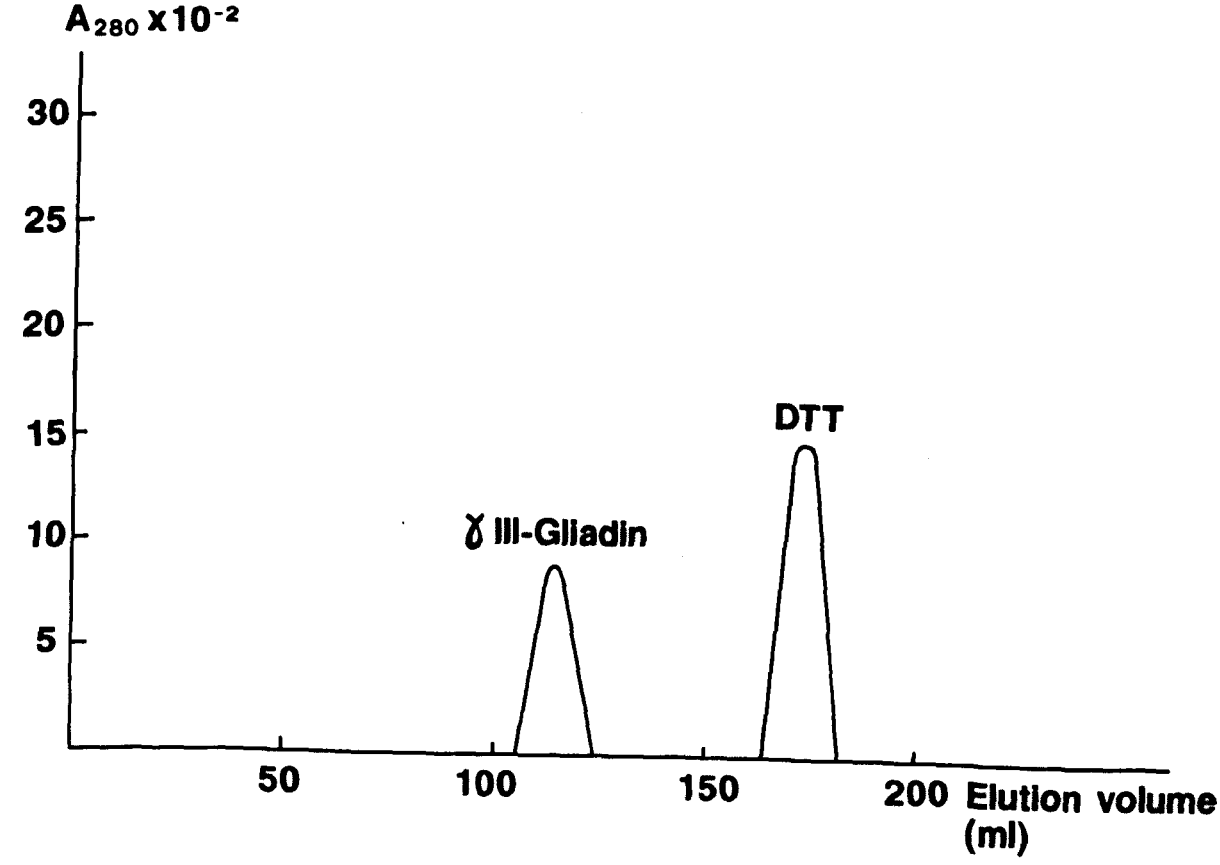

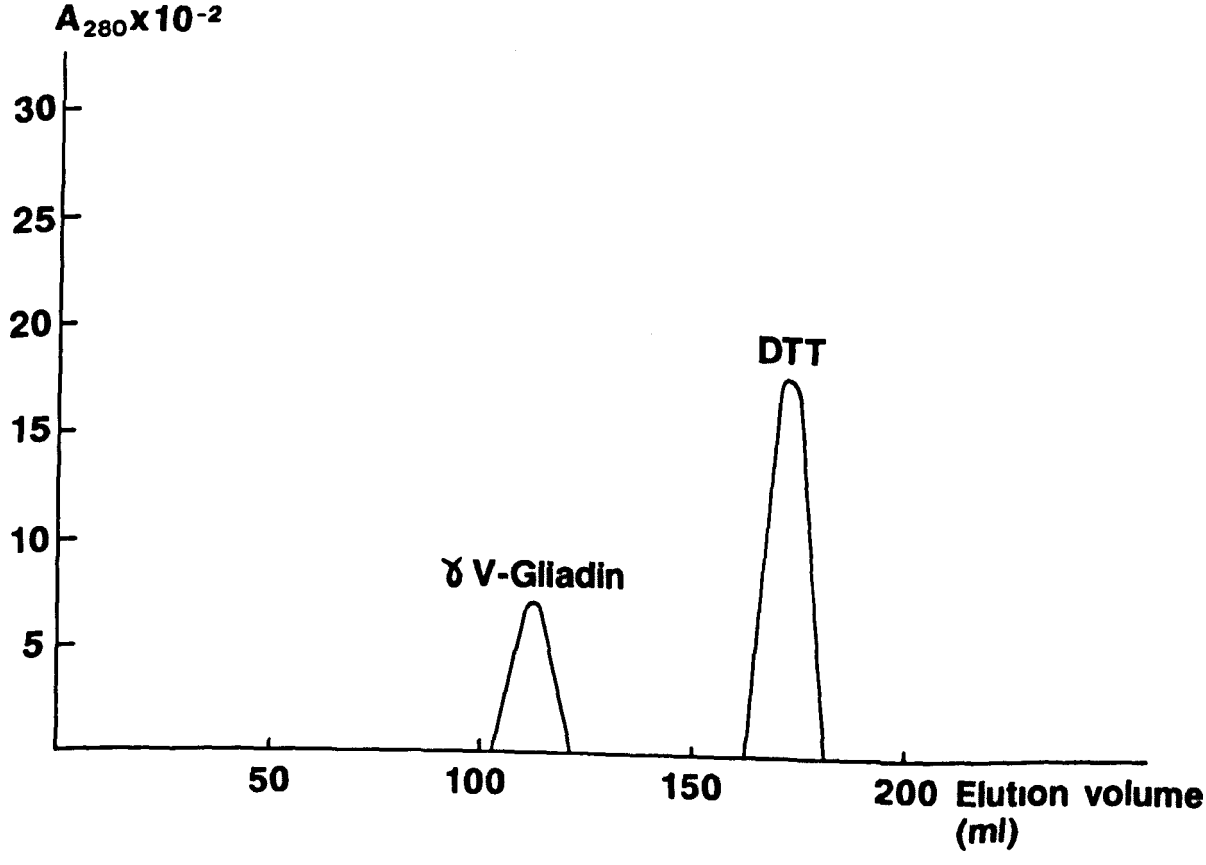

elution at 280nm. The second peak differed from the one preceeding it in a number of ways. Fractions from it neither appeared on SDS-PAGE gels nor emitted fluorescence light after excitation at 295nm. In addition, they gave negative results after Biuret assays and consistently eluted in a retention volume of approximately 172ml. It was concluded that this was not a protein peak. Instead, it was likely to have been due to the elution of DTT molecules used to reduce the protein samples. DTT is known to absorb at 280nm (Popineau and Pineau, 1985 b; personal communication, 1989) and in view of its size (M_r 154.2), is expected to be eluted close to the total volume of the column. The standard curve obtained by plotting the M_r of the proteins versus their respective K_{av} values (Figure 3.9) was linear with a negative slope.

ESTIMATION OF THE M_rS OF THE PURIFIED GLIADIN FRACTIONS

The elution volumes, corresponding K_{av} values and M_rs by gel filtration estimated for the three gliadin fractions are shown in Table 3.3. M_rs for the ω-gliadin, γ_{III}-gliadin and γ_V-gliadin were 90K, 41K and 44K respectively. The elution of each of these fractions was also accompanied by a non-protein peak similar to that described above. M_rs by gel filtration of gliadin fractions are not widely reported. Hamauzu and Yonezawa (1978) reported M_r values for gliadin fractions they referred to as gliadin-III and gliadin-IV, which corresponded to $\alpha+\beta$ gliadin and α-gliadin respectively as 37K and 33K. Popineau and Pineau (1985 b) also reported M_rs for γ_{44}-gliadin, γ_{46}-gliadin and γ_{50+51}-gliadin as 35K, 31K and 29.5K respectively. There was no agreement between these values and those estimated for the two purified γ-gliadin fractions. However, such disagreements in the estimation of M_rs of gliadin fractions in the presence of denaturants

Figure 3.9
STANDARD CURVE FOR THE ESTIMATION OF M_rS BY GEL FILTRATION CHROMATOGRAPHY

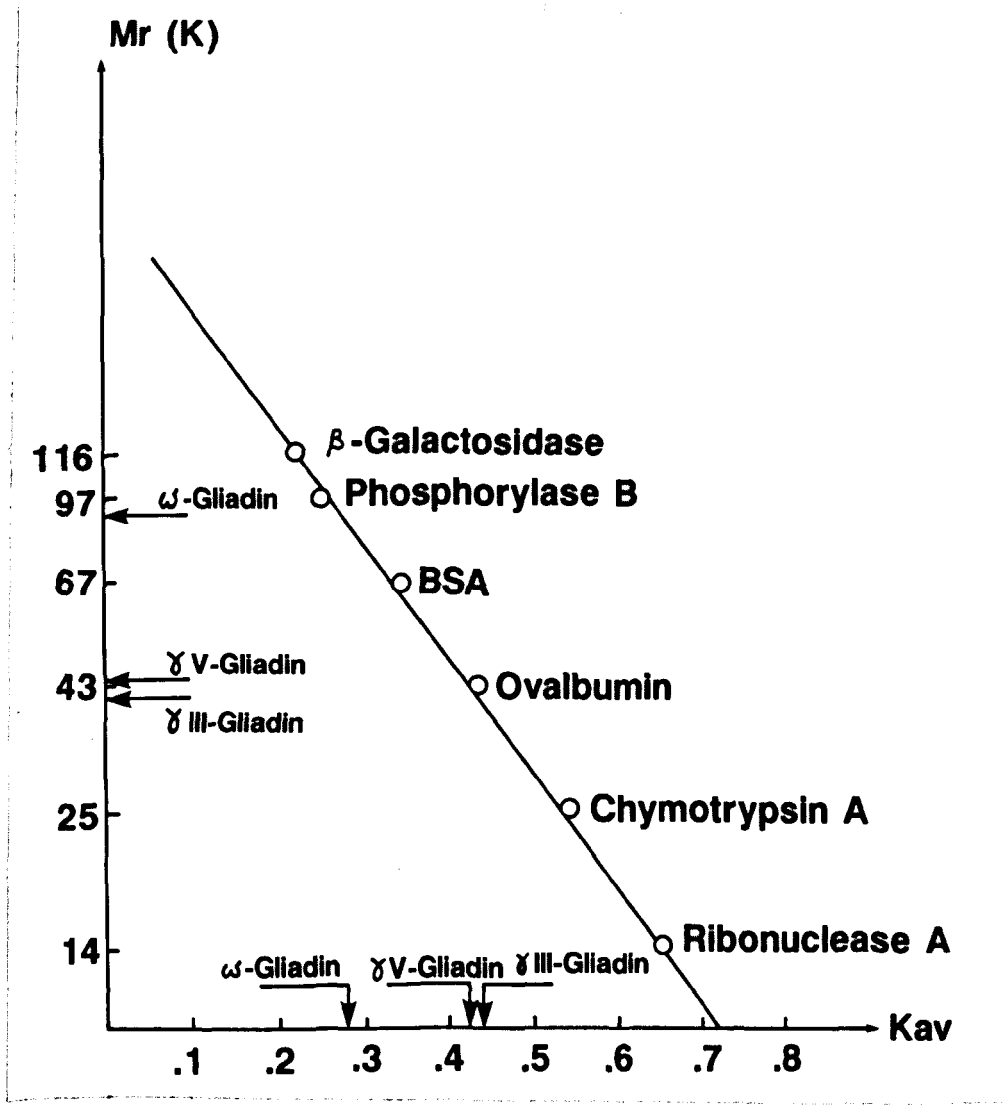

Table 3.3
PARAMETERS FOR M_r ESTIMATION BY GEL FILTRATION

Protein	V_e (ml)	K_{av}	M_r (K)
Ribonuclease A[1]	136	0.650	13.7
Chymotrypsinogen A[1]	124	0.540	25.0
Ovalbumin[1]	113	0.435	43.0
BSA[1]	103	0.345	67.0
Phosphorylase b[1]	93	0.250	97.4
ß-Galactosidase[1]	90	0.222	116.0
γ_{III}-gliadin	114	0.440	41.0
γ_V-gliadin	112	0.425	44.0
ω-gliadin	96	0.280	90.0
V_t of column	170ml[2]	172ml[3]	
V_o of column	66ml[4]		

1. molecular weight standards
2. by calculation
3. by volume of H_2O required to fill it completely
4. elution volume of Blue Dextran 2000

Table 3.4
PARAMETERS FOR M_r ESTIMATION BY SDS-PAGE

Protein	R_f		M_r	Mean M_r (K)	
ß-Galactosidase[1]	0.102	0.129[d]	116.0	-	-
Phosphorylase b[1]	0.128	0.182[d]	97.0	-	-
BSA[1]	0.192	0.273[d]	66.0	-	-
Ovalbumin[1]	0.308	0.416[d]	45.0	-	-
Gly 3-ph d'ase[1•]	0.385	0.506[d]	36.0	-	-
Carbonic anhydrase[1]	0.487	0.636[d]	29.0	-	-
Trypsinogen[1]	0.513	0.662[d]	24.0	-	-
Trypsin inhibitor[1]	0.615	0.779[d]	20.1	-	-
α-Lactalbumin[1]	0.795	0.987[d]	14.2	-	-
ω-gliadin	0.167	0.247[d]	80.0	72.0[d]	76.0
γ_V-gliadin	0.295	0.390[d]	47.0	46.0[d]	46.5
γ_{III}-gliadin	0.333	0.442[d]	41.0	41.0[d]	41.0

1. molecular weight standards
d duplicates
• glyceraldehyde 3-phosphate dehydrogenase

are known (Bunce *et al.*, 1985). Although those encountered using urea and SDS-PAGE are well reported, they are still not fully understood and there have been instances when wide variations in M_r have been reported using the same techniques (Booth and Ewart, 1969; Hamauzu *et al.*, 1974). Both urea and GuHCl are chaotropic agents known to destabilise the regular conformations of proteins. Their effects on M_rs estimated for gliadin fractions will therefore be expected to be similar.

2. SDS-PAGE

The mobilities of the three gliadins, and molecular weight standards on SDS-PAGE are

shown in Figure 3.10. The corresponding R_f values are given in Table 3.4, and the semi-logarithmic calibration curve obtained by plotting the molecular weights of the standard proteins against their respective R_fs is shown in Figure 3.11. M_rs estimated for the γ_{III}-gliadin and γ_V-gliadin fractions were 41K and 47K respectively and were reproducible in duplicate estimations. For the ω-gliadin however, 72K and 80K were obtained in duplicate estimates.

The M_r of the γ_{III}-gliadin was in good agreement with the values of Miflin *et al.* (1983), and that of the γ_V-gliadin M_r was similar to those reported by Popineau and Pineau (1988). Both the M_r by gel filtration and SDS-PAGE of the γ_{III}-gliadin were identical whereas for the γ_V-gliadin, they were 44K and 47K respectively.

The average M_r by SDS-PAGE of the ω-gliadin fraction was 76K and was higher than the value of 57.5K reported for the ω_1-gliadin fraction of Chinese Spring (Kasarda *et al.*, 1983). There was no agreement between the M_rs by gel filtration and by SDS-PAGE of the ω-gliadin fraction. Inaccuracies associated with estimations of M_rs of gliadin fractions are known to be more common among the ω-gliadins possibly as a result of their extended repetitive domains, but this is not fully understood. The inclusion of urea in SDS-PAGE gels is thought to cause increases of 30%, or more, in estimated M_rs of ω-gliadin fractions (Bunce *et al.*, 1985).

N-TERMINAL AMINO ACID SEQUENCE ANALYSIS

The retentions and recoveries of residues in the automated Edman degradation of the ω-gliadin, γ_V-gliadin and γ_{III}-gliadin together with the retentions of the corresponding PTH-amino acid standards, are shown in Tables 3.5 a, b and c respectively. Up to 10

Figure 3.10
M_r ESTIMATION: SDS-POLYACRYLAMIDE GEL ELECTROPHORESIS OF THE GLIADIN FRACTIONS AND MOLECULAR WEIGHT STANDARDS.

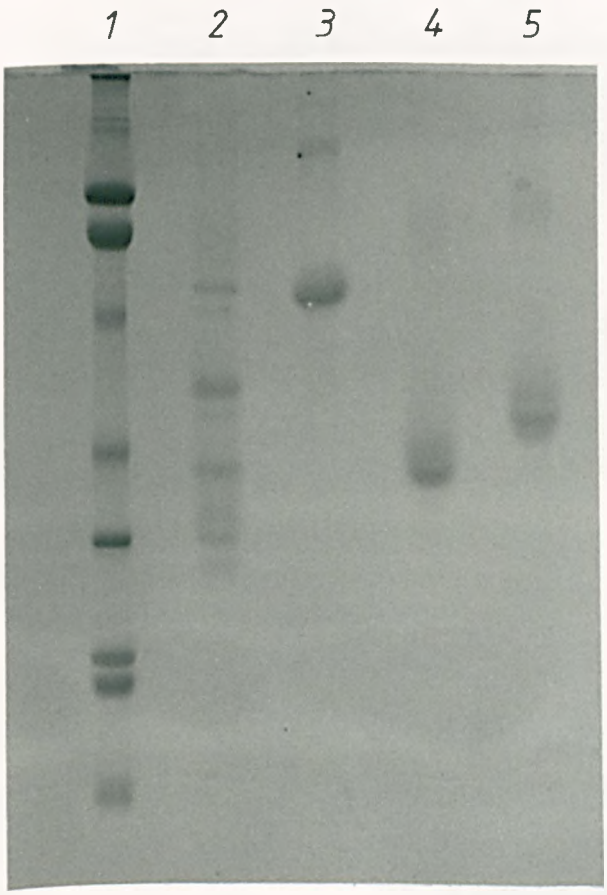

Lane	Fraction
1	molecular weight standards*
2	total gliadin standard
3	ω-gliadin
4	γ_{III}-gliadin
5	γ_{V}-gliadin

*. see text for details.

Figure 3.11
STANDARD CURVE FOR THE ESTIMATION OF M_rS BY SDS-PAGE

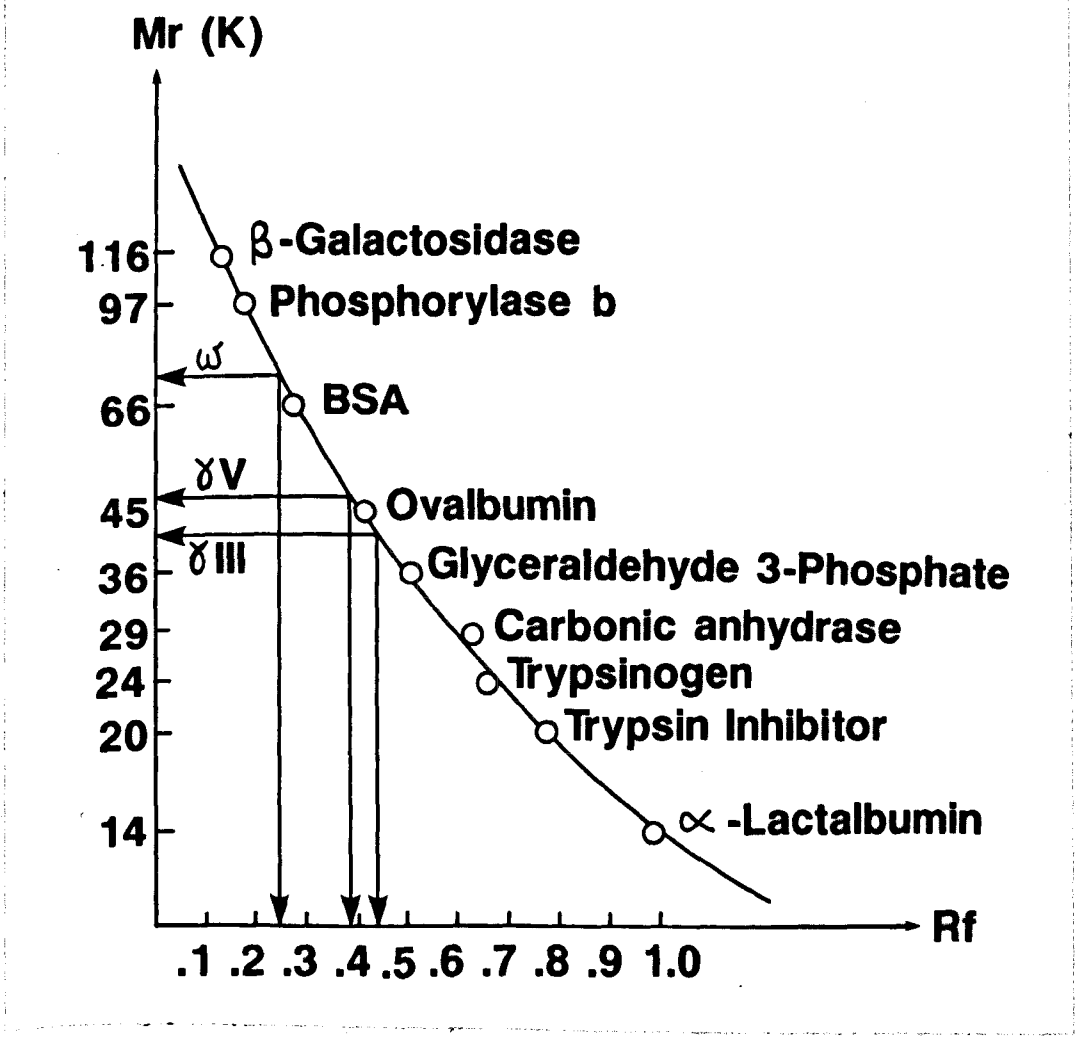

cycles were analysed for the ω-gliadin and 20 for each of the γ_{III}-gliadin and γ_V-gliadin. The N-terminal amino acid sequences deduced for the three fractions are summarised and compared to reported sequences of related gliadin fractions in Figure 3.12.

By comparing the retentions of peaks from the cycles of the Edman degradation and those of the PTH-amino acid standards, the N-terminal sequence of the ω-gliadin was deduced as a KEL-type sequence. The rest of the sequence was in good agreement with that of the ω_1-gliadin of Chinese Spring (Kasarda *et al.*, 1983). At cycle 5, two peaks with retentions corresponding to arginine and asparagine were recovered in comparable amounts. Serine has been reported at this position in the majority of N-terminal amino acid sequences of ω-gliadins (Kasarda *et al.*, 1983) but neither arginine nor asparagine has.

The retentions of peaks corresponded to single PTH-amino acid residues at most of the cycles of the Edman degradation of the γ_V-gliadin (Table 3.5b). However, two residues were detected at each of cycles 2-8 and 10 and their recoveries suggested that in each case, one was major and the other minor. The sequence based on the major PTH-amino acid residues, corresponded to an NIQ-type sequence which was similar to that reported for the γ_2-gliadin of *T. aestivum* (Kasarda *et al.*, 1983) except for the residues at positions 13 and 14 (Figure 3.12). The minor sequences at cycles 2-8 and 10 on the other hand, corresponded to a heptapeptide sequence, SGQVQWP and Q respectively. Each minor residue was identical to the residue five positions higher in the major sequence.

By similar comparisons of the retentions and recoveries of peaks, the N-terminal amino acid sequence of the γ_{III}-gliadin was also deduced to comprise major and minor sequences (Table 3.5 c; Figure 3.12). The first detected peak in the major sequence of

Table 3.5a
RECOVERIES OF RESIDUES IN THE AUTOMATED EDMAN DEGRADATION OF THE ω-GLIADIN FRACTION

PTH-Amino Acid Standard		ω-Gliadin			
Residue	Peak Retention (min)	Cycle	Peak Retention (min)	Recovery (pmol)	Residue
D	5.21	1	26.17	500	K
N	6.13	2	10.10	600	E
S	7.40	3	26.70	800	L
Q	7.80	4	7.83	800	Q
T	8.60	5	16.20	50	R
G	9.03		6.10	50	N
E	10.00	6	20.20	800	P
H	10.80	7	7.80	800	Q
A	13.57	8	7.80	700	Q
R	16.35	9	7.80	800	Q
Y	17.67	10	25.33	800	F
P	20.20				
M	21.37				
V	21.72				
W	24.62				
F	25.30				
I	25.87				
K	26.17				
L	26.70				

Table 3.5b
RECOVERIES OF RESIDUES IN THE AUTOMATED EDMAN DEGRADATION OF THE γ_V-GLIADIN FRACTION

PTH-Amino Acid Standard		γ_V-Gliadin			
Residue	Peak Retention (min)	Cycle	Peak Retention (min)	Recovery (pmol)	Residue
D	6.15	1	7.03	1000	N
N	7.05	2	27.01	1000	I
S	8.13		8.10	30	S
Q	9.43	3	9.40	900	Q
T	9.60		9.85	200	G
G	9.92	4	22.95	900	V
E	10.41		9.40	200	Q
H	11.04	5	6.15	700	D
A	14.53		22.95	200	V
R	15.20	6	19.06	900	P
Y	20.44		9.85	200	G
P	19.04	7	8.10	80	S
M	22.08		23.33	200	W
V	22.95	8	9.90	800	G
W	23.30		19.06	200	P
F	26.30	9	9.40	800	Q
I	27.00	10	22.95	600	V
K	27.55		9.40	100	Q
L	28.05	11	9.40	600	Q
		12	23.33	600	W
		13	19.03	800	P
		14	19.06	800	P
		15	9.42	600	Q
		16	9.42	600	Q
		17	28.05	500	L
		18	22.95	500	V
		19	19.06	400	P
		20	9.42	500	Q

Table 3.5c
RECOVERIES OF RESIDUES IN THE AUTOMATED EDMAN DEGRADATION OF THE γ_{III}-GLIADIN FRACTION

PTH-Amino Acid Standard		γ_{III}-Gliadin			
Residue	Peak Retention (min)	Cycle	Peak Retention (min)	Recovery (pmol)	Residue
D	6.45	1	10.83	300	G
N	7.80		22.11	100	P
S	8.25	2	27.50	500	I
Q	9.73	3	9.75	500	Q
T	10.50		10.85	100	G
G	10.85	4	23.22	500	V
E	12.00		9.75	100	Q
H	13.85	5	6.40	500	D
A	14.33		23.25	100	V
R	16.10	6	22.11	500	P
Y	17.40		9.79	80	Q
P	22.08	7	8.25	100	S
M	23.00		26.07	80	W
V	23.26	8	10.90	400	G
W	26.10		28.43	100	L
F	26.99	9	9.79	400	Q
I	27.51	10	23.25	300	V
K	28.02		9.75	80	Q
L	28.44	11	9.75	400	Q
		12	26.11	300	W
		13	28.44	300	L
			23.22	100	V
		14	9.80	300	Q
			22.05	80	P
		15	9.75	400	Q
		16	28.45	300	L
			8.25	50	S
		17	28.45	300	L
		18	23.25	300	V
		19	22.04	400	P
		20	9.79	300	Q

the γ_{III}-gliadin corresponded to glycine but the rest of the sequence was similar to that reported for the γ_2-gliadin of *T. aestivum* (Kasarda *et al.*, 1983) except for serine at position 16. Glycine has not been reported as the first residue in the sequence of any gliadin fraction to date and in view of the close similarity between the sequences of the γ_{III}-gliadin and the γ_2-gliadin of *T. aestivum*, it is likely that this may have been a sequencing error. In contrast to the the γ_V-gliadin, single minor residues were detected at cycles 1, 10, 13, 14 and 16 respectively in addition to a hexapeptide sequence, GQVQWL at cycles 3-8 for the γ_{III}-gliadin. Each minor residue was also identical to the residue five positions higher in the major sequence with the exception of serine at cycle 16. Serine was also expected as the second residue in the minor sequence. However, in view of the poor recoveries obtained for this residue, it is unlikely that yields lower than 30pmol were detected. The minor sequences detected in the N-terminal sequencing of the two γ-gliadins have not been reported for other gliadins. This is likely to have been the result of degradation in some polypeptides due to experimental handling rather than the manner of their biosyntheses. The degradation is likely to have involved the cleavage of a hexapeptide corresponding to NIQVDP in the γ_V-gliadin and a pentapeptide corresponding to GIQVD in the γ_{III}-gliadin. This in turn, would suggest that the peptide bonds adjacent to the proline residue at position 6 may be susceptible to cleavage in both the γ_{III}-gliadin and the γ_V-gliadin.

AMINO ACID COMPOSITION ANALYSIS

The amino acid compositions (mol %) determined for each of the purified gliadin fractions are shown in Table 3.6. The figures in parentheses are standard deviations

from triplicate determinations. Tryptophan and cysteine were not determined and asparagine and glutamine were determined as their corresponding free acids, aspartic acid and glutamic acid respectively.

The amino acid composition of the ω-gliadin was in good agreement with that reported for the ω_1-gliadin of Chinese Spring (Table 3.2) (Kasarda *et al.*, 1983) differing significantly from this only in the levels of glycine (2.3mol % ω-gliadin, 1.1mol % ω1-gliadin), valine (1.1mol % ω-gliadin, 0.4mol % ω1-gliadin) and lysine (1.0mol % ω-gliadin, 0.4mol % ω1-gliadin). In addition, the combined levels of glutamine/glutamic acid (40mol %) proline (30mol %) and phenylalanine (9mol %) was nearly 80% of the total of residues.

The amino acid compositions of the γ_{III}-gliadin and γ_V-gliadin differed from each other mainly in the levels of serine (6mol % γ_{III}-gliadin, 3mol % γ_V-gliadin), proline (20mol % γ_{III}-gliadin, 22mol % γ_V-gliadin) and lysine (1mol % γ_{III}-gliadin, 2mol % γ_V-gliadin). Both fractions contained approximately 37 mol % glutamine/glutamic acid and 5-6 mol % phenylalanine. In comparison with reported amino acid compositions for γ-gliadin (Table 3.2) (Charbonnier, 1973), the γ_{III}-gliadin and γ_V-gliadin contained higher levels of lysine (1-2 compared to .5mol %) and proline (20-22 compared to 16mol %) but lower levels of glutamine/glutamic acid (37 compared to 40). Their levels of proline (20-22mol %) and lysine (1-2mol %) were higher than that of total gliadin (18 mol % proline, and 0.6 mol % lysine). Serine content in the γ_V-gliadin (3.4mol %) was also lower than in total gliadin (5.5mol %).

Figure 3.12
N-TERMINAL AMINO ACID SEQUENCES OF THE ω-GLIADIN, γ_V-GLIADIN, γ_{III}-GLIADIN AND RELATED GLIADIN FRACTIONS

	1																			20
ω_1*-Gliadin	K	E	L	Q	S	P	Q	Q	S	F	S	H	Q	Q	Q	P	F	P	Q	Q
ω-Gliadin	K	E	L	Q	R	P	Q	Q	Q	F										
					N															
γ_2*-Gliadin	N	I	Q	V	D	P	S	G	Q	V	Q	W	L	Q	Q	Q	L	V	P	Q
γ_V-Gliadin	N	I	Q	V	D	P	S	G	Q	V	Q	W	P	P	Q	Q	L	V	P	Q
		S	G	Q	V	Q	W	P		Q										
γ_{III}-Gliadin	G	I	Q	V	D	P	S	G	Q	V	Q	W	L	Q	Q	L	L	V	P	Q
	P		G	Q	V	Q	W	L		Q			V	P		S				

*. Kasarda et al. (1983)

TABLE 3.6
AMINO ACID COMPOSITIONS OF ω-GLIADIN, γ_{III}-GLIADIN AND γ_{V}-GLIADIN

	(mol % ± SD)					
	ω-Gliadin		γ_{III}-Gliadin		γ_{V}-Gliadin	
Asn/asp	0.8	(0.25)	1.7	(0.15)	2.2	(0.15)
Gln/glu	39.7	(2.80)	37.3	(0.30)	37.4	(0.96)
Ser	5.7	(0.36)	6.0	(0.21)	3.4	(0.15)
Gly	2.3	(0.30)	3.9	(0.42)	3.3	(0.32)
His	5.0	(0.0)	1.2	(0.0)	1.0	(0.05)
Arg	0.7	(0.21)	1.4	(0.05)	1.6	(0.26)
Thr	1.6	(0.05)	2.1	(0.0)	2.1	(0.55)
Ala	0.9	(0.32)	3.2	(0.05)	2.7	(0.21)
Pro	29.6	(0.21)	20.0	(0.50)	21.9	(0.52)
Tyr	1.7	(0.70)	0.4	(0.05)	0.6	(0.0)
Val	1.1	(0.90)	4.2	(0.0)	3.4	(0.15)
Met	0.0	(0.0)	1.6	(0.05)	1.7	(0.06)
Ile	1.6	(0.11)	3.7	(0.10)	3.5	(0.11)
Leu	3.6	(0.20)	6.8	(0.15)	5.6	(0.25)
Phe	8.6	(0.45)	5.2	(0.10)	5.8	(0.17)
Lys	1.0	(0.72)	1.1	(0.0)	2.2	(0.11)

DISCUSSION

In studies to determine the relative molecular masses for the isolated gliadins, the γ_{III}-gliadin gave results with good agreement between:

1) M_rs by SDS-PAGE obtained in duplicate determinations for the same fraction.

2) M_rs by SDS-PAGE of the purified fractions and those reported for related gliadins.

3) M_rs by SDS-PAGE and by gel filtration for the same fraction in denaturing conditions.

On the same basis, the ω-gliadin gave the least consistent results and the γ_V-gliadin was intermediate between the two. The cause of disagreements in the M_rs of gliadins estimated in the presence of denaturants, have been explained in terms of various factors such as the presence of repetitive sequences and unusually high contents of proline (Hamauzu *et al.*, 1975; Hamauzu and Yonezawa, 1978; Bunce *et al.*, 1985). Another possible cause is experimental handling. However in the estimation of the M_rs of the ω-gliadin, γ_{III}-gliadin and γ_V-gliadin, a number of observations confirmed the accuracy and reliability of the protocols used. For instance, in the gel filtration experiments V_t was measured by the volume of water required to fill the column completely as $172cm^3$ and V_o was estimated from the elution volume of Blue Dextran 2000 as 66ml. Theoretically, V_o is about 35% of V_t (Darbre, 1987) and in the case of the column used, V_o represented 38% of V_t. The accuracy of V_t was also confirmed by the elution volume of DTT (M.Wt 154.2) used in reducing disulphide bonds in the protein samples. Being so small, DTT would be expected to elute in a volume equivalent to the total volume of the column. In all chromatographic runs residual DTT was eluted from the column with a retention of approximately 170ml. Similarly, in the estimation of M_rs by SDS-PAGE, the electrophoretic mobility of each fraction was consistent with those of corresponding

bands in the total gliadin standard and with the exception of the ω-gliadin, these were reproducible in duplicate estimates.

The proline-rich repetitive regions of gliadins have been suggested as a possible source of the over-estimation of M_rs in the presence of denaturants but this has not been conclusively demonstrated. The problem arises from the fact that the methods require calibration with known proteins. Hence, if the gliadins are systematically different from the standard proteins in their behaviour in the presence of these denaturants, then accurate molecular masses cannot be determined. This is further complicated by the fact that the action of denaturants such as urea and GuHCl are not fully understood and that denaturation by these agents, and by SDS, may generate different unfolded states. In summary, therefore, the discrepancies in the M_r values determined for the purified gliadins by SDS-PAGE and GuHCl-gel filtration, probably arise from differences between the gliadins or the standard proteins in their unfolding by these denaturants.

The presence of minor sequences in the two γ-gliadin fractions has to date, not been reported for any gliadins and suggested the presence of N-terminally truncated polypeptides in both fractions. Interestingly, in the ω-gliadin, SDS-PAGE band pattern of which suggested the presence of a single major protein, no minor sequences were detected. It is possible therefore, that the doublet of bands consistently observed in the SDS-PAGE band patterns of the γ_{III}-gliadin and the γ_{V}-gliadin corresponded to intact and truncated polypeptides. The fact that the proteins corresponding to these doublets could not be further fractionated could also mean that the cleavage of peptides from the N-termini of both fractions did not result in any significant changes in their chemical and physical properties and that each preparation was homogeneous. The cause of the

truncations was more difficult to ascertain. However, the doublet of bands from the γ_{III}-gliadin and γ_V-gliadin were also present in the SDS-PAGE pattern of the total gliadin standard. Hence it could have been the result of mechanical shearing through agitation during the extraction, or the result of prolonged exposure to 50mM acetic acid during dialysis to remove urea, although this is less likely. In other cases where gliadins have been exposed to extremes of pH, deamidation of asparagine and glutamine residues was reported (Popineau and Pineau, 1985 b) and not acid cleavage of peptides. Moreover, 50mM acetic acid can hardly be described as extreme acidic condition.

CONCLUSION

The average M_rs estimated for the γ_{III}-gliadin, γ_V-gliadin and the ω-gliadin were 41K, 46.5K and 76K respectively by SDS-PAGE, and 41K, 44K and 90K respectively by gel filtration. The ω-gliadin had a KEL-type N-terminal amino acid sequence and showed close similarity to the sequence of the ω_1-gliadin of Chinese Spring. The γ_V-gliadin had an NIQ-type sequence which was also very similar to the sequence of a γ_2-gliadin of *T. aestivum*. The N-terminal sequence of the γ_{III}-gliadin, however, had glycine as the first residue but was otherwise similar to the sequence of the γ_2-gliadin of *T. aestivum*. Both γ-gliadin fractions were pure preparations although minor populations of N-terminally truncated polypeptides were present in each. It was impossible to separate further the intact and truncated polypeptides as a result of close similarities in their properties. The cause of the truncations was more likely to have been due to mechanical shearing during extraction rather than acid hydrolysis. There was also a suggestion that the peptide bonds on either side of proline 6 may be susceptible to cleavage.

CHAPTER 4.

FLUORESCENCE AND CIRCULAR DICHROISM SPECTROSCOPY STUDIES OF THE PURIFIED GLIADIN FRACTIONS

INTRODUCTION

This chapter presents the physical characterisation of the folded conformations of the purified gliadin fractions in solution as an extension to their characterisation in terms of M_r, amino acid composition and N-terminal amino acid sequence. Broadly, this involved the use of the physical techniques of circular dichroism and fluorescence spectroscopy to derive information on their time-averaged conformations, flexibilities and stabilities to urea-induced denaturation. As introduction to these studies, a discussion of protein structural organisation and dynamics and the methods normally used to evaluate these are presented. The principles of circular dichroism and fluorescence spectroscopy, which were used in this project, and are sensitive to conformational transitions and structural dynamics in proteins, are also presented. Published work on the structures of gluten proteins including gliadin structural organisation are also briefly discussed as a background and finally, the approach adopted is summarised.

PROTEIN STRUCTURAL ORGANIZATION

Protein folding results in the transformation of the nascent linear polypeptide chain into a compact, relatively rigid three-dimensional structure which in favourable cases, can be

determined to atomic resolution by X-ray crystallography analysis. The folded conformation of a protein comprises different levels of structural organisation, is unique, and determines its functional properties. The primary structure refers to the sequence of amino acid residues in the linear polypeptide chain. Secondary structure refers to the local arrangement of the polypeptide backbone into regular structures such as α-helix and ß-sheets as a result of non-covalent interactions between amino acid side-chains close to one another in the linear sequence. It is stabilised and maintained by hydrogen bonding between the amide and carbonyl groups in the peptide units of the polypeptide backbone. Residues far apart in the linear sequence also interact as a result of covalent disulphide bonds between pairs of cysteine residues as well as non-covalent ionic interactions, hydrogen bonding and hydrophobic interactions. Together, these interactions produce a tightly folded conformation referred to as the tertiary structure. In proteins comprising more than one polypeptide chain, quarternary structure refers to the assembly of the individual chains into a multimeric unit stabilized by the specific interactions between the individual chains. A further structural feature referred to as a domain may also be found in proteins containing 200 or more residues. This can not be defined as rigidly as the other levels of organisation. Along a polypeptide chain, however, domains appear as separate units linked by short segments which are also part of the linear sequence. Interactions are more extensive within a particular domain than between different domains and this may give each domain a distinct identity which could be functional or structural. Structural domains are common among the gluten proteins and these are discussed in detail in later sections.

Different methods exist for analysing the structural organisation of proteins. Primary

sequence may be determined by direct amino acid sequencing or by deduction from known nucleotide sequences. Secondary structure may also be determined by direct or indirect means. Indirect techniques comprise predictive methods and computer-aided modelling both of which are based on the availability of sequence and structural details. Direct methods are mainly spectroscopic, such as circular dichroism (CD), optical rotatory dispersion (ORD), nuclear magnetic resonance (NMR), which are sensitive to protein molecular conformations. However, the only technique which completely resolves the three-dimensional structures of proteins with M_rs in excess of 15K is X-Ray crystallography. This requires 'diffraction quality' crystals for optimal analysis and may take several years to achieve. As a result, although a vast number of proteins have been isolated and characterised, the three-dimensional structures of only a few hundred have been determined to atomic resolution by X-Ray crystallography. Other techniques such as those based on the hydrodynamic properties of proteins like viscometric analysis and ultracentrifugation are also used to analyse the shape, conformation and size of proteins. X-Ray crystallography has not been applied to the study of prolamins and a number of reasons may be responsible for this. Firstly, purification of adequate quantities of homogeneous prolamin components is difficult to achieve due to their extensive polymorphism. Secondly, their unusual aqueous solubility suggests that they may not be readily 'crystallisable' although views contrary to this have been stated (Tatham *et al.*, 1990 b). Thus, prolamin structural analysis have been carried out extensively by CD, ORD, NMR (to a lesser extent) and hydrodynamic techniques. Fluorescence spectroscopy is also not known to have been applied to the study of prolamins despite its high sensitivity to conformational transitions and structural dynamics in proteins. The

basis of the technique is the fluorescence of aromatic residues. The gliadins and other prolamins, however, are intrinsically fluorescent due to their contents of tryptophan, phenylalanine and tyrosine. In this project, therefore, fluorescence spectroscopy was used to complement and extend the characterisation of the purified gliadins using CD.

PROTEIN STRUCTURAL TRANSITIONS AND DYNAMICS

Despite the seeming rigidity of the folded conformations of proteins, significant flexibility and movement of parts relative to one another occur within their matrices. In general, such flexibility, mobility or dynamics are assumed to be important for the functionality of proteins but this remains a largely unproven assumption (Careri *et al.*, 1979). These motions may be due to the vibrations of individual atoms, or the collective movements of a group of atoms covalently linked into one unit, or to movements of whole sections of the protein such as a domain or subunit. Each type of motion is well characterised in terms of the time scale over which it occurs and may be monitored by a wide range of techniques. Flexibility and mobility may occur either in solution or within the crystalline state. It is, however, particularly enhanced in solution. As solution studies are more convenient compared with the solid state, details of the structures, conformations and dynamics of proteins are determined in solution. This approach is supported by evidence which shows that the conformation of a protein in solution generally, approximates to that determined within a crystal lattice (Rupley, 1969; Makinen and Fink, 1977).

Structural dynamics in proteins may be monitored by fluorescence spectroscopy. Flexibility and movement of parts relative to each other are best described by the

rotation of fluorophores such as tryptophan. Fluorescence anisotropy is a measure of the average displacement of the fluorophore in its excited state and the time-course of these motions is revealed by time-resolved measurements. In a polarised field, the parallel ($\parallel$) and perpendicular ($\perp$) components of the fluorescence intensity decay at different rates and the anisotropy (r), is defined as the ratio of the difference between the parallel and the perpendicular intensities to the total intensities, i.e

$$r = \frac{I_{\parallel} - I_{\perp}}{I_{\parallel} + 2I_{\perp}} \qquad (2)$$

The overall rotational displacement of the protein molecule can be predicted with reasonable confidence. In comparing the predicted and observed average displacements, a faster than expected rotational displacement would indicate significant segmental motion within the molecule. Similarly, diffusion controlled collision of quenchers with fluorophores is based on the ability of small neutral molecules, such as acrylamide, to penetrate the protein matrix and quench the fluorescence of the fluorophore. Fluorescence quenching experiments thus provide information on the environment and accessibility of fluorophores to solvent and quencher molecules. A completely buried fluorophore, for instance, will not be accessible to quencher molecules whereas a completely exposed fluorophore will be. Like all other spectroscopic techniques, fluorescence is non-destructive and samples can be recovered after analysis. But the main advantage in using this technique to monitor dynamic processes within the protein matrix is its sensitivity. The phenomenon of fluorescence emission generally occurs on a nanosecond timescale. Hence, dynamic processes which also occur on a similar

timescale such as those described above, directly influence measured fluorescence parameters.

Structural transitions in protein molecules may also be monitored by CD spectroscopy. Protein CD spectra in the far-uv region (i.e. below 250nm), are primarily due to absorption by the peptide bonds in the polypeptide backbone. Thus, the main conformational arrangements of the backbone have distinct CD spectra associated with each as shown for the α-helix, ß-sheet and the 'unordered' or the so-called 'random coil' conformations in Figure 4.1 b. α-Helix spectra are characterised by negative minima around 210nm and 220nm and a positive maximum around 190nm. ß-Sheet spectra show a negative minimum around 215nm and this is accompanied by positive maximum around 195-200nm. Aperiodic structures such as ß-turns, have very weak and variable CD spectra to the extent that where these and ß-sheets are present, the spectra of the sheets predominate. 'Random' structures also give rise to weak CD spectra which are characterised by a negative minimum around 200nm and a maximum around 220nm which may be positive or negative. The strongest CD spectra on the whole, are those of the α-helix and when present these mask all the other spectra. The folded conformations of proteins also have distinct CD spectra in the near-uv region i.e. 250-340nm as a result of absorption by the aromatic side-chains and to a less extent, by chiral disulphide bonds if present. Under conditions in which the folded conformation is increasingly perturbed, a CD spectral scan in the far-uv region will visualize the approach to randomisation of structure as a gradual shift in the spectra of regular and aperiodic structures towards that of a 'random coil'. Under the same conditions, CD spectral scans in the near-uv region will also show shifts if the environment of the aromatic side-chains

becomes sufficiently perturbed. Both the backbone and side chain CD spectra therefore, provide a means of monitoring transitions in protein conformations.

PRINCIPLES OF CIRCULAR DICHROISM SPECTROSCOPY (based on Adler *et al.* (1973))

A beam of linearly polarized light is made up of two components consisting of right and left circularly polarized light with electronic vectors E_R and E_L respectively. Interaction of such a beam with an asymmetric molecule such as a protein, produces the phenomena of circular dichroism (CD) and optical rotatory dispersion (ORD). The asymmetric molecule is then said to be optically active. Of all the amino acids only glycine does not contain an asymmetric carbon atom yet most amino acids display only small ORD or CD spectra. It is, therefore, the conformations of proteins which arise from the asymmetry and arrangement of peptide units in space, which are responsible for their CD and ORD characteristics. E_R and E_L travel at different speeds through the molecule and give rise to optical rotation or rotation of the plane of polarization, measured in degrees of rotation as α_λ. ORD is the variation of α_λ with wavelength, λ. In a wavelength region where the molecule does not absorb light, absorption varies gradually with wavelength and a plot of α_λ versus λ gives a straight line. In an absorbance region, however, α_λ increases sharply in one direction, falls to zero at the absorption maximum and then rises sharply in the opposite direction. This behaviour is referred to as the Cotton effect, and it may be positive or negative. In the region of its Cotton effect, an optically active molecule will absorb E_R and E_L to differing extents. CD is defined as the difference in the extinction coefficients of the left and right handed circularly polarized light, i.e.

Figure 4.1
POSSIBLE ORD AND CD COTTON EFFECTS ASSOCIATED WITH A TYPICAL ABSORPTION BAND (a) AND CD SPECTRA OF THE MAJOR PROTEIN SECONDARY STRUCTURES (b).

a

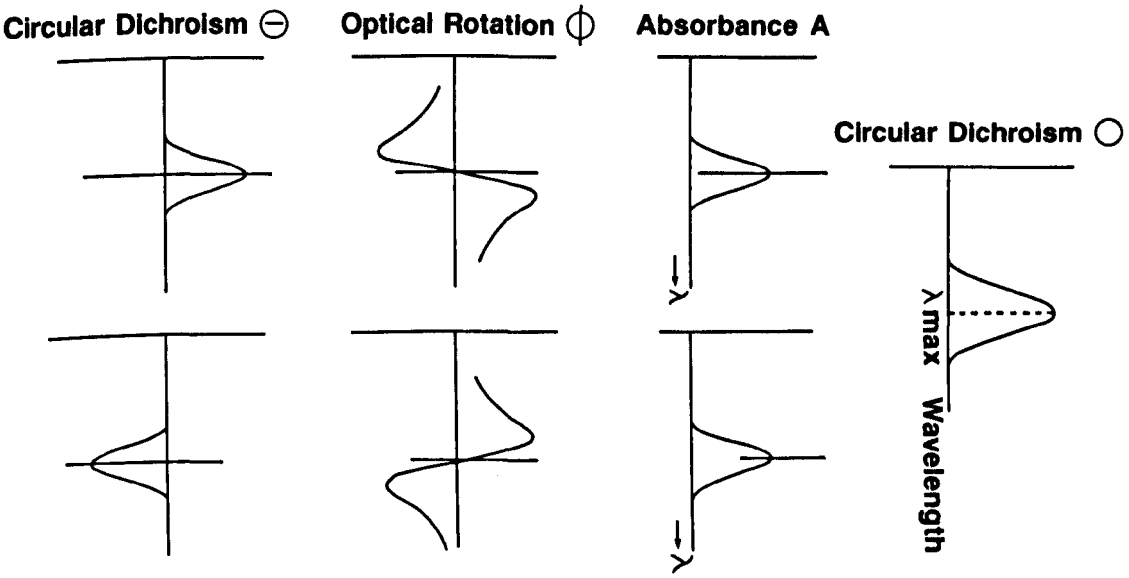

b

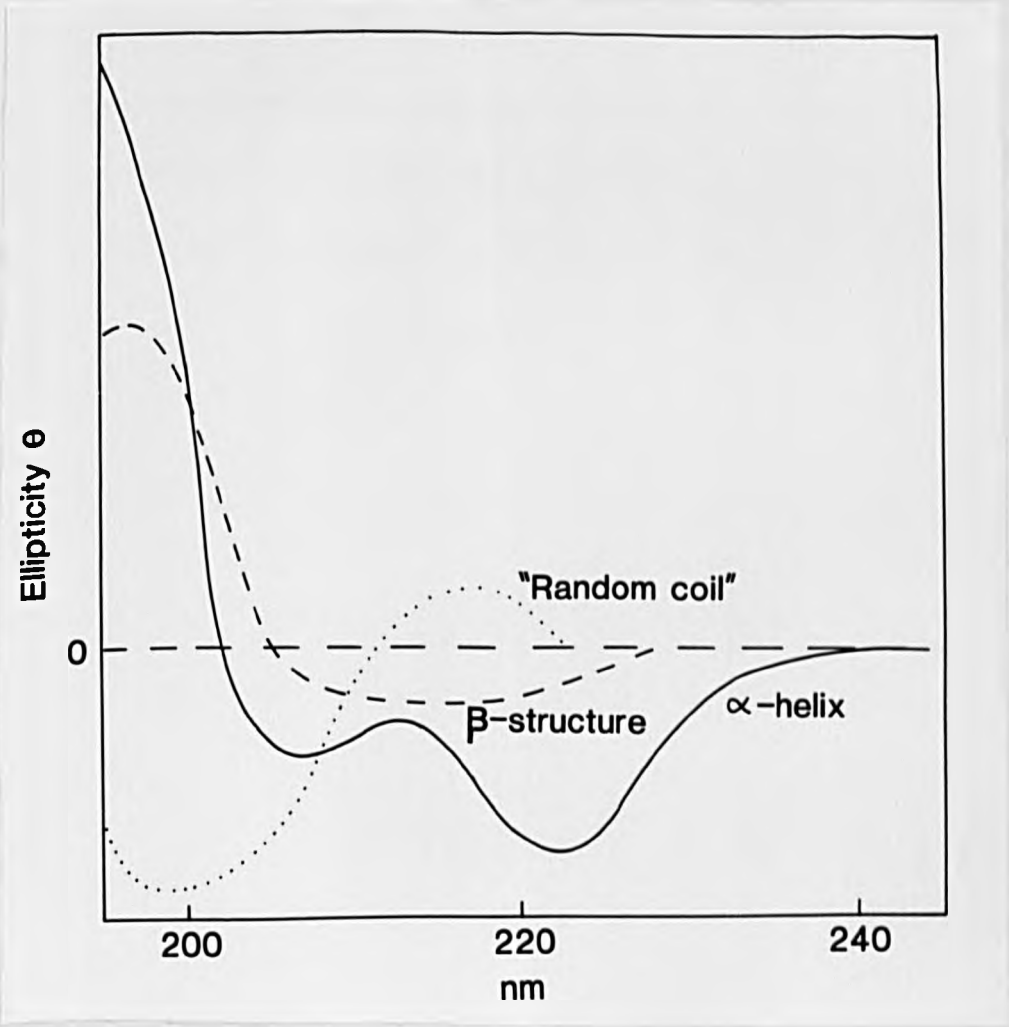

$$CD = (E_R - E_L) \qquad (3)$$

After CD has occurred, the emerging light beam is not linearly polarized but rather elliptically polarized. The ellipticity of the emerging beam, $[\theta]_\lambda$ which is proportional to $(E_L - E_R)$, is a measure of CD. Figure 4.1a shows a typical absorption band at wavelength λ and the possible ORD and CD Cotton effects associated with this. CD data are reported either as the molar ellipticity $[\theta]$ or the molar CD, $\Delta\varepsilon$. The two measurements are equivalent and are related by the following equation,

$$[\theta] = 3300\Delta\varepsilon \qquad (4)$$

The mean residue ellipticity for a protein or polypeptide $[\theta]_\lambda$ is calculated as

$$[\theta]_\lambda = \frac{\theta_{obs} \times M.W}{10 \times d \times c} \qquad (5)$$

where

λ = wavelength

θ_{obs} = observed ellipticity

MW = molecular weight

c = concentration in g ml^{-1}

d = path length in cm.

If the concentration of the protein or polypeptide is known in mg ml^{-1}, its molar concentration, c' can be obtained by dividing the concentration by 113, the average

residual molecular weight of amino acids. The molar ellipticity, [θ] is then calculated as,

$$[\theta] = \frac{\theta_{obs} \times 10}{d \times c'} \qquad (6)$$

The units of [θ] are degrees cm^2 $dmol^{-1}$.

As a result of superior instrumentation, CD has largely superceded ORD in the analysis of protein structures.

PRINCIPLES OF FLUORESCENCE SPECTROSCOPY (based on Bell and Hall (1981); Lakowicz (1981))

The absorption of a photon of energy by a chromophore causes electrons to move from a low energy ground state to a higher excited energy state. The electrons then return to the ground state via a number of possible pathways. One such pathway is the emission of a photon possessing lower energy than the absorbed photon in a process called fluorescence (Figure 4.2). Fluorescence essentially comprises two processes, absorption (or excitation) and emission. At any given energy state, most electrons occupy the lowest level available to them. The transition from ground to excited state occurs on a time-scale of 10-15ns with emission occurring after this. The lifetime of the molecule within the excited state depends on its stability as well as the other processes which compete with fluorescence. Emission occurs from the lowest energy level of the excited state and the return to the ground state by fluorescence always occurs via the excited state. The rate of depopulation of the excited state is described by an overall rate constant k which

is the sum of the individual rate constants for all the competing processes, i.e,

$$k = k_f + k_r \qquad (7)$$

where

k_f = rate constant of fluorescence

k_r = rate constant of various competing processes.

The quantum yield of fluorescence, q is defined as the ratio of the number of photons emitted to the number of photons absorbed i.e,

$$q = \frac{number\ of\ photons\ emitted}{number\ of\ photons\ absorbed} \qquad (8)$$

q, therefore, is also an expression of the efficiency of the fluorescence and from equations 7 and 8 above may further be represented as,

$$q = \frac{k_f}{k_f + k_r} \qquad (9)$$

The relaxation of the excited fluorophore to the ground state is defined by the fluorescence lifetime, T. This is an exponential process which is related to the rate constant of decay, k by the equation,

$$T = \frac{1}{k} \qquad (10)$$

Figure 4.2
POSSIBLE PATHWAYS BETWEEN THE EXCITED STATE AND THE GROUND STATE FOR AN ELECTRON.

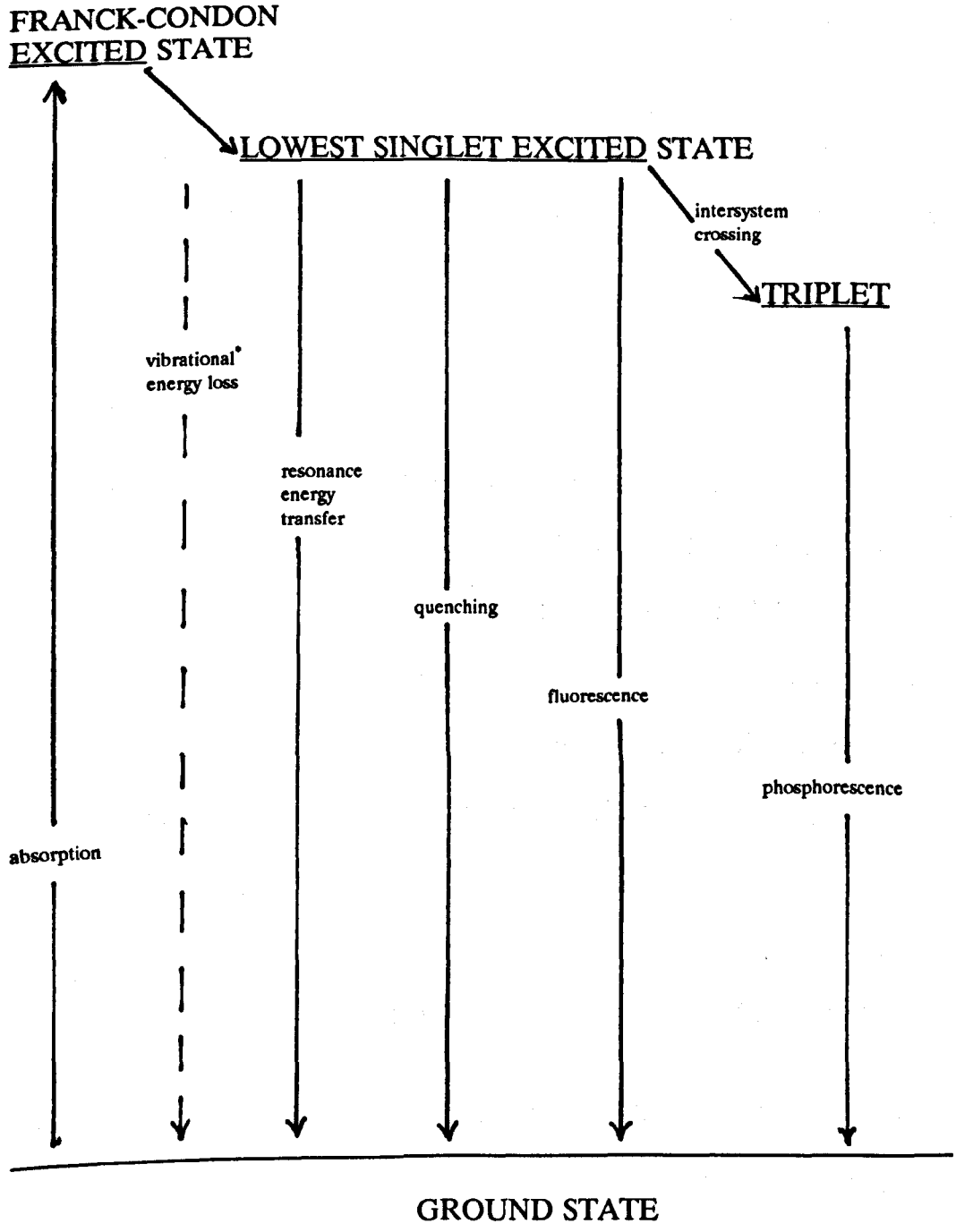

*. no radiation.

Solvent effects influence the efficiency of fluorescence. In a polar environment, the excited state is further stabilized by interactions with solvent molecules, whereas in a non-polar solvent such interactions are minimal. Hence, transfer of a fluorophore from a polar to a non-polar environment is accompanied by an increase in energy difference between the excited and ground states which also leads to a higher quantum yield. The two solvents commonly used to dissolve gliadins, 1% (v/v) acetic acid and 70% (v/v) ethanol are polar and non-polar respectively. The fluorescence lifetimes measured in these solvents will therefore be expected to reflect this difference.

PROTEIN FLUORESCENCE

The aromatic amino acid residues tryptophan, tyrosine and phenylalanine confer their fluorescence properties on protein molecules in which they occur. The absorption wavelengths of these three residues are in the order phenylalanine < tyrosine < tryptophan. Hence the fluorescence emission characteristics of a protein which contains all three residues, will be typical of tryptophan. Tyrosine fluorescence likewise, is observed in the absence of tryptophan and that of phenylalanine only in the absence of both tryptophan and tyrosine.

FLUORESCENCE ANALYSIS OF PROTEIN CONFORMATION AND STABILITY (based on Pace (1986))

Most of the physical properties of proteins are significantly altered under conditions which perturb their folded conformation. Urea and GuHCl reversibly denature proteins by disrupting the non-covalent forces which maintain their folded conformations. The

'unordered' or 'random' coil polypeptide can then be renatured to the native conformation by removal of the denaturant. As the fluorescence of tryptophan residues is sensitive to protein conformational transitions, both processes of denaturation and renaturation may be monitored by tryptophan fluorescence.

Figure 4.3 a shows the spectrum of native ribonuclease T1 and its corresponding spectrum after denaturation in 6M GuHCl. The transition from native to denatured protein is accompanied by a large drop in fluorescence intensity and a shift in the wavelength of maximum emission from 335nm to 355nm. In principle however, fluorescence intensity may increase or decrease upon denaturation and the magnitude of the intensity is not in itself useful for obtaining further information about the structure and stability of the protein. However, in instances such as the denaturation of ribonuclease T1 which proceeds via a considerable shift in wavelength of maximum emission, structural information such as the conformational stability or ΔG^{H20} can be obtained from analysis of the denaturation curve (Figure 4.3 b). For closely-related proteins such as the gliadins which may differ from each other only in a few amino acid residues, ΔG^{H20} values are a useful means of comparing their conformational stabilities in order to draw conclusions about the possible roles of key amino acids in their sequences. It is also possible to obtain indications of possible mechanisms involved in unfolding from denaturation curve analysis. In proteins comprising one or more domains, denaturation curve analysis may also provide clues about the relative stabilities associated with each domain. There are also examples where unexpected results from denaturation curve analysis have led to the unravelling of useful structural information. For instance, when the reduction of disulphide bonds and subsequent unfolding of insulin

Figure 4.3
FLUORESCENCE EMISSION SPECTRA OF NATIVE AND DENATURED RIBONUCLEASE T1 (a), & THE CORRESPONDING GuHCl DENATURATION CURVE (b).

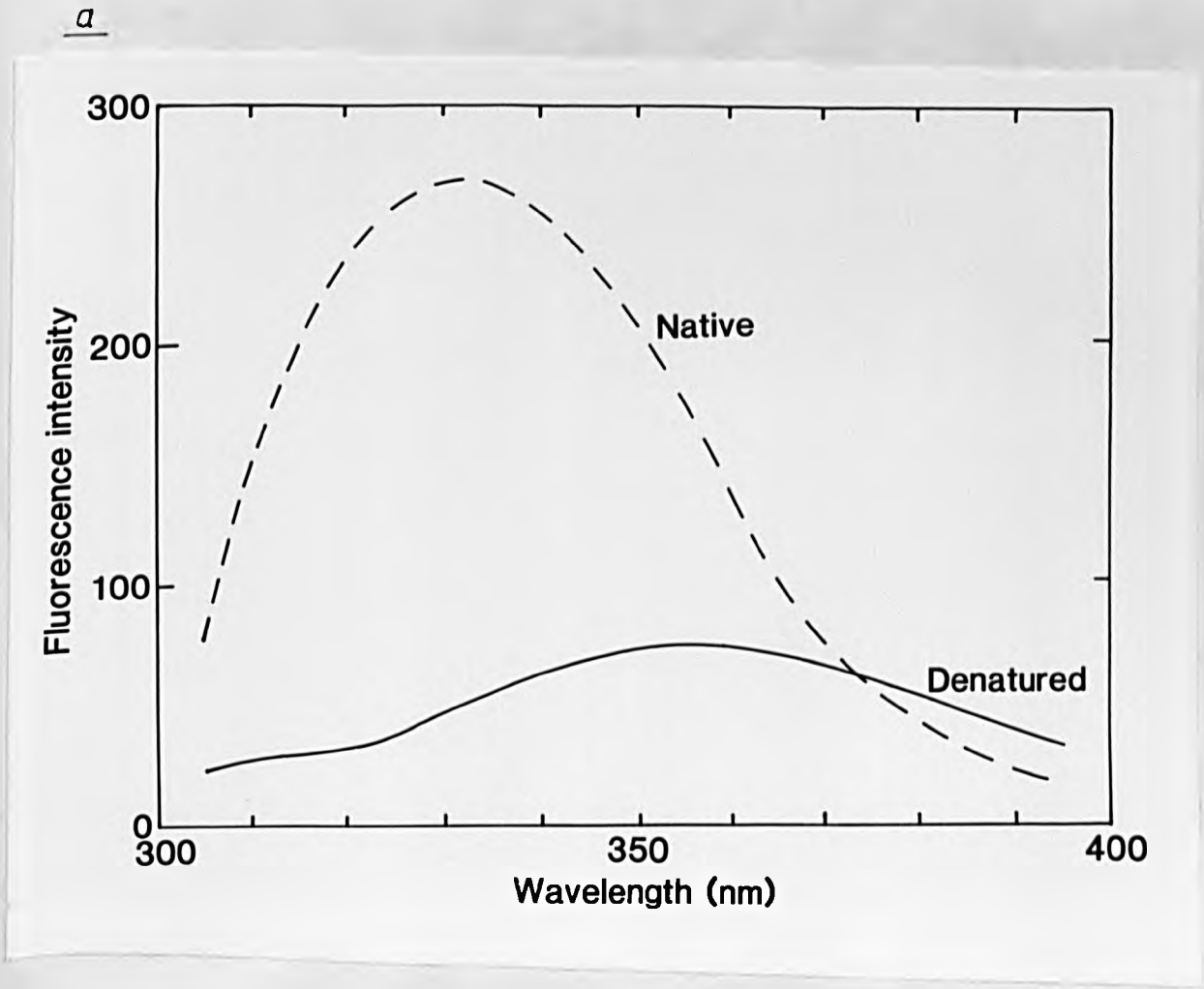

b

(based on Pace, 1986)

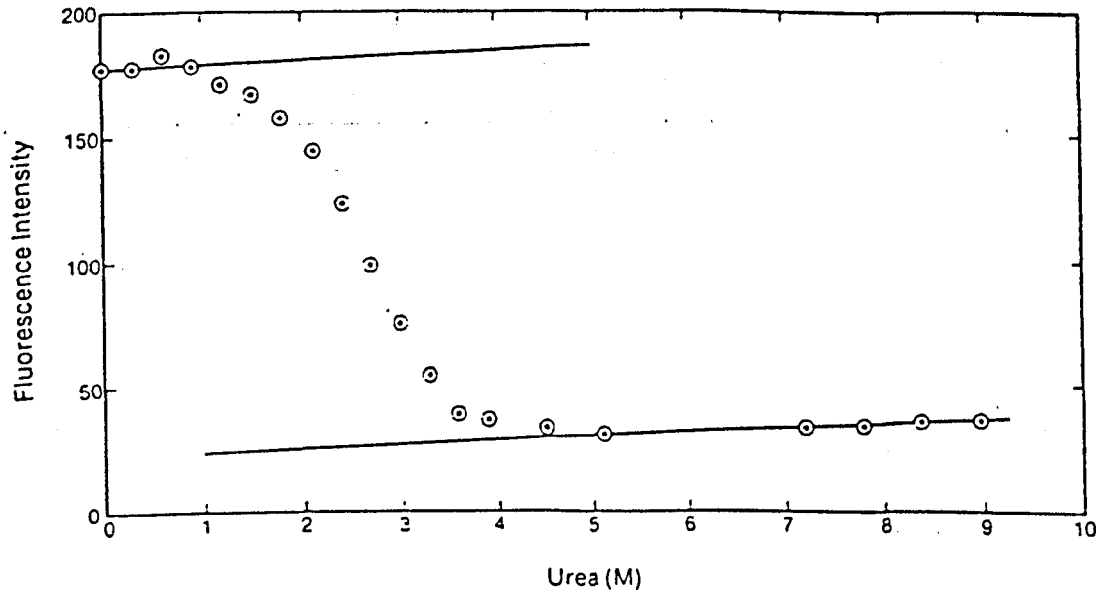

Urea denaturation curve for ribonuclease T_1 in 0.1 *M* Tris (pH 8.05), 30°. The fluorescence intensity was measured at 320 nm with excitation at 278 nm.

were found to be irreversible, it was suggested and later proven that the protein was synthesized in a different form. In order to undertake denaturation studies such as these, however, it is important initially to examine the spectra of the native and denatured forms of the protein under study. It is only when significant shifts in the wavelength of maximum emission exist between these that any of the information mentioned above relating to the structure and stability of a protein may be derived from denaturation curve analysis.

FLUORESCENCE QUENCHING ANALYSIS OF THE ENVIRONMENT OF TRYPTOPHAN RESIDUES.

An early strategy used in the study of the solution structures of proteins involved mapping out the residues which are exposed to and those shielded from the external aqueous environment (Kronman and Robbins, 1970). In later years, low molecular weight reagents were used to quench the fluorescence of tryptophan residues (Lehrer, 1975). These quenchers acted by decreasing the fluorescence intensity of tryptophan through physical collision. The ease with which the fluorescence of the fluorophore was quenched reflected its degree of accessibility to the quencher. Among the quenchers used, the ionic molecules I^-, NO_3^- and Cs^+ introduced additional electrostatic effects which led to inaccurate estimation of the degree of exposure (Lehrer, 1971 a; Burstein *et al.*, 1973; Lehrer, 1971 b). Molecular O_2 was also adopted as a neutral probe (Lakowicz and Weber, 1973) but it had the disadvantage of being small enough to penetrate the interior of proteins fairly rapidly to quench indiscriminately the fluorescence of buried residues as easily as exposed ones. Moreover, being a relatively

hydrophobic molecule, O_2 accumulated in apolar regions of proteins facilitating the quenching of buried residues (Eftink and Ghiron, 1976).

Eftink and Ghiron (1976) first reported the efficient quenching of tryptophan fluorescence by acrylamide and it was shown to be discriminating in sensing the degree of exposure of this residue. Tryptophan quenching by acrylamide, a small neutral molecule of molecular weight 154, is described by a modified form of the Stern-Volmer equation below,

$$\frac{F_0}{F} = (1 + K_{sv}[Q]) \, e^{V[Q]} \qquad (11)$$

where

F_0 = quenching in the absence of quencher

K_{sv} = dynamic quenching constant

V = static quenching constant.

Dynamic quenching is primarily due to collision of quencher with the excited state of the fluorophore while static quenching involves the formation of a complex between the quencher and the ground state of the fluorophore. Dynamic quenching results in a decrease in quantum yield upon addition of quencher but static quenching does not affect the lifetime of the excited state.

The Stern-Volmer equation (11) can be rearranged into the form below,

$$\frac{F_0/F}{e^{V[Q]}} = 1 + K_{sv}[Q] \qquad (12)$$

Figure 4.4
ACRYLAMIDE QUENCHING OF SINGLE TRYPTOPHAN-CONTAINING PROTEINS (based on Eftink & Ghiron, 1976).

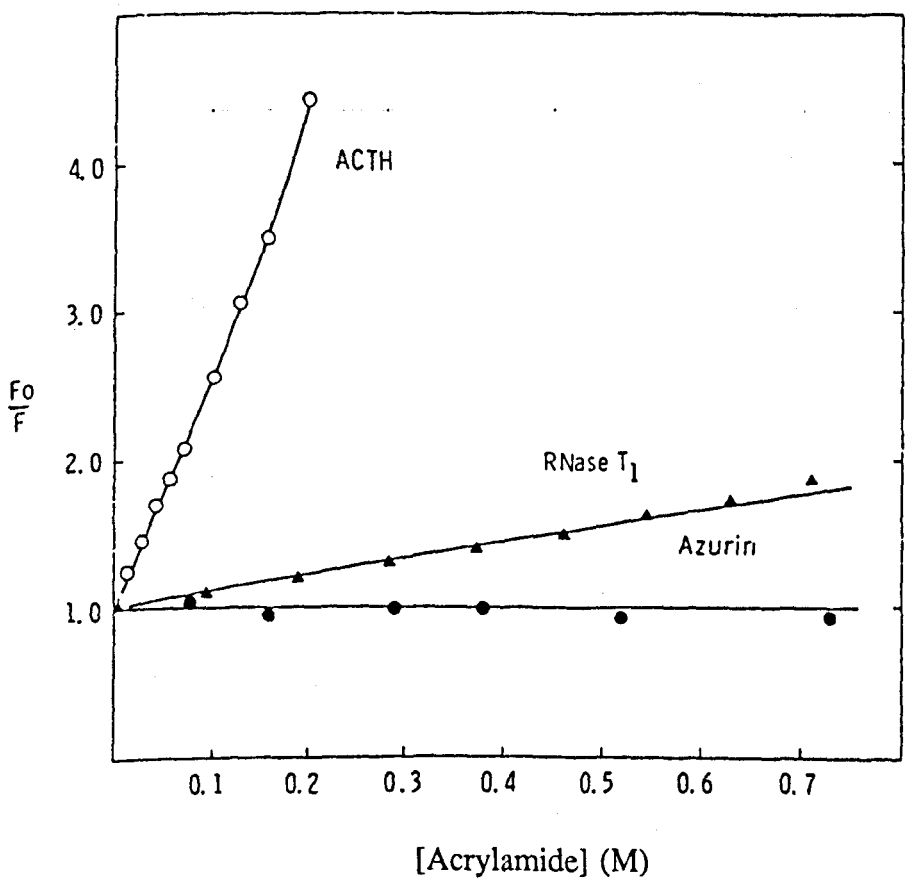

From this, a Stern-Volmer plot of F_0/F as a function of [Q] (quencher concentration) for quenching data, produces three broad types of responses as shown in Figure 4.4 and described below (Eftink and Ghiron, 1976).

1. UPWARD CURVATURE PLOTS eg. ACTH and BSA. In general, this type of plot describes a tryptophan residue accessible to bombardment by quencher molecules. In single tryptophan-containing proteins such as adrenocorticotropin (ACTH), it is indicative of static quenching in which the quencher and fluorophore form a complex before excitation and quenching is independent of the rate of collision of fluorophore and quencher. In multi-tryptophan containing proteins like bovine serum albumin (BSA), which is reported to be the only one known to display this type of curvature, such plots indicate the situation where all the fluorophore residues are accessible to quencher molecules or the situation where the observed fluorescence is dominated by a single residue.

2. *LINEAR PLOTS* eg. RNAse T1, azurin and ß-trypsin. Azurin possesses a single tryptophan residue believed to be completely buried and insulated from quencher or solvent molecules. The horizontal plot obtained for this protein describes the situation where the tryptophan residue is so buried that neither static nor collisional quenching occurs. In practice, few proteins will be expected to follow this sort of quenching behaviour. On a reference scale of possible topographical positioning of tryptophan residues in proteins, however, it represents one extreme (Table 4.1). The RNAse T1 plot on the other hand, is linear with a positive slope. This protein also possesses a single tryptophan residue believed to be completely enveloped within the matrix of the protein. While no static quenching is observed, significant collisional quenching occurs possibly

through intermittent exposure of the buried tryptophan residue. This type of quenching behaviour provided early evidence of the so called 'breathing motion' in protein matrices (Eftink and Ghiron, 1975). In multi-tryptophan containing proteins like ß-trypsin, a linear plot is indicative of a situation where the accessibility of exposed residues is nearly equal to the non-accessibility of buried residues to quencher molecules.

3. *DOWNWARD CURVATURE PLOTS* eg. lysozyme and chymotrypsin. In proteins containing multiple tryptophan residues, the quenching of their fluorescence may be selective with those residues which are more accessible being readily quenched before those which are less accessible. Stern-Volmer plots of the quenching behaviour of such proteins in general, show a downward curvature and studies of other multi-tryptophan containing proteins have also shown Stern-Volmer patterns similar to that of lysozyme and chymotrypsin (Burstein, 1968; Teale and Badley, 1970; Lehrer, 1971).

For single tryptophan-containing proteins, the kinetics of quenching can be divided into a collisional component characterized by K_{sv} and a static component characterized by V in the modified form of the Stern-Volmer equation (11). Plots of the quenching behaviour of this group of proteins give a straight line. Data can therefore be fitted to a linear regression analysis program and V estimated by decreasing or increasing a randomly chosen value until the highest correlation is obtained. As K_{sv} equals the slope of the final plot, the values of both quenching constants can be determined. Quantitative assignment of K_{sv} and V is relatively simple for single-tryptophan containing proteins, but for multi-tryptophan containing proteins, the static component V, is often masked and K_{sv} remains the single most important parameter (Eftink and Ghiron, 1976). For these

proteins, quantitative treatment of quenching data is further complicated by other difficulties. For instance, the emission may be heterogeneous and each fluorophore may have distinct characteristics which can not be resolved. There is also the possibility of radiation-less energy transfer occuring between various fluorophores although this has been demonstrated only in a few cases (Longworth and Ghiron, 1976). For such proteins, useful qualitative information can still be derived from their Stern-Volmer plots. K_{sv} is calculated as the slope of the curve and the values obtained are then compared with values determined for other proteins and inferences drawn from these. Table 4.1 shows typical acrylamide quenching parameters for selected single and multi-tryptophan proteins which differ in the extent of exposure of their tryptophan residues to solvent or quencher molecules. In general, the lower the K_{sv} value of a protein, the least accessible the tryptophan residues are eg. azurin, $K_{sv} = 0$; ACTH, $K_{sv} = 13.0$. V values were not reported for the multi-tryptophan containing proteins.

TABLE 4.1
ACRYLAMIDE QUENCHING PARAMETERS FOR SINGLE[1] AND MULTI[2]-TRYPTOPHAN CONTAINING PROTEINS (based on Eftink and Ghiron, 1976)

Protein	K_{sv} (M^{-1})	V (M^{-1})
Azurin[1]	0	0
HSA[1]	1.0	0.6
RNAse T[1]	1.1	0
Glucagon[1]	10.5	1.0
ACTH[1]	13.0	1.0
BSA[2]	3.7	-
Lysozyme[2]	3.5	-
Chymotrypsin[2]	1.0	-
Pepsin[2]	9.5	-

USE OF SYNCHROTRON RADIATION SOURCE FOR TIME-RESOLVED FLUORESCENCE ANALYSIS

Measurement of time-dependent depolarization of tryptophan fluorescence is useful for monitoring dynamic processes resulting from flexibility within protein molecules. The pulsed properties of a synchroton radiation source (SRS) provide a means of carrying out such measurements. Its main advantages are high accuracy and degree of reproducibility which are the result of unique properties such as a well defined time structure and polarization characteristics. Its disadvantages on the other hand, are its limited availability and high cost of operation. The SERC SRS at Daresbury is normally operated *in multi-bunch* mode during which it delivers high intensities with pulses every 2ns. Single-bunch mode operation is used for time-resolved measurements and this gives lower intensities as well as 0.2ns pulses spaced 320ns apart. The high aperture station HA 12.1 is one of two stations from which experiments utilising single-bunch mode operation are performed. The experimental set-up comprises a linear accelerator (LINAC), 30cm diameter storage rings, a spectrofluorimeter incorporating a sensitive photomultiplier (PM), and a multi-channel analyser (MCA) fitted with a log/linear ratemeter. Electrons are initially 'injected' into the storage rings via the LINAC in the form of a close bunch approximately 6cm long. They are then accelerated to within the speed of light with energy of the order of 2Gev. The accelerating field is created magnetically by constraining the electrons to travel round a closed path. This results in the emission of synchroton radiation in the form of a highly polarized electromagnetic radiation. The electron bunch passes a given point in the storage rings every 320ns. As it does so, a pulse of synchroton radiation lasting 0.2ns or the time taken for the bunch

to pass the point, is generated. Each pulse of photons is directed via a hole in the storage rings placed at an angle to the electron path, into vacuum sealed steel tubes and subsequently, via mirrors to the spectrofluorimeter. A Spex™ monochromator focuses polarised incident radiation of a defined wavelength onto a cuvette holder which may hold a protein solution or a light scatterer, usually Ludox™ solution. The tryptophan residues in the protein solution which are correctly orientated are simultaneously excited and the ensuing fluorescence emission is detected by the PM which in turn, transmits electronic impulses to the MCA/single photon counting (SPC) apparatus. The signals from the Ludox™ solution which are variously referred to as a 'system prompt' or a 'lamp profile', calibrate the time profile of the excitation pulse.

Single photon counting is a sophisticated concept involving the probability distribution for emission of a single photon after an excitation event. By sampling the single photon emission following a large number of excitation flashes, the experiment constructs this probability distribution (O'Connor and Phillips, 1984). The MCA data collection uses a number of channels, usually up to 1,024 and these are 'filled' individually over a specific length of time. The time calibration of an experiment, as distinct from the time profile of the excitation pulse, defines the time taken for each channel to record the maximum number of photons it collects. Both quantities are taken into account during data analysis. A computer program analyses the data from each experiment and up to three exponentials may be fitted to each set of data. In this way, different lifetimes and their relative contributions to the total fluorescence may be resolved as has been reported for three tryptophan residues of a lactate dehydrogenase (Waldman *et al.*, 1987).

BACKGROUND TO STRUCTURAL ANALYSIS OF GLIADIN FRACTIONS (based on Tatham *et al.* (1990 b).

Early analysis of structural aspects of gluten proteins comprised mainly the application of hydrodynamic techniques such as sedimentation equilibrium ultracentrifugation to determine their size and shape (Krejci and Svedberg, 1935; Lamm and Poulsen, 1936; Entrikin, 1941; Taylor and Cluskey, 1962; Wu and Dimler, 1964). From these studies, a high degree of asymmetry and low intrinsic viscosity associated with compact globular conformations were observed for gliadin fractions. Infra-red (IR) studies (Kretschmer, 1957) and wide angle X-ray scattering analysis (Grosskreutz, 1960) also gave a broad indication of a rich content of α-helices within the conformations of gluten proteins. Later, the application of ORD and CD dominated the analysis of the secondary structural content of gluten proteins and this led to further data acquisition. In a series of ORD (Wu and Dimler, 1964; Wu and Cluskey, 1965; Cluskey and Wu, 1966; Wu *et al.*, 1967; Cluskey and Wu, 1971) and CD (Cluskey and Wu, 1971) studies, the α-helix content of gliadins and glutenins in a series of buffers and solvents were reported as in Table 4.2. The reduced content of α-helix structure in 3M urea in both fractions suggested a partial denaturation. When urea concentration was increased to 8M, neither fraction was reported to have retained appreciable ordered structure. However, when both fractions were analysed in solvents which promote hydrogen bond formation an increased content of α-helix was observed. These early studies were limited to a great extent by the heterogeneity of the fractions studied, but, some remarkable results were obtained. For instance, Krejci and Svedberg (1935) extracted gliadins with aqueous ethanol and determined the M_r by ultracentrifugation of a major component as 34.5K.

TABLE 4.2
α-HELIX CONTENT OF WHOLE GLIADIN AND GLUTENIN FRACTIONS IN DENATURING AND NON-DENATURING BUFFERS.

Fraction	α-Helix Content (%)			
	1	2	3	4
Gliadins	19-21	29	23	34-35
Glutenins	10-12	17	14	38-43

1. in the presence of 3M urea
2. in the presence of 2mM HCl
3. in the presence of dilute acetic acid
4. in the presence of hydrogen bond-promoting solvents eg. trifluoroethanol and 2-chloroethanol.

Data based on reference numbers 29-30 & 147-149.

Later analysis of more homogeneous gliadin preparations has shown that the mean M_r of the α- and γ-type gliadins agrees well with this estimate.

More recent progress in the understanding of the structures and conformations of cereal prolamins, have been attributed to the following (Tatham *et al.*, 1990 b):

1. the availability of sequence data on specific prolamin components, and

2. improved methods of analysis.

Thus, structural information have been derived from spectroscopic analysis of purified fractions or synthetic peptides corresponding to known domains within prolamin polypeptides and also from the application of structure prediction algorithms.

STRUCTURAL ANALYSIS OF THE S-RICH PROLAMINS

Of the major prolamins, the S-rich fractions are the most widely studied. Within this class, the A-gliadins of wheat are believed to present the most complete picture of the structure of any group of cereal prolamins (Tatham *et al.*, 1990 b). These are α-type gliadins encoded by genes on chromosome 6A. The extensive structural data available on them is often referred to in the analysis of other prolamin types. Kasarda *et al.* (1968) reported CD spectra for A-gliadin which were typical of a protein rich in α-helix. The side chains were shown to adopt different conformations according to the polarity of the solvent in which it was dissolved but no effect was observed in the backbone conformation under the same conditions. Tatham *et al.* (1985 b, c) also determined the far-uv spectrum of a total α-gliadin preparation in 70% (v/v) aqueous ethanol and showed this to be similar to that reported for A-gliadin by Kasarda *et al.* (1968), but the near-uv spectrum in 70% (v/v) aqueous ethanol, in contrast, showed that the side chains were held in a fixed conformation. The thermal stability of the protein was also found to be unusually high, retaining considerable ordered structure when heated to 80°C in 70% (v/v) aqueous ethanol. The thermal denaturation was reversible and it was suggested that it involved helix-coil transition. Similar changes in the near-uv spectra was reported to indicate significant changes in the folded environment of the aromatic residues upon heating. Secondary structural content was estimated by deconvolution of CD spectra and structure prediction algorithms (Tatham *et al.*, 1985 b, Tatham and Shewry, 1985; Purcell *et al.*, 1988) but each method has its own inherent limitations. In general, the proportion of α-helix or ß-structure estimated varied according to the method of analysis used with the main methods being biased towards the presence of one

or the other secondary structure element. Predictive methods also, may not give correct estimates as a result of the repeat regions of prolamins (Tatham *et al.*, 1990 b). Thus, estimates obtained using this approach may not always reflect true differences in secondary structure content.

Unlike the α-type gliadins, the γ-type gliadins have not been so extensively studied. However, it is known that their far- and near-uv spectra, determined in 70% (v/v) aqueous ethanol, are similar to those of the α-type gliadins (Shewry *et al.*, 1985). They are therefore, rich in α-helix structure and unusually stable to thermal denaturation. Their thermal stability is not significantly altered by reduction and alkylation of their cysteine residues. ß-Sheets occur within their proline-rich N-terminal repetitive domain while the C-terminal non-repetitive domain is predominantly α-helical. Tatham *et al.* (1990 a) reported studies of two peptide fragments derived by the enzymic hydrolysis of an intact γ-type gliadin, one corresponding broadly to the proline-rich N-terminal domain and the other to the non-repetitive C-terminal domain. The overall structural characteristics of the two fragments were shown to be similar to that of the intact polypeptide. They also confirmed the presence of ß-structure (mainly ß-turns), in the N-terminal domain and α-helix in the C-terminal domain. A summary of the secondary structure contents estimated for various S-rich gliadins is shown in Table 4.3.

The generalized domain structures of representative S-rich and S-poor prolamins are shown in Figure 3.2 a and b. In general, S-rich prolamins share a number of common structural characteristics. At the same time, significant differences, notably in the occurence and regularity of ß-turns exist between them. This is influenced by the extent to which repeat motifs are conserved within individual domains. In the α-type gliadins

TABLE 4.3
SECONDARY STRUCTURE CONTENTS (%) OF S-RICH GLIADINS AND THE B1 HORDEIN (S-POOR) FRACTION OF BARLEY.

Fraction	α-Helix	ß-Sheets	Aperiodic Structures ß-Turn	Random coil
α-Gliadin[1]	36-37	11-12	52-53	
ß-Gliadin[1]	36-37	22-23	41-42	
γ-Gliadin[1]	33-34	20-21	46-47	
B1 Hordein[1]	28-30	8-10	60-62	
α-Gliadin[2]	34-35	6-7	36-37	24-25
γ_3-Gliadin[2]	32-33	14-15	42-43	15-17
B1 Hordein[2]	27-28	6-8	38-39	24-25

1. calculated by deconvolution of CD spectra
2. predicted from amino acid sequences
Data based on Shewry *et al.* (1987)

and the LMW/aggregated gliadins, not only are repeat motifs poorly conserved, they are also interspersed with other sequences. Thus, ß-turns in these groups of gliadins tend to be irregular and in the case of the LMW/aggregated type, they are interrupted by regions of other secondary structure. The repetitive domain of the γ-type gliadins on the other hand, is based on a highly conserved motif comprising the heptapeptide sequence PQQPFPQ. As a result, ß-turns in this group of gliadins may be regular enough to form a loose spiral structure. Popineau and Pineau (1988), studied α-, ß- and γ-gliadin fractions under different conditions and concluded on the basis of their hydrodynamic behaviour that the γ-gliadins did not possess the compact/globular shape associated with other S-rich gliadins. Tatham *et al.* (1990 b), however, suggested that this may not be a

universal characteristic of the γ-type gliadins as the M_r values (44K and 46K) reported by Popineau and Pineau (1988) were higher than those of other γ-gliadins and may have been the result of the presence of longer repetitive domains and consequently higher hydrodynamic volumes.

THE STRUCTURES OF THE S-POOR PROLAMINS

Among this group, the C hordein fraction of barley has been extensively studied, mainly as a model system due to the following reasons:

1. it is a homogeneous protein and so is ideally suited for structural analysis
2. amino acid sequence data on it are available.

The structural organisation of C hordein is shown in Figure 3.2 b. Its repetitive region based on the consensus octapeptide PQQPFPQQ, is rich in ß-turns (Tatham *et al.*, 1985 a). The far-uv spectra of the protein in 70% (v/v) aqueous ethanol showed that it was devoid of α-helix or ß-sheet but rich in ß-turns (Tatham *et al.*, 1985 a; Field *et al.*, 1986). Heating it to 70°C in 70% (v/v) aqueous ethanol or 0.1M acetic acid, or the addition of increasing concentrations of trifluoroethanol, all resulted in spectral shifts indicative of increased ß-turn structure. From near-uv CD scans of the protein in 70% (v/v) aqueous ethanol, the side chains were shown to be in a fixed conformation which was stable to heating. The spectral shifts which resulted from the addition of 4M urea however, suggested loss of ordered structure. NMR studies (Tatham *et al.*, 1985 c) have also confirmed the presence of ß-turns. It has been suggested on the basis of hydrodynamic studies (Field *et al.*, 1986; 1987; Tatham *et al.*, 1989) that these ß-turns may form a loose helix and that molecules of C hordein may be rod-shaped.

Less is known about the structure of ω-gliadins. However, short N-terminal amino acid sequences are homologous with that of C hordein. Structure prediction (Tatham et al. (1985 b), as well as near- and far-uv CD data recorded in various solvents at different temperatures (Tatham and Shewry, 1985) also suggest that, like C hordein, they are rich in ß-turns and that the proportion of these increases upon heating. Evidence from FT-IR spectroscopy also supports the presence of ß-turns (Purcell *et al.*, 1988). From hydrodynamic studies, Popineau and Pineau (1988) suggested that the ω-gliadins were non-globular and that their extended structures resulted from the presence of repetitive ß-turns.

THE APPROACH ADOPTED FOR THE PHYSICAL CHARACTERIZATION OF THE PURIFIED GLIADIN FRACTIONS

On the basis of the studies discussed above, a number of approaches could have been used to characterise the folded conformations of the gliadin fractions. Of the two spectroscopic techniques used, the application of CD to the study of prolamin groups is widely reported. Although the application of fluorescence is yet to be reported for any prolamin group, it was used because the gliadins contain tryptophan residues and the technique is very sensitive to fluctuations in the environment of this residue. The availabilities of both steady-state and time-resolved fluorescence facilities also meant that the conclusions from these studies could be compared with those from the CD experiments. In order to establish a basis for detailed denaturation studies, however, the conformations of native and fully denatured samples of each fraction had to be compared. Preliminary experiments were therefore carried out in which each fraction

was exposed to 0-10M urea and GuHCl. For simplicity, aliquots of each fraction were designated, according to different treatments, 'native' when dissolved in 1% (v/v) acetic acid or 70% (v/v) ethanol, 'denatured' when dissolved in urea or GuHCl and 'reduced/alkylated' after treatment with 40mM DTT and 100mM IAM according to the protocol of Waxdall *et al.* (1968) as described in Chapter 3. The conformations of each fraction under these conditions, were monitored initially by fluorescence emission wavelength scans. Similarly, their backbone and aromatic side chain conformations, were monitored by CD scans in the far- and near-uv wavelength regions respectively. SDS-PAGE was also used to monitor the effect of reduction and alkylation of cysteine residues on their conformations, which may result in reduction in electrophoretic mobility due to unfolding of the polypeptide chain. As a result of the complementary use of SDS-PAGE, further denaturation analyses were carried out using urea because unlike GuHCl it is uncharged. Moreover, in preliminary fluorescence analysis, greater quantum yields were observed in the presence of urea than GuHCl. Fluorescence quenching experiments were carried out in order to derive information on the environments of the individual tryptophan residues. Denaturation and reduction/alkylation did not appear to affect the quenching characteristics of tryptophan residues in any of the three fractions. Further quenching analyses were therefore confined to the 'native' conformations. Time-resolved lifetime and anisotropy measurements were carried out using the SERC SRS at Daresbury. Limited availability of this facility, however, meant that preliminary lifetime and anisotropy experiments were performed on only the γ_{III}-gliadin and the γ_{V}-gliadin fractions.

AIMS

The overall aims of the physical characterisation of the γ_{III}-gliadin, γ_{V}-gliadin and ω-gliadin fractions were as follows:

1. to use fluorescence and circular dichroism spectroscopy to monitor the native and denatured conformations of each fraction, and

2. to draw conclusions on the unfolding and refolding of their conformations *in vitro*.

MATERIALS

CD facilities were provided by the Department of Chemistry, University College, London. Time-resolved fluorescence experiments were carried out at the SERC Daresbury Laboratory with the SRS operated in single-bunch mode.

CHEMICALS

PRODUCT		SOURCE
Acetic acid (glacial)	AR	Fisons Ltd
Acrylamide	AR	BDH
Dithiothreitol	AR	Boehringer Mannheim
Ethanol (absolute) 'spectrosol grade'		Romil Chemicals
Guanidinium chloride (GuHCl) 'grade 1'		Sigma
Urea 'ultra pure grade'		Bethesda Research Laboratories

The water used for all the physical experiments was 'double filtered millipore grade' from local supplies.

SOLUTIONS

2M acrylamide and 10M urea were prepared by dissoving the appropriate weight of solute in a measured volume of 1% (v/v) acetic acid, and filtered. The acrylamide solution was stored in a dark reagent bottle.

EQUIPMENT

FLUORESCENCE SPECTROSCOPY

PRODUCT	SOURCE
LS-5B Luminescence spectrometer	Perkin-Elmer
3700 data station	"
FX-85 printer	Epson
F3-Water bath	Haake
Stoppered quartz cuvettes (1ml, 1cm lightpath)	Hellma Precision Instruments

CIRCULAR DICHROISM SPECTROSCOPY

PRODUCT	SOURCE
JASCO J-600 spectropolarimeter	Japan Spectroscopy Company
Stoppered cuvettes (1ml, 0.02/1.0cm lightpaths)	Hellma Precision Instruments

METHODS

SAMPLE PREPARATION

'Native' and 'denatured' γ_{III}-gliadin, γ_V-gliadin and ω-gliadin samples were prepared in 1% (v/v) acetic acid and in the same solvent containing 1 to 10M urea. Reduction and alkylation of cysteine residues was performed on each gliadin fraction according to the method of Waxdall *et al.* (1968), as described in Chapter 3 with the ω-gliadin which lacks this residue, acting as control. The buffer was 100mM sodium phosphate, pH 7.0, containing 40mM DTT and 100mM IAM. For subsequent analysis of 'reduced/alkylated' samples of each fraction, the sodium phosphate buffer was replaced by exhaustive dialysis against 1% (v/v) acetic acid. The concentration of protein in each sample was 1mg ml^{-1}.

DETERMINATION OF THE FLUORESCENCE EMISSION SPECTRA OF THE GLIADIN FRACTIONS

100μl aliquots of the 'native', 'denatured' and 'reduced/alkylated' samples of the γ_{III}-gliadin, γ_V-gliadin and ω-gliadin fractions each containing 100μg protein, were placed in separate 1ml (1cm lightpath) stoppered quartz cuvettes. Each sample solution was excited with incident light at 295nm and the emission spectrum was recorded in the wavelength range 300-450nm. The spectrum of a blank solution containing identical components as the sample except protein, was also recorded as described above. The blank spectrum was subtracted from the sample emission spectrum to obtain the corrected spectrum. The excitation and emission monochromator slits were set at 2.5 and 5.0 widths respectively and the temperature of the cuvette holder was thermostatically controlled at 20°C.

FLUORESCENCE QUENCHING ANALYSIS

'Native' samples of the three gliadin fractions each containing 70μg protein in a total volume of 700μl were measured into separate 1ml stoppered quartz cuvettes (1cm lightpath). Each solution was excited with incident light at 295nm and the initial emission in the absence of acrylamide was recorded at 350nm. 20μl aliquots of 2M acrylamide solution were successively added to each sample solution up to a final acrylamide concentration of 0.57M and the emission after each acrylamide addition was recorded at 350nm. A blank solution containing only 1% (v/v) acetic acid was also titrated with 2M acrylamide as above. The fluorescence emission of the blank solution was subtracted from the corresponding sample emission at each acrylamide concentration to obtain the corrected emission. Excitation and emission slit widths of 10.0 and 5.0 respectively were used and the temperature of the cuvette holder was thermostatically controlled at 20°C.

DATA ANALYSIS

F_0 and F values for each sample at every acrylamide concentration were corrected for acrylamide absorbance and dilution using an inner filter factor as reported by Parker (1968). Stern-Volmer plots of $[F_0/F]$ versus [Q] for each gliadin fraction were analysed by a linear regression program developed within the RBF group at University of Kent at Canterbury. K_{sv} was calculated as the slope of the curve.

TIME-RESOLVED LIFETIME AND ANISOTROPY MEASUREMENTS

Two separate operations were performed involving the initial collection of scatter data

using a standard solution of Ludox™ available on-site, followed by the collection of protein lifetime and anisotropy data. Each protein sample consisted of a 1ml aliquot containing 1mg of either the γ_{III}-gliadin or γ_{V}-gliadin fraction in either 1% (v/v) acetic acid or 70% (v/v) ethanol and each sample was placed in a separate stoppered quartz curvette (1cm lightpath).

SCATTER DATA COLLECTION

All previous data held in the memory of the SPC apparatus were cleared by turning the 'MEMORY' switch to 'EXT' and pressing the 'ERASE' button. The emission polarizer in the spectrofluorimeter was set to the 'magic angle' of 351.4° according to on-site instructions. The emission PM shutter was then closed and the Ludox™ sample placed in the sample chamber, after which the chamber was covered with a black cloth to prevent light leakage. The excitation wavelength was changed to 340nm by typing the command 'MO SP 340' and the excitation monochromator slits were turned down to 0.5. The emission photomultiplier (PM) shutter was then opened while the slits were adjusted until a reading of 25kHz registered on the ratemeter attached to the MCA. The SPC memory was then set to 2 and the 'PRESET' button was turned to 'COUNTS'. The SPC was tuned to collect 50K counts and collection of scatter data was started by pressing the 'COLLECT' button, and allowed to proceed until 50K counts registered in any one channel.

PROTEIN FLUORESCENCE DATA COLLECTION

LIFETIME ANALYSIS

With the emission PM shutter closed, the sample chamber was opened, the Ludox™ solution was replaced with a protein sample and the chamber was covered with a black cloth. The excitation wavelength was changed to 295nm by typing the command 'MO SP 295' and the excitation monochromator slits were adjusted as described above. The SPC memory was set to 3 and with the 'PRESET' button still on 'COUNTS' and the SPC tuned to collect 50K counts, protein data collection was started by pressing the 'COLLECT' button. After collection of data, the SPC memory was set to 'EXT' and the scatter data held in memory 2 and the protein data in memory 3 were transferred from the SPC apparatus to the local computer by typing the command 'OU'. The two sets of data were then transferred from the local computer to the mainframe by typing the 'TR' command.

ANISOTROPY ANALYSIS

The sequence of events used in the collection of both scatter and protein data in the anisotropy measurements was similar to that used in the lifetime measurements except for a few minor changes. After erasing all previous data from the SPC, the polarizer was released by loosening the screws holding it. The freedom of the polarizer to rotate was checked by typing the 'TU PA' command after which it moved to the parallel position. Scatter data was collected and stored using the Ludox™ solution as already described except that the SPC was tuned to collect 100K counts corresponding to 50K counts for each of the parallel and perpendicular components. After replacing the Ludox™

solution with the protein sample, the excitation wavelength was changed to 295nm and the excitation slit widths were adjusted as described above. The SPC memory was set to 'EXT', the 'PRESET' button switched to 'SECONDS' and the SPC dials were adjusted to read 200-300s or the time taken for 50K counts to register in any one channel for each of the parallel and the perpendicular components. The collection of anisotropy data was started by typing the 'R' command to initiate the 'ROTATE' program using a dwell time of 50s. Output of data from the SPC to the local computer and subsequent transfer to the mainframe were carried out as described above. Scatter data, parallel component and perpendicular component data were stored by convention, in memories 2, 3 and 4 respectively. All the time-resolved fluorescence experiments were carried out at 20°C. Single determinations were carried out for each fraction.

DATA HANDLING

The mainframe at Daresbury was accessed from University of Kent at Canterbury through the 'SGATE' commmand using the instruction 'CALL DLSWTCH'. Lifetime data were analysed by the 'FLUORFIT' program and anisotropy data by the 'FLUOROT' program. Each set of data was fitted to 1 or 2 exponentials between channels 1 and 900 out of a total of 1,024 available. Attempts to fit 3 exponentials were not successful. Lifetime (τ) and rotational correlation time (ϕ) values were calculated by the appropriate programs and the relative fluorescence intensity associated with each was given by an A value. In addition to evaluating rotational correlation times for each set of anisotropy data, 'FLUOROT' also automatically calculated a lifetime (τ^*) value fitted to one exponential.

CD ANALYSIS

A stock solution of 10M urea in 10mM acetic acid was serially diluted in steps of one molar, to give separate solutions containing 1-10M urea in 10mM acetic acid. A control solution containing only 10mM acetic acid was also prepared. For each gliadin fraction, 1mg protein was dissolved in 1ml of the solutions containing 0-10M urea to give 11 separate sample solutions. Far- and near-uv CD spectral scans were carried out on each sample solution in the wavelength ranges 190-260nm and 240-310nm respectively using a JASCO J-600 spectropolarimeter. A baseline was initially recorded for each of the wavelength ranges above by scanning the control solution. Far-uv CD spectra were also recorded for separate aliquots of 'reduced/alkylated' forms (after dialysis against acetic acid) of the γ_{III}-gliadin, γ_{V}-gliadin and ω-gliadin fractions, each containing 1mg ml^{-1} protein in 1% (v/v) acetic acid. The standard set of conditions used for the far- and near-uv CD scans are shown in Table 4.4.

DATA HANDLING

The CD spectra were analysed using the 'CONTIN 2' program as reported by Provencher and Glockner (1981). The raw sample spectra were initially corrected by subtracting the corresponding baseline. Each corrected spectrum was then converted to $\Delta\varepsilon$ or molecular CD units using a molar concentration factor of 1/113 or 8.85×10^{-3} (where 1 = concentration of protein in mg ml^{-1} and 113 = average residual molecular weight of amino acids) and the appropriate lightpath i.e 0.02cm for far-uv CD spectra and 1.0cm for near-uv CD spectra.

TABLE 4.4
STANDARD CONDITIONS FOR CD ANALYSIS

Condition	Far-uv region	Near-uv region
Data mode	CD	CD
Cell type	0.02cm	1.0cm
Band width	1nm	1nm
Slit width	auto	auto
Sensitivity	20/50 mdeg	5mdeg
Time constant	4s	4s
Start wavelength	260nm	310nm
End wavelength	190nm	240nm
Step resolution	2nm	0.2nm
Scan speed	10nm min^{-1}	10nm min^{-1}
Number of scans	1	1
Alternate	Off	Off

RESULTS

EMISSION SPECTRA ANALYSIS

The fluorescence emission spectra of the 'native', 'denatured' and 'reduced/alkylated' forms of the γ_{III}-gliadin, γ_{V}-gliadin and ω-gliadin fractions are shown in Figure 4.5 a, b and c respectively. In Figure 4.6 a, b and c the spectrum of the 'native' form of each fraction is compared with the spectrum recorded for the corresponding 'denatured' and 'reduced/alkylated' form after dialysis. The spectra recorded for all the fractions were reproducible in several wavelength scans.

For each fraction, the spectra of the 'reduced/alkylated' and 'denatured' forms all showed higher fluorescence emission intensities than the corresponding 'native' spectrum.

The wavelength of maximum emission for the 'native' gliadins, was around 350nm while for their equivalent 'denatured' and 'reduced/alkylated' forms, shifts ranging from 354-356nm were observed (Figure 4.5). After dialysis, the spectra of the 'denatured' and 'reduced/alkylated' ω-gliadin samples were similar to that of the 'native' ω-gliadin (Figure 4.6c). For the two γ-gliadin fractions also, the spectra of their dialysed 'denatured' forms were similar to that of their respective 'native' forms (Figure 4.6 a and b). The spectra of the corresponding 'reduced/alkylated' samples, however, each showed a wavelength of maximum emission around 354nm after dialysis (Figure 4.6 a and b). Thus, in the ω-gliadin fraction, the shifts in wavelength of maximum emission was due only to the presence of denaturant whereas in the two γ-gliadin fractions, the presence of denaturants as well as the reducing and alkylating agents DTT and IAM respectively, led to shifts in the wavelength of maximum emission. Unlike the effect of denaturants alone which was reversible in all three fractions, the effect of reduction and alkylation was not reversible in the two γ-gliadin fractions. Despite these differences, none of the observed shifts was great enough for further detailed denaturation analysis in any of the three fractions.

FIGURE 4.5
FLUORESCENCE EMISSION SPECTRA OF 'NATIVE' (A), 'DENATURED' (B) AND 'REDUCED/ALKYLATED' (C) γ_{III}-GLIADIN (a), γ_{V}-GLIADIN (b) AND ω-GLIADIN (c)

a.

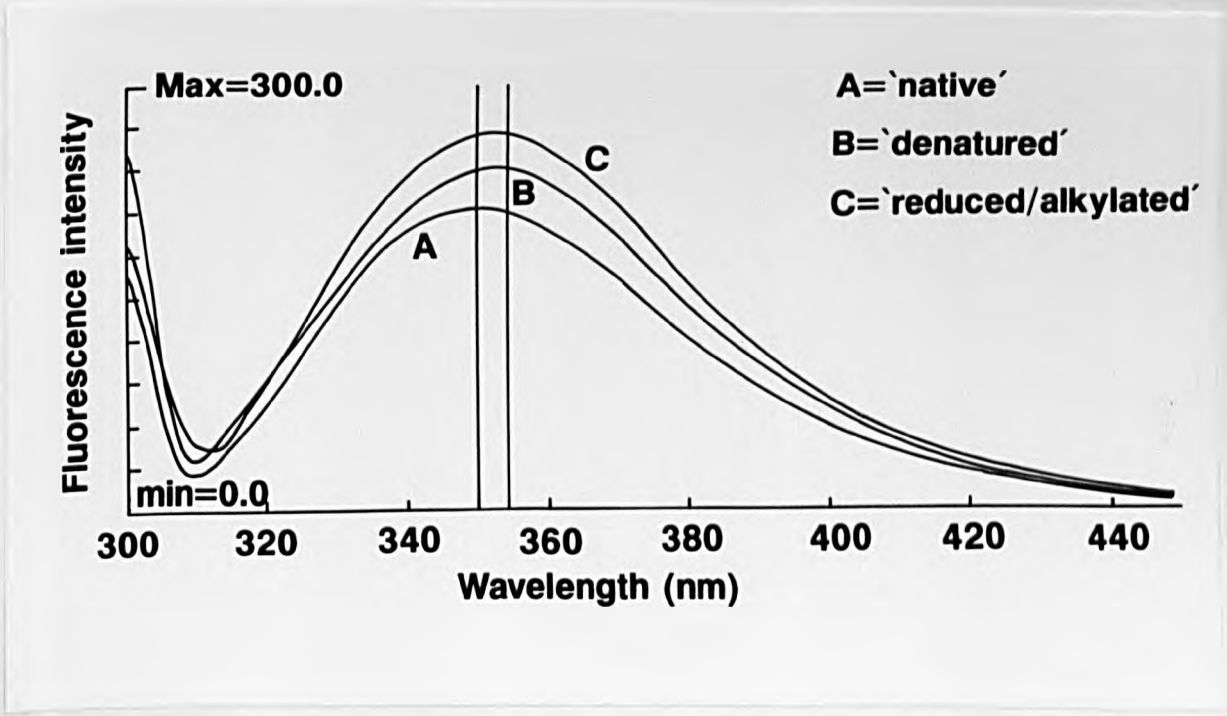

b.

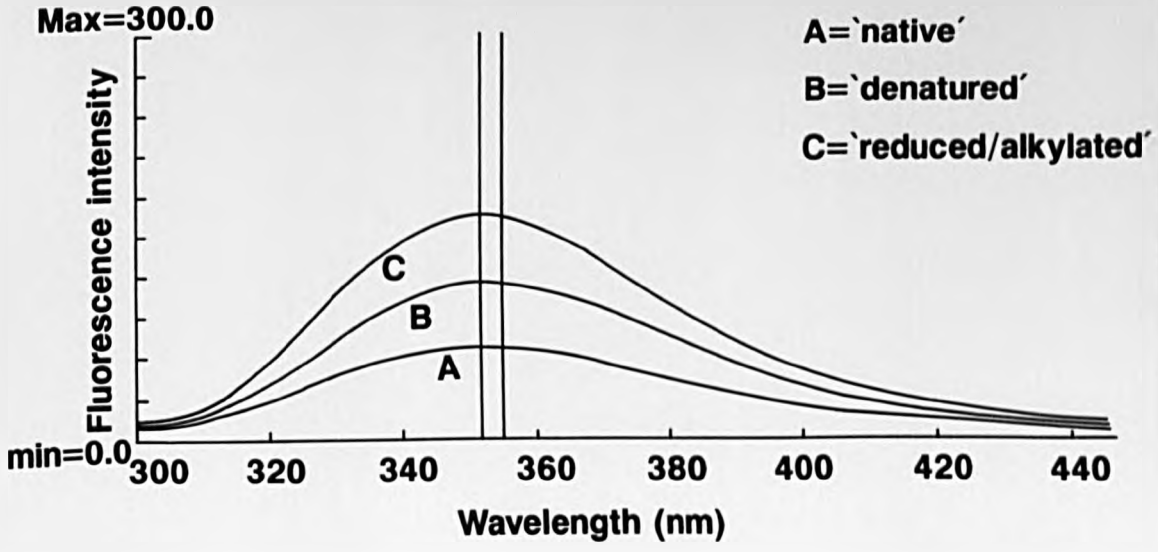
Max=300.0
min=0.0
Fluorescence intensity
A=`native´
B=`denatured´
C=`reduced/alkylated´
C
B
A
300
320
340
360
380
400
420
440
Wavelength (nm)

c.

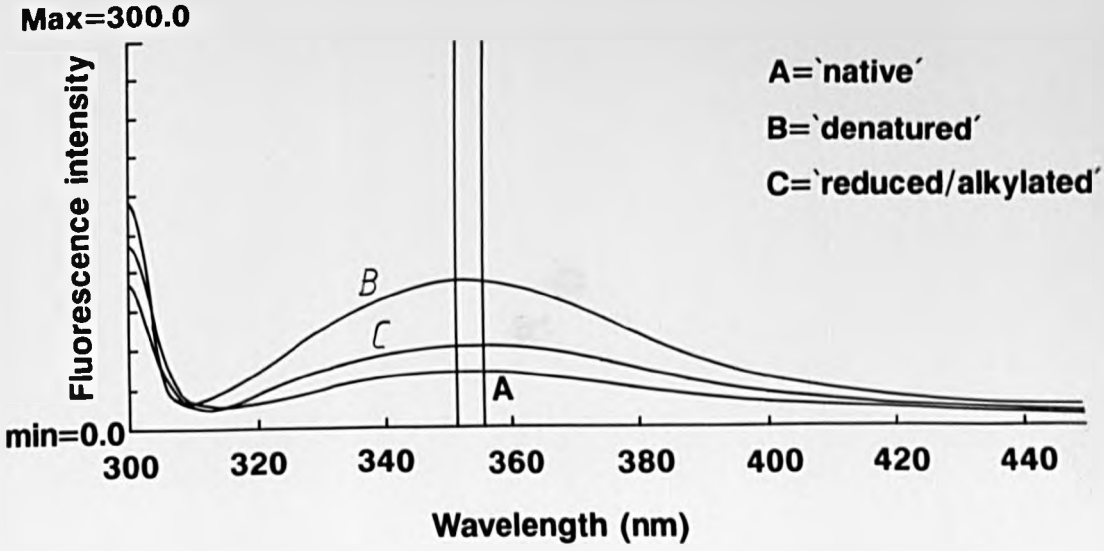
Max=300.0
Fluorescence intensity
min=0.0
A=`native´
B=`denatured´
C=`reduced/alkylated´
B
C
A
300
320
340
360
380
400
420
440
Wavelength (nm)

FIGURE 4.6 a.
COMPARISONS OF THE FLUORESCENCE EMISSION SPECTRA OF 'DENATURED' (B) AND 'REDUCED/ALKYLATED' (C) γ_{III}-GLIADIN AFTER DIALYSIS IN 1% (v/v) ACETIC ACID, WITH THE SPECTRUM OF THE 'NATIVE' PROTEIN.

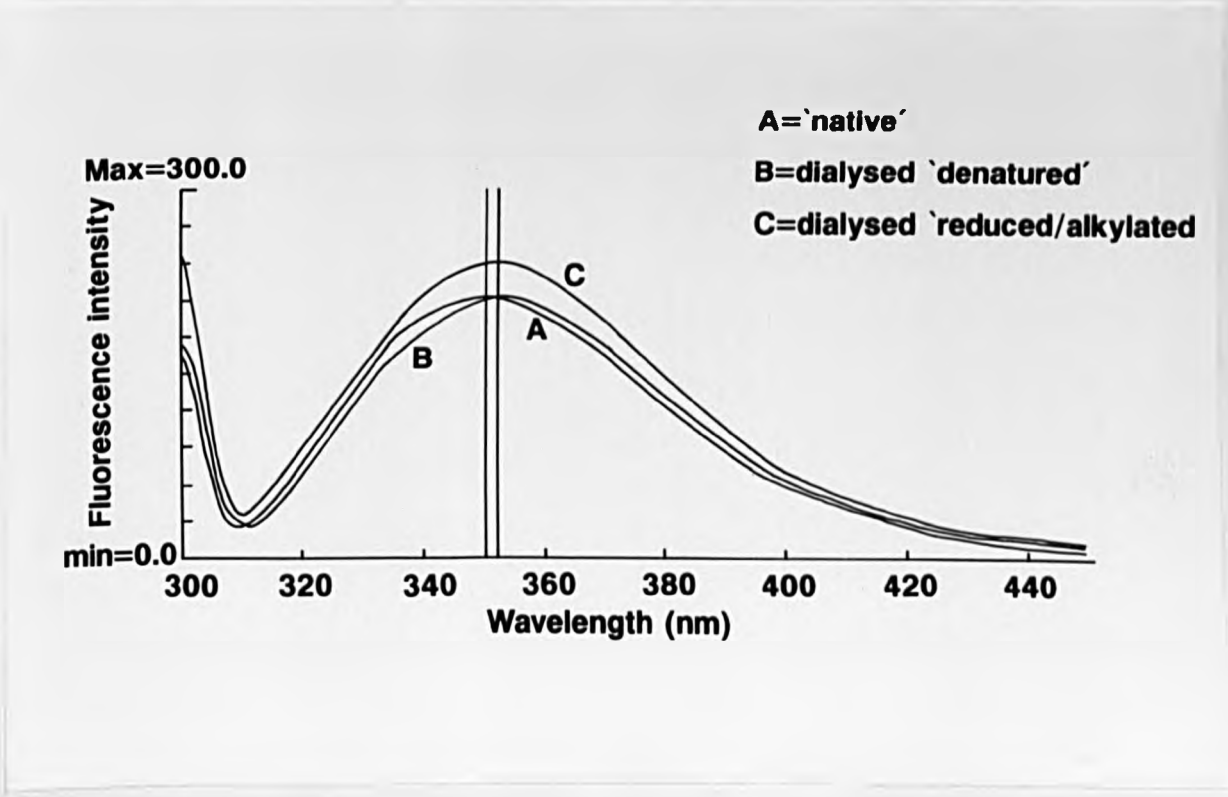

FIGURE 4.6 b.
COMPARISONS OF THE FLUORESCENCE EMISSION SPECTRA OF 'DENATURED' (B) AND 'REDUCED/ALKYLATED' (C) γ_V-GLIADIN AFTER DIALYSIS IN 1% (v/v) ACETIC ACID, WITH THE SPECTRUM OF THE 'NATIVE' PROTEIN.

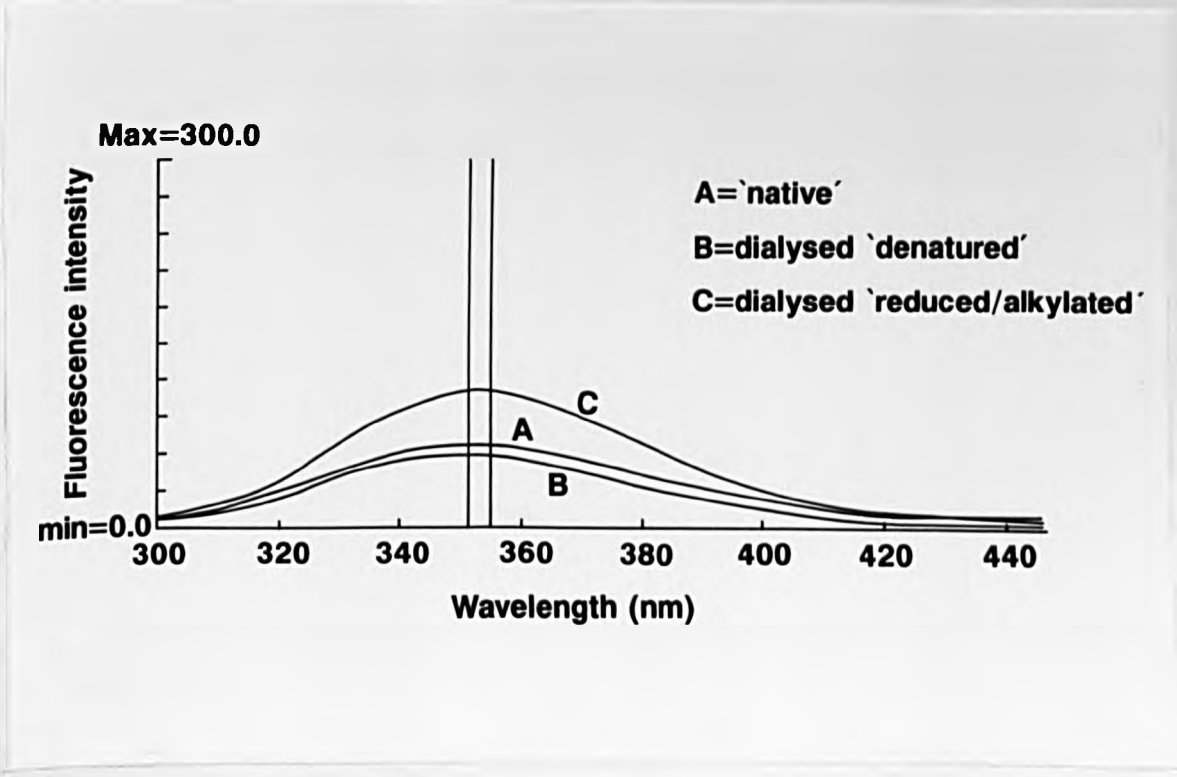

FIGURE 4.6 c.
COMPARISONS OF THE FLUORESCENCE EMISSION SPECTRA OF 'DENATURED' (B) AND 'REDUCED/ALKYLATED' (C) ω-GLIADIN AFTER DIALYSIS IN 1% (v/v) ACETIC ACID, WITH THE SPECTRUM OF THE 'NATIVE' PROTEIN.

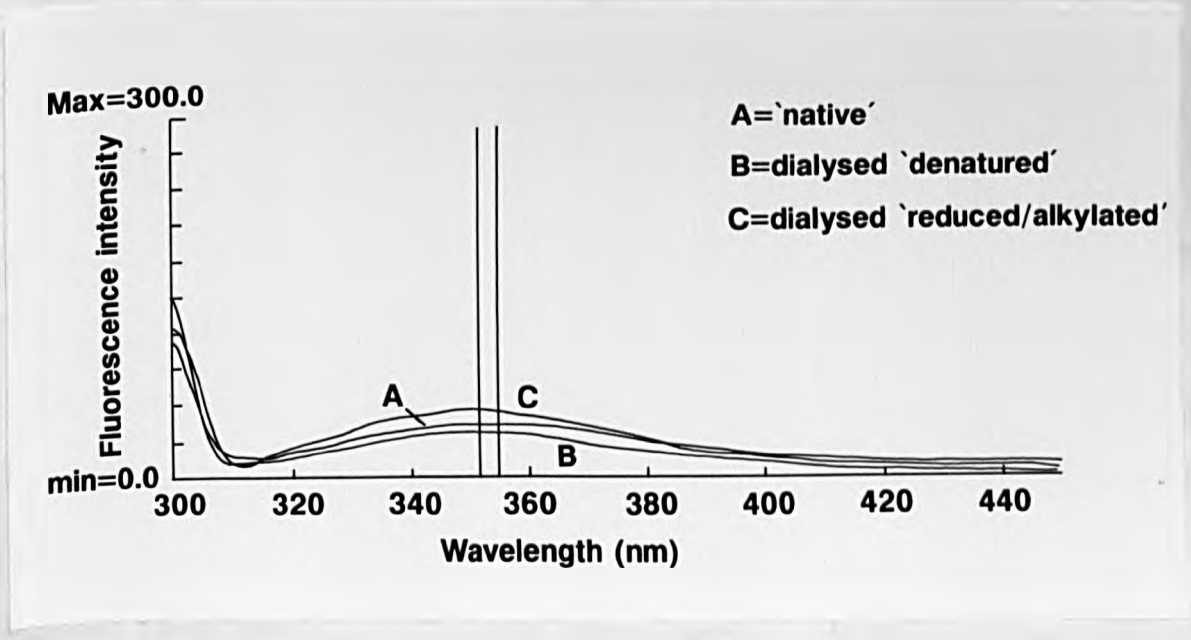

FLUORESCENCE QUENCHING ANALYSIS

Acrylamide quenching plots for the γ_{III}-gliadin, γ_V-gliadin and ω-gliadin fractions are shown in Figure 4.7. Up to an acrylamide concentration of 0.57M, the plot for each fraction showed an upward curvature, this being very marked in the ω-gliadin and the γ_{III}-gliadin fraction. As each fraction contains multiple tryptophan residues, these upward curvatures suggest either that the observed fluorescence is dominated by a single residue or that all tryptophan residues are accessible to quencher molecules in each fraction. Although the curvature of Stern-Volmer plots generally give an indication of the accessibility of tryptophan residues, in multi-tryptophan containing proteins, K_{sv} is a more reliable indicator. K_{sv} values obtained from the plots in Figure 4.7 are shown in Table 4.5. Compared with K_{sv} values of 0, 1.0 and 13 reported for azurin, HSA and ACTH respectively (Eftink and Ghiron, 1976), values of 12, 15 and 18 obtained for the γ_{III}-gliadin, γ_V-gliadin and ω-gliadin fractions respectively, suggested the presence of highly exposed tryptophan residues in all these fractions. Thus, on the basis of their Ksv estimates, the accessibility of tryptophan residues in the three fractions was in the order, ω-gliadin > γ_V-gliadin > γ_{III}-gliadin.

TIME-RESOLVED LIFETIME AND ANISOTROPY ANALYSES

LIFETIME

Lifetime parameters obtained for the γ_{III}-gliadin and γ_V-gliadin fractions in 1% (v/v) acetic acid and 70% (v/v) ethanol are shown in Table 4.6. In both fractions average lifetime values of 3ns and 4ns in 1% (v/v) acetic acid and 70% (v/v) ethanol respectively, were obtained when the data were fitted to a single exponential decay.

FIGURE 4.7
STERN-VOLMER PLOTS OF ACRYLAMIDE QUENCHING OF TRYPTOPHAN FLUORESCENCE IN γ_{III}-GLIADIN (+), γ_V-GLIADIN (◇) AND ω-GLIADIN (□).

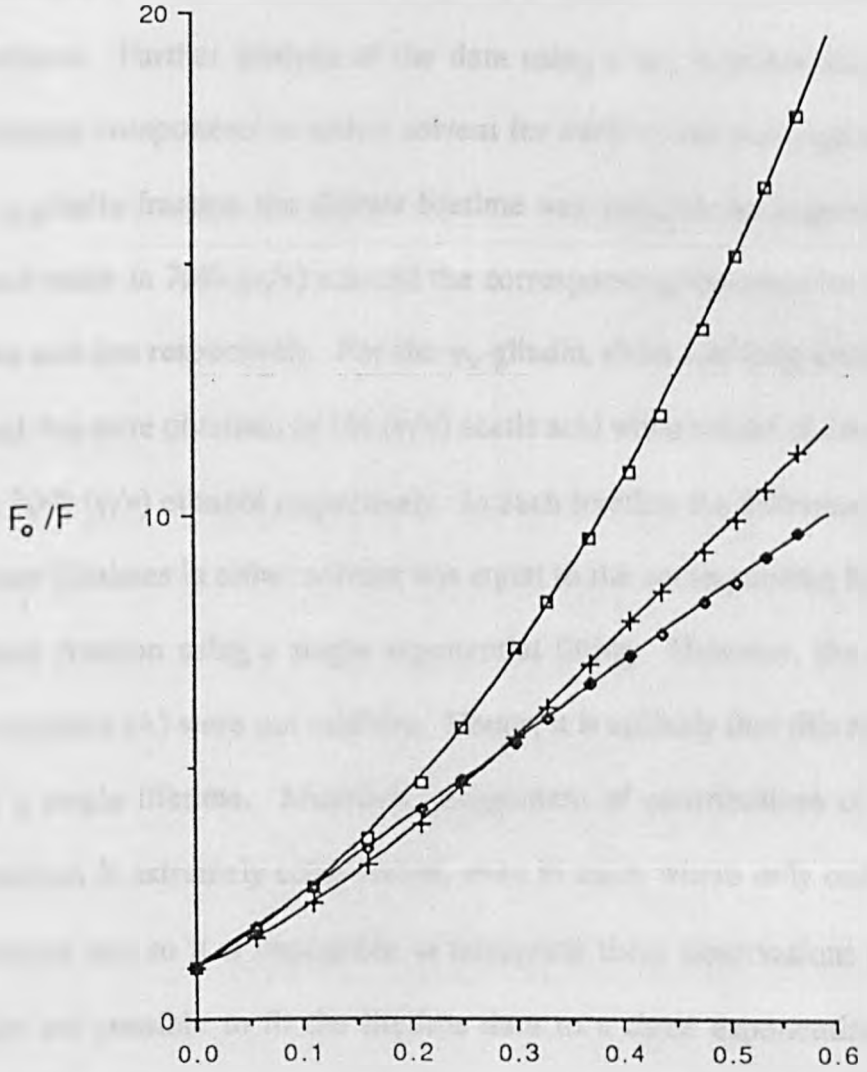

These values are both typical of tryptophan fluorescence in proteins which generally occurs on a 1-10ns timescale. The effect of solvent polarity accounted for the difference between τ values determined for both fractions in 1% (v/v) acetic acid and 70% (v/v) ethanol. Further analysis of the data using a two exponential decay fitting, gave two lifetime components in either solvent for each of the two γ-gliadin fractions. For the γ_{III}-gliadin fraction the shorter lifetime was 1ns and the longer 4ns in 1% (v/v) acetic acid while in 70% (v/v) ethanol the corresponding lifetimes for the same fraction were 1ns and 5ns respectively. For the γ_V-gliadin, short and long lifetime components of 1ns and 4ns were obtained in 1% (v/v) acetic acid while values of 2ns and 6ns were obtained in 70% (v/v) ethanol respectively. In each fraction the difference between the long and short lifetimes in either solvent was equal to the corresponding lifetime obtained for the same fraction using a single exponential fitting. However, the accompanying relative intensities (A) were not additive. Hence, it is unlikely that this represented the splitting of a single lifetime. Moreover, assignment of contributions of individual tryptophan residues is extremely complicated, even in cases where only one tryptophan residue is present and so it is impossible to interprete these observations in more detail. It was also not possible to fit the lifetime data to a three exponential decay as the analysis program 'crashed' each time an attempt was made. It was only possible to secure a three exponential fitting by constraining the analysis to a narrow range of channels. However, in each case, the values obtained were largely uninterpretable and this was taken as a further indication of the complexity of the emissions.

TABLE 4.5
ACRYLAMIDE QUENCHING PARAMETERS ESTIMATED FOR THE γ_{III}-GLIADIN, γ_V-GLIADIN AND ω-GLIADIN FRACTIONS

Fraction	K_w (M^{-1})
γ_{III}-gliadin	12.4
γ_V-gliadin	15.1
ω-gliadin	18.4

ANISOTROPY

Rotational correlation times (ϕ) estimated for each γ-gliadin fraction in 1% (v/v) acetic acid and 70% (v/v) ethanol are shown in Table 4.6. The data were fitted to one and two exponential decays respectively for each fraction in either solvent. However, in each case a single exponential fitting gave the more consistent results. For proteins of the sizes of the γ_V-gliadin and γ_{III}-gliadin fractions (M_rs 41K and 47K respectively), ϕ values in the order of 50ns would be expected for the rotation of the entire molecule. Hence, values of 2.7 and 4ns for the γ_V-gliadin fraction and 6nsec for the γ_{III}-gliadin fraction in 1% (v/v) acetic acid and 70% (v/v) ethanol respectively, were indicative of freely rotating tryptophan residues and suggested significant segmental motion and considerable degrees of flexibility within the matrices of each fraction. The faster rotational correlation times estimated for the γ_V-gliadin fraction in either solvent suggested that the degree of flexibility was higher in this fraction compared with the γ_{III}-gliadin fraction. The 'FLUOROT' program used to analyse the anisotropy data, also automatically evaluated a lifetime value fitted to a single exponential decay. For each γ-gliadin, τ^*

values obtained this way in either 1% (v/v) acetic acid or 70% (v/v) ethanol, compared well with those estimated using the 'FLUORFIT' program.

CD ANALYSIS OF THE CONFORMATIONS OF THE GLIADIN FRACTIONS

The far-uv CD spectra of the γ_{III}-gliadin, γ_V-gliadin and ω-gliadin fractions in the presence of 0-10M urea are shown in Figure 4.8 a, b and c respectively. In the absence of urea, the spectra of the γ_{III}-gliadin and γ_V-gliadin fractions each showed a negative maximum in the region of 205-210nm and a shoulder around 220nm, typical of the spectrum associated with α-helix conformation in proteins (Figure 4.1 b). The spectrum of the ω-gliadin fraction under the same conditions, had none of these characteristics. Instead, it showed a single negative maximum around 205nm similar to that reported by Tatham and Shewry, (1985) and indicative of the presence of ß-turns. In 2M urea, all three gliadin fractions showed unexpected increased spectral intensities. These were around 205-210nm for the γ-gliadins and fractions and around 205nm for the ω-gliadin fraction and suggested induced higher contents of α-helices in the γ-gliadin fractions and ß-turns in the ω-gliadin fraction. Between 2-10M urea, however, gradual decreases in intensity representing the loss of some regular structure from the backbone conformations was observed for all three fractions, but none of their spectra approached the spectrum of the so-called 'random-coil' conformation even in 10M urea (Figure 4.1). Above 8M urea, the spectrum of the ω-gliadin fraction showed a positive maximum around 222nm similar to that reported for poly(L-lysine) (Drake *et al.*, 1988). This is a synthetic molecule known to possess an extended conformation made up of 50% regular and 50% unordered structure. The likelihood, therefore, is that under these

extreme conditions of high denaturant concentration this fraction still retained some residual backbone structure.

Tatham and Shewry (1985) also reported near-uv CD spectra for ω- and γ-gliadin fractions and assigned absorptions at 262-268nm and 275-276nm to phenylalanine and tyrosine respectively. It was suggested that these side-chains were in a fixed conformation in all the gliadin fractions. In comparison with the ω-gliadin fraction, the α-, ß- and γ-gliadins each had higher spectral intensities within the wavelength range 260-320nm and this was also attributed to the absorption of the rigid cystine disulphide chromophore in the S-rich gliadins. Tryptophan absorption was not detected, however, Kasarda *et al* (1968) assigned a shoulder at 298nm in the spectra recorded for α-gliadin in aqueous solution, to tryptophan. The near-uv CD spectra of the γ_{III}-gliadin fraction in 0-10M urea are shown in Figure 4.9. In contrast to its far-uv CD spectra, the concentration of urea did not cause any significant spectral shifts in the near-uv CD spectra. The near-uv CD spectra of the γ_V-gliadin and ω-gliadin fractions which are not shown, followed similar patterns to that of the γ_{III}-gliadin fraction. None of the absorption characteristics attributed to the aromatic residues (Tatham and Shewry, 1985; Kasarda *et al.*, 1968) was observed in the spectra of any of three gliadin fractions. In contrast, the intensity of the spectra of the two γ-gliadin fractions between 260-320nm were similar to each other and were individually significantly higher than that of the ω-gliadin fraction within the same wavelength range, possibly as a result of the presence of disulphide bonds in the γ-gliadins. The likelihood therefore, is that the aromatic residues are not in a fixed conformation and that their environments did not alter significantly with increasing urea concentration in all three fractions.

TABLE 4.6
LIFETIME (τ) DATA FOR THE γ_{III}-GLIADIN AND γ_V-GLIADIN FRACTIONS

Fraction	Condition (1mg ml^{-1})	Ex'tial[1]	τ (ns)	A
γ_{III}-Gliadin	1% HAc[2]	1	3.0	0.13
		2	1.2	0.11
			4.3	0.60
	70% EtOH[3]	1	4.0	0.12
		2	1.1	0.07
			4.8	0.08
γ_V-Gliadin	1% HAc[2]	1	2.9	0.13
		2	1.1	0.10
			3.8	0.07
	70% EtOH[3]	1	4.2	0.12
		2	2.0	0.10
			6.0	0.05

1. Number of exponentials fitted
2. 1% (v/v) acetic acid
3. 70% (v/v) ethanol

TABLE 4.7
ROTATIONAL CORRELATION TIME (ϕ) DATA FOR THE γ_{III}-GLIADIN AND γ_V-GLIADIN FRACTIONS

Fraction	Condition (1mg ml^{-1})	Ex'tial[1]	ϕ (ns)	A	τ^* (ns)
γ_{III}-Gliadin	1% HAc[2]	1	5.8	0.13	3.0
		2	0.9	0.88	
			18.0	0.08	
	70% EtOH[3]	1	6.1	0.13	4.0
		2	1.2	0.08	
			15.9	0.08	
γ_V-Gliadin	1% HAc[2]	1	2.7	0.14	2.9
		2	10.9	0.06	
			0.6	0.11	
	70% EtOH[3]	1	4.1	0.14	4.1
		2	0.7	0.09	
			8.7	0.08	

τ^*. Lifetime calculated by 'FLUOROT'
1. *Number of exponentials fitted*
2. 1% (v/v) acetic acid
3. 70% (v/v) ethanol

Figure 4.8
THE FAR-UV CD SPECTRA OF THE γ_{III}-GLIADIN (a), γ_V-GLIADIN (b) AND ω-GLIADIN (c) FRACTIONS IN 0-10M UREA.

a

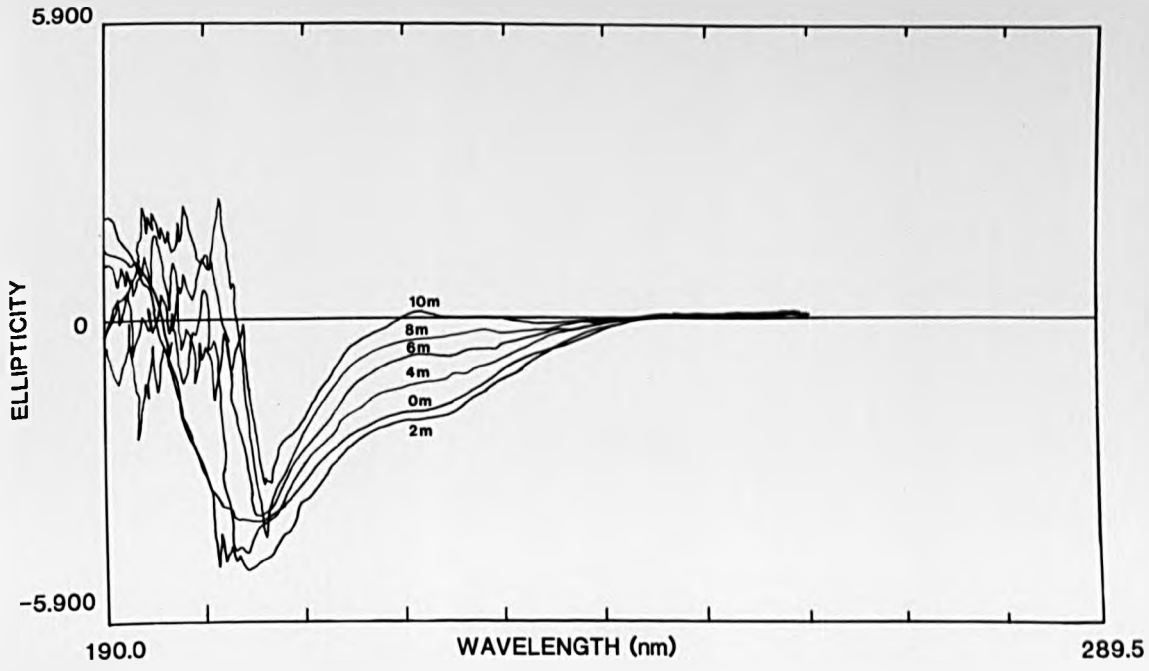

b

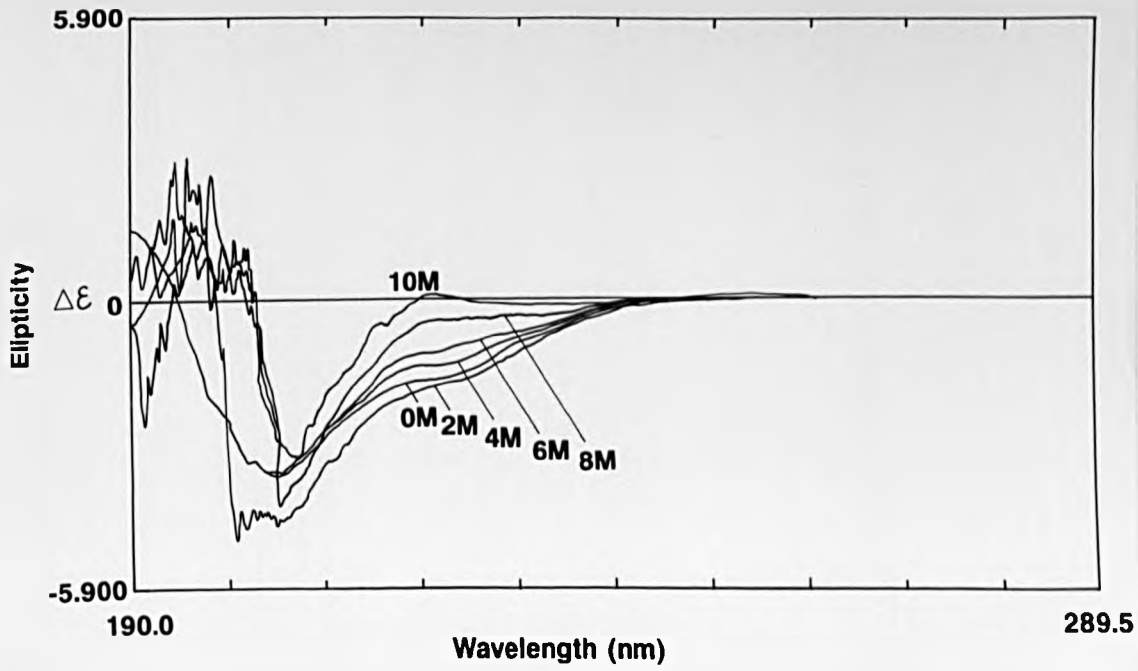
5.900
Ellpticity
Δε 0
10M
0M
2M
4M
6M
8M
-5.900
190.0
289.5
Wavelength (nm)

C

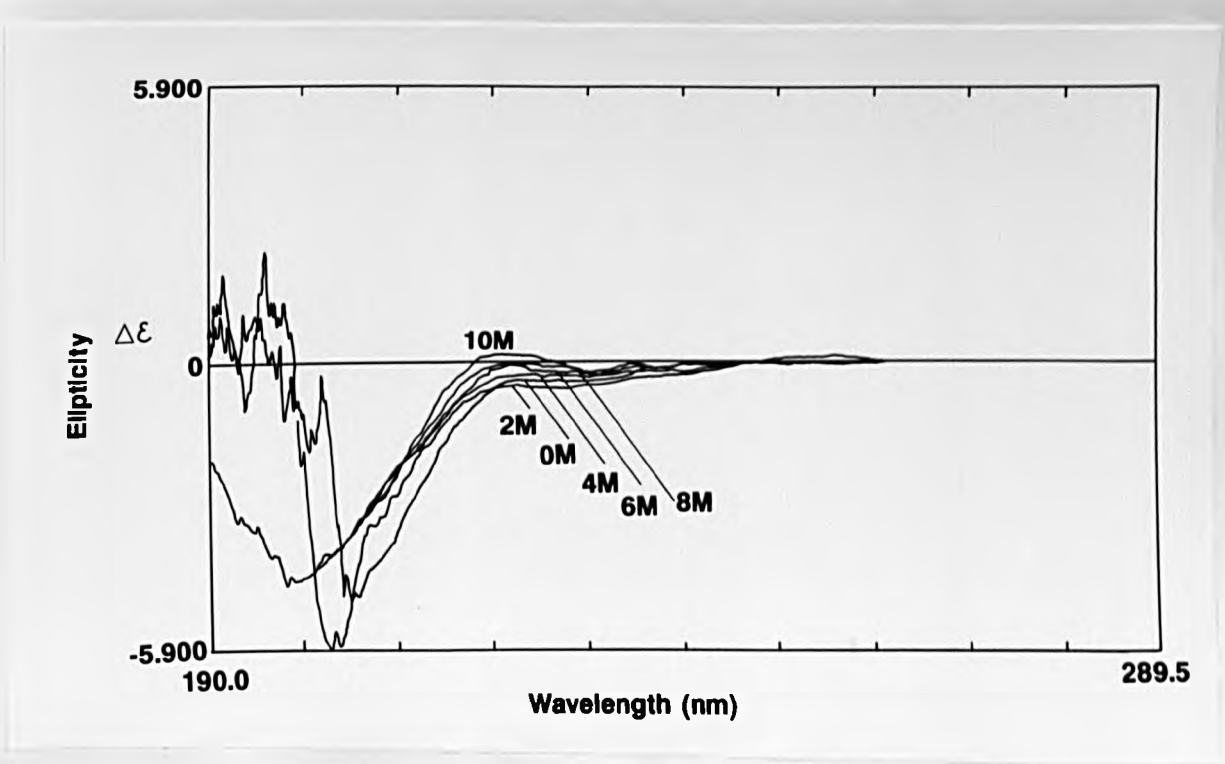
5.900
Ellpticity
Δε
0
-5.900
190.0
289.5
Wavelength (nm)
10M
2M
0M
4M
6M
8M

Figure 4.9
THE NEAR-UV CD SPECTRA OF THE γ_{III}-GLIADIN FRACTION IN 0-10M UREA.

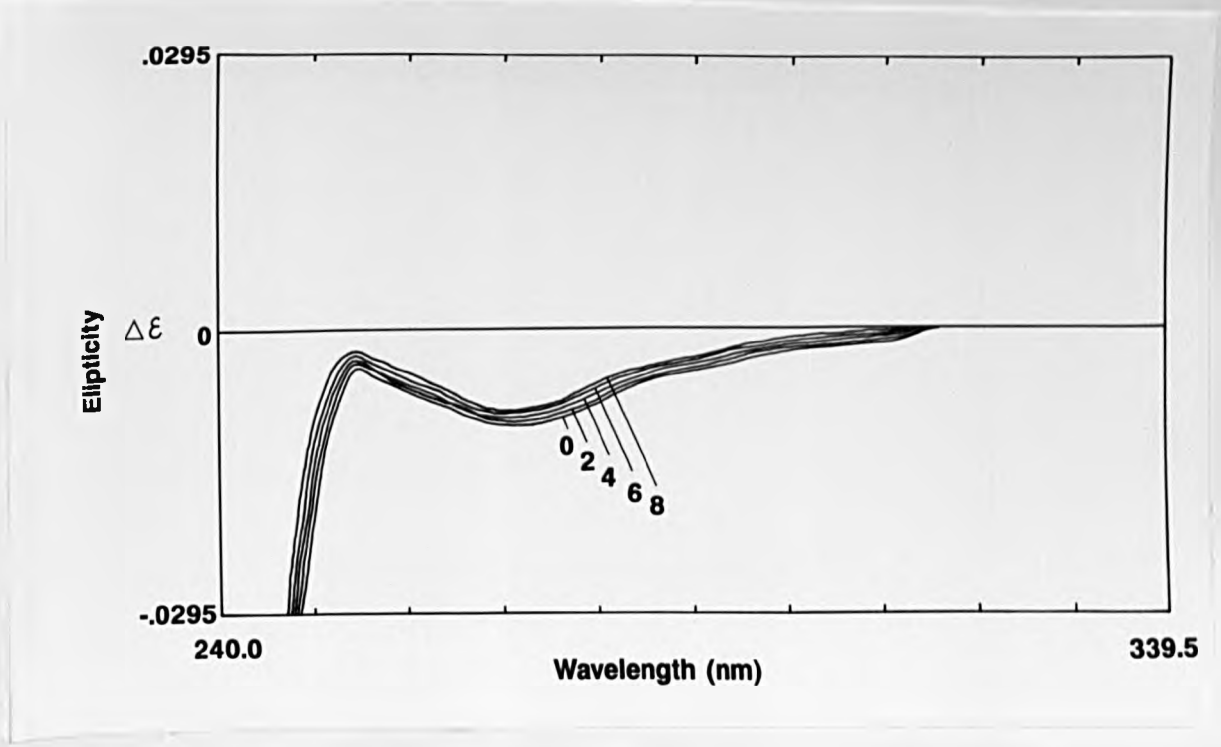

Figure 4.10
COMPARISONS OF THE FAR-UV CD SPECTRA OF 'NATIVE' AND 'REDUCED/ALKYLATED' γ_{III}-GLIADIN (a), γ_{V}-GLIADIN (b) AND ω-GLIADIN (c) AFTER DIALYSIS AGAINST 1% (v/v) ACETIC ACID.

a.

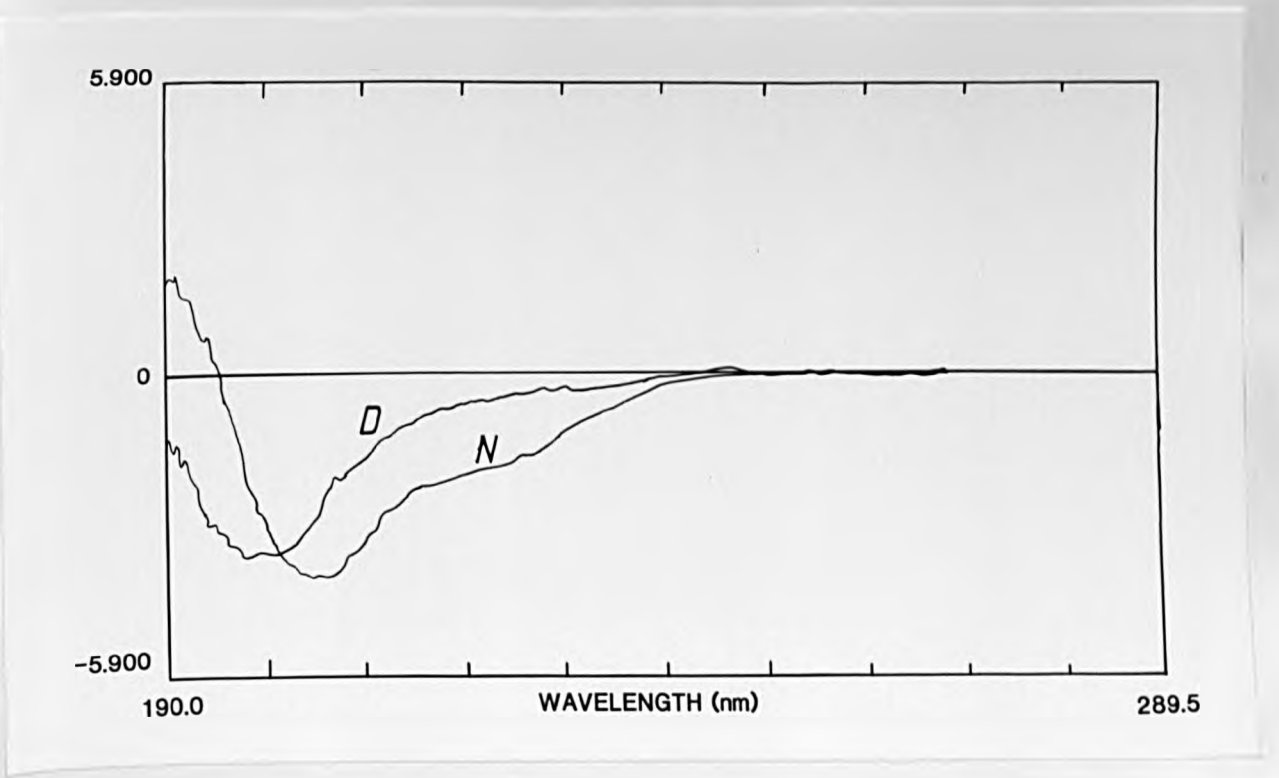

N 'NATIVE'

D 'DIALYSED REDUCED/ALKYLATED'

b.

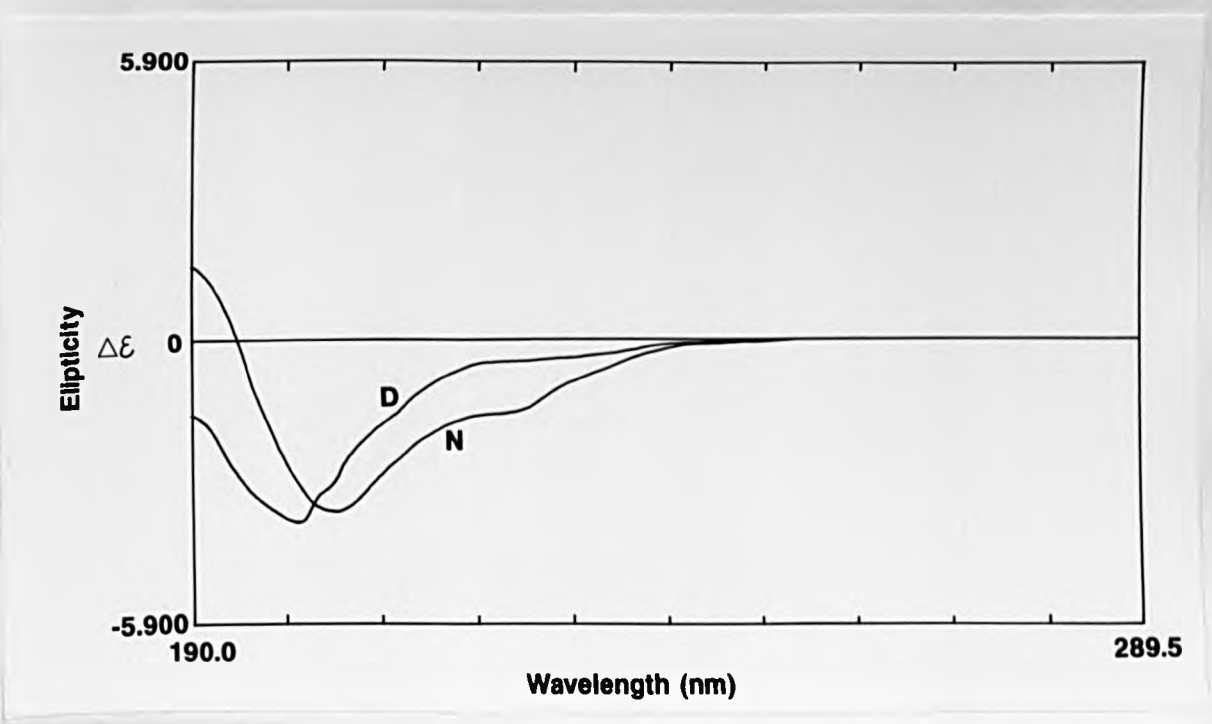

N 'NATIVE'

D DIALYSED 'REDUCED/ALKYLATED'

c.

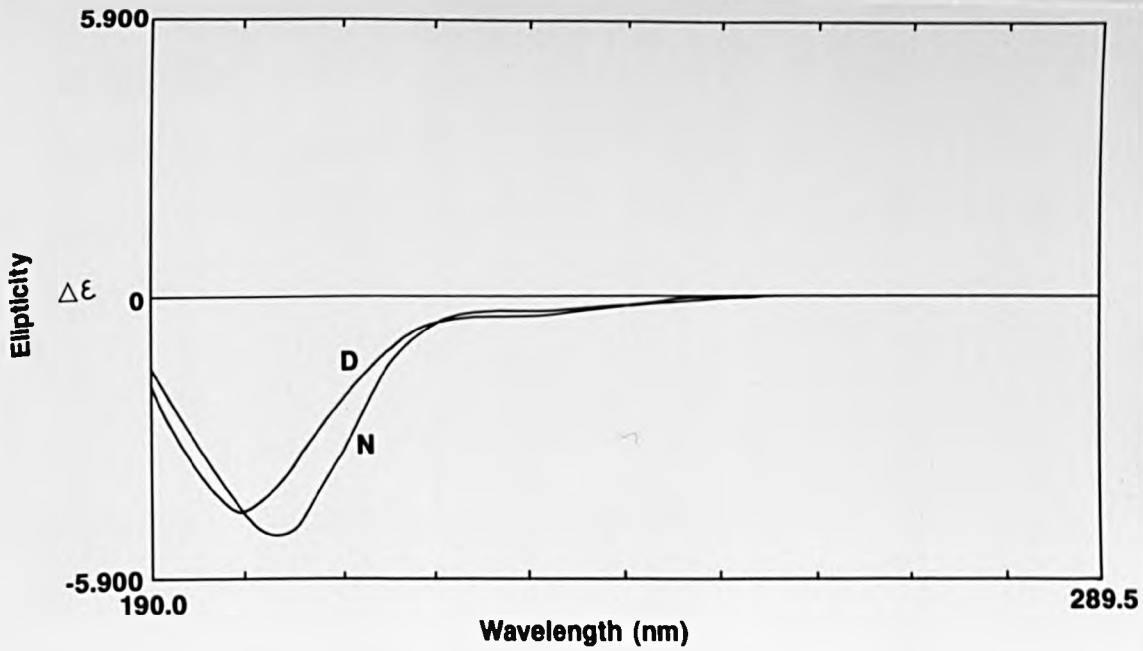

N 'NATIVE'

D DIALYSED 'REDUCED/ALKYLATED'

SDS-PAGE ANALYSIS OF THE EFFECT OF REDUCTION AND ALKYLATION ON THE CONFORMATIONS OF THE GLIADIN FRACTIONS

Comparisons of the electrophoretic mobilities of corresponding 'native' and 'reduced/alkylated' forms of each of the three fractions are shown in Figure 4.11. No difference in mobility was observed for the ω-gliadin fraction which was consistent with the earlier observations that with an absence of disulphide bonds, reduction and alkylation did not affect the overall conformation of this fraction. In contrast, the two γ-gliadin fractions showed differences in mobility between the two forms, the mobility of the 'reduced/alkylated' form being marginally retarded in each case. For these fractions, therefore, reduction and alkylation of the cysteine residues resulted in minor changes in their overall size when denatured by SDS.

DISCUSSION

Tryptophan fluorescence was used to monitor structural and dynamic properties of the three gliadin fractions. In multi-tryptophan proteins such as these, quantitative interpretation of fluorescence data may be complicated by the heterogeneity of the emissions. A useful qualitative description of the environment of tryptophan residues, however, can still be obtained from such data through comparison with reported data on other proteins. In all three fractions increases in quantum yield upon exposure to 10M urea were accompanied by minor shifts in the wavelength of maximum emission, generally in the order of 4-6nm. Such a shift to longer wavelength is characteristic of transfer to a more polar environment but an increase of intensity in the presence of denaturant is unusual suggesting that the tryptophan fluorescence is quenched in the

Figure 4.11
COMPARISONS OF THE SDS-PAGE MOBILITIES OF 'NATIVE' AND 'REDUCED/ALKYLATED' γ_{III}-GLIADIN, γ_V-GLIADIN AND ω-GLIADIN.

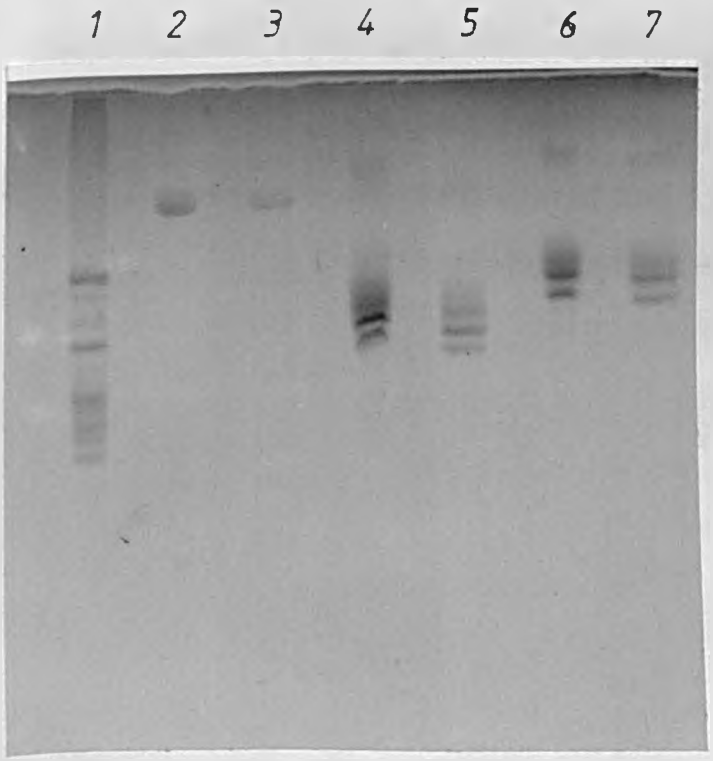

Lane	Fraction
1	total gliadin standard
2	'reduced/ alkylated' ω-gliadin
3	'native' ω-gliadin
4	'reduced/alkylated' γ_{III}-gliadin
5	'native' γ_{III}-gliadin
6	'reduced/alkylated' γ_V-gliadin
7	'native' γ_V-gliadin

native protein.

In the steady-state quenching analysis, the contribution of individual tryptophan residues in each fraction were not resolved. The quenching pattern, however, indicated a significant surface exposure of tryptophan residues in each fraction as shown by the average K_{sv} estimates (Table 4.5). This was also in agreement with the overall upward curvature of each of the individual plots. Further indication of the accessibility of the tryptophan residues was obtained in the case of the two γ-gliadins from the results of the time-resolved studies of their fluorescence anisotropy decays. Unlike the quenching estimates which were the average of three separate experiments, the time-resolved parameters were obtained from a single preliminary experiment. Yet, the average rotational correlation times of 6ns for the γ_{III}-gliadin fraction and 3.5ns for the γ_{V}-gliadin fraction, were generally typical of free rotation of tryptophan residues in proteins, consistent with highly accessible tryptophan residues and suggested considerable segmental mobility in these fractions. In addition, the complexity of the tryptophan emissions revealed by the analysis of the time-resolved lifetime and rotational correlation time data, also suggested that the observed fluorescence was unlikely to have been dominated by a single species. The near-uv CD spectra of the three fractions in 0-10M urea were also consistent with an unchanging environment of aromatic residues as would be expected for residues exposed to the solvent in the native state.

Tatham and Shewry (1985) attributed the high thermostability of the S-rich (α-, ß- and γ-) gliadins and the S-poor (ω-) gliadins to differing degrees of stabilisation by covalent and non-covalent forces. In the normally cysteine-deficient ω-gliadins whose secondary structural organisation comprises mainly ß-turns, hydrophobic interactions were reported

to be very important and were also suggested to have increased with rising temperature. In contrast, hydrogen bonding and to a lesser extent disulphide bonds, were proposed to have accounted for the stability of the α-helices which are the predominant regular secondary structural elements in the S-rich gliadins (Table 4.3). In the γ-gliadin fractions (Tatham and Shewry, 1985), thermal denaturation was also reported to have led to a transition between two defined conformations involving a helix to coil transition. The far-uv CD spectra of the γ_{III}-gliadin, γ_{V}-gliadin and ω-gliadin fractions, (Figures 4.8 a, b and c) showed that urea concentrations up to 2M induced higher contents of α-helices in the γ-gliadin fractions and ß-turns in the ω-gliadin. Only a limited, gradual loss of backbone structure occured in the presence of 2-10M urea. Covalent interactions could not have been responsible for the increased stability in up to 2M urea but a combination of hydrogen bonding and hydrophobic interactions is more likely. The major denaturing effect of urea on proteins in aqueous solution is thought to arise from the disruption of complex H-bonded structure of bulk water induced by high concentrations of urea; this, in turn, weakens the hydrophobic effect and hence destabilizes the native conformations of proteins. However, there may also be direct effects of urea if it can bind or interact intimately with amino acid side-chains in proteins. Urea molecules (M.wt 60) are small enough to penetrate the interior of proteins efficiently; it is possible that direct binding of urea by the proteins at concentrations up to 2M may have led to the observed increases in α-helix content in the γ_{III}-gliadin and γ_{V}-gliadin fractions, and in ß-turns in the ω-gliadin. Beyond 2M urea, the contribution of hydrogen bonding is likely to have gradually decreased in the presence of the denaturant, and hydrophobic interactions would appear to have been the main force responsible for maintaining the residual

structure in all three fractions. If indeed hydrophobic interactions largely account for the stability of gliadin fractions exposed to urea, this may further explain the earlier observations of irreversible binding of gliadin preparations to the SP-Trisacryl column (Chapter 2) which was also reported by Pratt (1990).

Against a background of the reported existence of defined conformations in the thermal denaturation of gliadin fractions (Tatham and Shewry, 1985) the observed shifts in the wavelength of maximum fluorescence emission upon exposure of the three fractions to urea, could also be significant. Although the average shift of 4-6nm was minimal compared to that of ribonuclease T1 for instance (Figure 4.4), it did indicate that in each fraction, urea induced a conformational form which was different, but only marginally, from the 'native' conformation. The difference in electrophoretic mobility observed on SDS-PAGE gels (Figure 4.11) between 'native' and 'reduced/alkylated' forms of the γ_{III}-gliadin and γ_{V}-gliadin was also consistent with the existence of only a marginal difference between the two conformations.

CONCLUSION

The physical techniques of fluorescence and CD spectroscopy were used to study the conformations of the γ_{III}-gliadin, γ_{V}-gliadin and ω-gliadin fractions and their stabilities to denaturant-induced unfolding. The CD spectra of all three fractions in the far- and near-uv region as well as their fluorescence characteristics all suggested open extended structures in which the aromatic side-chains were exposed and accessible to solvent molecules. In addition, preliminary time-resolved anisotropy studies suggested significant segmental mobility in the two γ-gliadin fractions consistent with their proposed extended

structures. All three fractions were relatively stable to urea-induced denaturation with each retaining some residual structure in the presence of 10M urea. The similarity of the far-uv spectrum of the ω-gliadin fraction in the presence of 10M urea to that reported for poly(L-lysine) suggested that, under these conditions, this fraction consisted of equilibrium proportions of ordered and unordered structures. The observed stability of the fractions to urea may have been due to the contribution of hydrophobic interactions and hydrogen bonding to a lesser extent. Covalent disulphide bonds may also be significant for maintaining α-helices in the two γ-gliadins since reduction and alkylation led to decreases in these secondary structure elements. Small shifts in the wavelengths of maximum fluorescence emission also indicated that urea and the disruption of disulphide bonds both induced a conformational form in each fraction which differed only marginally from the corresponding 'native' conformation.

CHAPTER 5

PHYSICAL STUDIES OF PEPTIDES DERIVED FROM A γ-TYPE GLIADIN

INTRODUCTION

The domains of polypeptide chains may be isolated as stable fragments by preparative separation methods after enzymic digestion of the native protein. As interactions are more extensive within, rather than between, separate domains, the conformational integrity of the domain polypeptides is usually retained after isolation, thus permitting a detailed characterization as has been reported for peptides derived from a wide variety of proteins. For instance, the thermal unfolding of papain was proposed to involve a biphasic transition as a result of the independent unfolding of its two domains (Hernández-Arana and Soriano-García, 1988). Similar unfolding patterns were also reported for the α-subunit of tryptophan synthase (Miles *et al.*, 1982) and ovomucoid (Baig and Salahuddin, 1978). Among the prolamins, structural studies of gluten protein fractions using synthetic peptides based on known sequences in the primary structure have also been reported (Tatham *et al.*, 1987; 1989), and recently, more direct conformational studies using peptides derived by the enzymic hydrolysis of a γ-type gliadin were reported (Tatham *et al.*, 1990 a). In all the above cases, the structural and functional characteristics of the domain fragments were related to those of the intact polypeptides from which they were derived.

The domains of gliadin fractions are well defined (Figure 3.2), and for the γ_{III}-gliadin,

γ_V-gliadin and ω-gliadin fractions, the protocol reported by Masson *et al.* (1989) could have been used to attempt the isolation of peptides corresponding to their respective domains. Studies of the peptide fragments would then have allowed the individual domains in the intact molecules to be probed and the structural changes which accompanied their denaturation (chapter 4), more confidently interpreted. However, to set up and adapt the digestion and isolation protocols required a lot of time. Hence, the corresponding domains from γ_{44}-gliadin which is related to the two purified γ-gliadins and were available as a gift from France, were used instead. Detailed studies of the γ_{44}-gliadin from the wheat cultivar Capitole, has been reported (Popineau and Pineau, 1985 b; Masson, 1988, Popineau and Pineau, 1988; Masson *et al.*, 1989). The close similarities in sequences between it, the γ_{III}-gliadin and γ_V-gliadin meant, therefore, that interpretation of data on it could be applied directly to the two purified γ-gliadins. The preliminary studies carried out on the γ_{44}-gliadin-derived peptide fragments are presented and discussed in this chapter.

STRUCTURAL ORGANIZATION OF THE γ-TYPE GLIADINS

The domain structure of the γ-type gliadins is shown in Figure 3.2 a. It includes two regions described below.

1. A proline-rich N-terminal domain preceded by a short unique N-terminal sequence of up to 12 residues. There are 125 residues in this domain, and beyond the unique N-terminus, the sequence consists predominantly of repeats of amino acids based on the consensus heptapeptide sequence PQQPFPQ.

2. A cysteine-rich C-terminal domain containing 8 cysteine residues known to form 4

intra-chain disulphide bonds. No repeat sequences have been reported to occur within this domain.

PHYSICAL CHARACTERISTICS OF THE DOMAIN REGIONS OF γ_{44}-GLIADIN (based on Tatham *et al.*, 1990 a and b)

Masson (1988) reported the isolation of two peptides obtained by limited chymotryptic digestion of an intact γ_{44}-gliadin. The peptides were isolated by open column gel filtration chromatography and SE-HPLC on a semi-preparative scale. Their M_rs by SDS-PAGE were 17K and 28K respectively. Amino acid composition analysis suggested that the 17K peptide corresponded broadly to the non-repetitive C-terminal domain and the 28K peptide to the repetitive proline-rich N-terminal domain. Although the higher M_r of the N-terminal peptide was not consistent with the total number of residues (125 compared with 150 residues in the C-terminal peptide), it was suggested that this was due to the presence of extended repeats of amino acid sequences within this region. Tatham *et al.* (1990 a) reported detailed analyses of the conformations and thermal stabilities of the 17K and 28K peptides by CD spectroscopy. It was shown initially that the far-uv spectrum of intact γ_{44}-gliadin was similar to that reported for other γ-gliadin fractions (Tatham and Shewry, 1985; Aibara and Morita, 1988) in having a conformation rich in α-helices. Comparison of the far-uv spectra of the two peptides with that of the intact γ_{44}-gliadin showed that the 17K fragment was also predominantly α-helical while the 28K fragment comprised mainly ß-turns. The α-helical content of a number of proteins or peptides may be compared using the ratio of their ellipticity ($\Delta\varepsilon$) at 208nm to that at 224nm. Ratios of 1:0.6 and 1:0.8 were reported for the γ_{44}-gliadin and the 17K peptide

derived from it respectively, suggesting that in the absence of the repetitive proline-rich domain, the content of α-helix in the non-repetitive C-terminal peptide was higher than that of the intact polypeptide. The stabilities to thermal denaturation of the intact γ_{44}-gliadin and the two peptide fragments were also reported. In the intact polypeptide, spectral shifts consistent with a gradual loss of α-helices with increasing temperature, were reported. The 17K peptide on the other hand, showed little evidence of these spectral shifts and was considered to be stable to heating. The spectrum of the 28K peptide however, showed an increase in ß-turn conformation upon heating. In addition, the presence of an isosbestic point between 212-213nm was considered as an indication of the existence of a transition between two conformations, one predominant at 20°C and the other at 80°C. Under cryogenic conditions, low temperature CD measurements also give detailed information on conformational equilibrium involving a more limited range of structures. Unlike the 28K peptide, the 17K peptide was reported not to have been affected by cooling, whereas the structural changes indicated by the spectral shifts observed for the intact polypeptide were attributed by the authors to changes resulting from the proline-rich repetitive domain. In an attempt to check whether or not the conformations assigned to each peptide fragment were related to that of the intact protein, the far-uv CD spectra obtained for the separate peptides in 70% (v/v) ethanol at room temperature were added together. Comparison of the resultant spectrum to that recorded for the intact γ_{44}-gliadin under the same conditions, indicated a broad agreement in the shapes of the two spectra.

PHYSICAL CHARACTERISATION OF UREA-INDUCED TRANSITIONS IN γ_{44}-GLIADIN DERIVED PEPTIDES

There was insufficient time to apply the enzymic digestion and preparative techniques mentioned above to isolate domain peptides from any of the three gliadin fractions. Instead, the γ_{44}-gliadin-derived peptides which corresponded broadly to the proline-rich repetitive N-terminal and non-repetitive C-terminal domains respectively were used. The quantities of the γ_{44}-gliadin-derived domain peptides available were generally in the order of 0.7mg and this affected the type and number of experiments performed. Thus, the same solutions used to record far-uv CD spectra were saved for subsequent use in recording their fluorescence emission spectra. Although it was intended to carry out preliminary steady-state acrylamide quenching studies, this was not possible in the end due to limited time availability.

AIMS

The overall aims of the studies undertaken were to investigate the effects of urea concentration on the conformations of the domain peptides derived from γ_{44}-gliadin and to attempt to relate any observed changes to the results of studies on conformation and stability of the intact γ_{III}-gliadin and γ_{V}-gliadins reported in the previous chapter.

MATERIALS

The two γ_{44}-gliadin derived peptides were gifts from Dr. Y. Popineau, INRA Laboratoire de Biochimie et Technologie des Protéines, Nantes, France. All other materials were the same as described in the physical characterization of the intact gliadin fractions in

chapter 4.

METHODS

Far-uv CD spectral scans were carried out on solutions of the N-terminal and C-terminal peptides, initially in the absence of urea and subsequently in the presence of 4M and 8M urea according to the protocol described for the intact gliadin fractions in chapter 4. The peptide concentrations were determined directly by weighing and were 0.2mg ml^{-1} in both cases. The baseline was obtained by scanning a solution of 10mM acetic acid and the recorded spectral data were analysed as described above for the intact polypeptides.

Separate aliquots of the solutions above, each containing 100μg of the N-terminal and C-terminal peptides in a total volume of 1ml, were prepared by dilution in appropriate solvents containing 0M, 4M and 8M urea. The fluorescence emission spectrum of each sample solution was recorded under each set of conditions, using the protocol described for the intact gliadin fractions in chapter 4.

RESULTS

The far-uv CD spectra of the C-terminal and N-terminal peptides in 0-8M urea are shown in Figure 5.1 and 5.2 respectively. The spectrum of the C-terminal peptide in the absence of urea showed a negative maximum around 205-210nm and a shoulder around 218nm. As urea concentration was increased to 4M and 8M the corresponding spectra showed a gradual decrease in the intensity around 205-210nm and this was also accompanied by a gradual smoothing of the shoulder around 220nm. All of these

observations were consistent with a gradual loss of α-helical content as observed for the intact γ_{III}-gliadin and γ_V-gliadin fractions above. Unlike the C-terminal peptide, the initial spectrum of the N-terminal peptide obtained in the absence of urea had a single negative maximum around 200nm, an indication of the presence of ß-turns within its conformation. In the presence of 4M urea the negative maximum was shifted to about 208nm and in 8M urea this was accompanied by a positive maximum at 220-225nm to give a spectrum resembling that of poly(L-lysine), thus suggesting that in the presence of 8M urea significant equilibrium proportions of both ordered and unordered structure were present within the repetitive N-terminal domain peptide. In Figure 5.3 the spectrum of the C-terminal peptide (C) and that of the N-terminal peptide (N) recorded in the absence of urea, were added to give a total or simulated spectrum (T). It was assumed on the basis of the domain structure of the γ-type gliadin shown in Figure 3.2 (a) that the C-terminal and the N-terminal peptides made up approximately 55% and 45% respectively of the intact polypeptide. The comparison of the simulated spectrum (T) and that of the intact γ_{III}-gliadin in the absence of urea (G) showed remarkable agreement. This suggested that although neither peptide was derived from the γ_{III}-gliadin their combined spectra in the absence of urea corresponded with that of the intact γ_{III}-gliadin under the same conditions. A similar agreement was also obtained when the simulated spectrum (T) was compared to the spectrum of the γ_V-gliadin fraction.

The fluorescence emission spectra of the N-terminal and C-terminal peptides in the absence of urea and in 4M and 8M urea are shown Figures 5.4 and 5.5 respectively. In each peptide, the wavelength of maximum emission was around 350nm in the absence

Figure 5.1
THE FAR-UV CD SPECTRA OF THE C-TERMINAL PEPTIDE IN 0-8M UREA.

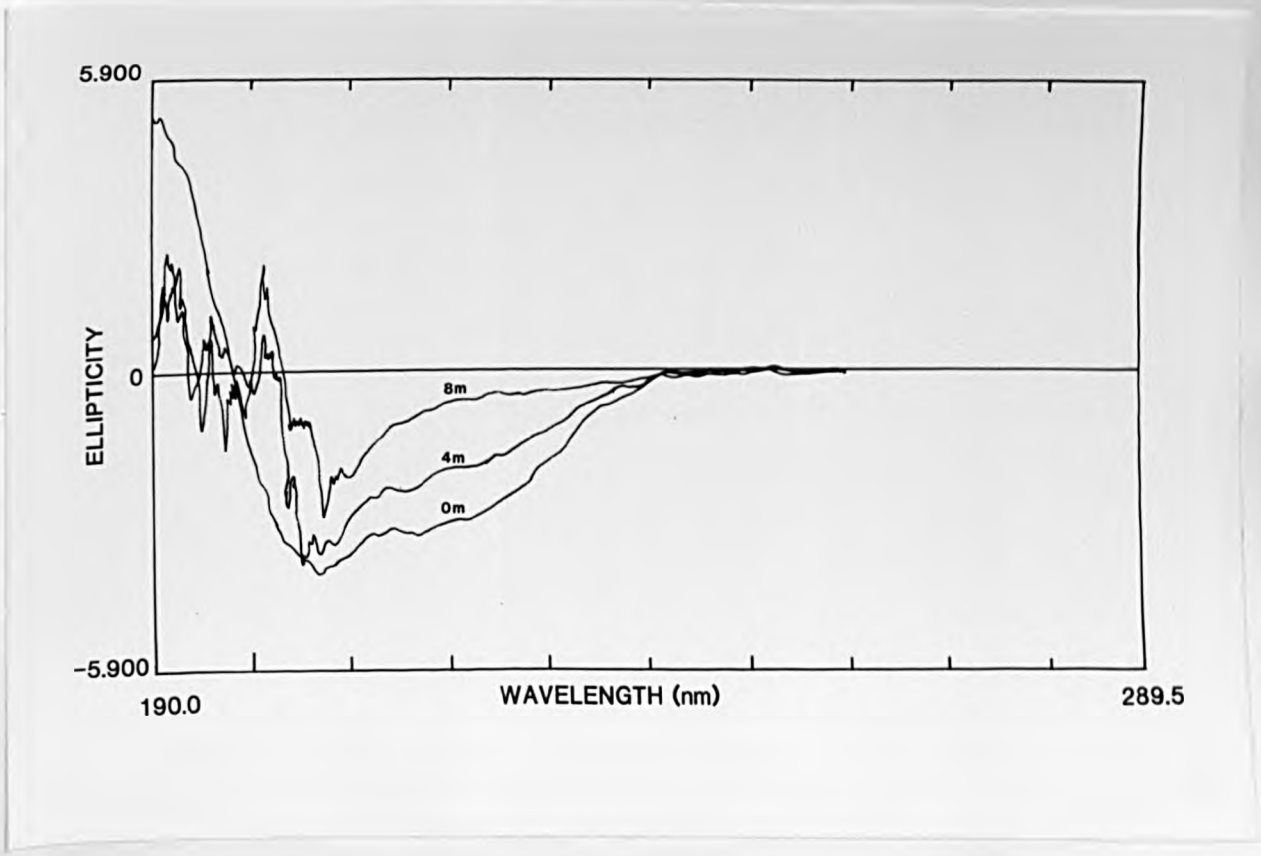

Figure 5.2
THE FAR-UV CD SPECTRA OF THE N-TERMINAL PEPTIDE IN 0-8M UREA.

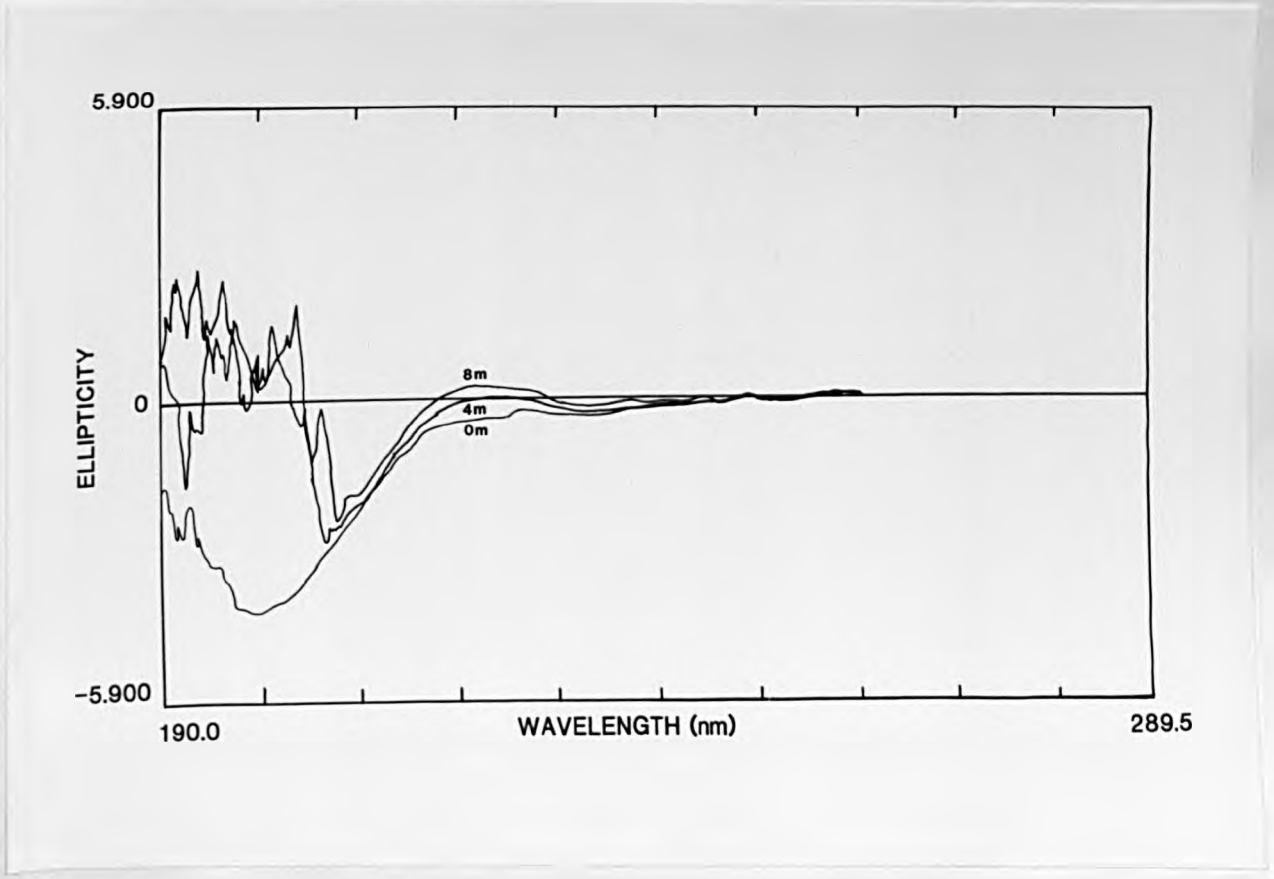

Figure 5.3
THE FAR-UV CD SPECTRA OF γ_{III}-GLIADIN (G) AND THE SUM (T) OF THE C-TERMINAL (C) AND N-TERMINAL (N) PEPTIDE SPECTRA, ALL IN THE ABSENCE OF UREA.

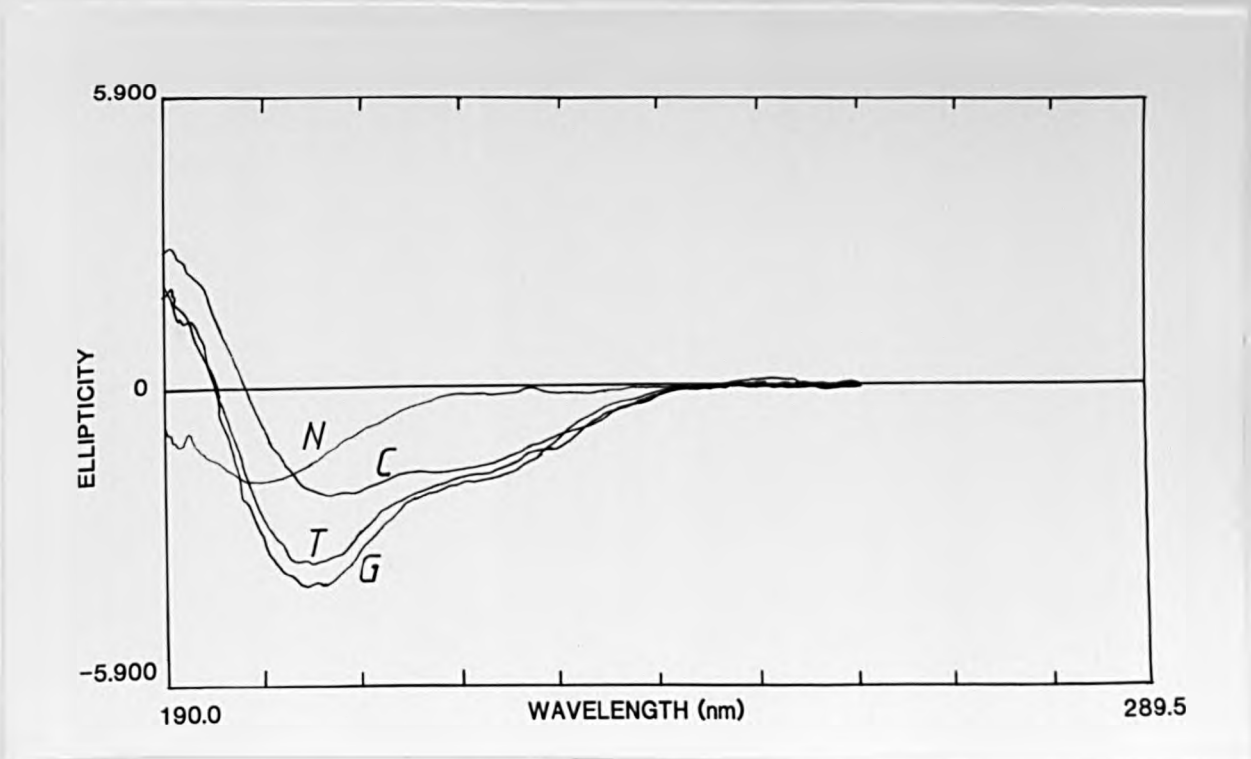

Figure 5.4
FLUORESCENCE EMISSION SPECTRA OF THE C-TERMINAL PEPTIDE IN 0-8M UREA.

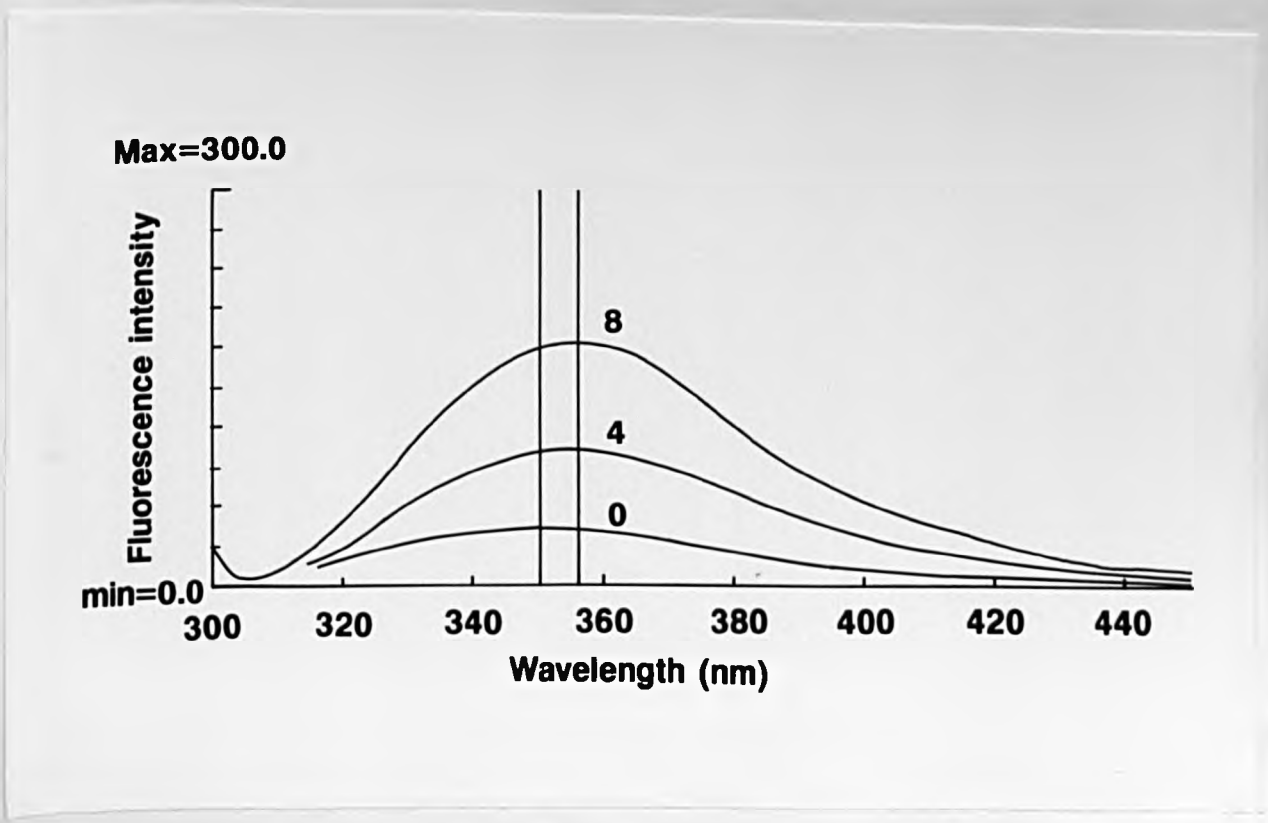

Figure 5.5
FLUORESCENCE EMISSION SPECTRA OF THE N-TERMINAL PEPTIDE IN 0-8M UREA.

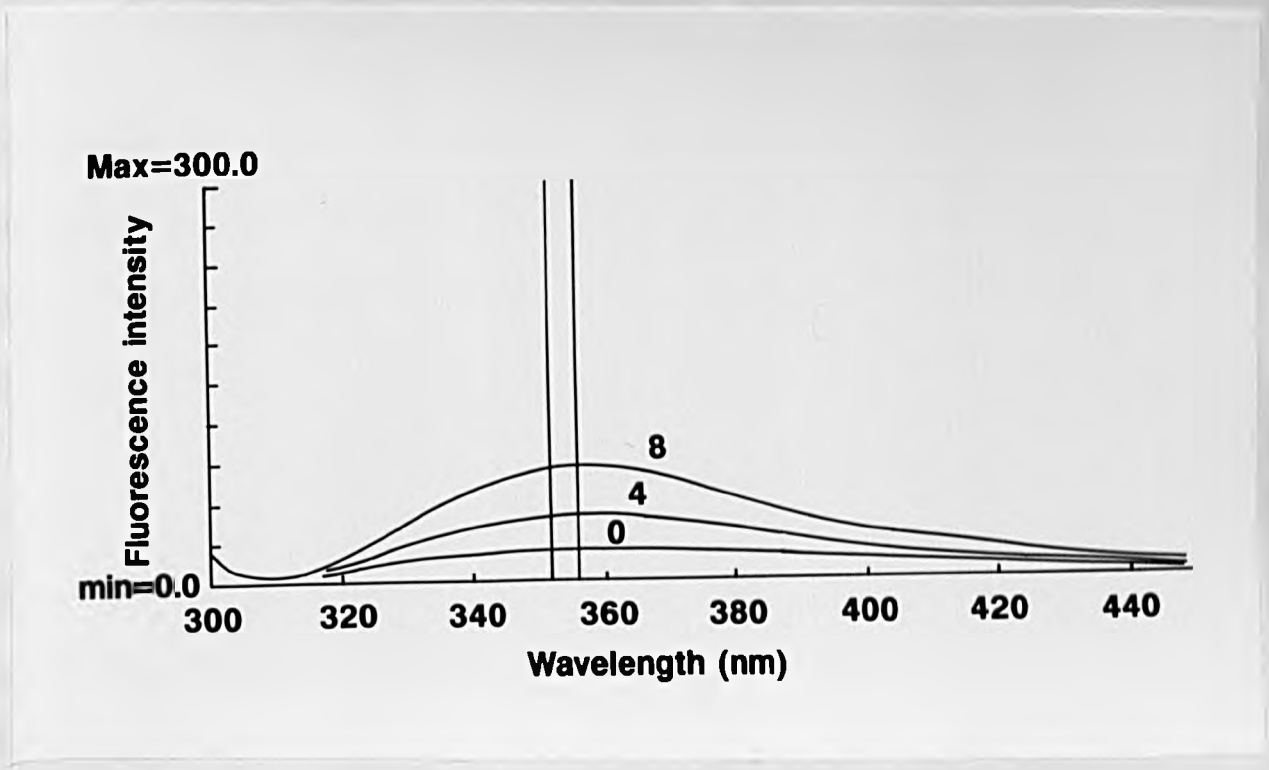

of urea. In the presence of 4M and 8M urea, however, the shift in the wavelength of maximum emission was of the order of 3nm for the N-terminal peptide and 5nm for the C-terminal peptide. In addition, at each urea concentration the fluorescence intensity of the N-terminal peptide was about half that of the C-terminal peptide. The differences in fluorescence emission intensity could have been due to differences in the characteristics of the fluorophores in each peptide including their environments and emissions, or in their numbers. The greater shift in the wavelength of maximum emission observed for the C-terminal peptide however, suggested that it was less stable to urea-induced transitions than the N-terminal peptide. The shifts also suggested the presence of closely-related, but different conformational states in both peptides, in the presence of urea.

DISCUSSION

The effect of increasing urea concentration on both the far-uv CD and fluorescence emission spectra of the two peptides followed similar patterns to those obtained for the intact γ_{III}-gliadin and γ_{V}-gliadin fractions under identical conditions. The two sets of spectra suggested that the C-terminal peptide was more susceptible to urea-induced denaturation than the N-terminal peptide. In the absence of urea, the non repetitive C-terminal domain was rich in α-helical content. Exposure to 4M and 8M urea led to a gradual decrease in the α-helical conformation. On the basis of the spectral shifts observed for the C-terminal peptide in 0-8M urea, its stability to urea-induced denaturation was not as great as its reported stability to thermal denaturation between 20°C and 80°C and cooling from +20°C to -100°C (Tatham *et al.*, 1990 a). The

repetitive N-terminal peptide on the other hand showed only slight shifts in spectra upon exposure to 0-8M urea. The similarities of the spectra obtained in 8M urea to that reported for poly(L-lysine) (Drake *et al.*, 1988) suggested the presence of equilibrium proportions of ordered and unordered structure in this domain fragment when exposed to 8M urea. The reported conformational mobility of this domain as a result of heating and cooling (Tatham *et al.*, 1990 a) was not observed upon exposure to urea. On the whole, therefore, the effects of urea concentration on the backbone conformations of both peptides appeared to contrast with their reported sensitivities to heating and cooling.

The combined conformation of the two peptides simulated from their individual far-uv CD spectra obtained in the absence of urea was, however, similar to the conformations of each of the γ_{III}-gliadin and γ_V-gliadin fractions under similar conditions. As these peptides were derived from the γ_{44}-gliadin of the wheat cultivar Capitole, and the γ_{III}-gliadin and γ_V-gliadin fractions were each from the cultivar Chinese Spring, these results justified the use of the two peptides and confirmed the existence of significant structural homology among the γ-type gliadins regardless of their source.

The yield of fluorescence intensity at each urea concentration (Figures 5.4 and 5.5) was also found to be about two times higher in the C-terminal peptide than in the N-terminal peptide. In DNA-derived primary sequences reported for gliadin fractions (Figure 2.1; Bartels *et al.*, 1986) tryptophan appears to be well conserved at positions 12, 154 and 158. This allows some speculations to be made. Firstly, it could be due to the fact that the number of fluorophores contributing to the observed fluorescence were twice as many in the C-terminal peptide as in the N-terminal peptide, a situation which is possible if

the emissions and environments of all the fluorophores were identical. As in the cases of the intact gliadin fractions, the shifts in the wavelength of maximum fluorescence emission in the presence of urea, suggested that different but closely-related conformations of each peptide were induced upon exposure to urea.

CONCLUSION

Although the experiments carried out were limited by the amounts of the two peptides available, some useful patterns emerged from this preliminary study. Firstly, the α-helix-rich conformation of the non-repetitive C-terminal domain peptide was found to be more susceptible to urea-induced denaturation than the ß-turns of the proline-rich repetitive domain peptide. Secondly, the conformation associated with each peptide fragment was directly related to the overall conformations of both the γ_{III}-gliadin and the γ_{V}-gliadin fractions. Finally, it may be that the environments and emission characteristics of the tryptophan residues are identical in the fragment peptides and the intact γ-gliadins. One way of testing the latter conclusion, would be to use time-resolved measurements to quantitate the contributions of each tryptophan residue. Although Waldmann *et al.* (1987), were able to do so for three tryptophan residues of a lactate dehydrogenase, they used site-directed mutagenesis to selectively replace these residues. As yet, successful application of site-directed mutagenesis to gluten proteins has not been reported. Still, the above approach would appear to be more appropriate in the light of these preliminary studies and also the existence of established techniques for isolating peptide fragments from gliadin fractions (Masson, 1988). In addition, analysis of the emissions will be facilitated by the use of peptides containing one and two tryptophan residues

instead of a 276-residue polypeptide containing three tryptophans. In this way, direct interpretation of data would then permit the conformations of the individual domains in the intact molecules to be studied in more detail. Furthermore, the problems associated with possible conformational changes as a result of selectively replacing tryptophan residues by site-directed mutagenesis, would not arise.

CHAPTER 6

GENERAL DISCUSSION

The overall aims of this project was to elucidate the pathway and mechanism of folding of gluten proteins. However, in view of their extensive polymorphism, two γ-gliadins and an ω-gliadin were purified to homogeneity for study as representative S-rich and S-poor fractions respectively. It is generally accepted that the isolation of individual gliadin components is best achieved using a preliminary step to purify the crude gliadin fraction to which the component belongs instead of directly from total gliadin (Platt and Kasarda, 1971; Charbonnier, 1974). Thus, in the procedure used to prepare the γ_{III}-gliadin, γ_{V}-gliadin and ω-gliadin fractions for physico-chemical analysis, ion-exchange chromatography on carboxymethyl cellulose CM52 was used initially to separate total gliadin into crude fractions enriched in ω-gliadins, γ-gliadins, β-gliadins and α-gliadins prior to further fractionation by gel filtration and semi-preparative RP-HPLC. It was essential to adopt a protocol that gave reasonable yields in a reproducible manner. In spite of the very good yields and consistent recoveries of the γ_{III}-gliadin, γ_{V}-gliadin and ω-gliadin, some of the stages of the purification were not rapid and may be worth modifying in future applications in order to improve the overall efficiency. For instance, the ion-exchange column buffer could be used to resuspend the total gliadin precipitate recovered after 70% (v/v) ethanol extraction instead of 8M urea. Not only will this avoid the need for dialysis to remove urea, it would also permit total gliadin to be loaded directly onto the ion-exchange column. In the absence of freeze-dried protein, total

gliadin recovery can be estimated from the extinctions of the protein solution at 260nm and 280nm (Dawson *et al.*, 1969) although this may require the use of gliadin standards. Another possible modification worth considering in future applications would be to use a batch process to prepare specific broad groups of gliadins prior to gel filtration and RP-HPLC. In cases where high performance separation equipment is available, the CM52 and Sephadex G-100 columns could also be substituted by the equivalent preparative IE-HPLC/FPLC and SE-HPLC/FPLC columns respectively. This would mean lower sample loads per run; however, the rapidity, superior resolution and reproducibility, should lead to an overall improvement in the efficiency of purification of gliadin fractions.

A modified purification protocol might provide a means of confirming the earlier conclusion that experimental handling may have contributed to the partial cleavage of N-terminal residues from some of the γ_{III}-gliadin and γ_{V}-gliadin polypeptides. In many other studies, gliadin fractions have been exposed to low pH buffers and dilute acids in the course of their purification, but as yet, loss of N-terminal peptides such as were described above have not been reported.

The true M_rs of most gliadins on the other hand, are not known and conflicting values are often reported. The basis of this disparity has been the subject of some research and is still not understood (Bunce *et al.*, 1985). In terms of similarities between M_rs determined by the same, or by different methods, as well as comparison with values previously reported for gliadin fractions, the γ_{III}-gliadin here gave the most consistent results, the ω-gliadin the least consistent and the γ_{V}-gliadin was intermediate between the two. The presence of repetitive sequences and their unusually high contents of

proline have been suggested as a possible source of the disparity in the M_rs of gliadins estimated in the presence of denaturants (Hamauzu *et al.*, 1975; Hamauzu and Yonezawa, 1978; Bunce *et al.*, 1985). In addition, it is also possible that this may be a reflection of systematic differences between the gliadins and the standard molecular weight markers in their unfolding behaviour in the presence of denaturants.

The combination of circular dichroism and fluorescence spectroscopy was used to study the time-averaged conformations, flexibility and stability to urea-induced denaturation of the three purified gliadins. These studies were intended to form the basis for further analyses of the unfolding and refolding of these fractions. However, it emerged after preliminary denaturation experiments that each fraction was unusually stable in the presence of urea. Increases of fluorescence intensity in the presence of denaturant suggested that the fluorescence of tryptophan residues were quenched in the native state. Similarly, exposure to 10M urea, and in the case of the two gliadin fractions reduction of disulphide bonds and alkylation of cysteine residues, resulted in conformational forms which were only marginally different from those of the native proteins. Denaturation curve analysis could therefore not be used to estimate the conformational stability, ΔG^{H20}, nor to speculate on the relative stabilities of individual domains and their possible mechanisms of folding. Time-resolved fluorescence, steady-state quenching and far- and near-uv CD analyses provided useful information on the overall folded conformations of the three purified fractions. For instance, Stern-Volmer constants deduced from steady-state quenching of tryptophan fluorescence, showed that there were significant differences between the conformations of the three fractions.

In summary, the native conformations of each fraction, defined in this thesis as the

conformations in 1% (v/v) acetic acid or 70% (v/v) ethanol, comprise open extended structures in which tryptophan residues are exposed to the solvent, and are possibly quenched. Each of the above conformations are significantly stable to chemical-induced denaturation; only marginally different conformational forms are present in the presence of denaturant and with the absence of disulphide bonds. It is likely that the key stabilising forces are hydrophobic forces although disulphide bonds and hydrogen bonding may also be significant. One of the broad aims of the physical characterisation was to investigate the applicability of circular dichroism and fluorescence spectroscopy to the unfolding and refolding of the purified gliadin fractions *in vitro*. In view of the lack of significant differences between the native and denatured conformations of each fraction, this may not be a suitable approach. However, it has been shown that the properties of the intact γ-gliadins could be regarded as the sums of those of peptide fragments corresponding to their N-terminal and C-terminal domains respectively. Hence, with the availability of methods for isolating such stable peptide fragments, the physical approaches adopted in this project could be applied to the analysis of peptide fragments instead of intact polypeptides, in order to probe the conformations of gliadins in more detail. Reported progress in protein engineering of cereal storage proteins (Tatham *et al.*, 1990 b), should also benefit future attempts at understanding details of the folding of gliadins, because it would afford the possibility of analysing both authentic and mutant proteins and peptides derived from them for clues about the role of specific residues in the primary sequences as has been reported for authentic and mutant proteins of *Staphylococcal nuclease* (Shortle, 1986; Wright and Freedman, 1989).

LITERATURE CITED.

1. ADLER, A.J., GREENFIELD, N.J. & FASMAN, G.D., 1973. In "Methods in Enzymology", (Hirs, C.H.W. & Timasheff, S.N., eds.), Florida: Academic Press, XXVII(D):675.

2. AIBARA, S. & MORITA, Y., 1988. *J. Cereal Sci.*, 7:237.

3. ANDERSON, O.D., LITTS, J.C., GAUTIER, M.-F. & GREENE, F.C., 1984. *Nucleic Acids Res.*, 12:8129.

4. ANDERSON, O.D., HALFORD, N.G., FORDE, J., YIP, R., SHEWRY, P.R. & GREENE, F.C., 1988. In "Proceedings of the 7th Wheat Genetics Symposium", Cambridge: IPSR, p 699.

5. ANONYMOUS, 1968. In "Recommendations on Gene Symbols and Stock Preservation for Wheat and its Relatives: Proceedings of the 3rd International Wheat Genetics Symposium.", London: Butterworths, p 466.

6. AUTRAN, J.-C., LEW, E.J-L., NIMMO, C.C. & KASARDA, D.D., 1979. *Nature*, 282:527.

7. BAIG, M.A. & SALAHUDDIN, A., 1978. *Biochem. J.*, 171:89.

8. BARTELS, D., ALTOSAAR, I., HARBERD, N.P., BARKER, R.F. & THOMPSON, R.D., 1986. *Theor. Appl. Genet.*, 72:845.

9. BELL, J.E. & HALL, C., 1981. In "Spectroscopy in Biochemistry", (Bell, J.E., ed.), Florida: CRC Press, 1:3.

10. BELTON, P.S., SHEWRY, P.R. & TATHAM, A.S., 1985. *J. Cereal Sci.*, 3:305.

11. BERNADIN, J.E., 1978. *Bakers Digest*, 52:20.

11. BIDLINGMEYER, B.A., COHEN, S.A. & TARVIN, T.L., 1984. *J. Chromatogr.*, 336:93.

12. BIETZ, J.A., HUEBNER, F.R., SANDERSON, J.E. & WALL, J.S., 1977. *Cereal Chem.*, 54:1070.

13. BIETZ, J.A., 1983. *J. Chromatogr.*, 255:219.

14. BIETZ, J.A., 1986. In "Advances in Cereal Science and Technology", (Pomeranz, Y., ed.), Minnesota: American Association of Cereal Chemists Inc., VIII:105.

15. BLOKSMA, A.H., 1975. *Cereal Chem.*, 52(II):170r.

16. BOOTH, M.R. & EWART, J.A.D., 1969. *Biochim. Biophys. Acta.*, 181:226.

17. BRANLARD, G. & DARDAVET, M., 1985. *J. Cereal Sci.*, 3:345.

18. BUNCE, N.A.C., WHITE, R.P. & SHEWRY, P.R., 1985. *J. Cereal Sci.*, 3:131.

19. BURNOUF, T. & BOURIQUET, R., 1980. *Theor. Appl. Genet.*, 58:107.

20. BURSTEIN, E.A., 1968. *Biofizika*, 13:718.

21. BURSTEIN, E.A., VEDENKINA, N.S. & IVKOVA, M.N., 1973. *Photochem. Photobiol.*, 18:263.

22. BUSHUK, W. & NG, P.K.W., 1987. In "GLUTEN PROTEINS": Proceedings of the 3rd International Workshop, Budapest, (Lásztity, R. & Békés, F., eds.), Singapore: World Scientific, p 206.

23. BYERS, M., MIFLIN, B.J., & SMITH, S.J.S., 1983. *J. Sci. Food Agric.*, 34:447.

24. CARERI, G., FASELLA, P. & GRATTON, E.A., 1979. *Rev. Biophys. Bioengng.*, 8:69.

25. CHARBONNIER, L., 1973. *Biochimie*, 55:1217.

26. CHARBONNIER, L., 1974. *Biochim. Biophys. Acta.*, 359:142.

27. CHARBONNIER, L. & MOSSÉ, J., 1980. *J. Sci. Food Agric.*, 31:54.

28. CLEMENTS, R.L., 1987. *Cereal Chem.*, 64(6):442.

29. CLUSKEY, J.E. & WU, Y.V., 1966. *Cereal Chem.*, 43:119.

30. CLUSKEY, J.E. & WU, Y.V., 1971. *Cereal Chem.*, 48:203.

31. COLE, E.W., TORRES, J.V. & KASARDA, D.D., 1983. *Cereal Chem.*, 60(4):306.

32. CREIGHTON, T.E., 1978. *Prog. Biophys. Mol. Biol.*, 33:231.

33. DANNO, G.I., KANAZAWA, K. & NATAKE, M., 1974. *Agric. Biol. Chem.*, 38:1947.

34. DARBRE, A. (ed.), 1986. In "Practical Protein Chemistry, A Handbook", Chichester: John Wiley, p10.

35. DAWSON, R.M.C., ELLIOT, D.C., ELLIOT, W.H. & JONES, K.M. (eds.), 1969. In "Data for Biochemical Research", Oxford: Clarendon Press, p 625.

36. DILL, D.B., ALSBERG, C.L., 1925. *J. Biol. Chem.*, 65:279.

37. DRAKE, A.F., SILIGARDI, G. & GIBBONS, W.A., 1988. *Biophys. Chem.*, 31:143.

38. EFTINK, M.R. & GHIRON, C.A., 1975. *Proc. Natl. Acad. Sci., U.S.A.*, 9:3290.

39. EFTINK, M.R. & GHIRON, C.A., 1976. *Biochemistry*, 15(3):672.

40. ELTON, G.A.H. & EWART, J.A.D., 1962. *J. Sci. Food Agric.*, 13:62.

41. ENTRIKIN, P.P., 1941. *J. Am. Chem. Soc.*, 63:2127.

42. EWART, J.A.D., 1968. *J. Sci. Food Agric.*, 19:617.

43. EWART, J.A.D., 1972. *J. Sci. Food Agric.*, 23:567.

44. EWART, J.A.D., 1975. *J. Sci. Food Agric.*, 26:1021.

45. EWART, J.A.D., 1977 a. *J. Sci. Food Agric.*, 28:191.

46. EWART, J.A.D., 1977 b. *J. Sci. Food Agric.*, 28:843.

47. EWART, J.A.D., 1981. *J. Sci. Food Agric.*, 32:1203.

48. FIELD, J.M., TATHAM, A.S., BAKER, A. & SHEWRY, P.R., 1986. *FEBS Lett.*, 200:76.

49. FIELD, J.M., TATHAM, A.S. & SHEWRY, P.R., 1987. *Biochem. J.*, 247:215.

50. FROMM, M.E., MORRISH, F., ARMSTRONG, C., WILLIAM, R., THOMAS, J. & KLEIN, T.M., 1990. *BIO/TECHNOLOGY*, 8 (September):833.

51. GORDON-KAMM, W.J., SPENCER, T.M., MANGANO, M-L., ADAMS T.R., DAINES, R.J., START, W.G., O'BRIEN, J.V., CHAMBERS, S.A., ADAMS, W.R. Jr., WILLETTS, N.G., RICE, T.B., MACKEY, C.J., KRUEGER, R.W., KAUSCH, A.P. & LEMAUX, P.G., 1990. *Plant Cell*, 2(7):603.

52. GROSSKREUTZ, J.C., 1960. *Biochim. Biophys. Acta.*, 38:400.

53. HAMAUZU, Z., TOYOMASU, T. & YONEZAWA, D., 1974. *Agric. Biol. Chem.*, 38:2445.

54. HAMAUZU, Z. & YONEZAWA, D., 1978. *Agric. Biol. Chem.*, 42(6):1283.

55. HAMAUZU, Z. & YONEZAWA, D., 1978. *Agric. Biol. Chem.*, 42(6):1283.

56. HARBERD, N.P., BARTELS, D. & THOMPSON, D., 1985. *Mol. Gen. Genet.*, 198:234.

57. HERNÁNDEZ-ARANA, A. & SORIANA-GARCÍA, M., 1988. *Biochim. Biophys. Acta.*, 954: 170.

58. HESSER, J.M., 1987. In "GLUTEN PROTEINS": Proceedings of the 3rd International Workshop, Budapest, (Lásztity, R. & Békés, F., eds.), Singapore: World Scientific, p 441.

59. HOPKINS, F.G., 1925. *Biochem. J.*, 19:787.

60. HOSENEY, C.R., 1986. In "Principles of Cereal Science and Technology", (Pomeranz, Y., ed.), Minnesota: American Association of Cereal Chemists Inc., p 6.

61. JACKSON, E.A., HOLT, L.M. & PAYNE, P.I., 1983. *Theor. Appl. Genet.*, 66:29.

62. JONES, R.W., TAYLOR, N.W. & SENTI, F.R., 1959. *Arch. Biochem. Biophys.*, 84:363.

63. KASARDA, D.D., BERNADIN, J.E. & THOMAS, R.S., 1967. *Science*, 155:203.

64. KASARDA, D.D., BERNADIN, J.E. & GAFFIELD, W., 1968. *Biochemistry*, 7:3950.

65. KASARDA, D.D., BERNADIN, J.E. & NIMMO, C.C., 1976. In "Advances in Cereal Science and Technology", (Pomeranz, Y., ed.), Minnesota: American Association of Cereal Chemists Inc., I:158.

66. KASARDA, D.D., AUTRAN, J-C., LEW, E.J-L., NIMMO, C.C. & SHEWRY, P.R., 1983. *Biochim. Biophys. Acta.*, 747:138.

67. KHAN, K. & BUSHUK, W., 1978. *Bakers Digest*, 52:14.

69. KHAN, K. & BUSHUK, W., 1979. *Cereal Chem.*, 56:505.

70. KREJCI, L. & SVERDBERG, T., 1935. *J. Am. Chem. Soc.*, 57:946.

71. KRETSCHMER, C.B., 1957. *J. Phys. Chem.*, 61:1627.

72. KRONMANN, M.J. & ROBBINS, F.M., 1970. In "Fine Structure of Proteins and Nucleic Acids" (Fasman, G.D., ed.), New York: Marcel Dekker, p 271.

73. LAEMMLI, U.K., 1970. *Nature*, 227:680.

74. LAFIANDRA, D., KASARDA, D.D. & MORRIS, R., 1984. *Theor. Appl. Genet.*, 68:531.

75. LAKOWICS, J. & WEBER, G., 1973. *Biochemistry*, 12:4171.

76. LAKOWICZ, J.R., 1981. In "Spectroscopy in Biochemistry", (Bell, J.E., ed.), Florida: CRC Press, 1:195.

77. LAMM, O. & POULSON, A., 1936. *Biochem. J.*, 30:528.

78. LÁSZTITY, R., BÉKÉS, F., öRSI, F., SMIED, I. & EMBER-KÁRPÁTI, M., 1987. In "GLUTEN PROTEINS": Proceedings of the 3rd International Workshop, Budapest, (Lásztity, R. & Békés, F., eds.), Singapore: World Scientific. p 343.

79. LEHRER, S.S., 1971 a. *Biochemistry*, 10:3254.

80. LEHRER, S.S., 1971 b. *Biophys. J.*, 11:72a.

81. LEHRER, S.S., 1975. In "Concepts in Biochemical Fluorescence (Chen, R. & Edelhoch, H., eds.), New York: Marcel Dekker.

82. LONGWORTH, J.W. & GHIRON, C.A., 1974. *Biochemistry*, 15(3):680.

83. MAKINEN, M.W. & FINK, A.L., 1977. *Ann. Rev. Biophys. Bioeng.*, 6:301.

84. MASSON, P., POPINEAU, Y. & PINEAU, F., 1989. *Lebens-Wiss. u-Technol.*, 22:157.

85. MECHAM, D.K., KASARDA, D.D. & QUALSET, C.O., 1978. *Biochem. Genet.*, 16:831.

86. MEREDITH, O.B. & WREN, J.J., 1966. *Cereal Chem.*, 43:169.

87. MIFLIN, B.J., MATTHEWS, J.A., BURGESS, S.R. & FAULKS, A.J., 1980. *Ann. Technol. Agric.*, 29:133.

88. MIFLIN, B.J., FIELD, J.M. & SHEWRY, P.R., 1983. In "Seed Proteins": *Ann. Proc. Phytochem. Soc. Europe*, (Daussant, J., Mossé, J. & Vaughan, J., eds.), London: Academic Press, 20:253.

89. MILES, E.W., YUTANI, K. & OGASAHARA, K., 1982. *Biochemistry*, 21:2586.

90. MOONEN, J.H.E., SCHEEPSTRA, A.A. & GRAVELAND, A., 1982. *Euphytica*, 31:677.

91. MOONEN, J.H.E., SCHEEPSTRA, A. & GRAVELAND, A., 1983. *Euphytica*, 32:735.

92. NIELSEN, T.B. & REYNOLDS, J.A., 1978. In "Methods in Enzymology", (Hirs, C.H.W. & Timasheff, S.N., eds.), Florida: Academic Press, XLVIII(F):3.

93. O'CONNOR, M. (ed.), 1983. *Ciba Found. Symp.*, 93.

94. O'CONNOR, D.V. & PHILLIPS, D., 1984. In "Time Correlated Single Photon Counting", London: Academic Press.

95. OKITA, T.W., CHEESEBROUGH, V. & REEVES, C.D., 1985. *J. Biol. Chem.*, 260:8203.

96. PACE, C.N., 1986. In "Methods in Enzymology", (Hirs, C.H.W. & Timasheff, S.N., eds.), Florida: Academic Press, 131(L):266.

97. PARKER, C.A., 1968. In "Photoluminescence of Solutions", New York: Elsevier, p 220.

98. PAYNE, P.I., CORFIELD, K.G. & BLACKMAN, J.A., 1979. *Theor. Appl. Genet.*, 55: 153.

99. PAYNE, P.I., CORFIELD, K.G., HOLT, L.M. & BLACKMAN, J.A., 1981 a. *J. Sci. Food Agric.*, 32:51.

100. PAYNE, P.I., HOLT, L.M. & LAW, C.N., 1981 b. *Theor. Appl. Genet.*, 60:229.

101. PAYNE, P.I., HOLT, L.M., LAWRENCE, G.J. & LAW, C.N., 1982. *Qual. Plant. Plant Foods Hum.*

Nutr., 31:229.

102. PAYNE, P.I., HOLT, L.M., WORLAND, A.J. & LAW, C.N., 1982. *Theor. Appl. Genet.*, 63:129.

103. PAYNE, P.I., HOLT, L.M., JACKSON, E.A & LAW, C.N., 1984. *Philos. Trans. R. Soc., London Ser. B.*, 304: 359.

104. PAYNE, P.I., 1987. *Ann. Rev. Plant Physiol.*, 38:141.

105. PERUFFO, A.D.B., POGNA, N.E., TEALDO, E., TUTTA, C. & ALBUZIO, A., 1985. *J. Cereal Sci.*, 3:355.

106. PLATT, S.G. & KASARDA, D.D., 1971. *Biochim. Biophys. Acta.*, 243:407.

107. POGNA, N.E., BOGGINI, G., CORBELLINI, M., CATTANEO, M. & PERUFFO, A.D.B., 1982 a. *Can. J. Plant Sci.*, 62:913.

108. POGNA, N.E., PERUFFO, A.D.B., BOGGINI, G. & CORBELLINI, M., 1982 b. *Genet. Agric.*, 36:143.

109. POPINEAU, Y. & GODON, B., 1982. *Cereal Chem.*, 59:55.

110. POPINEAU, Y. & PINEAU, F., 1985 a. *Lebens-Wiss. u-Technol.*, 18:133.

111. POPINEAU, Y & PINEAU, F., 1985 b. *J. Cereal Sci.*, 3:363.

112. POPINEAU, Y. & PINEAU, F., 1988. *Lebens-Wiss. u-Technol.*, 21:113.

113. PRATT, K., 1990. Ph.D Thesis, University of Kent at Canterbury.

114. PROVENCHER, S.W., GLöCKNER, J., 1981. *Biochemistry*, 20:33.

115. PURCELL, J.M., KASARDA, D.D. & WU, C-S.C., 1988. *J. Cereal Sci.*, 7:21.

116. RAFALSKI, J.A., SCHEETS, K., METZLER, M., PETERSON, D.M., HEDGCOTH, C. & SOLL, D.G., 1984. *EMBO J.*, 3:1409.

117. RAINERI, D.M., BOTTINO, P., GORDON, M.P. & NESTOR, E.W., 1990. *BIO/TECHNOLOGY*, 8 (January):33.

118. RUPLEY, J.A., 1969. In "Structure and Stability of Biological Macromolecules" (Timasheff, N. & Fasman, G.D., eds.), New York: Marcel Dekker, p 291.

119. SHEWRY, P.R., AUTRAN, J.-C., NIMMO, C.C., LEW, E.J-L. & KASARDA, D.D., 1980. *Nature*, 286:520.

120. SHEWRY, P.R., TATHAM, A.S., FORDE, J., MIFLIN, B.J. & KASARDA, D.D., 1984. In "GLUTEN PROTEINS": Proceedings of the 2nd International Workshop, Vageningen, (Graveland, A. & Moonen, J.H.E., eds.), Vageningen: Netherlands Organisation for Applied Scientific Research (TNO), p 51.

121. SHEWRY, P.R. & MIFLIN, B.J., 1985. In "Advances in Cereal Science and Technology",

(Pomeranz, Y., ed.), Minnesota: American Association of Cereal Chemists Inc., 7:1.

122. SHEWRY, P.R., TATHAM, A.S., FORDE, J., KREIS, M. & MIFLIN, B.J., 1986. *J. Cereal Sci.*, 4:97.

123. SHEWRY, P.R., FIELD, J.M. & TATHAM, A.S., 1987. In "Cereals in a European Context", (Morton, I.D., ed.), Weinheim: Ellis Horwood, p 421.

124. SHORTLE, D., 1986. *J. Cell. Biochem.*, 30:281.

125. SIGMA TECHNICAL DEPARTMENT, 1989. Personal communication.

126. SOZINOV, A.A. & POPERELYA, F.A., 1982. *Qual. Plant. Plant Foods Hum. Nutr.*, 31:243.

127. TATHAM, A.S. & SHEWRY, P.R., 1985. *J. Cereal Sci.*, 3:103.

128. TATHAM, A.S., DRAKE, A.F. & SHEWRY, P.R., 1985 a. *Biochem. J.*, 276:557.

129. TATHAM, A.S., MIFLIN, B.J. & SHEWRY, P.R., 1985 b. *Cereal Chem.* 62:405.

130. TATHAM, A.S., SHEWRY, P.R. & BELTON, P.S., 1985 c. *Biochem. J.*, 232:617.

131. TATHAM, A.S., DRAKE, A.F. & SHEWRY, P.R., 1989. *Biochem. J.*, 259:471.

132. TATHAM, A.S., MASSON, P. & POPINEAU, Y., 1990 a. *J. Cereal Sci.*, 11:1.

133. TATHAM, A.S., BELTON,P.S. & SHEWRY, P.R., 1990 b. In "Advances in Cereal Science and Technology", (Pomeranz, Y., ed.), Minnesota: America Association of Cereal Chemists Inc., X:1.

134. TAYLOR, N.W. & CLUSKEY, J.E., 1962. *Arch. Biochem. Biophys.*, 97:399.

135. TEALE, F.W.J. & BADLEY, R.A., 1970. *Biochem. J.*, 116:341.

136. THOMPSON, R.D., BARTELS, D., HARBERD, N.P. & FALVELL, R.B., 1983. *Theor. Appl. Genet.*, 67:87.

137. TKACHUK, R. & MELLISH, V.J., 1987. In "GLUTEN PROTEINS": Proceedings of the 3rd International Workshop, Budapest (Lásztity, R. & Békés, F., eds.), Singapore: World Scientific, p 111.

138. VASIL, V., REDWAY, F. & VASIL, I.K., 1990. *BIO/TECHNOLOGY*, 8 (May):429.

139. WALDMANN, A.D.B., CLARKE, A.R., WIGLEY, D.B., HART, K.W., CHIA, W.N., BARSTOW, D., ATKINSON, T., MUNRO, I. & HOLBROOK, J.J., 1987. *Biochim. Biophys. Acta.*, 913:66.

140. WALL, J.S., 1979. In "Recent Advances in the Biochemistry of Cereals", *Ann. Proc. Phytochem. Soc. Europe* (Laidman, D.L. & Wyn Jones, R.G., eds.), London: Academic Press, 16:275.

141. WAXDALL, M.J., KONINGSBERG, W.H., HENLEY, W.L. & EDELMAN, G.M., 1968. *Biochemistry*, 7:1959.

142. WOYCHIK, J.H., BOUNDY, J.A. & DIMLER R.J., 1961. *Arch. Biochem. Biophys.*, 94:477.

143. WOYCHIK, J.H., 1963. Proc. Seed Protein Conf., New Orleans, La., (January), p27.

144. WREN, J.J. & NUTT, J., 1967. *J. Sci. Food Agric.*, 18:119.

145. WRIGHT, G. & FREEDMAN, R.B., 1989. *Protein Engineering*, 2(8):583.

146. WRIGLEY, C.W. & SHEPHERD, K.W., 1973. *Ann. NY Acad. Sci.*, 209:154.

147. WU, Y.V. & DIMLER, R.J., 1964. *Arch. Biochem. Biophys.*, 107:435.

148. WU, Y.V. & CLUSKEY, J.E., 1965. *Arch. Biochem. Biophys.*, 112:32.

149. WU, Y.V., CLUSKEY, J.E. & SEXSON, K.R., 1967. *Biochim. Biophys. Acta.*, 133:83.